Titre: Title:	Synthèse topologique et géométrique des manipulateurs parallèles en translation
Auteur: Author:	Xiaoyu Wang
Date:	2006
Type:	Mémoire ou thèse / Dissertation or Thesis
Référence: Citation:	Wang, X. (2006). Synthèse topologique et géométrique des manipulateurs parallèles en translation [Ph.D. thesis, École Polytechnique de Montréal]. PolyPublie. https://publications.polymtl.ca/7784/

UNIVERSITÉ DE MONTRÉAL

SYNTHÈSE TOPOLOGIQUE ET GÉOMÉTRIQUE DES MANIPULATEURS PARALLÈLES EN TRANSLATION

XIAOYU WANG
DÉPARTEMENT DE GÉNIE MÉCANIQUE
ÉCOLE POLYTECHNIQUE DE MONTRÉAL

THÈSE PRÉSENTÉE EN VUE DE L'OBTENTION
DU DIPLÔME DE PHILOSOPHIÆ DOCTOR
(GÉNIE MÉCANIQUE)
AVRIL 2006

Your file Votre référence
ISBN: 978-0-494-24552-1
Our file Notre référence
ISBN: 978-0-494-24552-1

UNIVERSITÉ DE MONTRÉAL

ÉCOLE POLYTECHNIQUE DE MONTRÉAL

Cette thèse intitulée:

SYNTHÈSE TOPOLOGIQUE ET GÉOMÉTRIQUE DES MANIPULATEURS PARALLÈLES EN TRANSLATION

présentée par: WANG Xiaoyu

en vue de l'obtention du diplôme de: Philosophiæ Doctor

a été dûment acceptée par le jury d'examen constitué de:

M. GOURDEAU Richard, Ph.D., président

M. BARON Luc, Ph.D., membre et directeur de recherche

M. CLOUTIER Guy, Doct., membre et codirecteur de recherche

M. BIRGLEN Lionel, Ph.D., membre

M. HAYES John D., Ph.D., membre

à ma femme Yuhong et à toute ma famille

REMERCIEMENTS

Je tiens, tout particulièrement, à remercier mon directeur de recherche Prof. Luc Baron, ainsi que mon codirecteur de recherche Prof. Guy Cloutier pour m'avoir fait confiance et m'avoir adroitement dirigé au cours de mes recherches.

Je remercie très sincèrement les membres du jury pour avoir accepté de lire et d'évaluer ma thèse.

Ma reconnaissance va à l'ensemble de mes collèges du laboratoire de CAE pour leur précieuse aide tant au niveau de la langue français qu'au niveau de la connaissance scientifique.

Mes remerciements iront aussi vers ceux qui m'ont poussé au cours de ces travaux de recherche.

Enfin, un grand merci à toute ma famille ; ma mère, mon père, mon frère et surtout ma femme pour leur amour et pour leur soutien inconditionnel.

RÉSUMÉ

Cette thèse présente une contribution à la synthèse topologique et géométrique des manipulateurs parallèles (MPs). Notre intérêt s'est porté sur les MPs à 3 degrés de liberté, et plus particulièrement, aux MPs en translation (MPTs).

La topologie d'un manipulateur est, en général, la description de la structure de sa chaîne cinématique, *i.e.*, la nature de tous ses couples cinématiques et leur arrangement alors que la géométrie est un ensemble de contraintes dimensionnelles et géométriques sur les positions et orientations relatives entre les couples cinématiques.

Ce travail consiste à développer les outils de synthèse topologique et géométrique permettant de générer et d'évaluer systématiquement les MPTs de toutes topologies et géométries.

L'objectif premier de cette thèse est de proposer une approche générale de synthèse topologique permettant de déterminer la topologie d'un MP en fonction de ses degré de liberté de manipulateur et degré de mobilité de l'effecteur. Le deuxième objectif consiste à proposer une méthode de synthèse topologique permettant de déterminer la topologie d'un MP de sorte que son effecteur n'ait que 3 degrés de mobilité en translation à travers un espace de travail. Le troisième objectif est de développer un nombre raisonnable de modèles géométriques qui peuvent s'appliquer aux MPTs de toutes topologies et géométries.

Dans le cadre de ce travail, une revue de la littérature a été réalisée afin d'identifier la problématique et de positionner nos travaux de recherche par rapport aux travaux réalisés dans les domaines concernés. Par la suite, le problème de synthèse

topologique et géométrique a été étudié.

La première problématique abordée est d'identifier les particularités topologique et géométrique des manipulateurs spatiaux. Pour cela, nous avons effectué une analyse des architectures connues et proposé des définitions pour la ***topologie*** et la ***géométrie***. Puis, nous avons proposé une représentation topologique originale des manipulateurs qui permet de décrire adéquatement la chaîne cinématique et de caractériser la propriété cinématique. Cette représentation a une structure de graphe, ce qui permet une description numérique sous forme de matrice et de générer systématiquement les topologies.

La deuxième problématique abordée est de formaliser la topologie en fonction du degré de liberté de manipulateur et la mobilité de l'effecteur. Pour celle-ci, nous avons d'abord précisé les termes : ***degré de liberté de manipulateur*** (DDL), ***degré de mobilité*** (ou ***mobilité***) ***de l'effecteur*** (DDM), et ***nature de la mobilité de l'effecteur*** (NDM). Afin d'établir le lien entre la topologie et les DDL, DDM, et NDM, nous avons introduit la notion de ***configuration initiale*** et nous avons proposé, basée sur cette configuration, une représentation numérique de la topologie et de la géométrie. Par la suite, nous avons effectué une analyse systématique de l'espace tangentiel à la configuration initiale et nous avons établi le lien entre la topologie et les DDL et DDM. Selon la théorie des groupes de Lie, ce lien est aussi valide dans l'espace de déplacement voisinant la configuration initiale. Cependant, cette analyse ne permet pas d'établir de façon rigoureuse le lien entre la topologie et la NDM, car l'espace tangentiel dépend de la configuration de manipulateur.

Nous avons donc procédé à l'analyse de l'espace de déplacement et nous avons proposé pour la première fois une approche de synthèse qui permet de déterminer

la topologie d'un MP qui ne génère que le déplacement en translation à l'intérieur d'un voisinage de son espace de travail. Les deux analyses ont abouti à une approche originale de la synthèse topologique et géométrique des MPTs.

Afin d'automatiser le processus de synthèse, nous avons développé des modèles géométriques qui peuvent s'appliquer aux MPTs de toutes topologies et géométries. Pour ceci, nous avons proposé une méthode originale de définir un référentiel à chaque membrure, qui permet de traiter de façon uniforme les joints prismatiques, les joints rotoïdes et les joints rotoïdes très éloignés. Pour la première fois, les problèmes des modèles géométriques direct et inverse des MPTs ont été systématiquement étudiés.

Les travaux présentés dans cette thèse permettent de produire un environnement de synthèse topologique et géométrique des MPTs. Une étude systématique de la littérature nous a permis de valider l'originalité de nos travaux et notre contribution en ce qui concerne la synthèse topologique et géométrique. Des applications de nos approches nous ont permis de proposer de nouvelles topologies et de nouvelles géométries. L'ensemble des méthodes, des techniques proposées et des travaux fondamentaux que nous avons réalisés pourront être utilisés à l'étude théorique et à la conception cinématique des MPTs

ABSTRACT

This thesis presents a contribution to the topological and geometric synthesis of parallel manipulators (PMs). Focus was put on 3-degree-of-freedom (DOF) PMs, and especially on translational PMs (TPMs).

The topology of a manipulator is, in general, the description of the structure of its kinematic chain, *i.e.* the type of its kinematic pairs and their general arrangement, while its geometry is a set of dimensional and geometric constraints on the relative position and orientation of its kinematic pairs.

This work is aimed at developing topological and geometric synthesis tools in order that TPMs of all topologies and geometries can be generated and evaluated systematically.

The first objective of this thesis is to propose a general topological and geometric synthesis approach allowing of the determination of the topology of a PM according to its manipulator's DOF and its end-effector's (EE) DOF. The second objective is to derive topologies of PMs which generate only translational displacement. The third objective is to develop a reasonable number of kinematic models which can apply to TPMs of all topologies and geometries.

First of all, a literature review was carried out in order to pinpoint key issues concerning the topological and kinematic synthesis of PMs and base our research on the most recent achievements in the related fields. After that, the synthesis problem was studied.

The first problem addressed in this thesis is to identify the particular aspects of spa-

tial manipulator topologies and geometries. To this end, analysis of known spatial manipulator architectures was performed and the terms ***topology*** and ***geometry*** were redefined in order to take into consideration the structure characteristics proper to spatial manipulators. The analysis also leads to a topological representation with which kinematic chain structure and the mobility can be better characterized. The representation has a graph structure and can be easily adapted for matrix form numerical representation, making it possible for topologies to be generated systematically.

The second problem is to formulate relations between the topology of a PM and its manipulator's DOF and EE's DOF. To better characterize a manipulator as a mechanism and its EE as a rigid body, appropriate definitions were made on the ***manipulator's degree of freedom*** (DOF), the ***end-effector's degree of mobility*** (DOM), and the ***nature of the end-effector's mobility*** (NOM). In order to establish relations between topology and DOF and DOM, the concept of ***initial configuration*** was introduced which lead to an integrated topology and geometry representation. From the analysis of a set of linear equations established in displacement tangent space at the initial configuration, topology and geometry conditions were then derived for a PM to have a given DOF and DOM in the tangent space. According to the group theory, the PM will have the given DOF and DOM within a neighborhood of the initial configuration. However, tangent space analysis does not ensure that the NOM will not change once the PM leaves the initial configuration.

Analysis in displacement space was then performed and a new topological synthesis approach was proposed. With this approach, the resulting PMs will only generate translational displacement within an entire neighborhood of the initial configuration. The analyses in tangent space and in displacement space together lead to a

new topological and geometric synthesis approach of TPMs.

In order to achieve automatic synthesis, a kinematic model was proposed which takes both topology and geometry as design variables and can therefore apply to TPMs of all topologies and geometries. This was done by performing a special frame assignment, which enables prismatic joints and revolute joints to be treated in a unified way. Then for the first time, the forward and inverse kinematic problems of TPMs were systematically studied.

The work presented in this thesis makes it possible to create a platform for automatic topological and geometric synthesis of TPMs. Its originality comes from the fact that the main problems addressed here are open problems in kinematic synthesis of TPMs which are identified through a systematic literature review. Applications of the results from this work have allowed us to propose new topologies and geometries of 3-DOF PMs. The results of this work can be used for theoretical studies and kinematic design of TPMs.

TABLE DES MATIÈRES

DÉDICACE iv

REMERCIEMENTS v

RÉSUMÉ vi

ABSTRACT ix

TABLE DES MATIÈRES xii

LISTE DES FIGURES xviii

LISTE DES NOTATIONS ET DES SYMBOLES xxii

LISTE DES TABLEAUX xxv

INTRODUCTION 1

0.1 Contexte 1

0.2 Topologie et géométrie 2

0.3 Synthèse des manipulateurs spatiaux 2

0.4 Synthèse des MPs 3

0.5 Objectifs 4

CHAPITRE 1 REVUE CRITIQUE DE LA LITTÉRATURE 6

1.1 La terminologie 7

1.2 Historique 14

1.3 MP versus MS 17

1.4 Représentation topologique 21

1.4.1 Vues perspectives 21

1.4.2 Dessin d'assemblage 22
1.4.3 Schéma cinématique 23
1.4.4 Représentation par graphes, matrices, schémas structurel et fonctionnel 23
1.4.5 Graphe d'agencement 24
1.4.6 Représentation alpha-numérique 25
1.5 Synthèse topologique 27
1.5.1 Approche basée sur la théorie de graphe 27
1.5.2 Théorie des groupes de Lie et synthèse topologique 27
1.5.2.1 Théorie des groupes de Lie 27
1.5.2.2 Synthèse topologique basée sur la théorie des groupes de Lie 31
1.5.3 Synthèse basée sur la théorie des visseurs 32
1.6 Synthèse géométrique des MPs 35
1.6.1 Modélisation cinématique 36
1.6.2 Résolution des problèmes des modèles géométriques 38
1.6.2.1 Solution numérique 38
1.6.2.2 Solution algébrique 39
1.7 Conclusion 39

CHAPITRE 2 ORGANISATION GÉNÉRALE DE LA THÈSE 41
2.1 Les travaux proposés 41
2.2 Chapitre 3 : topologie et diagramme topologique des MSs et MPs . 43
2.3 Chapitre 4 : analyse de mobilité des MPs à 3 DDLs 45
2.4 Chapitre 5 : synthèse topologique des MPTs basée sur la cinématique instantanée 47
2.5 Chapitre 6 : synthèse topologique des MPTs basée sur analyse de déplacement 50

2.6 Chapitre 7 : modélisation topologique et géométrique des MPTs . . 52
2.6.1 Paramétrage topologique et géométrique 52
2.6.2 Modélisation géométrique 53

CHAPITRE 3 TOPOLOGY OF SERIAL AND PARALLEL MANIPULATORS AND THEIR TOPOLOGICAL DIAGRAMS 56
3.1 Introduction 57
3.2 Basic Definitions and Background 59
3.3 Topology : Revised for the Topological Synthesis 62
3.4 Topological diagrams 64
3.4.1 Topological representation : a review 64
3.4.2 Kinematic composition 67
3.4.3 Essential constraints 69
3.4.4 Simplified diagram 70
3.4.5 Topological diagram 71
3.5 Additionnal Examples of Topological Diagrams 73
3.5.1 Serial manipulators 73
3.5.2 Parallel manipulators 75
3.6 Kinematic Synthesis Methodology 76
3.7 Conclusion 78

CHAPITRE 4 MOBILITY ANALYSIS OF THREE-DEGREES-OF-FREEDOM PARALLEL MANIPULATORS 84
4.1 Introduction 85
4.2 Nomenclature 87
4.3 Degree of Freedom and Mobility : Revisited 88
4.4 Kinematics of PMs of General Topology and Geometry 90
4.5 Tangent Space Formulation 92
4.6 Tangent Space Analysis of 3-legged PMs 95

4.6.1 Isoconstrained PMs of 3-DOF 97
4.6.2 Overconstrained PMs of 3 DOFs 104
4.6.3 Underconstrained PMs of 3 DOFs 108
4.7 Conclusion 113

CHAPITRE 5 TOPOLOGICAL AND GEOMETRICAL SYNTHESIS OF THREE DEGREE-OF-FREEDOM FULLY PARALLEL MANIPULATORS BY INSTANTANEOUS KINEMATICS . . 119
5.1 Introduction 120
5.2 Kinematic modelling 123
5.3 Tangent Space Analysis 130
5.4 The Synthesis Procedure 133
5.5 Synthesis Examples 136
5.6 Conclusion 142

CHAPITRE 6 SYNTHESIS OF TRANSLATIONAL PARALLEL MANIPULATORS BASED ON FINITE DISPLACEMENT . . . 149
6.1 Introduction 150
6.2 Kinematic modelling and definitions 152
6.3 Possible subchain topologies for TPMs 157
6.3.1 Subchains with only one (n)-H (hpyer) revolute link 158
6.3.2 Subchains with only one (hyper) skew revolute link 158
6.3.3 Subchains with at least two (hyper) skew revolute links . . 160
6.4 Analysis of the EE orientation space of PMs of 3 DOF 165
6.4.1 PMs with a T-subchain 166
6.4.2 PMs with an I-subchain 166
6.4.3 PMs with three A-subchains 169
6.4.4 PMs with three Z-subchains 175
6.5 Topological synthesis of TPMs 180

6.6 Conclusion 181

CHAPITRE 7 TOPOLOGICAL AND GEOMETRIC MODELLING OF TRANSLATIONAL PARALLEL MANIPULATOR 185

7.1 Introduction 186

7.2 Nomenclature 188

7.3 Topological Representation 189

7.4 Geometric Representation 192

7.5 kinematic modelling of general PMs 193

7.6 Kinematic model of TPMs 198

7.7 Inverse kinematics of TPMs 201

7.7.1 Subchains of $R^1R^1R^2R^2R^2$ 202

7.7.1.1 Solve q_1 and q_2 202

7.7.1.2 Solve q_3, q_4, and q_5 209

7.7.2 Subchains of $R^1R^1R^2R^2R^1$ 215

7.7.2.1 Solve q_3 and q_4 215

7.7.2.2 Solve q_1, q_2, and q_5 216

7.8 Forward kinematics of TPMs 219

7.8.1 Position manifold 220

7.8.2 Numerical solution 224

7.9 Jacobian matrix 226

7.9.1 Jacobian matrix of subchains 227

7.9.2 Jacobian matrix of TPMs 228

7.10 Synthesis procedure 229

7.11 Conclusion 231

7.12 Appendix 1 : Inverse kinematics of TPMs 232

7.12.1 Subchains of $R^1R^1R^1R^2R^2$ 232

7.12.2 Subchains of $R^1R^2R^2R^2R^1$ 234

7.12.3 Subchains of $R^1R^2R^2R^1R^1$ 236
7.12.3.1 Solve q_2 and q_3 236
7.12.3.2 Solve q_1, q_4, and q_5 237
7.13 Appendix 2 : Position manifold 240

CHAPITRE 8 DISCUSSION GÉNÉRALE 247

CONCLUSION 252

RÉFÉRENCES 255

LISTE DES FIGURES

FIG. 1.1	Illustration des couples cinématiques inférieurs	8
FIG. 1.2	Joints d'ordre un et deux	10
FIG. 1.3	Corps d'ordre deux et trois	10
FIG. 1.4	Les chaînes cinématiques série, arborescente, fermée, et parallèle	11
FIG. 1.5	Un mécanisme	12
FIG. 1.6	Deux mécanismes de différentes topologies	13
FIG. 1.7	Deux mécanismes de même topologie mais de géométries différentes	13
FIG. 1.8	MP breveté en 1931 (GWINNETT, 1931)	14
FIG. 1.9	Le premier MP (POLLARD, 1940)	15
FIG. 1.10	Plateforme de Gough (GOUGH, 1956)	15
FIG. 1.11	Schéma de la plateforme de Stewart (STEWART, 1965)	16
FIG. 1.12	Le premier simulateur de vol (Courtoisie de Klaus Cappel)	16
FIG. 1.13	Un MS	17
FIG. 1.14	Un MP	18
FIG. 1.15	3-RRR (GOSSELIN ET HAMEL, 1994)	19
FIG. 1.16	3-PRRR (KIM ET TSAI, 2002)	19
FIG. 1.17	3-RRRRR (ZLATANOV ET AL., 2002)	20
FIG. 1.18	Vues perspectives	22
FIG. 1.19	Dessin d'assemblage	22
FIG. 1.20	Symboles des joints cinématiques (ISO, 1981)	23
FIG. 1.21	Représentation par schéma structurel, graphe, et schéma fonctionnel	24
FIG. 1.22	les symboles des graphes d'agencement (PIERROT, 1991)	25
FIG. 1.23	les symboles des graphes d'agencement (BARON, 1997)	25

FIG. 1.24 Puma200 25
FIG. 1.25 Stanford 25
FIG. 1.26 4-Barres plan 26
FIG. 1.27 4-Barres sphériques 26
FIG. 1.28 Mécanisme de bennett 26
FIG. 1.29 MP de Y-Star 32
FIG. 3.1 Lower Kinematic Pairs 60
FIG. 3.2 Four-bar linkages having the same kinematic structure *RRRR* and different modility 61
FIG. 3.3 Parallel manipulators having the same kinematic structure 3-*PRRR* and very different kinematic properties 61
FIG. 3.4 Kinematic joint symbols (ISO, 1981) 64
FIG. 3.5 Layout graph symbols (PIERROT, 1991) 65
FIG. 3.6 Layout graph symbols (BARON, 1997) 65
FIG. 3.7 Structural schema, graph, and functional schema 66
FIG. 3.8 Kinematic Composition of a Planar 3-$\underline{\text{R}}$RR parallel manipulator 67
FIG. 3.9 Kinematic Composition of a Spherical 3-$\underline{\text{R}}$RR parallel manipulator 68
FIG. 3.10 Graphic symbols of the six essential constraints 69
FIG. 3.11 Diagram of a planar parallel manipulator with essential constraints on the relative joint locations 70
FIG. 3.12 Diagram of a spherical parallel manipulator with essential constraints on relative joint locations 70
FIG. 3.13 Diagram of a spherical parallel manipulator with constraints on relative non-adjacent joint Locations 71
FIG. 3.14 Diagram of 3-UPU 71
FIG. 3.15 Some additional symbols for complex constraints 72

FIG. 3.16 Diagram with Constraint Vertices 72
FIG. 3.17 Complex Joints 73
FIG. 3.18 Diagram of Delta (CLAVEL, 1988) 73
FIG. 3.19 Diagram of parallel manipulator proposed by (KIM ET TSAI, 2002) 74
FIG. 3.20 Joint grouping priority order 74
FIG. 3.21 PUMA manipulator 74
FIG. 3.22 A serial manipulator designed by Victor Scheinman, photo by Les Earnest, scanned by Bruce Baumgart 75
FIG. 3.23 4-DOF Flight Simulator by Koevermans W.P. et al., drawing by Merlet, J.P 75
FIG. 3.24 5-DOF by Hesselbach J. et al., drawing by Merlet, J.P. . . . 76
FIG. 3.25 6-DOF Decoupled Manipulator by Nabla, drawing by Merlet J.P 76
FIG. 3.26 Illustration of design spaces 77
FIG. 4.1 6-$\underline{S}$PRS PM 88
FIG. 4.2 An overconstrained PM of topology 2-$\underline{P}$RRR and 1-$\underline{P}$RS$\underline{P}$RSR^2 89
FIG. 4.3 Reference frames $\mathcal{F}_{j,i}$ attached to links 0 to m_j of the sub-chain j 90
FIG. 4.4 A new isoconstrained spherical PM 103
FIG. 4.5 An isoconstrained TPM of topology 3-$\underline{P}R^1R^2R^2R^2$ 107
FIG. 4.6 The overconstrained TPM of topology 3-$\underline{P}R^2R^2R^2$(KIM ET TSAI, 2002) 107
FIG. 4.7 An isoconstrained spherical PM of topology 3-$PP\underline{R}RR$ . . . 108
FIG. 4.8 An overconstrained spherical PM of topology 3-$\underline{R}RR$ (GOSSELIN ET HAMEL, 1994) 109
FIG. 4.9 A TPM with redundant passive joints 112

FIG. 4.10 A TPM without redundant passive joint (KONG ET GOSSELIN, 2002) 112
FIG. 5.1 Example 1 : A new architecture of PMs generating 1-DOF of translation and 2-DOF of rotation of topology R3R-R4R-P5R 138
FIG. 5.2 Example 2 : An isotropic architecture of translational PM of topology 3-RUU 140
FIG. 5.3 Example 3 : An existing architecture of translational PM of topology 3-UPU 141
FIG. 7.1 Two links coupled by a revolute joint 189
FIG. 7.2 End-effector reference frame 193
FIG. 7.3 Link reference frames 195
FIG. 7.4 Reference frame definition for $link(i, j)$ 196
FIG. 7.5 Topologies of 5-revolute-joint subchains 199

LISTE DES NOTATIONS ET DES SYMBOLES

MP : manipulateur parllèle

MS : manipulateur sériel

MPT : manipulateur parallèle en translation

MGD : modèle géométrique direct

MGI : modèle géométrique inverse

DDL : degré de liberté

DDM : degré de mobilité

NDM : nature de mobilité

DDC : dimension de l'espace de configuration

b : indice identifiant le référentiel global

e : indice identifiant le référentiel de l'effecteur

$\mathcal{F}_i$: référentiel de la $i^{ième}$ membrure

${}^d\boldsymbol{\rho}_c$: vecteur de position 3×1 de l'origine du référentiel $\mathcal{F}_c$ par rapport au référentiel $\mathcal{F}_d$

$\boldsymbol{\rho}_i$: vecteur de position 3×1 de l'origine du référentiel $\mathcal{F}_i$ par rapport au référentiel $\mathcal{F}_{i-1}$

$\boldsymbol{p}_i$: vecteur de position 3×1 de l'origine du référentiel $\mathcal{F}_i$ par rapport au référentiel $\mathcal{F}_b$

${}^d\mathbf{Q}_c$: matrice d'orientation 3×3 du référentiel $\mathcal{F}_c$ par rapport au référentiel $\mathcal{F}_d$

$\mathbf{Q}_c$: matrice d'orientation 3×3 du référentiel $\mathcal{F}_c$ par rapport au référentiel $\mathcal{F}_b$

$\mathbf{R}_{\boldsymbol{z}}(\theta)$: matrice de rotation 3×3 autour de l'axe $\boldsymbol{z}$ avec l'angle θ :

$$\mathbf{R_z}(\theta) = \begin{bmatrix} \cos(\theta) & -\sin(\theta) & 0 \\ \sin(\theta) & \cos(\theta) & 0 \\ 0 & 0 & 1 \end{bmatrix}$$

$\mathbf{R_{hz}}(\theta)$: matrice de transformation homogène de rotation 4×4 autour de l'axe $\boldsymbol{z}$ avec l'angle θ

$\mathbf{R_x}(\alpha)$: matrice de rotation 3×3 autour de l'axe $\boldsymbol{x}$ avec l'angle α :

$$\mathbf{R_x}(\alpha) = \begin{bmatrix} 1 & 0 & 0 \\ 0 & \cos(\alpha) & -\sin(\alpha) \\ 0 & \sin(\alpha) & \cos(\alpha) \end{bmatrix}$$

$\mathbf{R_{hx}}(\alpha)$: matrice de transformation homogène de rotation 4×4 autour de l'axe $\boldsymbol{x}$ avec l'angle α

$\mathbf{B_x}(a)$: matrice de transformation homogène de translation 4×4 le long de l'axe $\boldsymbol{x}$ avec une distance de a

$\mathbf{B_z}(d)$: matrice de transformation homogène de translation 4×4 le long de l'axe $\boldsymbol{z}$ avec une distance de d

$\mathbf{C}_i$: matrice de transformation homogène 4×4 du référentiel $\mathcal{F}_i$ par rapport au référentiel $\mathcal{F}_{i-1}$

$\mathbf{H}_i$: matrice de transformation homogène 4×4 du référentiel $\mathcal{F}_i$ par rapport au référentiel $\mathcal{F}_b$

${}^d\mathbf{H}_c$: matrice de transformation homogène 4×4 du référentiel $\mathcal{F}_c$ par rapport au référentiel $\mathcal{F}_d$

$\boldsymbol{e}_i$: $k^{ième}$ vecteur canonique qui est défini comme

$$\boldsymbol{e}_k \equiv \left[\underbrace{0 \ \cdots \ 0}_{k-1} \ 1 \ \underbrace{0 \ \cdots \ 0}_{n-k} \right]^T$$

dont la dimension est implicite et dépend du contexte

${}^{d}\mathbf{T}_{c}$:	opérateur tangentiel du référentiel $\mathcal{F}_c$ par rapport au référentiel $\mathcal{F}_d$ décrit dans le référentiel $\mathcal{F}_b$
${}^{f,d}\mathbf{T}_{c}$:	opérateur tangentiel du référentiel $\mathcal{F}_c$ par rapport au référentiel $\mathcal{F}_d$ décrit dans le référentiel $\mathcal{F}_f$
${}^{d}\boldsymbol{t}_{c}$:	torseur de vitesse du référentiel $\mathcal{F}_c$ par rapport au référentiel $\mathcal{F}_d$ décrit dans le référentiel $\mathcal{F}_b$
${}^{f,d}\boldsymbol{t}_{c}$:	torseur de vitesse du référentiel $\mathcal{F}_c$ par rapport au référentiel $\mathcal{F}_d$ décrit dans le référentiel $\mathcal{F}_f$

LISTE DES TABLEAUX

TAB. 2.1 L'intersection de deux sous-espaces de $\mathbb{R}^3$ 49
TAB. 2.2 Les sous-chaînes admissibles pour composer un MPT 51
TAB. 2.3 Les combinaisons des sous-chaînes pour un MPT 52
TAB. 6.1 Possible subchain topologies for TPMs 164

INTRODUCTION

0.1 Contexte

La majorité des manipulateurs sont actuellement des manipulateurs sériels (MSs). À cause de leur architecture sérielle ouverte, toutes les imperfections (jeux, flexions et frottements, par exemples) s'amplifient et additionnent leurs néfastes négatifs le long de la chaîne cinématique. Ces manipulateurs présentent donc des faiblesses au niveau de la rigidité, de la précision, et ont un rapport charge sur poids relativement faible. Ces manipulateurs s'avèrent alors peu adaptés à des tâches qui exigent une grande rigidité et une bonne précision.

Il existe des manipulateurs d'une autre architecture mécanique, nommés manipulateurs parallèles (MPs), qui sont caractérisés par des chaînes cinématiques fermées. Un MP met ses éléments en parallèle et son effecteur est simultanément supporté par plusieurs chaînes cinématiques. Les MPs présentent donc une plus grande rigidité et un meilleur rapport charge sur poids par rapport aux MSs.

Malgré le grand potentiel que présentent les MPs, leur utilisation industrielle reste encore marginale. Ceci s'explique d'une part, par la problématique commune à la synthèse de tous les manipulateurs spatiaux, et d'autre part, par la complexité des modèles cinématiques particulière aux MPs.

Ce travail est motivé par le besoin grandissant d'outils de synthèse topologique et géométrique des manipulateurs spatiaux et par le besoin de mettre en valeur des MPs.

0.2 Topologie et géométrie

Au niveau de la cinématique, un manipulateur est défini par sa topologie et sa géométrie. Par topologie nous désignons combien de solides dont un manipulateur est composé, comment ces solides sont reliés par quels types de couples cinématiques, et quels sont les caractéristiques de la disposition de ces couples cinématiques (parallélisme, perpendicularité, par exemple). Un manipulateur se distingue d'autres manipulateurs de la même topologie par sa géométrie. La géométrie est donc un ensemble de paramètres particuliers qui permettent de déterminer les positions et orientations relatives des couples cinématiques d'un manipulateur. La synthèse topologique et géométrique d'un manipulateur consiste ainsi à déterminer sa topologie et sa géométrie en fonction des tâches pour lesquelles il est envisagé.

0.3 Synthèse des manipulateurs spatiaux

Aujourd'hui, les principales méthodes de synthèse des manipulateurs spatiaux ne permettent pas, en toute généralité, de déterminer automatiquement la topologie et la géométrie d'un manipulateur en vue de satisfaire à une tâche donnée. La synthèse topologique est souvent réalisée en faisant appel à nos connaissances antérieures, à notre expérience, et à notre intuition, afin de déterminer le plus possible des topologies qui conviennent a priori aux contraintes de satisfaction des exigences cinématiques. Pour chacune de ces topologies, une synthèse géométrique est par la suite effectuée afin de comparer la performance de chaque design. Cette démarche est longue, ardue, et loin d'être optimale à cause des contraintes de temps qui deviennent de plus en plus primordiales. Il devient nécessaire d'utiliser des méthodes de synthèse plus systématiques qui permettent de définir à la fois la topologie et la géométrie.

0.4 Synthèse des MPs

La mise en parallèle de plusieurs chaînes cinématiques conduit à des avantages au niveau des performances cinématique, statique et dynamique, mais entraîne aussi des inconvénients qui se résument dans la liste suivante :

- espace de travail limité ;
- les modèles géométriques direct et inverse complexes ;
- découplage difficile des mouvements en translation et en rotation ;
- plus de singularités ;
- difficile d'obtenir une performance dans l'espace d'orientation qui est comparable à celle des MSs.

Afin de pallier ces inconvénients, une des principales méthodes que nous trouvons dans la littérature est de découpler le mouvement de 6 degrés de liberté (DDLs) en deux mouvements de 3 DDLs en mettant en série deux MPs à 3 DDLs. La synthèse des MPs à 3 DDLs est donc fondamentale et utile à la synthèse des MPs à 6 DDLs. L'importance de la synthèse des MPs à 3 DDLs se justifie aussi par le fait qu'un grand nombre d'applications n'exigent que 3 DDLs.

Les questions posées par la synthèse des MPs sont de plusieurs types. La première à laquelle nous sommes confrontés est de déterminer la topologie afin d'obtenir le DDL du manipulateur et le degré de mobilité (DDM) de l'effecteur désirés. Ceci est plus problématique pour les MPs que les MSs à cause des contraintes imposées par la mise en boucle des chaînes cinématiques. Observant les topologies connues des MPs à 3 DDLs, nous constatons que le DDL ne se calcule pas simplement par le nombre de couples cinématiques, ce qui est la cas pour les MSs. La deuxième question porte sur la nature de mobilité (NDM) de l'effecteur, c'est-à-dire le type de mouvement que peut réaliser l'effecteur qui se caractérise par le DDM en translation, le DDM en rotation, et le couplage entre le mouvement

en translation et le mouvement en rotation. Il s'agit de déterminer la topologie en fonction de la NDM, citons les manipulateurs sphériques, les manipulateurs en translation (MPTs). Une autre question importante est la représentation topologique. La problématique réside dans la représentation des caractéristiques de la disposition des couples cinématiques. Les représentations existantes ne permettent pas, soit de les représenter, soit de les discerner aisément d'autres informations.

À partir de ce constat, nous proposons d'étudier la synthèse topologique et géométrique des MPs à 3 DDLs, en particulier, des MPTs.

0.5 Objectifs

L'objectif de cette thèse est de combler les lacunes dans la synthèse des MPTs en proposant une approche de synthèse permettant de définir à la fois la topologie et la géométrie.

Pour commencer, le premier chapitre présente une étude bibliographique mettant en valeur les travaux réalisés dans le domaine de la cinématique des manipulateurs. L'objectif de cette étude consiste à identifier les problématiques, à positionner notre recherche, et à baser notre étude sur les réalisations les plus récentes.

Le deuxième chapitre présente une synthèse des travaux que nous avons réalisés dans le cadre de cette thèse par articles.

Le troisième chapitre aborde les concepts fondamentaux sur la topologie et la géométrie. Il est usuel de considérer que la topologie et la géométrie sont les concepts évidemment bien définis. Pourtant ce n'est pas le cas pour les MPs spatiaux. Effectuant une analyse des architectures connues des manipulateurs, nous identifions les caractéristiques de la disposition relative des couples cinématiques

qui sont essentiels pour déterminer le DDL, le DDM, et la NDM. Puis, nous proposons une définition des termes ***topologie*** et ***géométrie***, ce qui est essentiel pour la synthèse topologique et géométrique. Nous élaborons une méthode originale de représentation plus fidèle de la topologie d'un manipulateur.

Le quatrième et le cinquième chapitres détaillent une analyse de l'espace tangentiel de l'espace de déplacement afin de formuler la topologie et la géométrie en fonction des DDL et DDM. Nous introduisons le concept de configuration initiale et proposons une représentation numérique de topologie et géométrie permettant d'introduire la topologie en tant que nouvelle variable de synthèse. Nous abordons la synthèse topologique et géométrique en fonction de la NDM basée sur cette analyse et proposons une approche itérative de synthèse permettant de générer la topologie et la géométrie simultanément.

Le sixième chapitre porte sur le déplacement en orientation et vise à compléter notre approche de synthèse topologique dont une partie est proposée dans les quatrième et cinquième chapitres. L'objectif premier de ce chapitre est de déterminer quelles sont les topologies de chaîne cinématique sérielle permettant à l'effecteur les déplacements en translation avec une orientation constante. Le second objectif est de déduire les conditions pour l'effecteur de maintenir une orientation constante sous les contraintes imposées par la mise en parallèle des chaînes cinématiques sérielles.

Le septième chapitre présente la modélisation cinématique. Nous proposons des modèles cinématiques pouvant s'appliquer à plusieurs topologies. Nous détaillons la résolution des problèmes des modèles géométriques direct et inverse.

Enfin, nous présentons une conclusion générale sur l'ensemble de nos travaux entrepris dans le cadre de cette thèse suivie de recommandations.

CHAPITRE 1

REVUE CRITIQUE DE LA LITTÉRATURE

Les contraintes pesant sur la conception des manipulateurs ont beaucoup augmenté tant du point de vue de l'amélioration des performances cinématique, statique et dynamique que de celui de la réduction des temps consacrés à la synthèse topologique et géométrique. L'amélioration des performances est dictée par des tâches exigeant de plus en plus de rigidité, de précision, de vitesse, et de capacité d'accélération de la part des manipulateurs. La réduction des temps consacrés à la synthèse topologique et géométrique est dictée par des critères économiques. Ces contraintes ont conduit à de nombreuses évolutions dans le domaine de conception des manipulateurs.

La performance cinématique a été améliorée grâce à l'adoption des architectures parallèles et des techniques d'optimisation de la géométrie. Les temps consacrés à la synthèse géométrique ont été réduits grâce à l'usage de plus en plus courant de l'outil informatique et de l'extension de ses capacités de calcul. Par contre, la problématique d'intégrer la synthèse topologique à celle géométrique des manipulateurs spatiaux n'est pas encore abordée. Afin de mettre en valeur de différentes topologies et géométrie des MPs, il faut développer un environnement de synthèse topologique et géométrique de ces derniers

Comme nous l'avons mentionné dans l'introduction, ce travail porte sur la synthèse topologique et géométrique des MPTs. Afin de bien asseoir les bases de cette thèse, une étude bibliographique est nécessaire. Ce chapitre se divise principalement en sept parties. Dans la première, nous commençons par présenter la terminologie. La

seconde partie présente une brève historique des manipulateurs. Dans la troisième partie, nous comparons des différents aspects des MPs avec les MSs. La quatrième partie présente la représentation topologique. La cinquième partie détaille les principales méthodes de synthèse topologique. Dans la sixième partie, nous présentons la synthèse géométrique. Une conclusion est présentée à la fin.

1.1 La terminologie

Par définition, la robotique est hautement interdisciplinaire. Étant donné le nombre très important de chercheurs oeuvrant dans les domaines concernés, nous pouvons imaginer la quantité de publications réalisées depuis les dernières décennies. Chacun amenant les définitions, notations, et conventions de sa propre discipline, il est compréhensible qu'il règne une certaine confusion relative à la terminologie dans la vaste littérature. Afin de faciliter la compréhension de ce manuscrit, il est nécessaire de préciser les définitions et les conventions adoptées

Les définitions suivantes proviennent, sauf indication contraire, des travaux de (ANGELES, 2003).

Cinématique : l'étude des mouvements en fonction du temps, indépendamment des causes qui les produisent ;

Couple cinématique : un ensemble de conditions particulières auxquelles est assujetti un corps rigide par rapport à un autre, qui limite des mouvements de l'un par rapport à l'autre et qui détermine leur DDLs relatifs (DDLs de couple), également désigné «liaison cinématique» ;

Couple cinématique inférieur : un couple cinématique constitués de deux corps qui ont une surface, une ligne ou un point commun ;

Joint : réalisation physique d'un couple cinématique (IFToMM, 2003) ;

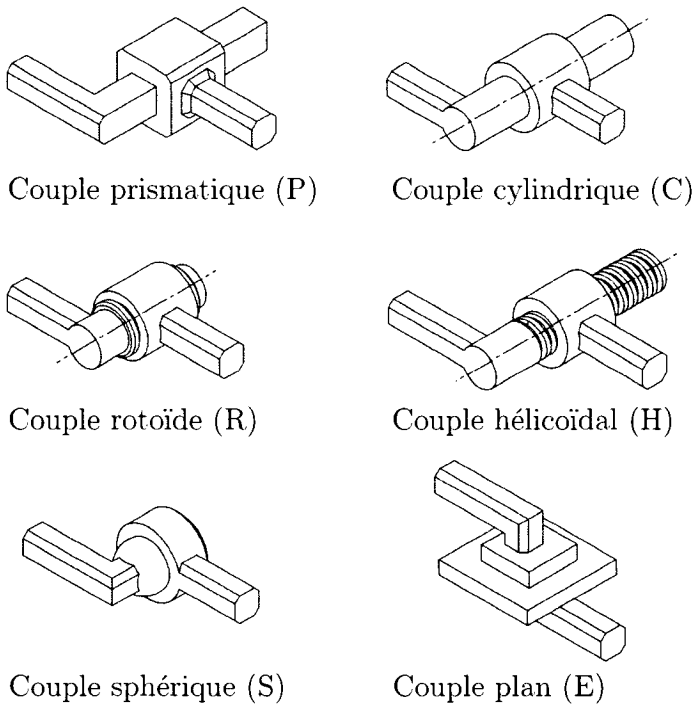

FIG. 1.1 Illustration des couples cinématiques inférieurs

Variables articulaires : les variables décrivant la position relative entre deux corps liés par un joint (PARALLEMIC, 2002).

Tel que montré à la Fig. 1.1, il n'existe que six couples cinématiques inférieurs soit : rotoïde (R), prismatique (P), cylindrique (C), sphérique (S), plan (E) et hélicoïdal (H).

Couple rotoïde : joint de type pivot réduisant le mouvement entre deux corps à une rotation autour d'un axe qui leur est commun. La situation relative entre les deux corps est donnée par l'angle autour de l'axe.
Symbole normalisé : R ;

Couple prismatique : joint de type glissière réduisant le mouvement relatif entre les deux corps à une translation le long d'un axe. La situation relative entre les deux corps est mesurée par une distance .

Symbole normalisé : P ;

Couple cylindrique : joint de type cylindrique réduisant le mouvement relatif entre les deux corps à une translation le long et une rotation autour d'un axe qui leur est commun. La situation relative entre les deux corps est mesurée par une distance et un angle autour de l'axe.
Symbole normalisé : C ;

Couple sphérique : joint de type sphérique réduisant le mouvement relatif entre les deux corps aux rotations autour d'un point qui leur est commun.
Symbole normalisé : S ;

Couple plan : joint de type plan réduisant le mouvement relatif entre les deux corps aux translations sur un plan et à la rotation autour de la normale de ce plan qui leur est commun.
Symbole normalisé : E ;

Couple hélicoïdal : joint de type hélicoïdal réduisant le mouvement relatif entre les deux corps à une rotation autour et une translation proportionnelle à la rotation le long d'un axe qui leur est commun. La situation relative entre les deux corps est mesurée par une distance ou un angle autour de l'axe.
Symbole normalisé : H ;

Degrés de mobilité d'un corps : le nombre de variables indépendantes pour déterminer les mouvements d'un corps ;

Pose d'un corps : la position et l'orientation de celui-ci ;

Degrés de liberté d'un couple : les mouvements relatifs permis par un couple ;

Ordre d'un joint : le nombre de corps liés par un joint moins un (voir Fig. 1.2) ;

Ordre d'un corps : le nombre de joints reliant un corps aux autres corps (voir Fig. 1.3) ;

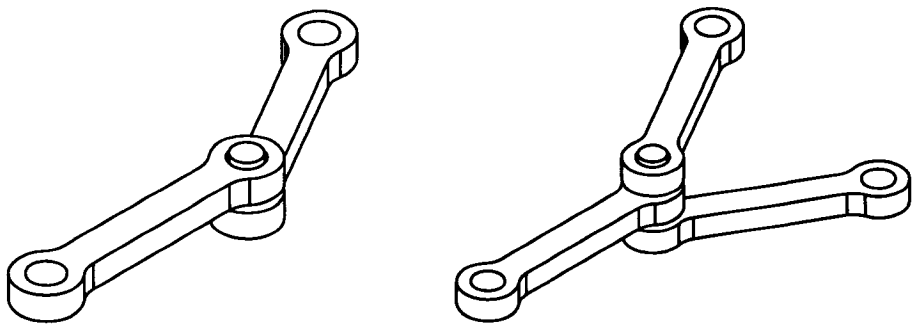

FIG. 1.2 Joints d'ordre un et deux

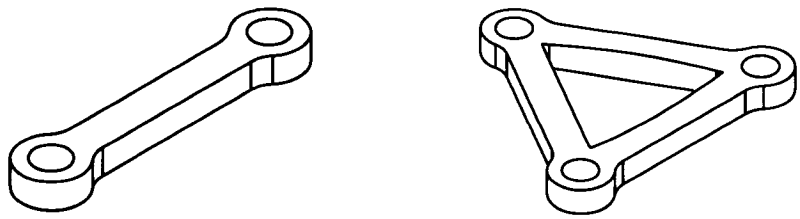

FIG. 1.3 Corps d'ordre deux et trois

Chaîne cinématique : un ensemble de corps appelés membrures en général rigides (solide) assemblés par des joints (voir Fig. 1.4) ;

Chaîne cinématique ouverte : une chaîne cinématique dont toutes les variables articulaires sont indépendantes ;

Chaîne cinématique sérielle : une chaîne cinématique ouverte dont les corps sont liés l'un après l'autre consécutivement. Le premier et le dernier corps ne sont liés qu'à un autre corps ;

Chaîne cinématique arborescente : une chaîne cinématique ouverte dont au moins un corps est lié à plus de deux corps ;

Chaîne cinématique fermée : il existe au moins une boucle dans la chaîne cinématique ;

Chaîne cinématique parallèle : il n'existe que deux corps qui sont liés à plus de deux corps ;

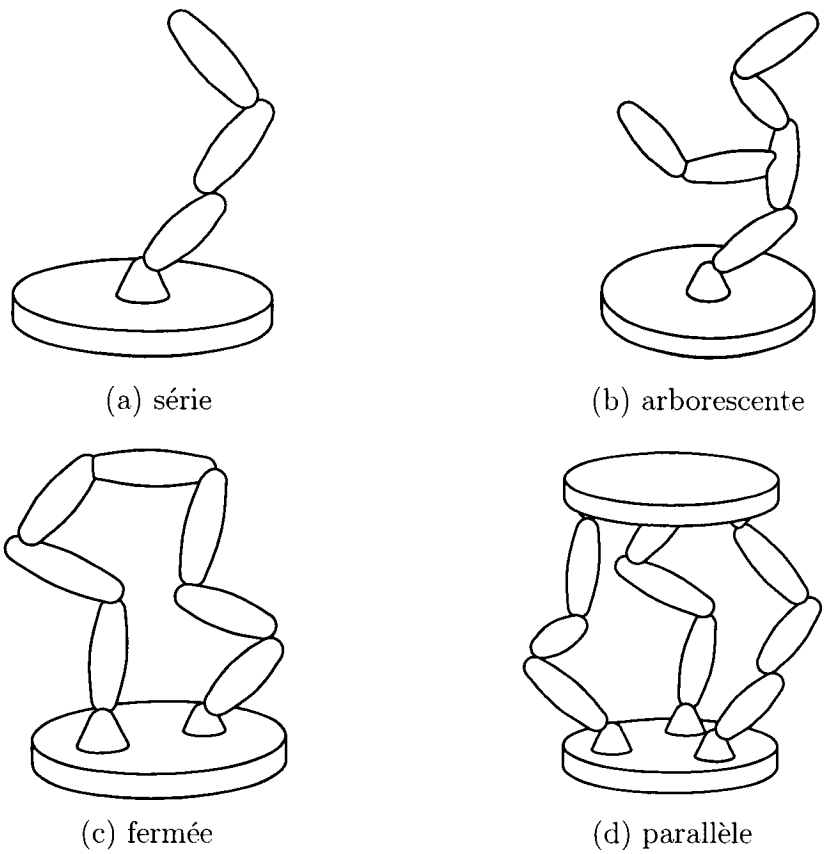

(a) série (b) arborescente

(c) fermée (d) parallèle

FIG. 1.4 Les chaînes cinématiques série, arborescente, fermée, et parallèle

Mécanisme : une chaîne cinématique dont un corps est désigné comme la base, certains autres comme des effecteurs, et certains joints commes joints actionnés (TSAI, 2001) (voir Fig. 1.5).

À propos des MPs, Jean-Pierre Merlet (MERLET, 1997) donne les définitions suivantes :

Un manipulateur parallèle généralisé est un mécanisme en chaîne cinématique fermée dont l'organe terminal (effecteur) est relié à la base par plusieurs chaînes cinématiques indépendantes ;

Un manipulateur parallèle est constitué d'un organe terminal à n DDLs et

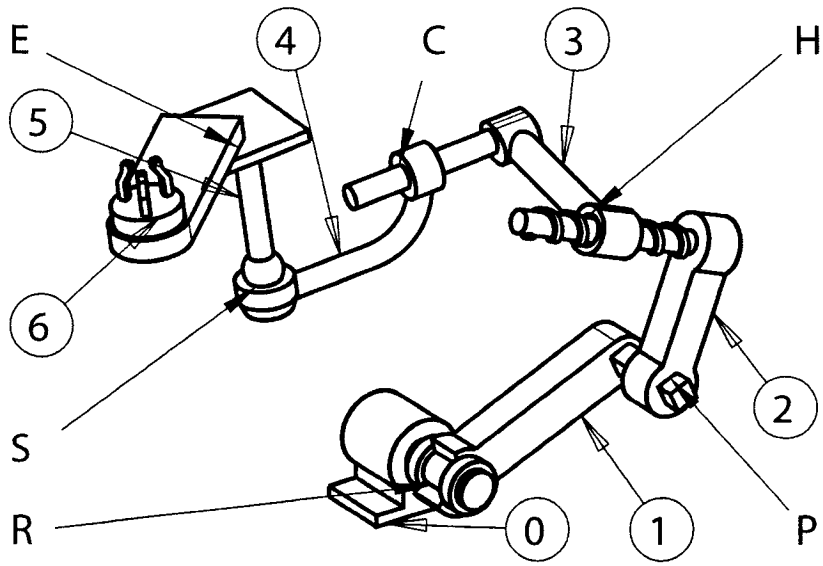

FIG. 1.5 Un mécanisme
Corps 0 : la base, corps 6 : l'effecteur, joint R : joint actionné

d'une base fixe, reliés entre eux par au moins deux chaînes cinématiques indépendantes, la motorisation s'effectuant par n actionneurs simples ;

Un manipulateur pleinement parallèle est un manipulateur parallèle dont le nombre de chaînes est strictement égal au nombre de DDLs de l'organe terminal ;

Un manipulateur sériel est un mécanisme en chaîne cinématique sérielle.

Dans l'étude des propriétés cinématiques des mécanismes, nous utilisons les termes «*topologie*» et «*géométrie*». Nous proposons les définitions suivantes :

La ***topologie*** *d'un mécanisme est une description qualitative des propriétés d'un mécanisme tel que :*

- *l'ordre de chaque corps ;*
- *l'ordre de chaque joint ;*
- *le type de chaque joint ;*

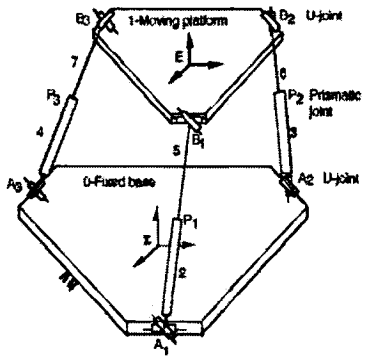

(a) 3-UPU (TSAI, 1996)

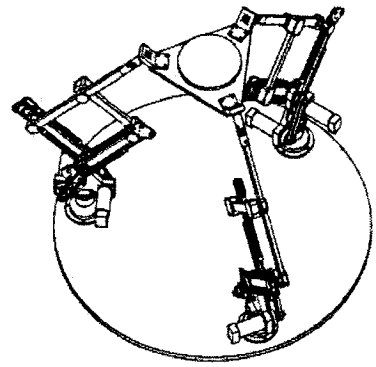

(b) un MP de l'Université Laval du Canada

FIG. 1.6 Deux mécanismes de différentes topologies

- *l'identification de la base, de l'effecteur et des joints actionnés ;*
- *un graphe décrivant les relations entre tous les joints et corps ;*
- *les contraintes géométriques tel qu'une perpendicularité, un parallélisme, etc.*

La ***géométrie*** *d'un mécanisme est une description quantitative. Ce sont les valeurs numériques déterminant les positions et orientations relatives des joints de chaque corps du mécanisme (distance, angle entre les axes des joints, par exemple).*

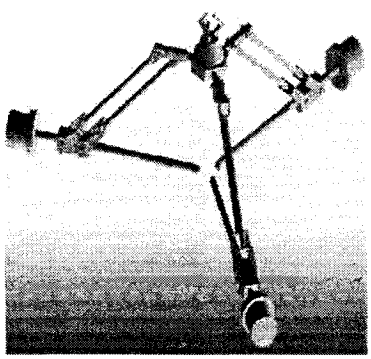

(a) Y-Star (HERVE ET SPARACINO, 1992)

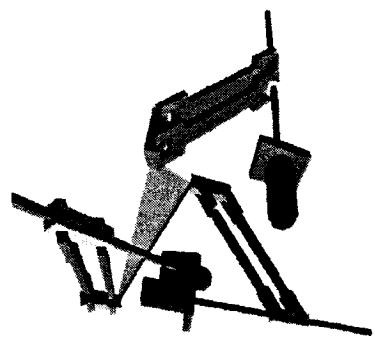

(b) une géométrie proposée par Baron (BARON, 2001)

FIG. 1.7 Deux mécanismes de même topologie mais de géométries différentes

La figure 1.6 montre deux mécanismes dont les topologies sont différentes tandis que la Fig. 1.7 montre deux mécanismes de même topologie mais de géométries

différentes.

1.2 Historique

Le premier schéma d'un manipulateur humanoïde fut l'oeuvre de Léonard de Vinci aux alentours de 1495 (WIKIPEDIA, 2006). Ce n'est qu'en 1961 que le premier manipulateur industriel a été réalisé : c'est un MS (ENGELBERGER, 1964). Au cours du dernier siècle, une architecture de manipulateur, fondamentalement différente, a aussi vu le jour : il s'agit d'un MP. En 1931, cette architecture a été brevetée aux États-unis (GWINNETT, 1931)(Fig. 1.8), mais nous ne savons pas s'il s'agit de la première conception d'un MP ni si un MP de cette architecture a jamais été construit (BONEV, 2003).

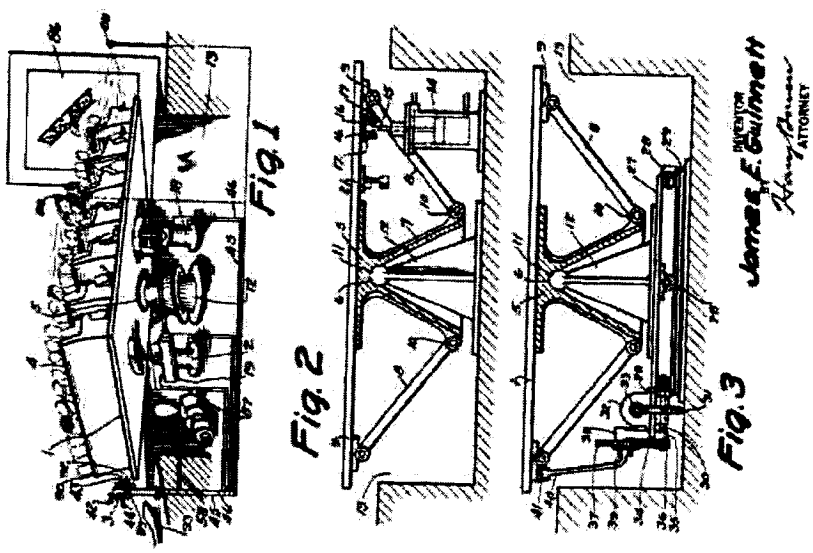

FIG. 1.8 MP breveté en 1931 (GWINNETT, 1931)

Une décennie plus tard, un nouveau MP a été inventé par Willard L.V. Pollard (POLLARD, 1940). Le MP de Pollard est bien connu comme la première réalisation

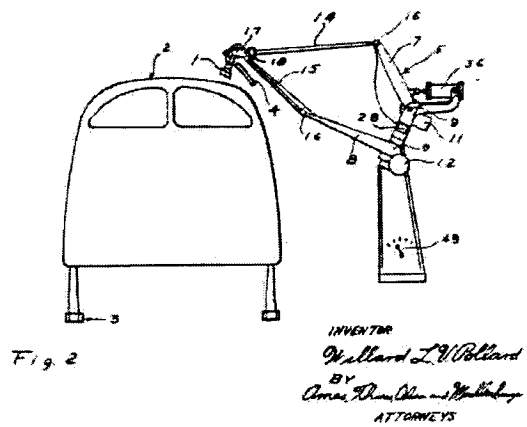

FIG. 1.9 Le premier MP (POLLARD, 1940)

de MP. Cette invention ingénieuse représente un MP de 5 DDLs composé de trois parties en séries (Fig. 1.9).

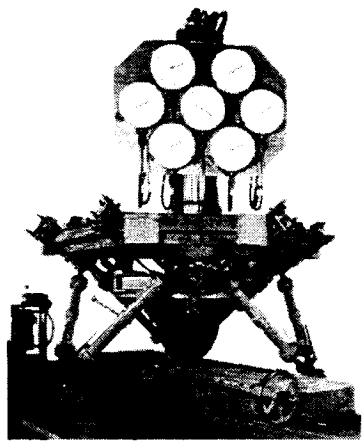

FIG. 1.10 Plateforme de Gough (GOUGH, 1956)

Seize ans après, de l'autre côté de l'Atlantique, un nouveau MP a vu le jour grâce à Gough V.E.(GOUGH, 1956). Ce MP sert de machine à tester les pneus (Fig. 1.10).

En 1965, le fameux article de Stewart D. a été publié (STEWART, 1965). Dans cet article, a été présenté une plateforme de mouvement à 6 DDLs pour l'usage de la simulation de vol (Fig. 1.11).

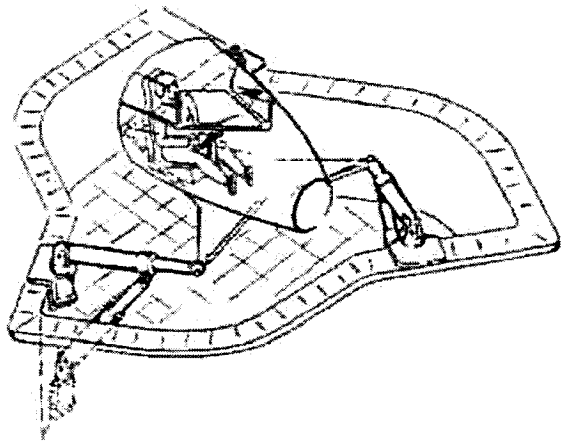

FIG. 1.11 Schéma de la plateforme de Stewart (STEWART, 1965)

En 1971, le bureau de brevet et de marque du commerce des États-unis a accordé un brevet à M. Klaus Cappel pour son invention et l'usage de cette invention comme simulateur de vol (BONEV, 2003). Le premier simulateur de vol a été aussi construit (Fig. 1.12).

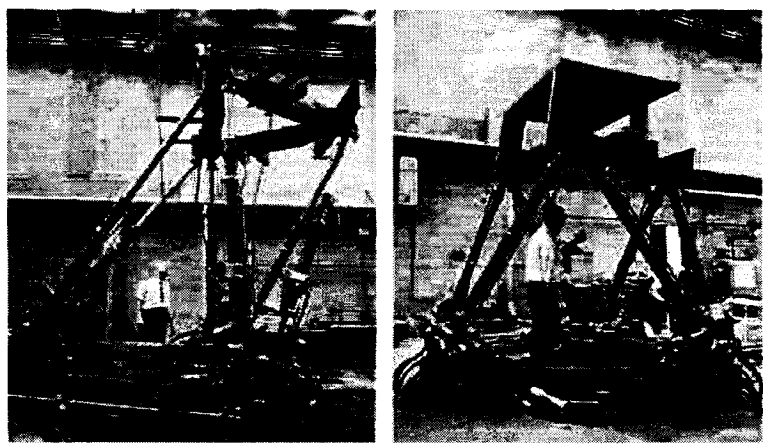

FIG. 1.12 Le premier simulateur de vol (Courtoisie de Klaus Cappel)

Ce n'est qu'en 1978 que Hunt a introduit le concept de MP et suggéré, dans son livre (HUNT, 1978), l'utilisation de ce type de structure en robotique. Depuis cette date, un grand nombre de chercheurs se sont intéressés aux MPs et les recherches systématiques ont été effectuées.

Il est à noter que dans de nombreuses applications, 6 DDLs ne sont pas exigés ; certains DDLs sont même non désirables pour des situations particulières (ANGELES, 2002). Les MPs ayant moins de 6 DDLs attirent alors de plus en plus l'attention des chercheurs, le MP de Delta (CLAVEL, 1988), le MP de Y-Star (HERVE ET SPARACINO, 1992), l'Oeil agile (GOSSELIN ET HAMEL, 1994), et l'appareil le ShaDe (BIRGLEN, 2002) sont juste quelques exemples que l'on pourrait qualifier de grand succès.

1.3 MP versus MS

Comme nous l'avons mentionné dans l'introduction, la synthèse des MPs et celle des MSs ont des problématiques communes. Afin de bien identifier la particularité de la synthèse des MPs et de tirer avantage des techniques développées dans la synthèse des MSs, nous effectuons une analyse des caractéristiques des MPs par rapport aux MSs.

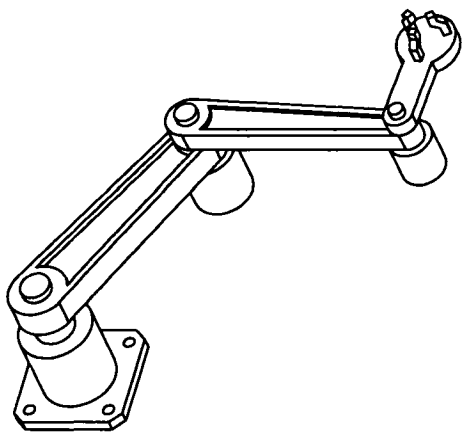

FIG. 1.13 Un MS

La Fig. 1.13 illustre un MS tandis que la Fig. 1.14 un MP.

Pour les MPs, l'effecteur est relié à la base par plusieurs chaînes cinématiques et

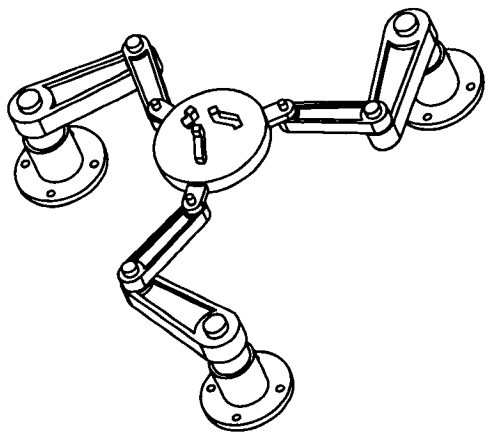

FIG. 1.14 Un MP

généralement, un seul joint de chacune de ces chaînes est actionné et mesuré, alors que les autres joints sont laissés libres. Contrairement à un MS traditionnel à chaîne cinématique ouverte, un MP est constitué de chaînes cinématiques fermées. Ainsi, au lieu de mettre en série les actionneurs (chaque actionneur doit porter les suivants) et les imperfections des axes (jeux, flexions, frottements, qui s'amplifient et additionnent leurs effets néfastes le long de la chaîne cinématique), le MP met ces éléments en parallèle, ce qui permet à la fois de rigidifier la structure mécanique, d'améliorer la précision et de diminuer la puissance des moteurs. Les joints près de la base sont préférablement choisis comme joints actionnés. Les actionneurs ne constituent donc pas une charge pour les autres actionneurs et il peut normalement être évité d'utiliser des transmissions mécaniques entre les joints actionnés et les actionneurs. Le poids d'un MP est ainsi généralement plus faible que celui d'un MS de rigidité équivalente. Il génère donc des accélérations élevées et aussi des temps de cycle plus faibles. Une autre conséquence non négligeable de la parallélisation des systèmes d'actionnement réside dans la symétrie inhérente à la structure mécanique qui induit une standardisation des actionneurs de chaque axe du manipulateur (CHAILLET ET PERRARD, 2001). Par ailleurs, l'adoption d'une topologie et d'une géométrie identiques pour chacune des chaînes cinématique rend

possible d'adopter la méthode de fabrication modulaire. En plus des tâches traditionnellement remplies par les MSs, les MPs s'avèrent aussi très prometteurs pour de nouvelles applications tels que les appareils Haptiques (BIRGLEN ET AL., 2002).

Puisque les MPs ont des caractéristiques complémentaires aux MSs, ils peuvent potentiellement répondre aux besoins auxquels les MSs ne peuvent satisfaire.

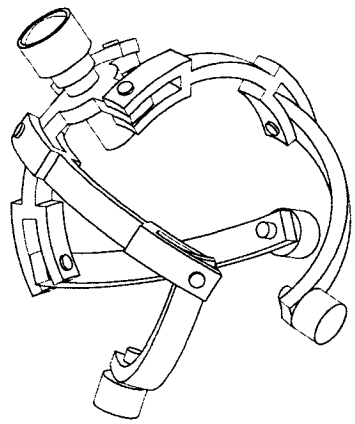

FIG. 1.15 3-RRR (GOSSELIN ET HAMEL, 1994)

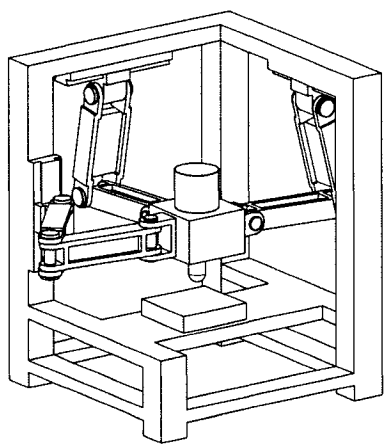

FIG. 1.16 3-PRRR (KIM ET TSAI, 2002)

Les avantages s'accompagnent aussi de nombreux inconvénients. Pour un MP, la mise en boucle de plusieurs chaînes cinématiques impose un nombre important de contraintes supplémentaires par rapport aux MSs, ce qui aboutit à un modèle

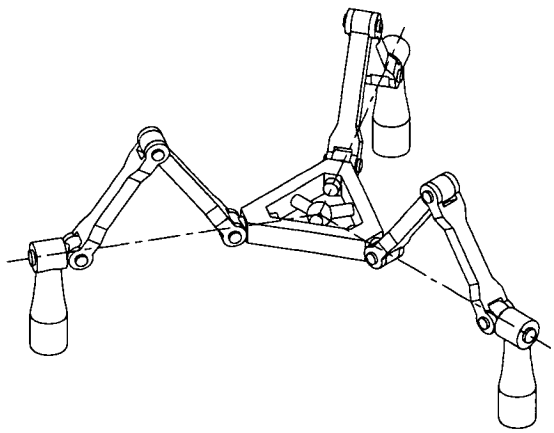

FIG. 1.17 3-RRRRR (ZLATANOV ET AL., 2002)

cinématique beaucoup plus complexe. Une chaîne cinématique d'une seule boucle constituée de 6 joints rotoïdes peut admettre 16 configurations différentes (RAGHAVAN ET ROTH, 1990) ; le modèle géométrique direct d'un MP sphérique à 3 DDLs se réduit à un polynôme de 8ième degré (GOSSELIN ET AL., 1994) ; le modèle géométrique direct de Stewart-Gough peut avoir jusqu' à 40 solutions réelles (DIETMAIER, 1998). Ce qui nous intéresse le plus est le lien entre la topologie et le DDL, le DDM, et la NDM. C'est une problématique principale que nous allons aborder. Ceci se justifie en observant les trois MPs montrés par Fig. 1.15, 1.16 et 1.17 qui sont tous à 3 DDLs et sont tous constitué des joints de 1 DDL. Par contre, les nombres de joints de chacun de ces MPs sont différents, soit 9, 12, et 15 respectivement. La nature de mobilité de l'effecteur mérite encore plus d'attention, car le premier produit les mouvements sphériques, le second génère les mouvements en translation, tandis que le troisième, dépendant de la configuration, peut être un MP sphérique ou un MP en translation (ZLATANOV ET AL., 2002).

1.4 Représentation topologique

Afin d'effectuer la synthèse topologique et géométrique, il est essentiel d'identifier tous les éléments déterminants de la topologie et de la décrire de façon systématique.

En général, la représentation topologique des manipulateurs spatiaux est un exercice difficile. Il en existe plusieurs types, chacune d'entre elles permet une représentation plus ou moins bonne, mais s'accompagne souvent d'une perte d'information ou de certaine confusion. Parmi celles-ci, nous pouvons citer la représentation topologique par : vue en perspective, schéma cinématique, dessin d'assemblage, et graphe d'agencement (COMPANY, 2000).

1.4.1 Vues perspectives

Dans ce type de représentation, les joints et les corps composant le mécanisme ne sont pas facilement visibles et identifiables. Nous pouvons voir l'aspect général du mécanisme et la disposition des joints et des corps , mais pas de manière précise. En plus, ce type de représentation nécessite souvent la numérotation, la nomenclature et des explications supplémentaires. La Fig. 1.18 est un exemple de ce type de représentation. Il est à noter que certains logiciels de simulation sont munis d'une fonction de visualisation tridimensionnelle de l'architecture des manipulateurs particuliers permettant de montrer la topologie et la géométrie (GOURDEAU, 1997).

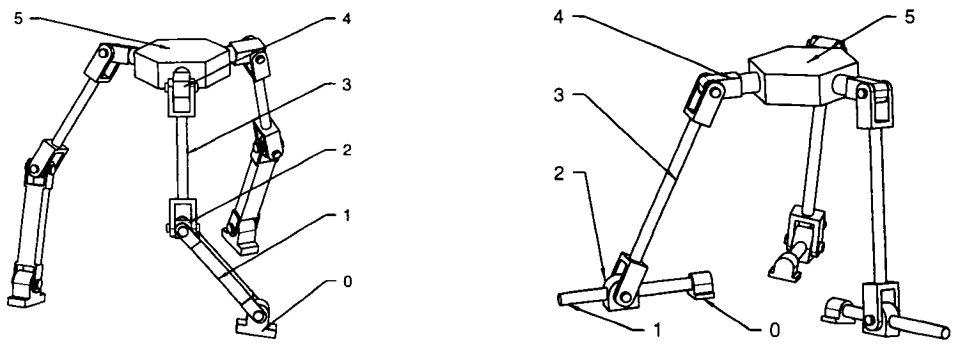

FIG. 1.18 Vues perspectives

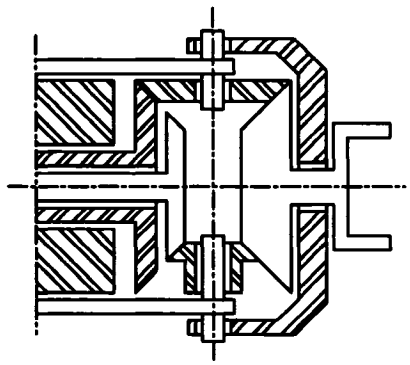

FIG. 1.19 Dessin d'assemblage

1.4.2 Dessin d'assemblage

Des dessins d'assemblage permettent de fournir toute l'information topologique et géométrique. Mais pour des mécanismes spatiaux complexes, nous avons besoin de plusieurs vues, vues de coupe ou vues de section, les inconvénients deviennent évidents. La Fig. 1.19 montre un exemple de ce type de représentation.

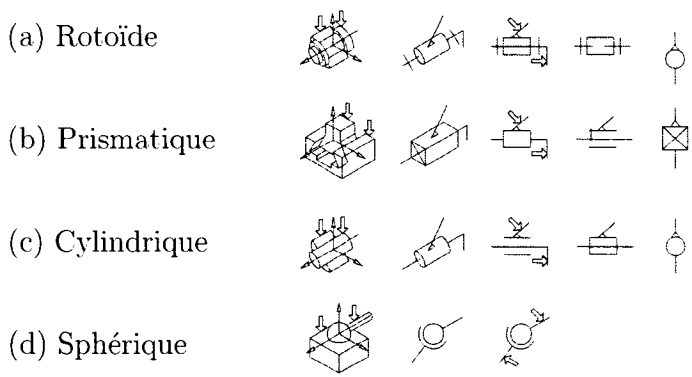

FIG. 1.20 Symboles des joints cinématiques (ISO, 1981)

1.4.3 Schéma cinématique

Il existe plusieurs conventions sur la représentation schématique de mécanismes. Il s'agit de la norme (ISO, 1981) résumée à la Fig. 1.20. Ce type de schémas, très pratiques pour représenter l'agencement des différents joints et corps composant un mécanisme, possèdent à la fois la simplicité et la lisibilité pour les mécanismes plans et les mécanismes spatiaux simples, mais manifestent de l'inadéquation pour les mécanismes spatiaux complexes.

1.4.4 Représentation par graphes, matrices, schémas structurel et fonctionnel

Du point de vue cinématique, un mécanisme contient un ensemble de corps et un ensemble de joints. Ces ensembles de corps et joints peuvent être représentés sous une forme abstraite appelée *graphe*. Dans une representation par graphe, les sommets représentent les corps alors que les lignes les joints du mécanisme. Pour distinguer les différents types de joints et corps, les lignes et sommets sont notés

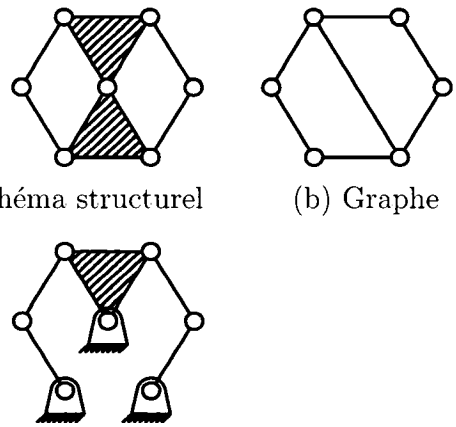

(a) Schéma structurel (b) Graphe

(c) Schéma fonctionnel

FIG. 1.21 Représentation par schéma structurel, graphe, et schéma fonctionnel

ou colorés (Fig. 1.21 b). Puisque les graphes sont propices à la représentation numérique, les mécanismes peuvent donc être représentés sous la forme de matrice.

Dans une représentation structurelle, chaque corps est représenté par un polygone dont les sommets représentent les joints. Spécifiquement, un corps binaire est représenté par une ligne avec deux sommets, un corps ternaire un triangle hachuré avec trois sommets, et un corps quaternaire un quadrilatère hachuré avec quatre sommets, *etc.* Pour distinguer les différents types de joints et corps, les polygones et sommets sont notés ou colorés (Fig. 1.21 a). Nous pouvons remarquer qu'une représentation fonctionnelle fournit un peu plus de détails qu'une représentation structurelle (Fig. 1.21 c).

1.4.5 Graphe d'agencement

Proposée par (PIERROT, 1991), la convention de représentation (voir Fig. 1.22) donne plus de facilité à la représentation topologique sur papier. Les symboles sont

Nom de joint	Représentation	
	Joint passif	Joint actionné
Rotoïde	R	R
Prismatique	P	P

FIG. 1.22 les symboles des graphes d'agencement (PIERROT, 1991)

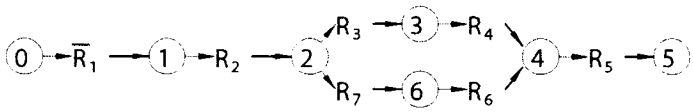

FIG. 1.23 les symboles des graphes d'agencement (BARON, 1997)

d'une forme géométrique simple et uniformisée, un rectangle simplement avec une lettre significative. On peut aisément dessiner une topologie sur papier. Fig. 1.23 montre une représentation similaire (BARON, 1997).

1.4.6 Représentation alpha-numérique

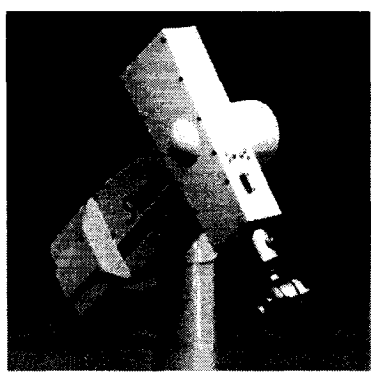

FIG. 1.24 Puma200

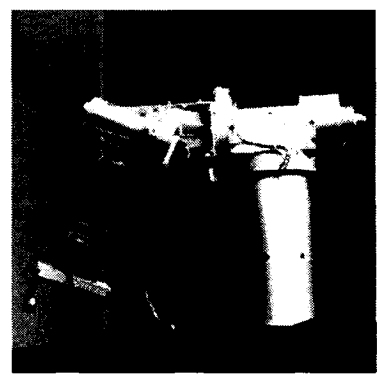

FIG. 1.25 Stanford

La méthode de représentation alpha-numérique est très répandue en robotique. La topologie d'un mécanisme est représentée par une série de symboles normalisés

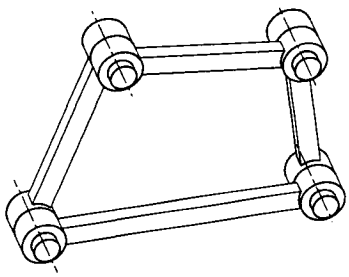

FIG. 1.26 4-Barres plan

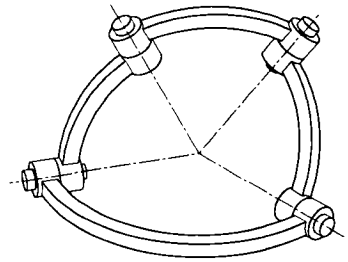

FIG. 1.27 4-Barres sphériques

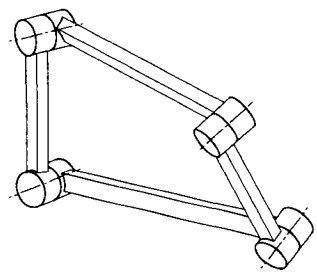

FIG. 1.28 Mécanisme de bennett

des couples cinématiques. Par exemple, la topologie du manipulateur Puma200 (Fig. 1.24) est représentée par RRRRRR, celle du manipulateur Stanford (Fig. 1.25) par RRPRRR. Néanmoins, cette méthode représente très peu les propriétés cinématiques tel que le DDL, le DDM, et la NDM. Il est évident que les trois mécansimes montrés dans les Fig. 1.26, 1.27 et 1.28 ont une même représentation topologique alpha-numérique, mais leurs propriétés sont fort différentes. Cette méthode est donc souvent accompagnée par des paramètres de Denavit-Hartenberg (DENAVIT ET HARTENBERG, 1954) pour décrire un mécanisme.

Une exploration de la littérature ne nous a pas permis de trouver de représentations symboliques de mécanismes qui permettent de représenter aisément les dispositions spéciales et indispensable pour le fonctionnement des mécanismes. Ces dispositions spéciales peuvent être un parallélisme, une perpendicularité ou bien d'autres.

1.5 Synthèse topologique

1.5.1 Approche basée sur la théorie de graphe

Un apport théorique de la synthèse de mécanismes provient des travaux de (DOBRJANSKYJ ET FREUDENSTEIN, 1967). Il s'agit d'une approche basée sur la théorie de graphe, une représentation abstraite de la structure cinématique, ce qui ressemble un peu à la représentation symbolique de la structure des composés chimiques. L'information essentielle d'une structure cinématique est l'agencement des corps et des joints et celle-ci peut être représentée par un graphe (FREUDENSTEIN ET WOO, 1974). L'avantage évident de cette méthode est que les graphes peuvent être énumérés systématiquement en effectuant l'analyse combinatoire (FREUDENSTEIN ET MAKI, 1979). Quand nous mettons en place des algorithmes d'ordinateur en exprimant les graphes sous la forme de matrice, il est possible d'automatiser le processus de synthèse.

Cette approche a permis à de nombreux autres auteurs de réaliser la synthèse des mécanismes plans. Cependant, dans le cas des mécanismes parallèles spatiaux, elle n'a pas encore été adaptée afin de prendre en compte les positions et orientations particulières entre les joints qui sont susceptible d'influencer la nature de mouvements générés.

1.5.2 Théorie des groupes de Lie et synthèse topologique

1.5.2.1 Théorie des groupes de Lie

La théorie des groupes est l'un des outils les plus puissants de la physique mathématique. Un **groupe** G est un ensemble sur lequel une loi de composition (produit ou

multiplication) $\varphi : G \times G \to G$ a été définie, tel que

1. L'ensemble est fermé par cette loi : si $a \in G$ et $b \in G$, alors $\varphi(a, b) \in G$. Cette condition est souvent appelée la **règle de groupe**.
2. La loi est associative : $\varphi[\varphi(a, b), c] = \varphi[a, \varphi(b, c)]$.
3. Il existe un élément neutre e, tel que $\varphi(e, a) = \varphi(a, e) = a$, pour tout élément $a \in G$.
4. Tout élément $a \in G$ possède un inverse unique a^{-1} dans G tel que $\varphi(a^{-1}, a) = e$.

Un sous-ensemble H de G est appelée **sous-groupe** de G s'il est lui-même un groupe, avec la même loi de multiplication que G.

Un **groupe de Lie** est une variété différentielle réelle ou complexe munie d'une structure de groupe, les opérations sur ce groupe devant également être différentiables. La dimension d'un groupe de Lie est la dimension de la variété qui lui est associée (LEDERMANN, 1973).

Un **groupe de Lie matriciel** est un groupe de Lie dont tout élément est une matrice carrée inversible, la règle de groupe étant la multiplication matricielle.

Une **algèbre de Lie** $\mathcal{G}$ est un espace vectoriel sur lequel a été défini un produit(appelée crochet de Lie) $[\ ,\ ] : \mathcal{G} \times \mathcal{G} \to \mathcal{G}$, tel que $\forall x, y, z \in \mathcal{G}$ and $\alpha \in \mathbb{R}$

1. $[x + y, z] = [x, z] + [y, z]$
2. $[z, x + y] = [z, x] + [z, y]$
3. $[\alpha x, y] = [x, \alpha y] = \alpha[x, y]$
4. $[x, y] = -[y, x]$
5. $[x, [y, z]] + [y, [z, x]] + [z, [x, y]] = 0$

Il est possible d'associer à tout groupe de Lie G une algèbre de Lie $\mathcal{G}$ dont l'espace vectoriel est l'espace tangentiel de G ; G s'obtient par exponentiation des éléments

de $\mathcal{G}$; la dimension de G est la dimension de l'espace vectoriel de $\mathcal{G}$ (McCarthy, 1990).

Le fait que le groupe de Lie et l'algèbre de Lie correspondent parfaitement à l'ensemble des déplacements des corps rigides est une clef voûte de l'analyse et de la synthèse des mécanismes (Herve, 1978).

Nous rappelons, dans un premier temps, la représentation de l'ensemble des déplacements d'un solide par un groupe de Lie. Nous vérifions d'abord si les déplacements d'un solide satisfont à tous les quatre axiomes des groupes de Lie. D'après (Herve, 1999), deux déplacements de suite de pose d'un solide engendrent un nouveau déplacement qui est le produit de composition de ces deux déplacements, l'ensemble des déplacements est donc fermé par la loi de composition (multiplication de deux matrices de transformations homogènes). Étant donnés trois déplacements consécutifs, effectuer les deux premiers et ensuite le dernier amène le solide à la même pose qu'effectuer le premier et ensuite les deux derniers, la loi de composition est donc associative ; il est évident que l'absence de déplacement est un déplacement neutre équivalent à la matrice identité de transformation homogène ; tout déplacement a un inverse unique qui déplace le solide à sa pose précédente. L'ensemble des déplacements des solides est ainsi un groupe, plus précisément un groupe de Lie. Si $\mathbf{H}(t)$ est la matrice de transformation homogène représentant la pose d'un solide, qui est en fonction du temps, alors nous avons le groupe spécial matriciel Euclidien :

$$SE(3) \equiv \{\mathbf{H}(t) | t \in \mathbb{R}+\} \tag{1.1}$$

avec le produit matriciel comme règle de groupe.

Par la suite, nous nous intéressons à l'algèbre de Lie associée au groupe de Lie de déplacements d'un solide. L'opérateur tangentiel $\mathbf{T}(t)$ (McCarthy, 1990) est

défini comme

$$\mathbf{T}(t) = \dot{\mathbf{H}}(t)\mathbf{H}(t)^{-1} \tag{1.2}$$

où le point désigne la dérivée par rapport au temps. Puisque

$$\mathbf{H}(t)\mathbf{H}(t)^{-1} = \mathbf{1} \tag{1.3}$$

où $\mathbf{1}$ est une matrice identité, nous avons

$$\dot{\mathbf{H}}(t)\mathbf{H}(t)^{-1} + \mathbf{H}(t)\dot{\mathbf{H}}(t)^{-1} = \mathbf{0} \tag{1.4}$$

Si une opération ψ est définie, tel que

$$\psi(\mathbf{T}(t_1), \mathbf{T}(t_2)) = \mathbf{T}(t_1)\mathbf{T}(t_2) - \mathbf{T}(t_2)\mathbf{T}(t_1), \tag{1.5}$$

les équations (1.2)$\sim$(1.5) nous permettent de prouver que ψ est un crochet de Lie (HERVE, 1978). Nous avons donc l'algèbre de Lie associée à $SE(3)$

$$\mathcal{SE}(3) \equiv \{\mathbf{T}(t) | t \in \mathbb{R}\} \tag{1.6}$$

dont le crochet de Lie est défini comme

$$[\mathbf{T}(t_1), \mathbf{T}(t_2)] = \mathbf{T}(t_1)\mathbf{T}(t_2) - \mathbf{T}(t_2)\mathbf{T}(t_1) \tag{1.7}$$

Tous les théorèmes mathématiques des groupes peuvent ainsi être employés pour l'analyse et la synthèse des manipulateurs. Le point important pour nos travaux dans le cadre de cette thèse est que la propriété des déplacements de l'effecteur des MPs peut être analysée dans l'espace tangentiel de l'espace de déplacements.

1.5.2.2 Synthèse topologique basée sur la théorie des groupes de Lie

La synthèse de mécanismes basée sur la théorie des groupes de Lie a été formalisée de façon systématique grâce aux travaux de (HERVE, 1999). Cette approche de synthèse et des exemples de son application sont présentés dans les paragraphes qui suivent.

Les déplacements relatifs d'un solide par rapport à un autre relié par un joint est un sous-groupe de Lie. La mise en série de deux joints entre trois solides permet un ensemble de déplacements relatifs entres les deux solides à chacune des deux extrémités de la chaîne cinématique. Cet ensemble est représenté par l'ensemble des produits de composition des éléments des deux sous-groupes de Lie qui représentent respectivement les déplacements relatifs permis par les deux joints. En mettant en série des joints, nous pouvons donc construire des générateurs des sous-groupes de Lie des déplacements. Par exemple, un générateur du sous-groupe de Lie des translations spatiales peut être réalisé en mettant en série trois joints prismatiques. Cependant, l'indépendance des trois sous-groupes de Lie des trois joints reste à vérifier. Ceci est le principe de la synthèse des MSs basée sur la théorie des groupes de Lie.

Si deux chaînes cinématiques sérielles sont mises en parallèle, l'ensemble des déplacements du solide partagé par ces deux chaînes est représenté par l'intersection de deux sous-ensembles des déplacements associés respectivement aux chaînes cinématiques sérielles. La synthèse des MPs est donc transformée en la synthèse des MSs dont les sous-groupes de Lie de déplacements doivent avoir une intersection qui convient au sous-ensemble des déplacements demandés. Un grand succès d'application de cette approche a été la synthèse du MP de Y-Star (HERVE, 1991). C'est un MP composé de trois chaînes cinématiques identiques n'ayant que des déplacements en translation (Fig 1.29). Quelques autres topologies ont été réalisées, toujours par

les mêmes chercheurs.

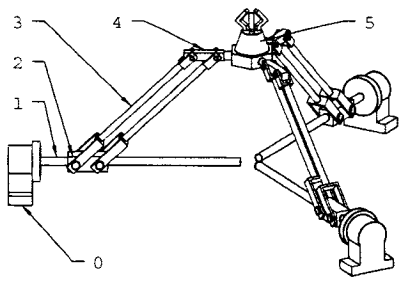

FIG. 1.29 MP de Y-Star

Bien que la synthèse topologique soit élégamment formalisée, la résolution du problème demeure toutefois fort difficile pour les MPs, car réaliser une synthèse de plusieurs chaînes cinématiques sérielles en fonction de l'intersection de leurs sous-ensembles des déplacements est tout un défi comparable à celui engendré par la problématique originale.

1.5.3 Synthèse basée sur la théorie des visseurs

L'opérateur tangentiel défini dans l'équation (1.2) a la forme suivante :

$$\mathbf{T} = \begin{bmatrix} 0 & -\omega_z & \omega_y & v_x \\ \omega_z & 0 & -\omega_x & v_y \\ -\omega_y & \omega_x & 0 & v_z \\ 0 & 0 & 0 & 1 \end{bmatrix} \tag{1.8}$$

Si

$$\boldsymbol{\omega} \equiv \begin{bmatrix} \omega_x \\ \omega_y \\ \omega_z \end{bmatrix}, \qquad \boldsymbol{v} \equiv \begin{bmatrix} v_x \\ v_y \\ v_z \end{bmatrix} \tag{1.9}$$

alors, les éléments de l'opérateur tangentiel peuvent être assemblés dans une matrice colonne, tel que

$$\boldsymbol{t} \equiv \begin{bmatrix} \boldsymbol{\omega} \\ \boldsymbol{v} \end{bmatrix} \tag{1.10}$$

Dans l'étude cinématique, cette matrice colonne est appelé **torseur de vitesse** (STRAMIGIOLI ET BRUYNINCKX, 2001). De façon similaire, un **torseur de force** est défini comme

$$\boldsymbol{w} \equiv \begin{bmatrix} \boldsymbol{m} \\ \boldsymbol{f} \end{bmatrix} \tag{1.11}$$

Les torseurs de vitesse et les torseurs de forces sont généralisés en leur donnant le nom **visseur**. Symbole : **$**. Un ***n*-système de visseurs** est toutes les combinaisons linéaires de n visseurs indépendants.

Dans l'étude des visseurs, un concept important est la notion **réciprocité**. Le **produit réciproque** est défini comme

$$\mathbf{\$}_1 \circ \mathbf{\$}_2 \equiv \mathbf{\$}_1^T \mathbf{\Gamma} \mathbf{\$}_2 \tag{1.12}$$

où

$$\mathbf{\Gamma} \equiv \begin{bmatrix} \mathbf{O} & \mathbf{1} \\ \mathbf{1} & \mathbf{O} \end{bmatrix} \tag{1.13}$$

et $\mathbf{O}$ est une matrice zéro 3×3 tandis que $\mathbf{1}$ est la matrice identité 3×3.

Deux visseurs sont réciproques si leur produit réciproque est égal à 0. Deux systèmes de visseurs sont réciproques si chaque visseur d'un système est réciproque à tous les visseurs de l'autre système (STRAMIGIOLI ET AL., 2002).

La théorie des visseurs a été employée à la synthèse des MPs, en particulier des MPs ayant moins de 6 DDLs.

Parmi les premiers travaux visant à utiliser la théorie des visseurs aux MPs, nous pouvons citer ceux de (AGRAWAL, 1991). La cinématique instantanée de chaque chaîne cinématique sérielle (sous-chaîne) a été modélisée comme un système de visseurs, appelé le système de torseurs de vitesse instantanée. Les contraintes exercées sur l'effecteur par chaque souschaîne ont été représentées par un autre système de visseurs, appelé le système de torseurs de force instantanée. Les deux systèmes de visseurs sont réciproques.

Dans les travaux de (LEGUAY-DURAND ET REBOULET, 1997), une revue systématique de la théorie des visseurs dans le contexte de la conception des MPs a été présentée. Les auteurs ont précisé une méthodologie de synthèse des MPs basée sur cette théorie. La chaîne cinématique parallèle est décomposée en souschaînes sérielles qui partagent le même effecteur et la même base. Ensuite, chacune de ces souschaînes est représentée par un système de torseurs de vitesse et un système de torseurs de force qui doivent être réciproques. La mobilité de l'effecteur de la chaîne parallèle est déterminée par l'intersection des systèmes de torseurs de vitesse. Les DDMs contraints sont déterminés par l'union des systèmes de torseurs de force.

Pour obtenir les DDMs, les conditions nécessaires sont les suivantes : 1) chacune des souschaînes possède au moins les mêmes DDMs requis pour l'effecteur ; 2) l'union des systèmes de torseurs de force équivaut aux DDMs qui doivent être éliminés.

Étant donné les DDMs, la synthèse topologique se réduit à déterminer les systèmes de torseurs de force, puis les systèmes de torseurs de vitesse, la topologie proprement dite, pouvant être générés par la définition de réciprocité.

Quelques années plus tard, des travaux similaires ont été présentés dans la littérature (FRISOLI ET AL., 2000). Cette méthodologie a permis de trouver de nouvelles topologies des MPs (KONG ET GOSSELIN, 2001).

Les topologies issues de cette méthodologie peuvent garantir la mobilité requise pour les déplacements infinitésimaux mais pas pour les déplacements à travers un espace de travail parce que les systèmes de torseurs de vitesse changent avec la configuration.

1.6 Synthèse géométrique des MPs

En effet, la synthèse géométrique des MPs est un problème d'optimisation : étant donnée la topologie d'un MP, trouver la géométrie de celui-ci de sorte d'optimiser ses performances. Parmi les divers problèmes (configurations singulières, dextérité, espace de travail,*etc.*), celui du modèle géométrique en est un essentiel afin de mettre en place une solution d'optimisation.

L'étude du modèle géométrique comporte quatres parties principales

- Modélisation cinématique : trouver la représentation mathématique du lien entre les variables articulaires et la pose de l'effecteur, établir le modèle géométrique proprement dit ;
- Problème du modèle géométrique direct (MGD) : trouver la pose de l'effecteur à partir des variables articulaires ;
- Problème du modèle géométrique inverse (MGI) : trouver les variables articulaires à partir de la pose de l'effecteur ;
- Matrice Jacobienne : trouver les matrices qui associent la vitesse de l'effecteur aux vitesses articulaires en définissant une relation linéaire entre ces derniers.

1.6.1 Modélisation cinématique

Les travaux théoriques liés à la modélisation cinématique des mécanismes spatiaux remontent aux années 50.

La propriété cinématique (position, orientation, vitesse, et accélération) d'un solide est identique à celle d'un référentiel qui lui est attaché. Un solide peut donc être représenté par des géométries primitives (point, line, et plan) et des vecteurs.

La notation la plus répandue pour les MSs est celle de (DENAVIT ET HARTENBERG, 1954). Elle permet une modélisation en effectuant un paramétrage minimum des chaînes cinématiques ouvertes simples constituées de joints rotoïdes et prismatiques de façon systématique. Afin de faciliter la formulation dynamique, une variante de cette notation, appelée Denavit-Hartenberg modifié (CRAIG, 1986) est largement adoptée dans la littérature. Il est à noter que la singularité des paramètres se produit dans certaines situations, deux axes s'approchent d'une configuration parallèle par exemples. Dans ce cas-ci, les paramètres sont fort sensibles à la disposition des joints, un petit changement de l'orientation relative entre deux joints peut introduire une très grande variation de certains paramètres. Pour pallier ce défaut, les auteurs de (HAYATI ET MIRMIRANI, 1985) ont proposé une modélisation basée sur la notation de Denavit-Hartenberg en introduisant un cinquième paramètre. Pourtant, ce cinquième paramètre s'accompagne de nouveaux problèmes de singularité. Une modélisation beaucoup plus élaborée a été proposée par (ZHUANG ET AL., 1992) en vue d'éviter toute singularité de paramètre et a visé principalement l'étalonnage robotique. Cette modélisation s'avère plutôt encombrant pour la synthèse géométrique.

Le paramétrage de Denavit-Hartenberg modifié par (KHALIL ET KLEINFINGER, 1986) est un exemple adapté à la modélisation des chaînes cinématiques non sérielles

qu'ils soient arborescentes ou fermées. Ce paramétrage est systématique et adapté à une génération automatique de la géométrie.

La plupart des modélisations cinématiques réalisées dans l'étude des MPs sont les modélisations personnalisées dans le but de réduire le nombre de paramètres et de simplifier le modèle géométrique (BARON ET AL., 2002). Ceci est du aux particularités très présentes des topologies des MPs étudiés. Pour réduire la complexité du modèle géométrique, le parallélisme, l'intersection, et la perpendicularité sont souvent adoptés dans la disposition des joints. Un modèle géométrique ainsi établi de façon personnalisée n'est pas adapté à un MP d'une topologie différente. En outre, lors de la définition du référentiel d'un solide, le point d'origine de celui-ci est toujours localisé sur l'axe d'un joint, d'une part, le problème d'instabilité numérique peut se produire si des joints se trouvent très éloignés par rapport au référentiel global, ce qui est inévitable durant une synthèse géométrique automatisée ; d'autre part, un joint prismatique n'a pas d'axe, la définition du référentiel devient problématique, car de différentes définitions conduisent à de différents modèles géométriques et induisent aussi de l'instabilité numérique potentielle.

Toutes ces modélisations cinématiques s'effectuent sur une topologie donnée et très peu de travail a été réalisé en prenant la topologie comme une variable de synthèse.

Dans sa thèse, Ramstein a fait des démarches dans le but d'introduire la topologie comme variable de synthèse (RAMSTEIN, 1999). Mais seules des topologies de MSs sont abordées de manière significative. Son algorithme d'optimisation choisit très rapidement une seule topologie de MS et ne se concentre ensuite que sur la synthèse géométrique. Ceci peut s'expliquer par le fait que la topologie est représentée par des variables non continues, la nature d'un joint ne peut être que zéro ou un, ce qui fait en sorte que la nature d'un joint ne peut évoluer de façon continue, chaque croisement de l'algorithme génétique conduit à un changement dramatique

de topologie.

1.6.2 Résolution des problèmes des modèles géométriques

Dans la littérature, on estime que le MGI des MPs est beaucoup plus simple que le MGI des MSs et on compare toujours le niveau de difficulté du MGD des MPs à celui du MGI des MSs. Nous remarquons que ce n'est pas le cas. À l'origine de cette fausse impression est la hyperparticularité de la chaîne cinématique des MPs étudiés. Si chaque chaîne cinématique reliant l'effecteur à la base d'un MP à 6 DDLs a une topologie générale, son MGI est aussi difficile que le MGI des MSs à 6 DDLs et le niveau de difficulté de son MGD est tel qu'il n'est pas comparable à celui du MGI des MSs, car il peut admettre plusieurs millions de solutions (GOSSELIN, 1988). Depuis des années, on ne cesse d'employer de nouvelles techniques de solutions, citons les travaux de (BOUDREAU ET AL., 1998), (BARON ET ANGELES, 2000), et (WANG ET OEN, 2002). Dans les parties qui suivent, nous présentons les techniques essentielles pour la solution du modèle géométrique.

1.6.2.1 Solution numérique

Le modèle géométrique des MPs est généralement un système d'équations hautement non linéaires, les méthodes numériques restent toujours les principaux outils pour le solutionner. L'efficacité de ce type de solution dépend d'une connaissance d'un estimé initial de la solution qui peut parfois être problématique ou même conduire à une divergence du processus de résolution ; les algorithmes s'arrêtent, en général, à la première solution, trouver la totalité des solutions exige des techniques complexe et beaucoup de temps de calcul. Bien que les solutions numériques puissent être suffisamment efficaces sous certaines conditions, elles ne fournissent

pas de compréhension théorique telles que les singularités, le nombre de modes d'assemblage, et la NDM.

Les inconvénients des solutions numériques peuvent être palliés en employant les techniques polynomiales. Il s'agit de ramener la solution d'un système d'équations non linéaires à celle d'un système de polynômes en vue de réduire la complexité du problème.

1.6.2.2 Solution algébrique

Il existe des géométries qui peuvent induire un modèle géométrique moins complexe. C'est le cas pour les MPs à 6 DDLs dont la position et l'orientation sont découplées et pour les MPs à 3 DDLs. Il est possible que le système d'équations associé au modèle géométrique se réduit à un polynôme monovariable à moins de 5 degrés dont la solution est une fonction explicite des paramètres géométriques et les variables articulaires des joints actionnées. Ce type de solution permet de trouver le nombre exact de solutions et permet une compréhension théorique au niveau des singularités, du mode d'assemblage, du DDL, et du DDM.

La solution algébrique est en fait la solution la plus avantageuse tant pour la synthèse géométrique et l'analyse cinématique que pour les applications en temps réel, car elle n'exige pas de résolution itérative, ce qui permet d'économiser énormément le temps de calcul.

1.7 Conclusion

Nous venons de présenter une étude bibliographique de synthèse topologique et de synthèse géométrique ainsi que les techniques les entourant. Nous constatons qu'il

n'existe pas de représentation topologique des manipulateurs sur papier ayant à la fois une grande simplicité et permettant de représenter adéquatement les caractéristiques de la disposition relative des joints (parallélisme, intersection, et perpendicularité par exemple) ; il n'existe pas non plus de représentation topologique continue permettant d'intégrer la topologie en tant que variable dans la synthèse des MPs.

Les travaux portant sur la synthèse topologique des MPs s'appuient principalement sur la théorie des groupes de Lie et la théorie des visseurs. La synthèse basée sur la théorie des groupes de Lie s'effectue en disposant judicieusement des joints afin que l'intersection des sous-ensembles générés par des souschaînes cinématiques soit un sous-ensemble requis. C'est un exercice généralement extrêmement difficile qui exige une compréhension très approfondie de la théorie des groupes de Lie et la théorie de synthèse de mécanismes. Il demeure un problème ouvert de mettre en place des algorithmes pour générer automatiquement des topologies avec cette approche.

La problématique liée à la méthode de synthèse basée sur la théorie des visseurs est qu'elle s'appuie sur l'analyse de la cinématique et de la statique sur une seule configuration, le problème sur la propriété cinématique globale reste à aborder.

En ce qui concerne la synthèse géométrique, la modélisation cinématique s'effectue généralement sur une seule topologie de façon personnalisée et peu adaptée pour s'appliquer à plusieurs topologies.

La plupart des travaux ne s'occupent que d'une seule partie de la synthèse topologique et géométrique. Les travaux proposés dans cette thèse traitent les deux parties, et ce dans un esprit de les intégrer afin de produire un environnement de synthèse topologique et géométrique automatisée des MPTs.

CHAPITRE 2

ORGANISATION GÉNÉRALE DE LA THÈSE

Cette thèse est présentée sous la forme d'une thèse par articles. Les résultats et les discutions des travaux réalisés sont présentés en détail dans les articles présentés aux chapitres 3, 4, 5, 6 et 7 qui ont été ou seront soumis pour publication dans les revues internationales reconnues dans les domaines de la robotique et de la conception de mécanisme. Ce chapitre consiste à présenter en français une synthèse générale des travaux réalisés dans cette thèse.

2.1 Les travaux proposés

Notre recherche porte sur la synthèse topologique et géométrique des MPTs.

Du point de vue cinématique, un manipulateur est défini par la topologie et la géométrie. La topologie d'un manipulateur est au sens large la structure de la chaîne cinématique, une propriété généralement indépendante des dimensions. Elle est, de toute évidence, une description qualitative de la chaîne cinématique. Étant donné la topologie d'un manipulateur, la géométrie est alors un ensemble de paramètres définissant les position et orientation relatives entre les couples cinématiques adjacents. Il est à noter que la topologie implique aussi les position et orientation relatives particulières de certains couples cinématiques. C'est surtout le cas pour les MPs à mobilités restreintes.

La synthèse de manipulateurs comporte, traditionnellement, deux étapes :

Synthèse topologique : cette étape consiste à définir toutes les topologies admissible pour une tâche donnée ;

Synthèse géométrique : ayant choisi une topologie qui convient a priori aux contraintes de satisfaction de la tâche, cette étape est de déterminer la géométrie de manière à optimiser la performance du manipulateur.

En vue de produire un environnement de conception cinématique automatisée, nous proposons une approche de synthèse des MPTs permettant de prendre en considération la topologie et la géométrie simultanément. En résumé, les objectifs de ce travail sont les suivants :

1. Réaliser une étude de l'aspect topologique et géométrique des manipulateurs permettant d'identifier les dispositions particulières des couples cinématiques afin de décrire la topologie de façon adéquate ; par la suite, proposer une méthode de représentation topologique efficace pour la synthèse et la documentation des manipulateurs ;
2. Déduire les conditions topologiques et géométriques pour un MP d'avoir 3 DDMs ;
3. Proposer une approche de synthèse topologique et géométrique en fonction de la NDM ;
4. Déterminer la topologie de toutes les sous-chaînes cinématiques admissibles pour composer un MPT ;
5. Proposer un modèle géométrique prenant en compte la topologie et la géométrie simultanément et, s'appuyant sur ce modèle, proposer les solutions aux problèmes des MGD et MGI.

2.2 Chapitre 3 : topologie et diagramme topologique des MSs et MPs

À la suite de l'étude bibliographique menée dans le chapitre précédent, nous constatons que l'aspect topologique et géométrique des manipulateurs spatiaux n'a pas été abordé de façon rigoureuse. Bien que la topologie des mécanismes ait fait l'objet de recherche depuis de longues années, on a traité uniquement la nature des couples cinématiques et l'agencement général de ces derniers indépendamment de toute dimension. Ceci ne pose pas de problème significatif aux mécanismes plans, est néanmoins loin d'être suffisant pour les mécanismes spatiaux. La complexité du modèle géométrique fait en sorte que le DDM et la NDM des mécanismes spatiaux ne peuvent plus être déterminés uniquement par la nature des couples cinématiques et leur agencement général, car ils dépendent aussi des position et orientation relatives entre les couples cinématiques. Il est donc nécessaire que la topologie comporte un aspect dimensionnel et sa représentation en reflète conséquemment.

Nous introduisons les nouveaux concepts suivants :

Composition cinématique : la composition cinématique d'un manipulateur est un ensemble d'informations sur les nombre et nature de tous ses couples cinématiques et leur agencement général ;

Contraintes essentielles : les contraintes essentielles d'un manipulateur sont les positions et orientations relatives particulières entre certains de ses couples cinématiques qui sont requises pour qu'il possède des propriétés cinématiques particulières telles que le DDL, le DDM, la NDM, *etc.*

En conséquence, nous redéfinissons

Topologie : la topologie d'un manipulateur est la composition cinématique et les contraintes essentielles ;

Géométrie : la géométrie d'un manipulateur est un ensemble de contraintes dimensionnelles et géométriques sur les positions et orientations relatives entre

ses couples cinématiques qui lui sont particulières par rapport à tous les autres manipulateurs de la même topologie.

À partir d'une analyse topologique des manipulateurs dont l'architecture est connue, nous avons identifié des contraintes essentielles suivantes :

- parallélisme ;
- perpendicularité ;
- coïncidence ;
- intersection ;
- alignement ;
- équidistance ;
- contrainte coplanaire ;
- contrainte concourante.

Un symbole a été proposé pour chacune de ces contraintes. Ensuite, nous inspirant de la représentation des mécanismes au moyen de graphes, nous proposons de représenter la composition cinématique sous forme de diagramme. La nature d'un couple cinématique est identifiée par une lettre significative en majuscule. En superposant les symboles de contraintes essentielles sur les liens, nous complétons la représentation topologique que nous appelons ***diagramme topologique***.

Certaines combinaisons de couples cinématiques sont très fréquentes parmi les topologies connues. Nous introduisons donc le concept de ***joint complexe***, une combinaison de plusieurs couples cinématiques, afin de simplifier la représentation d'un nombre très important de manipulateurs.

Nous avons montré par de nombreux exemples que notre approche est simple et efficace pour représenter adéquatement la topologie d'un manipulateur. Il y a une très bonne correspondance entre un diagramme topologique et les manipulateurs visés. Le diagramme topologique peut être facilement adapté à une représentation numérique sous forme de matrice permettant ainsi la génération automatisée des topologies.

Ayant identifié les aspects fondamentaux de la topologie et de la géométrie des

manipulateurs, nous pouvons entamer notre recherche sur la synthèse topologique et géométrique.

2.3 Chapitre 4 : analyse de mobilité des MPs à 3 DDLs

Pour la synthèse des manipulateurs, la topologie et la géométrie doivent satisfaire, avant tout, au DDL requis. Traditionnellement, le degré de liberté ou mobilité d'un mécanisme est défini comme le nombre de variables indépendantes pour décrire sa configuration (McCarthy, 1990). Pour les manipulateurs sériels ou plans, plusieurs formules généralisées de Chebyshev-Grubler-Kutzbach bien connues permettent de calculer le degré de liberté en fonction de la topologie (Angeles et Gosselin, 1988). Cependant, pour les mécanismes en chaîne cinématique fermée, il n'existe pas d'équation simple à cette fin. Il est donc nécessaire d'effectuer une analyse systématique afin de déduire les conditions topologiques et géométriques pour qu'un MP ait 3 degrés de libertés.

Afin de mieux caractériser un MP en ce qui concerne le degré de liberté du mécanisme et le degré de mobilité de l'effecteur, nous distinguons

degré de liberté (DDL) : le DDL d'un MP est le nombre de variables indépendantes pour décrire sa configuration ;

degré de mobilité (DDM) : le DDM d'un MP est le nombre de variables indépendantes pour décrire les position and orientation (pose) de son effecteur ;

degré de motorisation : la degré de motorisation d'un manipulateur est le nombre de couples cinématiques qui peuvent déterminer la pose de son effecteur.

Au voisinage d'une configuration non singulière d'un MP, le déplacement de tous les solides est continu. L'analyse de mobilité peut donc s'effectuer dans l'espace tangentiel à une configuration initiale.

Les équations structurelles dans l'espace tangentiel sont données comme les suivantes :

$$\mathbf{t}_e = \sum_{i=1}^{m_j} \left({}^{i-1}\hat{\mathbf{t}}_{j,i}\dot{q}_{j,i} \right) = \sum_{i=1}^{m_k} \left({}^{i-1}\hat{\mathbf{t}}_{k,i}\dot{q}_{k,i} \right),\ \forall j,\ k \in \{1,\ 2,\ 3\}\ ,\ j \neq k \tag{2.1}$$

où $\hat{\mathbf{t}}$ désigne le torseur de vitesse normalisé dont la structure correspond à la nature du joint et la valeur numérique correspond à la géométrie, et $\dot{q}$ est la vitesse articulaire. Il s'agit d'un système d'équations linéaires et la mobilité du MP est dictée par celui-ci. Si le nombre d'équations est égal au nombre de joints passifs, le MP est isocontraint. Les torseurs de vitesse des joints passifs de chaque sous-chaîne liant l'effecteur à la base peuvent être assemblés dans une matrice $\mathbf{W}_j$ $(j = 1, 2, 3)$ et la matrice

$$\mathbf{W}_B \equiv \begin{bmatrix} \mathbf{W}_1 & -\mathbf{W}_2 & \mathbf{O}_3 \\ \mathbf{O}_1 & \mathbf{W}_2 & -\mathbf{W}_3 \end{bmatrix} \tag{2.2}$$

est appelée la matrice des joints passifs. La matrice

$$\mathbf{A} \equiv \begin{bmatrix} \boldsymbol{x}_1 & \mathbf{0} & \mathbf{0} & \mathbf{W}_1 & \mathbf{O} & \mathbf{O} \\ \mathbf{0} & \boldsymbol{x}_2 & \mathbf{0} & \mathbf{O} & \mathbf{W}_2 & \mathbf{O} \\ \mathbf{0} & \mathbf{0} & \boldsymbol{x}_3 & \mathbf{O} & \mathbf{O} & \mathbf{W}_3 \end{bmatrix} \tag{2.3}$$

où $\boldsymbol{x}_j$ $(j = 1, 2, 3)$ désigne le torseur de vitesse normalisée du joint actionné de la $j^{ième}$ sous-chaîne, est appelée la matrice des joints. À la suite d'une analyse de l'équation (2.1), les conditions topologiques et géométriques pour le MP d'avoir 3 DDMs et d'être isocontraint sont déduites comme les suivantes :

1. les combinaisons des nombres de joints passifs des trois sous-chaînes sont $(2, 5, 5)$, $(3, 4, 5)$, et $(4, 4, 4)$;
2. la matrice des joints passifs $\mathbf{W}_B$ est une matrice carrée inversible ;

3. le rang de la matrice des joints **A** est égal à 15.

Si le nombre d'équations est supérieur au nombre de joints passifs, le MP devient surcontraint. Dans ce cas-ci, le MP ne peut être assemblé et avoir le DDM demandé que sous des conditions géométriques particulières. Analysant la solution de l'équation (2.1), nous constatons que chaque MP surconstraint est équivalent à un MP isocontraint dont les vitesses à certains joints sont égal à 0. En ce qui concerne la cinématique, il n'est donc pas nécessaire de traiter le cas des MPs surcontraints séparément, car ils ne sont que des MPs isocontraints avec des géométries particulières. De façon similaire, chaque MP souscontraint a un équivalent dans les PMs isocontraints et peut s'obtenir en ajournant des joints à son équivalent. En conséquence, du point de vue cinématique, la synthèse topologique et géométrique des MPs isocontraints incluent celles des MPs surcontraints et souscontraints.

2.4 Chapitre 5 : synthèse topologique des MPTs basée sur la cinématique instantanée

Ayant déduit les conditions topologiques et géométriques pour un MP d'avoir le DDL et le DDM requis, le problème qui suit dans la synthèse est de définir la topologie à partir de la NDM. Pour cela, nous caractérisons la NDM dans l'espace tangentiel et la décrivons avec trois torseurs de vitesse dont la combinaison linéaire forme l'espace tangentiel du déplacement de l'effecteur.

Soient $\mathbf{o}_i$ et $\mathbf{c}_i$ $(i = 1, 2, 3)$ vecteurs unitaires 3×1, et

$$\mathbf{G}_U \equiv \begin{bmatrix} \mathbf{o}_1 & \mathbf{o}_2 & \mathbf{o}_3 \end{bmatrix}, \quad \mathbf{G}_L \equiv \begin{bmatrix} \mathbf{c}_1 & \mathbf{c}_2 & \mathbf{c}_3 \end{bmatrix}, \quad \mathbf{G} \equiv \begin{bmatrix} \mathbf{G}_U \\ \mathbf{G}_L \end{bmatrix},$$

Nous décrivons l'espace tangentiel du déplacement de l'effecteur de la manière

suivante :

$$\{\mathbf{t}_e\} = Im(\mathbf{G}) \tag{2.4}$$

où $Im(\mathbf{G})$ désigne l'image de la matrice $\mathbf{G}$. Si

$$\mathbf{A}_i \equiv \begin{bmatrix} \boldsymbol{x}_i & \mathbf{W}_i \end{bmatrix},\ i = 1,\ 2,\ 3 \tag{2.5}$$

d'après l'équation (2.1), nous avons

$$\mathbf{t}_e \in Im(\mathbf{A}_i),\ i = 1,\ 2,\ 3 \tag{2.6}$$

En comparant l'équation (2.4) avec l'équation (2.6), il en résulte que

$$Im(\mathbf{G}) = Im(\mathbf{A}_1) \cap Im(\mathbf{A}_2) \cap Im(\mathbf{A}_3) \tag{2.7}$$

L'équation (2.7) nous permet de déduire la topologie et la géométrie à partir de la NDM.

Tel que montré par les équations (2.2) et (2.5), chaque colonne de la matrice $\mathbf{A}_i$ $(i = 1, 2, 3)$ est un torseur de vitesse normalisée. En effet, elle contient les coordonnées Plückoniennes normalisées de l'axe d'un joint. Afin d'exploiter la structure spéciale d'un torseur de vitesse normalisé, nous partitionnons la matrice $\mathbf{A}_i$ $(i = 1, 2, 3)$ en deux parties, une partie composée des 3 premières lignes, l'autre partie composée des 3 dernières lignes, soit

$$\mathbf{A}_i = \begin{bmatrix} \mathbf{A}_{Ui} \\ \mathbf{A}_{Li} \end{bmatrix},\ i = 1,\ 2,\ 3 \tag{2.8}$$

En conséquence, l'équation (2.7) peut se réécrire comme les suivantes :

$$Im(\mathbf{G}_U) = Im(\mathbf{A}_{U1}) \cap Im(\mathbf{A}_{U2}) \cap Im(\mathbf{A}_{U3}) \tag{2.9}$$

$$Im(\mathbf{G}_L) = Im(\mathbf{A}_{L1}) \cap Im(\mathbf{A}_{L2}) \cap Im(\mathbf{A}_{L3}) \tag{2.10}$$

Nous remarquons que seuls les joints rotoïdes sont impliqués dans l'équation (2.9).

Les équations (2.9) et (2.10) nous montrent que la synthèse peut s'effectuer dans $\mathbb{R}^3$ auquel nous sommes le plus habitués. La dimension de $Im(\mathbf{G}_U)$ et $Im(\mathbf{G}_L)$, dépendant de la NDM, peut être 0, 1, 2, et 3 qui correspondent respectivement à trois sous-espaces de $\mathbb{R}^3$, soit un point, une ligne, un plan, et un espace tridimensionnel. Nous résumons l'intersection de deux sous-espaces de $\mathbb{R}^3$ dans le tableau 2.1.

TAB. 2.1 L'intersection de deux sous-espaces de $\mathbb{R}^3$

	point	ligne	plan	tridimensionnel
point	point	point	point	point
ligne		point	point	ligne
plan			ligne	plan
tridimensionnel				tridimensionnel

Étant données $\mathbf{G}_U$ et $\mathbf{G}_L$, nous pouvons aisément déduire $\mathbf{A}_{Ui}$ et $\mathbf{A}_{Li}$ $(i = 1, 2, 3)$, la topologie et la géométrie proprement dit, en utilisant les résultats des travaux présentés dans la section précédente et le Tableau 2.1.

Cette approche de synthèse ne garantit la NDM qu'à une seule configuration. Il nous reste à étudier comment déterminer si un MP peut maintenir la NDM partout dans un espace de travail.

2.5 Chapitre 6 : synthèse topologique des MPTs basée sur analyse de déplacement

La synthèse des MPTs basée sur l'analyse de l'espace tangentiel nous permet de déduire la topologie et la géométrie de manière que le DDL, le DDM, la isocontrainte, et la NDM soient satisfaits à une configuration initiale. Afin de vérifier s'ils sont satisfaits à travers un espace de travail, nous allons analyser d'abord le déplacement de l'effecteur avec une orientation constante qui est permis par une sous-chaîne particulière, puis les orientations atteignables sous les contraintes de toutes les sous-chaînes.

L'idée principale est qu'en imposant une contrainte d'orientation à l'effecteur, sa capacité de déplacement en translation est réduite ; une sous-chaîne admissible doit avoir la pleine capacité en translation sous une telle contrainte. Sous la contrainte d'une sous-chaîne, l'orientation de l'effecteur est définie par l'equation (2.11).

$$\mathbf{R_z}(\theta_0)\mathbf{R_x}(\alpha_0)\left[\prod_{i=1}^{m}[\mathbf{R_z}(\theta_i)\mathbf{R_x}(\alpha_i)]\right]\mathbf{R_z}(\theta_e)\mathbf{R_x}(\alpha_e)\mathbf{R_z}(\theta_E) = \mathbf{Q}_e \qquad (2.11)$$

Afin de caractériser les différentes situations des joints rotoïdes, nous introduisons les notions suivantes :

Membrure rotoïde : une membrure portant deux joints rotoïdes ;

Membrure rotoïde de travers : une membrure portant deux joints non parallèles ;

Angle de membrure : l'angle entre les axes de deux joints d'une membrure rotoïde de travers ;

Membrures rotoïdes de travers supplémentaires : deux membrures rotoïdes de travers dont les angles de membrure sont égals ou supplémentaires ;

Membrure rotoïde de H : une membrure portant deux joints rotoïdes parallèles ;

Membrure rotoïde de n-H : une chaîne de $(n-1)$ membrures rotoïdes de H ;

Hyper membrure rotoïde : les membrures définies ci-dessus avec la présence des joints prismatiques entre les joints rotoïdes.

Sous-chaîne-T : une sous-chaîne n'ayant que des joints prismatiques ;

Sous-chaîne-I : une hyper membrure rotoïde de n-H ;

Sous-chaîne-A : une sous-chaîne composée d'une seule (hyper) membrure rotoïde de travers et des (hyper) membrures rotoïdes de n-H ;

Sous-chaîne-Z : une sous-chaîne composée de deux (hyper) membrures rotoïdes de travers supplémentaires et des (hyper) membrures rotoïdes de n-H ;

Sous-chaîne-Y : une sous-chaîne ayant au moins deux (hyper) membrures rotoïdes de travers non supplémentaires.

Analysant l'équation (2.11), nous avons déduit les sous-chaînes admissibles pour composer un MPT (tableau 2.2).

TAB. 2.2 Les sous-chaînes admissibles pour composer un MPT

	3-joint	4-joint	5-joint	6-joint
Sous-chaîne-T	Oui	Non	Non	Non
Sous-chaîne-I	Non	Oui	Non	Non
Sous-chaîne-A	Non	Non	Oui	Non
Sous-chaîne-Z	Non	Non	Oui	Oui
Sous-chaîne-Y	Non	Non	Non	Oui

Nous avons aussi déduit les combinaisons des sous-chaînes nécessaires pour que le MP soit isocontraint et pour éliminer la possibilité des déplacements en orientation de l'effecteur dans un espace de travail (Tableau 2.3).

TAB. 2.3 Les combinaisons des sous-chaînes pour un MPT

	T	I	A	Z	Y
Sous-chaîne-T					Y
Sous-chaîne-I			Y		
Sous-chaîne-A		Y	A	Y	
Sous-chaîne-Z					Y

où "A" représente une sous-chaîne-A, "Y" représente une sous-chaîne-Y.

Les résultats présentés dans les Tableaux 2.2 et 2.3 complètent ainsi notre approche de synthèse topologique des MPTs. Une modélisation topologique et géométrique et la résolution des problèmes des MGD et MGI sont nécessaire afin d'effectuer une synthèse conjointe topologique et géométrique.

2.6 Chapitre 7 : modélisation topologique et géométrique des MPTs

Après le problème de synthèse topologique, le problème à aborder lié à la synthèse conjointe topologique et géométrique est le paramétrage topologique et géométrique.

2.6.1 Paramétrage topologique et géométrique

Pour représenter la nature d'un joint, nous introduisons un couple (κ, w) où κ est un entier naturel identifiant l'orientation du joint par rapport aux autres joints de la même sous-chaîne et w est un nombre réel non négatif qualifiant la nature du joint, 0 correspondant à un joint prismatique. Ce paramétrage de la nature de

joint permet un passage continu d'un joint rotoïde vers un joint prismatique. La topologie d'un MP de n DDLs est donc représentée par n matrices tel que

$$\begin{bmatrix} \kappa_{j,1} & \kappa_{j,2} & \cdots & \kappa_{j,m_j-1} & \kappa_{j,m_j} \\ w_{j,1} & w_{j,2} & \cdots & w_{j,m_j-1} & w_{j,m_j} \end{bmatrix}, j = 1, 2, \cdots, n \tag{2.12}$$

où m_j désigne le nombre total de joints de $j^{ième}$ sous-chaîne.

Afin de représenter la géométrie et d'éviter toute singularité au niveau du paramétrage, nous introduisons le concept de la configuration initiale. Le paramétrage géométrique s'est ensuite effectué sur la configuration initiale. L'orientation d'un joint est représentée par un vecteur unitaire $\hat{\boldsymbol{n}}$ tandis que la position par un couple $(\hat{\boldsymbol{m}}, w)$ où $\hat{\boldsymbol{m}}$ est un vecteur unitaire représentant la direction du moment du vecteur $\hat{\boldsymbol{n}}$ (étant aligné avec l'axe du joint) par rapport à l'origine du référentiel global et w est la nature du joint. Les coordonnées Plückoniennes de l'axe du joint s'obtiennent à partir du triplet $(\hat{\boldsymbol{n}}, \hat{\boldsymbol{m}}, w)$ tel que

$$\boldsymbol{l} = \begin{bmatrix} w\hat{\boldsymbol{n}} \\ \hat{\boldsymbol{m}} \end{bmatrix} \tag{2.13}$$

La topologie et la géométrie d'un MP de n dlls sont donc représentées par n matrices tel que

$$\begin{bmatrix} \hat{\boldsymbol{n}}_{j,1} & \hat{\boldsymbol{n}}_{j,2} & \cdots & \hat{\boldsymbol{n}}_{j,m_j-1} & \hat{\boldsymbol{n}}_{j,m_j} \\ \hat{\boldsymbol{m}}_{j,1} & \hat{\boldsymbol{m}}_{j,2} & \cdots & \hat{\boldsymbol{m}}_{j,m_j-1} & \hat{\boldsymbol{m}}_{j,m_j} \\ w_{j,1} & w_{j,2} & \cdots & w_{j,m_j-1} & w_{j,m_j} \end{bmatrix}, j = 1, 2, \cdots, n \tag{2.14}$$

2.6.2 Modélisation géométrique

À la configuration initiale, un référentiel est défini pour chacune des membrures de la façon suivante :

1. les origines de tous les référentiels coïncident ;
2. l'axe $\boldsymbol{z}$ du référentiel est dans le sens du vecteur $\hat{\boldsymbol{n}}$;
3. l'axe $\boldsymbol{y}$ du référentiel est dans le sens du vecteur $\hat{\boldsymbol{m}}$;
4. le sens de l'axe $\boldsymbol{x}$ du référentiel se définit en utilisant la règle de la main droite ;
5. la variable articulaire q est définie tel que $\theta = wq$ où θ désigne l'angle de rotation du référentiel par rapport à son orientation initiale.

La pose d'un référentiel par rapport au référentiel précédent le long de la sous-chaîne se calcule par

$$\mathbf{C}_{j,i} = \mathbf{B}_{\mathbf{x}}(-\frac{1}{w_{j,i}})\mathbf{R}_{\mathbf{hz}}(w_{j,i}q_{j,i})\mathbf{B}_{\mathbf{x}}(\frac{1}{w_{j,i}})\mathbf{G}_{\mathbf{h}j,i} \tag{2.15}$$

où $\mathbf{G}_{\mathbf{h}j,i}$ est une matrice de transformation homogène de rotation entre ces référentiels à la configuration initiale. L'équation donnant la position d'un référentiel par rapport au référentiel précédent est :

$$\boldsymbol{\rho}_{j,i} = \begin{bmatrix} \frac{1}{w_{j,i}}\cos(w_{j,i}q_{j,i}) - \frac{1}{w_{j,i}} \\ \frac{1}{w_{j,i}}\sin(w_{j,i}q_{j,i}) \\ 0 \end{bmatrix} = \begin{bmatrix} -\frac{2}{w_{j,i}}\sin^2\left(\frac{w_{j,i}q_{j,i}}{2}\right) \\ \frac{1}{w_{j,i}}\sin(w_{j,i}q_{j,i}) \\ 0 \end{bmatrix} \tag{2.16}$$

Il est évident que si $w_{j,i}$ approche 0, nous avons

$$\lim_{w_{j,i}\to 0} \boldsymbol{\rho}_{j,i} = \begin{bmatrix} 0 \\ q_{j,i} \\ 0 \end{bmatrix} \tag{2.17}$$

ce qui correspond à un joint prismatique.

Pour un MP de n DDLs, le modèle géométrique est donné par

$$\mathbf{H}_{j,0}\left(\prod_{i=1}^{m_j}\mathbf{C}_{j,i}\right)\mathbf{C}_{j,e} = \mathbf{H}_{k,0}\left(\prod_{i=1}^{m_k}\mathbf{C}_{k,i}\right)\mathbf{C}_{k,e}$$
$$\forall j,\ k = 1,\ 2,\ \cdots,\ n,\ j \neq k \tag{2.18}$$

Le problème du MGI des MPTs peut, en effet, se transformer en la résolution des problèmes correspondant respectivement aux trois sous-chaînes. En exploitant la particularité des sous-chaînes, nous avons déduit les solutions explicites pour toutes les sous-chaînes ayant 5 joints. Le problème du MGD est résolu par des méthodes numériques. La matrice Jacobienne est formée implicitement comme un système d'équations linéaires et elle s'obtient aisément par la résolution de ce dernier.

L'ensemble de ces travaux nous permettra de mettre en place un environnement de synthèse topologique et géométrique automatisée des MPTs.

CHAPITRE 3

TOPOLOGY OF SERIAL AND PARALLEL MANIPULATORS AND THEIR TOPOLOGICAL DIAGRAMS

Xiaoyu Wang, Luc Baron and Guy Cloutier.
Département de génie mécanique, École Polytechnique de Montréal.
P.O. 6079, station Centre-Ville, Montréal, Québec, Canada, H3C 3A7.
xiaoyu.wang@polymtl.ca

(Submitted to the *Journal of Mechanism and Machine Theory*)

Abstract

This paper deals with manipulator topology. The term topology was first introduced into robotics to characterize the kinematic structure of a manipulator without reference to its dimensions. Its dimension-independent aspect does not pose a considerable problem to planar manipulators, but makes it no longer appropriate to describe spatial manipulators especially spatial parallel manipulators, because such properties as the degree of freedom of a manipulator and the degree of mobility of its end-effector as well as the nature of their mobilities are highly dependent on some dimensional elements. In order to address this import issue in kinematic synthesis, we introduce the essential geometric constraints into the concept of topology. We also propose a topological representation providing a better correspondance between the physical manipulator and its kinematic properties, a necessity for the topological synthesis and documentation. The essential constraints can also improve the efficiency of the topological synthesis methods.

Keywords : Parallel manipulator, Topology, Geometry, Kinematics, Representation, Diagram.

3.1 Introduction

As far as the kinematics is concerned, a mechanism is a kinematic chain with one of its links designated as the *base* and another as the *end-effector* (EE). A manipulator is a mechanism with all or some of its joints actuated. Driven by the actuated joints, the EE and all links undergo constrained motions with respect to the base (TSAI, 2001). A parallel manipulator is a mechanism whose EE is connected to its base by at least two independent kinematic chains (MERLET, 1997). The early research works on manipulators mostly dealt with a specific design ; each one being described in a particular way. With the number of designs increasing, the consistency, preciseness and conciseness of topological description of manipulators become more and more important. To describe how a manipulator is kinematically constructed, many different terms and definitions have been proposed. The words *architecture* (HUNT, 1982a), *structure* (HUNT, 1982b), *topology* (POWELL, 1982), and *type* (FREUDENSTEIN ET MAKI, 1965; YANG ET LEE, 1984) all found their way into the literature, describing kinematic chains without reference to dimensions. However, the kinematic properties of spatial manipulators are highly sensitive to some dimensional elements. The problem is that with the original definition of the term topology (the term topology is preferred here to other terms), manipulators of the same topology are sometimes producing a completely different mobility of their EE, and hence, are too different to be classified in the same category. It is therefore necessary to take into account some dimensional elements when dealing with topology.

Words used to define geometic details are equally diverse. *Parameter* (DENAVIT ET

HARTENBERG, 1954), *dimension* (CHEN ET ROTH, 1969; CHEDMAIL, 1998) and *geometry* (PARK ET BOBROW, 1995) are among the terms used to this end. As for the kinematic representation of parallel manipulators, one can hardly find a method which is adequate for a wide range of manipulators and commonly accepted and used in the literature. However, in the classification (BALKAN ET AL., 2001; SU ET AL., 2002), comparison studies (GOSSELIN ET AL., 1995; TSAI ET JOSHI, 2001) (equivalence, isomorphism, similarity, difference, etc.) and manipulator kinematic synthesis, an effective kinematic representation is essential.

This work is aimed at identifying and introducing essential geometrical constrains into the topology and proposing a new topological representation accordingly. The representation should work for all serial and parallel manipulators and be as much precise and concise as possible. It should also be appropriate to facilitate the automatic topological and geometrical synthesis of such manipulators.

Section 2 of this paper presents some definitions and background on the kinematics of serial and parallel manipulators. It underlines the importance of geometric constraints in determining the kinematic properties of mechanisms. Section 3 introduces the concepts of kinematic composition, essential constraints, a new separation between topology and geometry. In Section 4, the kinematic representations are reviewed and their limitations identified. Based on this review, we propose a new representation of the topology of manipulators, called topological diagrams. Several examples of topological diagrams of both serial and parallel manipulators is presented in Section 5. Finally, section 6 discusses the advantages and limitations of using these topological diagrams, and how it can improve the efficiency of topological synthesis algorithms.

3.2 Basic Definitions and Background

Some basic concepts and definitions about kinematic chains are necessary to review for the discussion on topology and topological representation. A *kinematic chain* is a set of rigid bodies, also called *links*, coupled by *kinematic pairs*. A kinematic pair is, then, the coupling of two rigid bodies so as to constrain their relative motion. We distinguish upper and lower kinematic pairs. Upper kinematic pairs constrain two rigid bodies such that they keep a line or point contact, while lower kinematic pairs constrain two rigid bodies such that a surface contact is maintained (ANGELES, 2003). A *joint* is a particular mechanical implementation of a kinematic pair (IFToMM, 2003). As shown in Fig. 3.1, there are six lower kinematic pairs corresponding to the types of joints, i.e., prismatic (P), revolute (R), cylindrical (C), helical (H), planar (E) and spherical (S) (ANGELES, 1982). Since all these pairs can be obtained by combining the R and P pairs, it is sufficient to deal only with them in the kinematic modeling. To characterize links, the notions of *simple link*, *binary link*, *ternary link*, *quaternary link* and *n-link* is introduced to indicate how many other links a link is connected to, where n is the degree of connectivity of that link (BARON, 1997). Similarly, *binary joint*, *ternary joint* and *m-joint* indicate how many links are connected to a joint, where m is the degree of connectivity of that joint. These basic concepts constitute a common basis for the kinematic analysis and synthesis of both serial and parallel manipulators.

For kinematic analysis, the kinematic description of a mechanism includes basic information and parameters. The basic information is which link is connected to which other links by what types of joints. This basic information is often referred to as *structure*, *architecture*, *topology*, or *type*, respectively, by different authors. This basic information alone is of little interest, because the kinematic properties of the corresponding mechanisms can vary too much to characterize a mechanism.

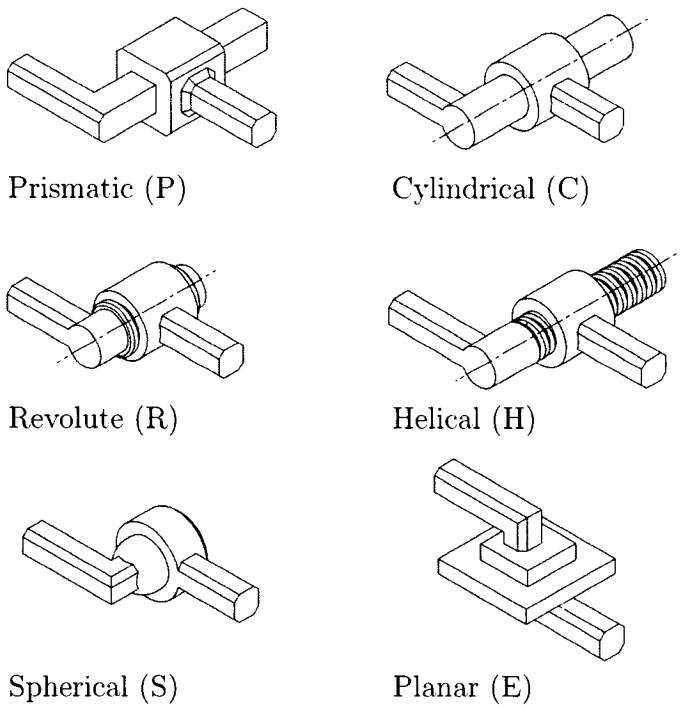

FIG. 3.1 Lower Kinematic Pairs

This can be demonstrated by the single-loop 4-bar linkages shown in Fig. 3.2. Without reference to dimensions, all mechanisms shown in Fig. 3.2 are of the same kinematic structure, i.e., $RRRR$ in a single loop structure, but have very different kinematic properties, and therefore are used in different applications. For example, mechanism a) produces planar motion and b) spherical motion, while c) is a Bennett mechanism (BENNETT, 1903) which produces spatial motion. Finally, mechanism d) allows no relative motion of its links. Moreover, figure 3.3 shows three parallel manipulators having the same kinematic structure, i.e., 3-$PRRR$, but producing very different kinematic properties. For example, mechanism a) has 3 degrees of freedom (DOFs) and its EE has no mobility. Conversely, mechanism b) has 3 DOFs and its EE has also 3 DOFs (here, they are in translation). Finally, mechanism c) allows no motion of its joints, and hence its EE has no mobility.

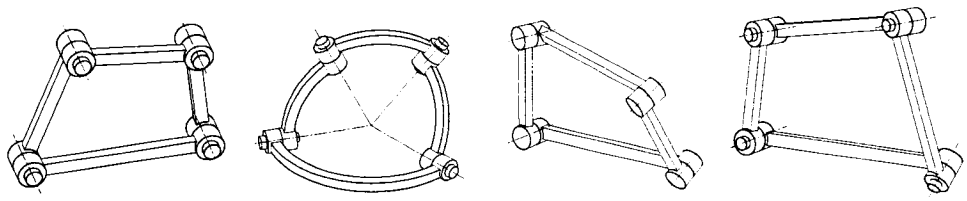

FIG. 3.2 Four-bar linkages having the same kinematic structure $RRRR$ and different modility

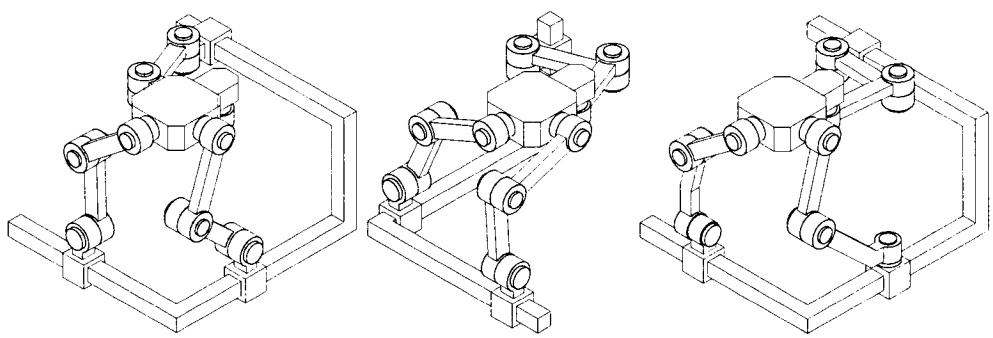

FIG. 3.3 Parallel manipulators having the same kinematic structure 3-$PRRR$ and very different kinematic properties

A particular mechanism is thus described, in addition to the basic information, by a set of parameters which define the relative position and orientation of each joint with respect to its neighbors. For complex closed-loop mechanisms, an often ignored problem is that certain parameters must take particular values in order for the mechanism to be functional and have the intended kinematic properties. More attention should be payed to these parameters which play a qualitative role in determining some important kinematic properties of the mechanism. For kinematic synthesis, not only do the eligible mechanisms have particular kinematic structures, but also they feature some particular relative positions and orientations between certain joints. If this particularity is not taken into account when formulating the

synthesis model, a great number of mechanisms generated with the model will not have the required kinematic properties and have to be discarded.

In the next section, we investigate the special joint dispositions and give a new definition of the term topology by introducing the essential constraints.

3.3 Topology : Revised for the Topological Synthesis

Since the sixties, a very large number of manipulator designs have been proposed in the literature or disclosed in patent files. The kinematic properties of these designs were studied mostly on a case by case basis and the characteristics of their kinematic structure were often not investigated explicitly. The constraints on the relative joint locations which are essential for a manipulator to meet the kinematic requirements were also rarely put into the kinematic representation. Constraints are introduced mainly to meet the functional requirements, to simplify the kinematic model, to optimize the kinematic performances, or for manufacturing considerations. These constraints can be revealed by investigating the underlying design ideas.

For a serial manipulator to generate planar motion, all its revolute joints need to be parallel and all its prismatic joints should be perpendicular to the revolute joints. For a serial manipulator to generate spherical motion, the axis of all revolute joints must be concurrent (McCarthy, 1990). For a parallel manipulator with three identical legs to produce only translational motion, the revolute joints of the same leg must be arranged in one or two directions (Wang et al., 2003a). A typical example of simplifying the kinematic model is the decoupling of the position and orientation of the EE of a 6-joint serial manipulator. This is realized by having three consecutive R joint axes concurrent. A comprehensive study was presented in (Ozgoren, 2002) on the inverse kinematic solutions of 6-R serial manipulators.

The study reveals how the inverse kinematic problem is simplified by making joint axes parallel, perpendicular or intersecting.

Optimizing the kinematic performance also gives rise to special relative joint locations. Isotropic parallel manipulators having orthogonal actuated joint axes proposed in (WENGER ET CHABLAT, 2000; WANG ET AL., 2003b) are examples of this kind. In summary, these special constraints are the special relative joint locations, *i.e.*, parallelism, perpendicularity, intersection, coplanarity, *etc.* To facilitate the kinematic analysis, kinematic synthesis, classification and comparison studies of manipulators, the terms kinematic composition, essential constraint, topology, geometry and their definitions are revisited for the topological synthesis as follows :

- the *kinematic composition* of a manipulator is the essential information about the number of its links, which link is connected to which other links by what types of joints and which joints are actuated ;
- the *essential constraints* are the minimum conditions for a manipulator of given kinematic composition to have the required DOF of the mechanism and degree-of-mobility (DOM) of its EE ;
- the *topology* of a manipulator is its kinematic composition plus the essential constraints ;
- The *geometry* of a manipulator is a set of constraints on the relative locations of its joints which are unique to each of the manipulators of the same topology.

Hence, topology also has a geometrical aspect such as parallelism, perpendicularity, coplanar, and even numerical values and functions on the relative joint locations which used to be considered as geometry. By our definition, geometry no longer includes relative joint locations which are common to all manipulators of the same topology because the later are the essential constraints and belong to the topology category. A manipulator can thus be much better characterized by its topology.

3.4 Topological diagrams

3.4.1 Topological representation : a review

The basic notions about link and joint introduced in Section 2 were used to describe manipulator kinematics. With these notions, the general spatial arrangement of links and joints of a manipulator can be described with ease. For example, the kinematic chain associated with a serial manipulator is constructed with binary links, two simple links and binary joints; while that associated with a parallel manipulator is composed of binary links, two multiple-links and binary joints. The limitation

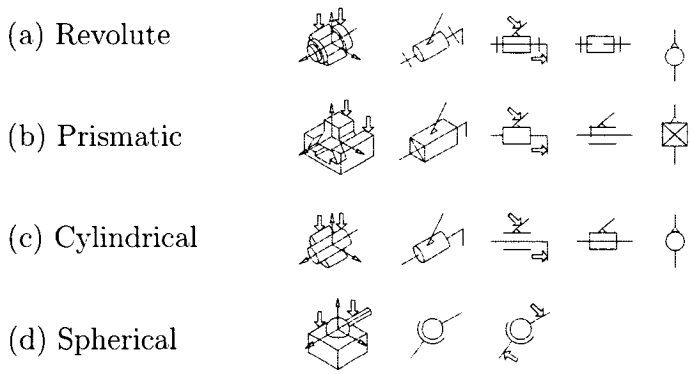

FIG. 3.4 Kinematic joint symbols (ISO, 1981)

of such description is obvious since the information about the joint types and which joints are actuated can not be provided without lengthy notations. Alphanumeric representation, 3-U<u>P</u>U or 3-<u>R</u>RR for example, may be the most effective one for kinematic composition, which is widely used in the literature. In general, the number indicates the number of identical kinematic chains, the sequence of upper case letters indicates the joint types along each kinematic chain and the actuated joints are identified by underlines. One of the more visual representation methods is the

Joint name	Representation	
	Passive joint	Actuated joint
Revolute	R	R
Prismatic	P	P

FIG. 3.5 Layout graph symbols (PIERROT, 1991)

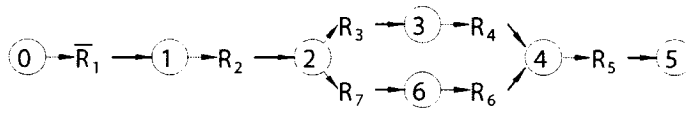

FIG. 3.6 Layout graph symbols (BARON, 1997)

kinematic diagram, i.e., a drawing of a mechanism showing its essential elements in simplified form with graphical symbols (Fig. 3.4). Although a great deal of effort has been made to normalize the graphical symbols for kinematic diagrams, e.g. (SMITH, 1886; ISO, 1981; THE ASSOCIATION OF GERMAN ENGINEERS, 1993), the practice in the literature is just far from normalized. Similar to the kinematic diagram, the kinematic layout graph (Fig. 3.5) was proposed in (PIERROT, 1991). With the kinematic layout graph, each joint is represented by an uppercase letter indicating the joint type surrounded by a rectangle; joints carried by the same link are connected by a line. The kinematic layout graph or its variants (Fig. 3.6) can be found in a number of recent publications. The common problem with the above kinematic representations is the poor correspondence between the representation and the intended manipulators. One kinematic diagram or layout graph may correspond to many manipulators with quite different kinematic properties. For planar mechanisms, there exist three similar representations, *i.e.*, structural schema, graph, and functional schema (see Fig. 3.7). The graph representation proposed in (CROSSLEY, 1962; CROSSLEY, 1965) is based on an abstract kinema-

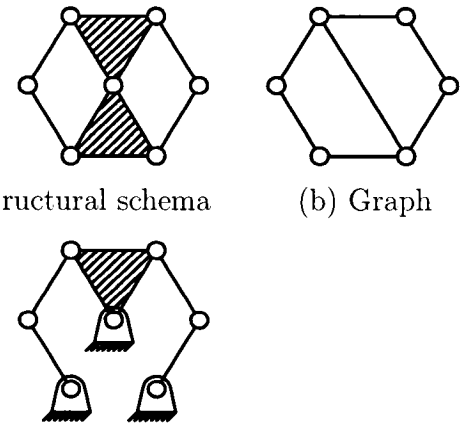

(a) Structural schema (b) Graph

(c) Functional schema

FIG. 3.7 Structural schema, graph, and functional schema

tic representation similar to the symbolic representation of chemical compound. With graph representation, the vertices denote links while edges denote joints. To distinguish different joints, the edges can be labeled or numbered. Since a graph can be easily represented by matrices, automatic synthesis algorithms can be implemented and kinematic chains can be systematically enumerated using graph theory and combinatorial analysis. When used with spatial mechanisms, the graph representation suffers from the same drawbacks as the kinematic diagram and the kinematic layout graph. For spatial manipulators, joint and link locations are often so complex that perspective views and section views have to be used to represent the kinematic chains. Although the perspective views and section views are simplified as much as possible, the special features of the joint locations, parallelism and perpendicularity for example, can hardly be recognized by anyone not familiar with spatial mechanism. The topological and geometrical features can not be distinguished without complementary notations. A new representation of layout graph with graphical symbols for geometric constraints was proposed in (WANG ET AL., 2004). Only one example of this representation was given, whether it is suitable

for a wide range of manipulators remains to be seen. Denavit-Hartenberg notation (DENAVIT ET HARTENBERG, 1954) and the initial configuration matrix (WANG ET AL., 2003a) were used for implicit topological representation when emphasis was put on geometric synthesis and visual representation could be compromised. In summary, the existing kinematic representations are only suitable for kinematic composition or kinematic geometry. There is a lack of topological representation.

3.4.2 Kinematic composition

Taking the basic ideas of graph and layout graph, we propose that the kinematic composition be represented by a diagram having the graph structure so as to be eventually adapted for automatic synthesis. The joint type is designated as an upper case letter, *i.e.*, **R** for revolute, **P** for prismatic, **H** for helical, **C** for cylindrical, **S** for spherical and **E** for planar. Actuated joints are identified by a line under the corresponding joint. The letters denoting joint types are placed at the vertices of the diagram, while the links are represented by edges. But there is a problem

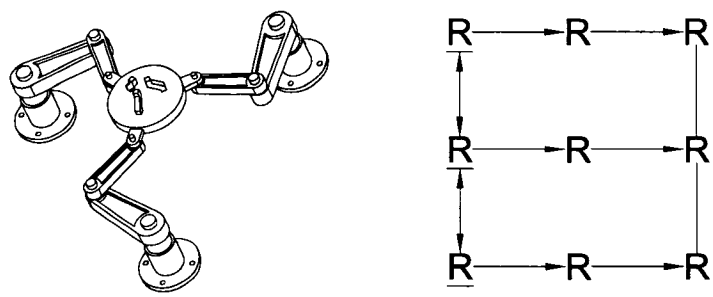

a) Physical manipulator b) Diagram

FIG. 3.8 Kinematic Composition of a Planar 3-$\underline{\text{R}}$RR parallel manipulator

for non serial mechanisms. If a link carries more than two joints, then this link corresponds to more than one edge. From the diagram, edges corresponding to

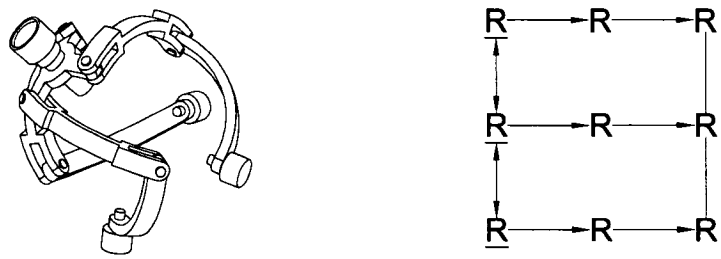

a) Physical manipulator b) Diagram

FIG. 3.9 Kinematic Composition of a Spherical 3-RRR parallel manipulator

one link can not be identified and the fact that no motion is permitted between them is not reflected. A simple way to solve this problem, while keeping the graph structure, is the use of an arrow at the edge end. Each joint has two joint elements, to which element a link is connected is indicated by the presence or absence of the arrow. Any link connected to the same joint element is actually rigidly attached and no relative motion is possible. "→R→R→R→" is a serial mechanism while "→R↔R↔R←" or "—R—R—R—" is a single link having three revolute joints. In this way, the diagram always has a graph structure. The kinematic composition of a planar parallel manipulator is shown in Fig. 3.8. The most left column represents the base carrying three actuated revolute joints while the most right column the end-effector. The end-effector is connected to the base by three identical kinematic chains composed of three revolute joints respectively. It is noteworthy that a very different manipulator shown in Fig. 3.9 has exactly the same kinematic composition. The diagram must bear additional information in order to appropriately represent the topology.

3.4.3 Essential constraints

Essential constraints are defined as the geometrical constrains necessary (but not necessary sufficient) to obtain the desired DOM of the EE and the DOF of the mechanism. There are six and only six of such geometrical constrains that qualify to an essential constrain, i.e.,

 Joint axes are skew and do not intersect;

 Joint axes are parallel and do not intersect;

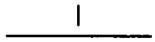 Joint axes are perpendicular and do not intersect;

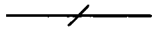 Joint axes are skew and intersect;

 Joint axes are parallel and intersect (aligned);

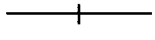 Joint axes are perpendicular and intersect.

FIG. 3.10 Graphic symbols of the six essential constraints

Superimposing the essential constraint symbols on the kinematic composition diagrams shown in Fig. 3.8 and 3.9, we obtain the the topological diagrams shown in Fig. 3.11 and 3.12. As we can see that the topology of the planar parallel manipulator is fully represented by the diagram. However, the diagram shown in Fig. 3.12 still does not reflect the fact that two joint axes intersect the third joint axis at the same point.

In order to characterize the relative situations of non-adjacent joint axes, we introduce subscripts and superscripts into the diagram. Axes of the joints with the same subscript are concurrent while those with the same superscript are parallel.

Fig. 3.13 and 3.14 show diagrams with subscripts and superscripts.

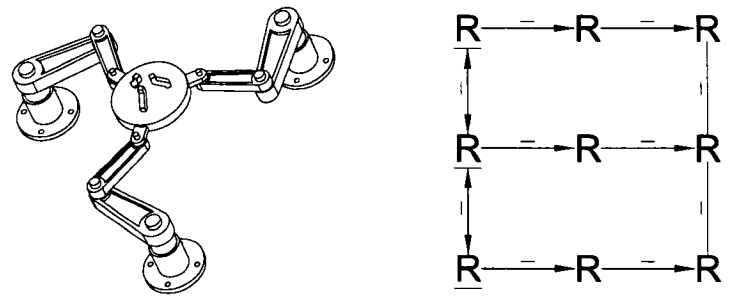

a) Physical manipulator b) Topological diagram

FIG. 3.11 Diagram of a planar parallel manipulator with essential constraints on the relative joint locations

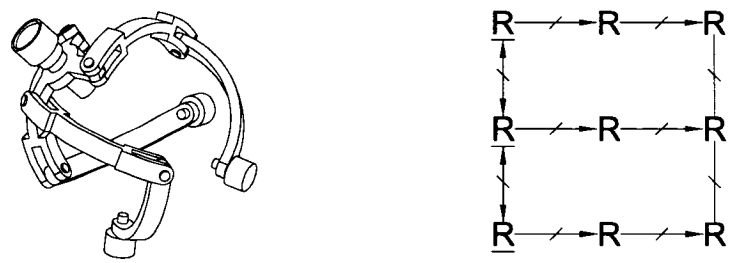

a) Physical manipulator b) Diagram

FIG. 3.12 Diagram of a spherical parallel manipulator with essential constraints on relative joint locations

3.4.4 Simplified diagram

For the sake of representation simplicify, complex constraints are introduced and expressed by constraint vertices. A constraint vertex is indicated by a rectangle. Inside the rectangle, either a meaningful symbol or a notation index can be placed. Some symbols are proposed as shown in Fig. 3.15. An example is shown in Fig. 3.16.

Some special constraints on relative locations of revolute joints can be found in a

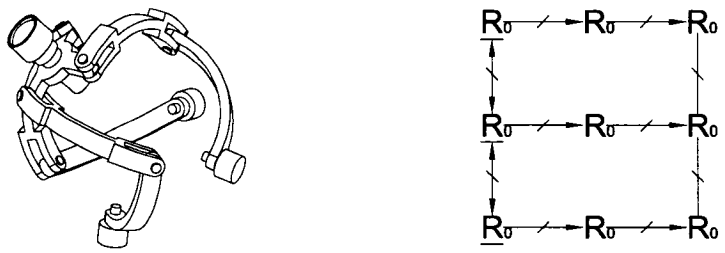

a) Physical manipulator b) Topological diagram

FIG. 3.13 Diagram of a spherical parallel manipulator with constraints on relative non-adjacent joint Locations

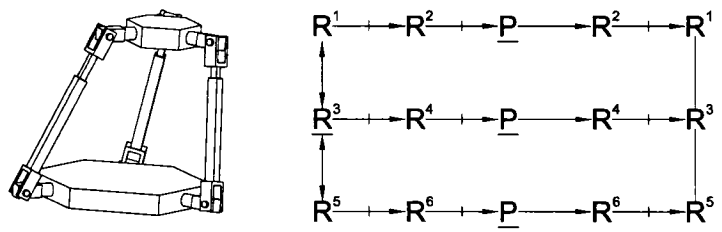

a) Physical manipulator b) Topological diagram

FIG. 3.14 Diagram of 3-UPU

large number of manipulator designs, introducing the following complex joints can greatly simplify their representations. These complex joints are shown in Fig. 3.17, where the *PI* joint is proposed by Angeles (ANGELES, 2002). Two examples are shown in Fig. 3.18 and Fig. 3.19.

3.4.5 Topological diagram

The diagram containing information on both the kinematic composition and the essential constraints is referred here as the *topological diagram*. A summary of topological diagram is given in the following paragraphs.

Coplanar

Concurrent

Intersect at equal angle

Axes (points) forming the edges (vertices) of an equilateral polygon

Equal link length

FIG. 3.15 Some additional symbols for complex constraints

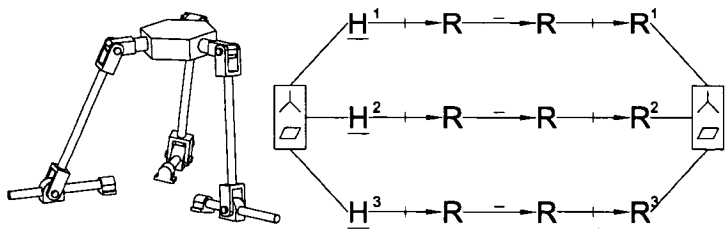

a) Physical manipulator b) Diagram of a subtopology

FIG. 3.16 Diagram with Constraint Vertices

A topological diagram has vertices and edges. There are joint vertices and constraint vertices. Joint vertices are marked by an upper case letter or a circled graphic symbol denoting a joint, while constraint vertices are indicated by a rectangle denoting special constraints on joints connected to it. Edges connecting joint vertices denote links. The leftmost edge corresponds to the base while the rightmost edge to the end-effector. Links have two kinds of extremities, *i.e.* with an arrow and without arrow. Links connected to the same joint element of a joint have the same kind of extremities pointing to this joint, they are rigidly attached. The ways to indicate the essential constraints are :

1. superimpose graphical symbols on edges;
2. add subscripts to joint vertices to indicate the concurrent joint axes;
3. add superscripts to joint vertices to indicate which joints are parallel;
4. add constraint vertices.

Ⓗ Two consecutive parallel revolute joints

Ⓔ Three parallel revolute joints

Ⓟ PI joint

Ⓐ Two revolute joints with general relative location

Ⓧ Two intersecting revolute joints

Ⓣ Two revolute joints intersecting at right angle

Ⓨ Tree concurrent revolute joints

Ⓤ Universal joint

FIG. 3.17 Complex Joints

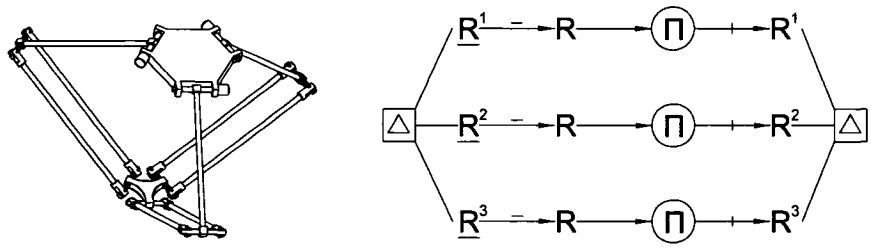

a) Physical manipulator b) Diagram

FIG. 3.18 Diagram of Delta (CLAVEL, 1988)

Joints can be grouped into complex joints to simplify the topological diagram. Actuated joints will not be grouped with non actuated joints. When different grouping is possible, the order from high priority to low priority is shown in Fig. 3.20

3.5 Additionnal Examples of Topological Diagrams

3.5.1 Serial manipulators

Two examples are shown in Fig. 3.21, and 3.22.

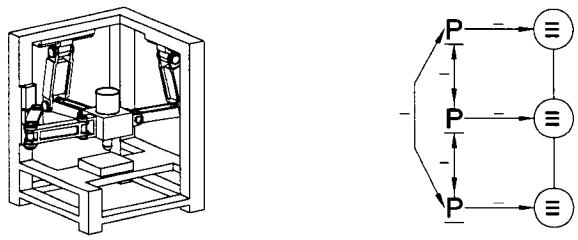

FIG. 3.19 Diagram of parallel manipulator proposed by (KIM ET TSAI, 2002)

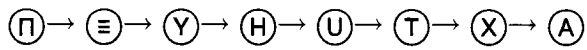

FIG. 3.20 Joint grouping priority order

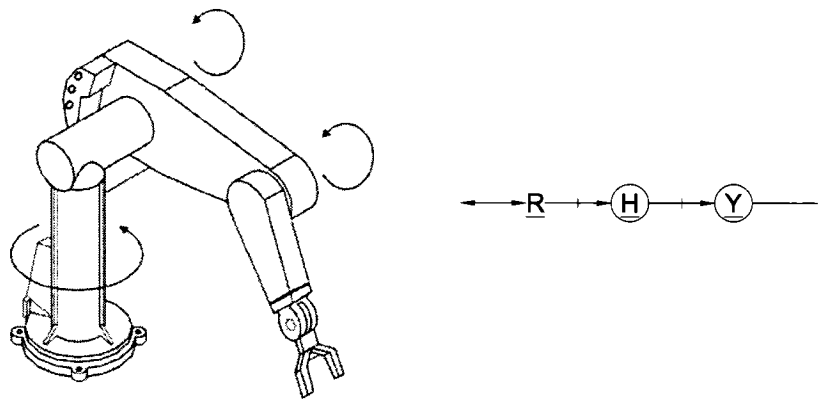

FIG. 3.21 PUMA manipulator

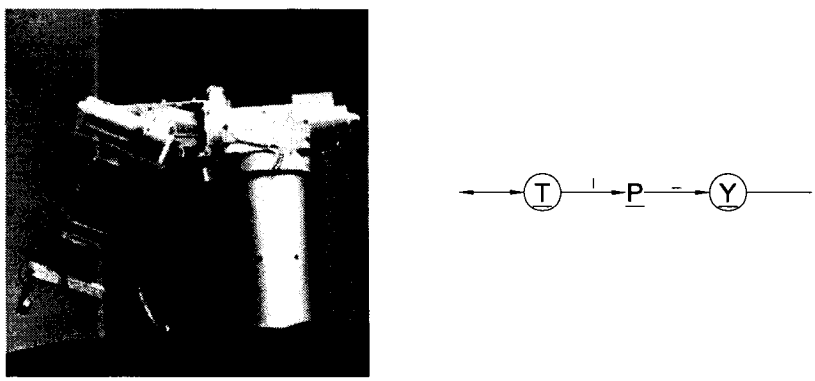

FIG. 3.22 A serial manipulator designed by Victor Scheinman, photo by Les Earnest, scanned by Bruce Baumgart

3.5.2 Parallel manipulators

Three examples are shown in Fig. 3.23, 3.24, and 3.25.

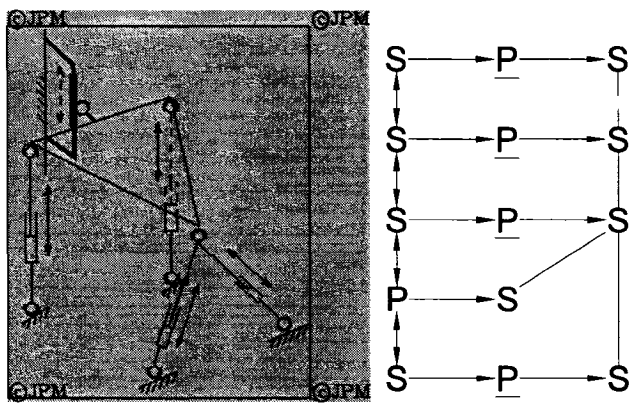

FIG. 3.23 4-DOF Flight Simulator by Koevermans W.P. et al., drawing by Merlet, J.P

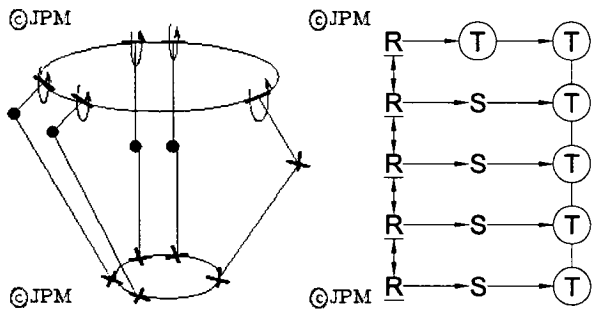

FIG. 3.24 5-DOF by Hesselbach J. et al., drawing by Merlet, J.P.

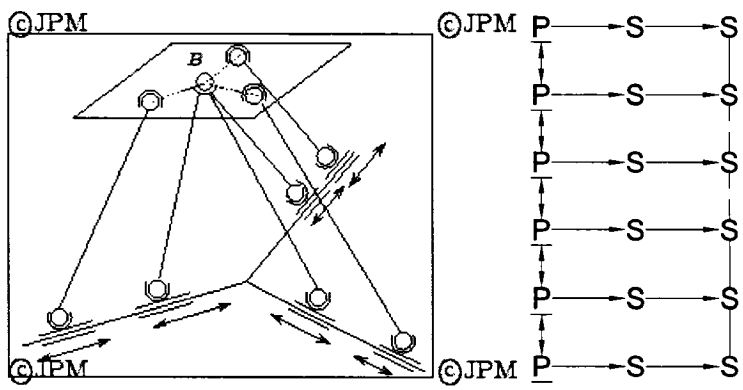

FIG. 3.25 6-DOF Decoupled Manipulator by Nabla, drawing by Merlet J.P

3.6 Kinematic Synthesis Methodology

There exist three major synthesis approaches for spatial manipulators. The first one consists of three steps :

1. Determine the possible kinematic compositions;
2. For each kinematic composition, a parametrization is performed;
3. With some of the parameters as design variables, the search for suitable designs is performed.

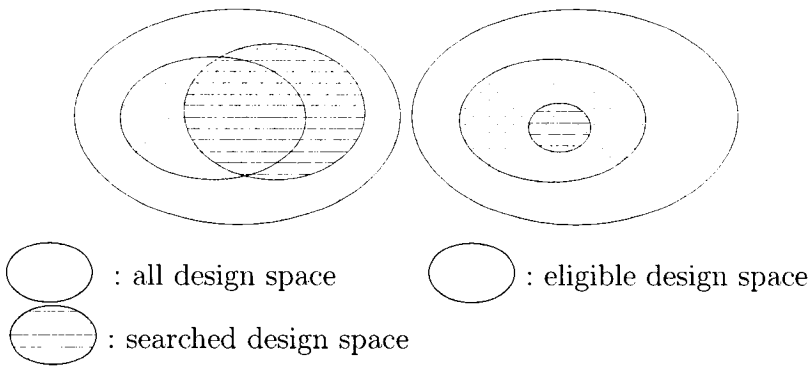

FIG. 3.26 Illustration of design spaces

The choice of the design variables is usually done by resorting to experience and intuition. As shown in Section 2, given a kinematic composition, particular geometric constraints must be satisfied in order for the manipulator to have required kinematic properties. This approach inevitably suffers from the poor correspondance between the suitable design space and the searched design space (illustrated in Fig. 3.26). With the second approach, synthesis based on screw theory or instantaneous kinematics for instance, the synthesis model is formulated as implicit functions with joint types and link geometries as unknowns. It is obvious that the synthesis can not be performed without the implication of all link geometries, making it not suitable for qualitative synthesis. The third approach is based on group theory. This approach is limited to kinematic chains whose displacements form a Lie group.

The systematic analysis of the essential constraints can improve these synthesis approaches. Since the essential constraints are relative locations between lines or between points and lines, they can be easily formulated into the kinematic model. Only parameters which are not under the essential constraints are taken as design variables, a good correspondance between the intended manipulators and the

synthesis model can therefore be achieved. With the kinematic compositions and essential constraints, qualitative or topological synthesis can be performed.

3.7 Conclusion

By introducing the essential constraints into the concept of topology, we believe that both serial and parallel manipulators can be better characterized, and would easier the topological and geometrical synthesis procedures. However, the topological synthesis of spatial manipulator is no longer dimension-independent, since most of the topological syntheses becomes a search for some special geometrical constraints, which play a key role in determining the required kinematic properties. On the other hand, it is necessary to identify the essential constraints when performing geometrical synthesis in order for the design space to correspond to the intended topology. The proposed topological diagrams are comprehensive, and enables the kinematic composition to be described precisely. The essential constraints are appropriately reflected, while the geometry is completely extracted from the diagrams. The graph structure makes it possible to implement computer algorithms in order to perform systematic enumeration, comparison and classification of serial and parallel manipulators. The topological diagram is also a useful tool for manual or automatic synthesis. It is highly flexible and can be extended with ease by introducing new joint or constraint symbols.

Acknowledgment

The authors acknowledge the financial support of NSERC (National Science and Engineering Research Council of Canada) under grants OGPIN-203618 and RGPIN-138478.

References

ANGELES, J. (1982). *Spatial Kinematic Chains. Analysis, Synthesis, Optimization.* Springer-Verlag, Berlin.

ANGELES, J. (2002). The qualitative synthesis of parallel manipulators. In *Proceedings of the WORKSHOP on Fundamental Issues and Future Research Directions for Parallel Mechanisms and Manipulators*, Quebec City, Quebec, Canada.

ANGELES, J. (c2003). *Fundamentals of robotic mechanical systems : theory, methods, and algorithms.* Mechanical engineering series : Mechanical engineering series (Springer). Springer, New York, 2nd ed. edition.

BALKAN, T., KEMAL OZGOREN, M., SAHIR ARIKAN, M., AND MURAT BAYKURT, H. (2001). A kinematic structure-based classification and compact kinematic equations for six-dof industrial robotic manipulators. *Mechanism and Machine Theory*, **36**(7), 817 - 832.

BARON, L. (c1997). *Contributions to the estimation of rigid-body motion under sensor redundancy.* PhD thesis, McGill University.

BENNETT, G. (1903). A new mechanism. *Engineering.*

CHEDMAIL, P. (1998). Optimization of multi-dof mechanisms. In Angeles, J. and Zakhariev, E., editors, *Computational Methods in Mechanisms System*, pages 97–130. Springer Verlag.

CHEN, P. AND ROTH, B. (1969). A unified theory for finitely and infinitesimally seperated position problems of kinematic synthesis. *ASME Journal of Engineering for Industry, Series B*, **91**, 203–208. Record Number : 2800.

CLAVEL, R. (1988). Delta, a fast robot with parallel geometry. *Proceedings of the 18th International Symposium on Industrial Robots*, pages 91 – 100.

CROSSLEY, F. (1962). Contribution to gruebler's theory in number synthesis of plane mechanisms. *American Society of Mechanical Engineers – Papers*, pages 5 –.

CROSSLEY, F. (1965). Permutations of kinematic chains of eight members or less from graph – theoretic viewpoint. *Developments in Theoretical and Applied Mechanics*, **2**, 467 – 486.

DENAVIT, J. AND HARTENBERG, R. S. (1954). Kinematic notation for lower-pair mechanisms based on matrices. In *American Society of Mechanical Engineers (ASME)*.

FREUDENSTEIN, F. AND MAKI, E. (1965). On a theory for the type synthesis of mechanism. In *Proceedings of the 11th International Congress of Applied Mechanics*, Springer, Berlin, pages 420–428.

GOSSELIN, C. M., RICARD, R., AND NAHON, M. A. (1995). Comparison of architectures of parallel mechanisms for workspace and kinematic properties. *American Society of Mechanical Engineers, Design Engineering Division (Publication) DE*, **82**(1), 951 – 958.

HUNT, K. H. (1982a). Geometry of robotics devices. *Mechanical Engineering Transactions*, **7**(4), 213–220. Record Number : 2700 1982.

HUNT, K. H. (1982b). Structural kinematics of in parallel actuated robot arms. Record Number : 2710 Proceedings Title : Design and Production Engineering Technical Conference Place of Meeting : Washington.

IFToMM (2003). Iftomm terminology. *Mechanism and Machine Theory*, **38**, 913–912.

ISO (1981). Kinematic diagrams - graphical symbols. ISO 3952-1, 1981.

Kim, H. S. and Tsai, L.-W. (2002). Evaluation of a cartesian parallel manipulator. In Lenarcic, J. and Thomas, F., editors, *Advances in Robot Kinematics, Theory and Applications*, pages 19–28. Kluwer Academic Publishers.

McCarthy, J. M. (1990). *An Introduction to Theoretical Kinematics*. The MIT Press, Cambridge, Massachusetts, London, England.

Merlet, J.-P. (c1997). *Les robots paralleles*. Hermes, Paris.

Ozgoren, M. (2002). Topological analysis of 6-joint serial manipulators and their inverse kinematic solutions. *Mechanism and Machine Theory*, **37**(5), 511 – 547.

Park, F. C. and Bobrow, J. E. (1995). Geometric optimization algorithms for robot kinematic design. *Journal of Robotic Systems*, **12**(6), 453 – 463.

Pierrot, F. (1991). *Robots pleinement paralleles legers : Conception, Modelisation et Commande*. PhD thesis, Universite Montpellier II, Montpellier, France.

Powell, I. (1982). The kinematic analysis and simulation of the parallel topology manipulator. *Marconi Rev. (UK)*, **45**(226), 121 – 38.

Smith, R. (1886). Diagrams of kinematics. *Engineer*.

Su, H., Collins, C., and McCarthy, J. (2002). Classification of rrss linkages. *Mechanism and Machine Theory*, **37**(11), 1413 – 1433.

THE ASSOCIATION OF GERMAN ENGINEERS (1993). Symbols for the kinematic structure description of industrial robots. Guideline 2681.

TSAI, L.-W. (2001). *Mechanism design : enumeration of kinematic structures according to function.* Mechanical engineering series : CRC mechanical engineering series. CRC Press.

TSAI, L.-W. AND JOSHI, S. (2001). Comparison study of architectures of four 3 degree-of-freedom translational parallel manipulators. *Proceedings - IEEE International Conference on Robotics and Automation*, **2**, 1283 – 1288.

WANG, X., BARON, L., AND CLOUTIER, G. (2003a). Design manifold of translational parallel manipulators. In l'Agence spatiale canadienne, editor, *Proceedings of 2003 CCToMM Symposium on Mechanisms, Machines, and Mechatronics*, Montreal, Quebec, Canada, pages 231–239.

WANG, X., BARON, L., AND CLOUTIER, G. (2003b). Kinematic modelling and isotropic conditions of a family of translational parallel manipulators. *IEEE International Conference on Control and Automation*, Montreal, Quebec, Canada, pages 173 – 177.

WANG, X., BARON, L., AND CLOUTIER, G. (2004). The design of parallel manipulators of delta topology under isotropic constraint. In Huang, T., editor, *Proceedings of the 11th World Congress in Mechanism and Machine Science*, volume 1, Tianjin, China, pages 202–206. China Machinery Press.

WENGER, P. AND CHABLAT, D. (2000). Kinematic analysis of a new parallel machine tool : The orthoglide. In Lenarcic, J. and Parenti-Castelli, V., editors, *Recent Advances in Robot Kinematics*, pages 305– 314. Kluwer Academic Publishers.

YANG, D. AND LEE, T. (1984). Feasibility study of a platform type of robotic manipulator from a kinematic viewpoint. *Journal of Mechanisms, Transmissions and Automation in Design*, **106**, 191–198.

CHAPITRE 4

MOBILITY ANALYSIS OF THREE-DEGREES-OF-FREEDOM PARALLEL MANIPULATORS

Xiaoyu Wang, Luc Baron and Guy Cloutier.
Département de génie mécanique, École Polytechnique de Montréal.
P.O. 6079, station Centre-Ville, Montréal, Québec, Canada, H3C 3A7.
xiaoyu.wang@polymtl.ca

(Submitted to the *Journal of Mechanism and Machine Theory*)

Abstract

This paper presents a systematic study of the degree of freedom (DOF) of parallel manipulators (PMs) and the degree of mobility (DOM) of their end-effector (EE). Kinematic models of PMs of general topology and geometry are established and the pose of the EE is formulated as implicit functions in terms of the topology and geometry. Analysis is then carried out in the displacement tangent space. Since in the vicinity of a non-singular configuration, displacement of any link is continuous, the DOM in the tangent space is the DOM in the displacement space which is a neighborhood of that configuration. At a non-singular configuration, the DOM of a link can not change when the configuration change. Topological and geometrical conditions are thus derived for PMs to have a given DOF and its EE to have given DOM, while being isoconstrained when the actuated joints are locked. The kinematic analysis provides insight into the DOF and the DOM of overconstrained

and underconstrained PMs while allowing them to be treated as isoconstrained PMs.

Keywords : Parallel manipulator, Kinematics, Mobility.

4.1 Introduction

A parallel manipulator (PM) is a closed-loop mechanism in which the end-effector (EE) is connected to the base through at least two independent kinematic chains (subchains) (MERLET, 1997). It has been demonstrated in a great number of applications that PMs offer better performance than serial manipulators (SMs). The first application of PMs dates back from the 50s when a PM was proposed for a tire testing device (GOUGH, 1956). Similarly, another PM was successfully used for a flight simulator shortly thereafter (STEWART, 1965). It was more than a decade later that PMs started attracting the attention of robotic researchers (HUNT, 1978). The main advantages of PMs can be explained by the intrinsic properties of their closed-form mechanical structure and their actuator layout. In contrast with SMs which have a cantilever-like structure, the load on the EE of PMs is shared among the subchains forming a bridge-like structure, offering a better stiffness and positioning accuracy. Each subchain of a PM has only one joint actuated. It is therefore possible to use identical actuators, each of them not having to carry the others, and install them on the base or near to, thus reducing the system inertia and improving the acceleration capacity. As these performance potentials were realized, more topologies have been proposed. However, the closed-loop nature of PMs implies also very complex kinematic models, singularities and limited workspace (GOSSELIN ET ANGELES, 1990), making the applications of PMs not as successful as expected (MERLET, 2002a). One effective way to overcome these drawbacks is to separate the rotation generating structure from the position generating structure

and connect them in series to improve the overall performance and reduce the design complexity (BROGARDH, 2002). In most of the industrial applications, a full 6-degrees-of-freedom (DOF) capacity is not necessary and sometimes even undesirable (ANGELES, 2002). So the design of PMs with less than 6-DOFs became an important issue in order to take advantage of such structures.

The design work focuses mainly on two different EE mobility, i.e., the spherical PM, namely SPM, and the translational PM, namely TPM. One among others an example of SPM is the Agile Eye (GOSSELIN ET HAMEL, 1994). Based on the intuition of researches many different TPMs have been proposed such as the Delta from Clavel (CLAVEL, 1988), Y-Star from Herve (HERVE, 1991), the 3-UPU from Tsai (TSAI, 1996), and Orthoglide from Wenger and Chablat (WENGER ET CHABLAT, 2000). Based on a more systematic synthesis approaches using either group theory or screw theory, many additional TPMs have recently been proposed. Recently, some special topologies have attracted the attention. For example, the singularity-free TPM (CARRICATO ET PARENTI-CASTELLI, 2002), the linear TPM (KONG ET GOSSELIN, 2002) or the fully decoupled TPM independently proposed by Gosselin (GOSSELIN ET AL., 2004) and Tsai (KIM ET TSAI, 2002).

Kinematic modelling, analysis and synthesis of these PMs have been investigated on a case by case basis. Only a few works have focused on a systematic studies of the degree of mobility (DOM) of the EE and the DOF of a PM as a whole. Why the EE of some overconstrained PMs has multiple DOMs and why the EE of some underconstrained PMs can be isoconstrained by the actuators. This paper is aimed at the formulation and analysis of the DOF of PMs of general topology and geometry and the corresponding DOM of their EE. Topological and geometric conditions for a PM and its EE to have the given DOF and DOM to be isoconstrained are derived. This formulation allow to explain how an isoconstrained PM becomes an underconstrained or an overconstrained one and how they can be dealt within a

unified formulation.

4.2 Nomenclature

- b : subscript to identify the base;
- e : subscript to identify the end-effector;
- $\mathcal{F}_i$: reference frame attached to *link* i;
- ${}^d\boldsymbol{\rho}_c$: 3×1 position vector of the origin of $\mathcal{F}_c$ in $\mathcal{F}_d$;
- $q_{j,i}$: joint variable of i^{th} joint of j^{th} subchain;
- $\boldsymbol{\rho}_i$: 3×1 position vector of the origin of $\mathcal{F}_i$ in $\mathcal{F}_{i-1}$;
- $\boldsymbol{p}_i$: 3×1 position vector of the origin of $\mathcal{F}_i$ in $\mathcal{F}_b$
- $\mathbf{A}_i$: 3×3 orientation matrix of $\mathcal{F}_i$ with respect to $\mathcal{F}_{i-1}$;
- ${}^d\mathbf{Q}_c$: 3×3 orientation matrix of $\mathcal{F}_c$ with respect to $\mathcal{F}_d$;
- $\mathbf{Q}_c$: 3×3 orientation matrix of $\mathcal{F}_c$ with respect to $\mathcal{F}_b$;
- $\mathbf{C}_i$: 4×4 homogeneous transformation matrix of $\mathcal{F}_i$ in $\mathcal{F}_{i-1}$;
- $\mathbf{H}_i$: 4×4 homogeneous transformation matrix of $\mathcal{F}_i$ in $\mathcal{F}_b$;
- ${}^d\mathbf{H}_c$: 4×4 homogeneous transformation matrix of $\mathcal{F}_c$ in $\mathcal{F}_d$;
- $\mathbf{R_{hz}}(\theta)$ 4×4 homogeneous rotation matrix around z axis of θ;
- $\mathbf{R_{hx}}(\alpha)$ 4×4 homogeneous rotation matrix around x axis of α;
- $\mathbf{B_x}(a)$ 4×4 homogeneous translation matrix along x axis of a;
- $\mathbf{B_z}(d)$ 4×4 homogeneous translation matrix along z axis of d;
- $\boldsymbol{e}_k$: the k^{th} canonical vector which is defined as $\mathbf{e}_k \equiv \left[\underbrace{0 \cdots 0}_{k-1} 1 \underbrace{0 \cdots 0}_{n-k}\right]^T$ whose dimension is implicit and depends on the context;
- ${}^d\mathbf{T}_c$: tangent operator of $\mathcal{F}_c$ in $\mathcal{F}_d$ expressed in $\mathcal{F}_b$;
- ${}^{f,\,d}\mathbf{T}_c$: tangent operator of $\mathcal{F}_c$ in $\mathcal{F}_d$ expressed in $\mathcal{F}_f$;
- ${}^d\boldsymbol{t}_c$: tangent vector of $\mathcal{F}_c$ in $\mathcal{F}_d$ expressed in $\mathcal{F}_b$;
- ${}^{f,\,d}\boldsymbol{t}_c$: tangent vector of $\mathcal{F}_c$ in $\mathcal{F}_d$ expressed in $\mathcal{F}_f$;

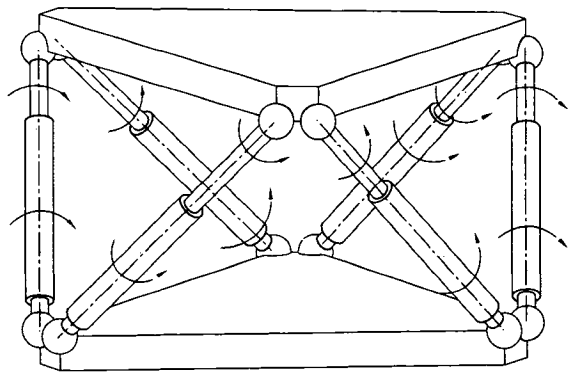

FIG. 4.1 6-SPRS PM

– $\boldsymbol{t}_c$: tangent vector of $\mathcal{F}_c$ in $\mathcal{F}_b$ expressed in $\mathcal{F}_b$.

4.3 Degree of Freedom and Mobility : Revisited

Traditionally, the DOF or DOM of a mechanism are defined as the number of independent variables needed to uniquely specify its configuration (MCCARTHY, 1990). For a SM, this is straightforward, because when the term redundant is not mentioned, the number of joints, the number of actuators, the DOF of the mechanism, and the DOM of the EE are all equal to the same number. But for general PMs, there is usually no set of independent variables which can uniquely specify its configuration. Theoretically, the number of actuators can be less than the DOF of the mechanism. For example, the 6-SPRS PM [1] shown in Fig. 4.1 has more DOF than actuators. In fact, the rotation of both the proximal and the distal links around their axes are extra DOFs. As a consequence, when a PM is said to have n DOF, it is not clear whether we are refering to the DOF of the mechanism, the number of actuators, or the DOM of the EE.

[1] S : spherical joint, P : prismatic joint, R : revolute joint. The underline indicates an actuated joint.

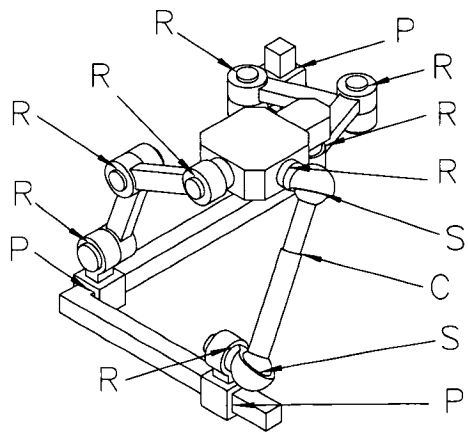

FIG. 4.2 An overconstrained PM of topology 2-PRRR and 1-PRSPRSR[2]

In this work, the following definitions are adopted :

- **Configuration** : the configuration of a PM is a specific arrangement of all its links under its structure constraints with each link having a specific pose;
- **Degree of freedom** : the degree of freedom, namely DOF, of a PM is the number of independent variables to describe its configuration;
- **Degree of mobility** : the degree of mobility, namely DOM, of a PM is the number of independent variables to describe the pose of its EE;
- **Degree of actuation** : the degree of actuation, namely DOA, of a PM is the minimum number of joints which can determine the pose of its EE.

Only a fully parallel PM has its DOF equal to its DOM and DOA. The complexity of mobility analysis can be illustrated by the overconstrained PM of topology 2-PRRR and 1-PRSPRSR[2] shown in Fig. 4.2. This PM has 3 DOMs, 4 DOAs, and 7 DOFs.

[2]The cylindrical joint, namely C, in modelled as a P and R joints, where the P is underlined since it is actuated.

4.4 Kinematics of PMs of General Topology and Geometry

As far as the kinematics is concerned, a manipulator is a kinematic chain which is a set of rigid bodies, also called *links*, coupled by *kinematic pairs*. In turn, a kinematic pair is the coupling of two links so as to constrain their relative motion (ANGELES, 2003). Each kinematic pair has two pair elements carried respectively by the two links it couples. Depending on the nature of the pair elements, a kinematic pair can be an upper or lower kinematic pair. A joint is a particular mechanical implementation of a kinematic pair (IFToMM, 2003). There are six types of joints corresponding to the *lower kinematic pairs*—spherical (S), cylindrical (C), planar (E), helical (H), prismatic (P), and revolute (R) (TSAI, 2001). All these joints can be realized by combining only the R and P joints. So in this work, without loss of generality, a PM is modelled as a kinematic chain having only P and R joints, the Denavit-Hartenberg notation (DENAVIT ET HARTENBERG, 1954) is used for each subchain. As shown in Fig. (4.3), the i^{th} link of j^{th} subchain is identified by (j, i),

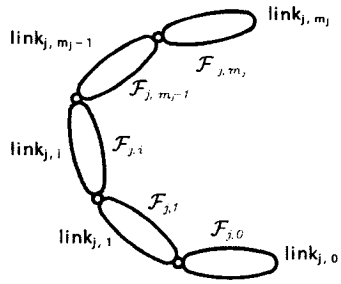

FIG. 4.3 Reference frames $\mathcal{F}_{j,i}$ attached to links 0 to m_j of the subchain j

the base being $(j, 0)$, and the EE being (j, m_j). The base and the EE are identified differently when treated in different subchains in order to unify the mathematic expression. A reference frame is attached to each link and denoted by $\mathcal{F}_{j,0}$ to $\mathcal{F}_{j,m_j}$. The *pose*, i.e., position and orientation, of a link is represented by an homogeneous transformation.

The sequence of links in the j^{th} subchain has a corresponding sequence of homogeneous transformations $\mathbf{C}_{j,0}$ to $\mathbf{C}_{j,m_j}$ that defines the pose of each link relative to the preceding link in the chain. The product of these transformations define the pose of the EE relative to the base.

$$\mathbf{H}_e = \mathbf{H}_{j,\,m_j} = \prod_{i=1}^{m_j} \mathbf{C}_{j,\,i}\left(q_{j,\,i}\right) \tag{4.1}$$

For a PM of n DOFs, its subchains are closed by attaching their end link frames together. The structure equations are thus obtained by equating the transformation products of all its subchains :

$$\mathbf{H}_e = \prod_{i=1}^{m_k} \mathbf{C}_{k,\,i}\left(q_{k,\,i}\right) = \prod_{i=1}^{m_j} \mathbf{C}_{j,\,i}\left(q_{j,\,i}\right),\ \forall j,\ k \in \{1,\ 2,\ \cdots,\ n\},\ j \neq k. \tag{4.2}$$

The possible configurations of the PM and the possible poses of the EE are determined by eq.(4.2). In general, eq.(4.2) is equivalent to a $6 \times (n-1)$ nonlinear algebaic system, for which closed-form solutions are rarely available. The complexity of such a system is illustrated by the forward kinematic problem (FKP) of generalized 3-DOF spherical PMs that can be reduced to a univariate 8^{th} degree polynomial whose solutions can only be computed by numerical means (GOSSELIN ET AL., 1994). The FKP of the Stewart-Gough platform of general geometry is another a good example, which admits up to 40 real solutions (DIETMAIER, 1998). Even a single-loop $6R$ chain of general geometry can have up to 16 configurations (RAGHAVAN ET ROTH, 1990). Therefore, we can not expect realistically to obtain a good understanding of the DOF, DOM, and DOA of a PM by directly solving eq.(4.2), not to say to derive such formula as that of Chebyshev-Grubler-Kutzbach in terms of the number of links and joints and degree of freedom of movement allowed at each joint (ANGELES ET GOSSELIN, 1988). It is reasonable that we turn our attention toward the displacement tangent space. From one hand, in the vicinity of a

non-singular configuration, the displacement of any link is continuous, the DOF or DOM in the tangent space is the DOF or DOM in the displacement space which is a neighborhood of that configuration (STRAMIGIOLI ET BRUYNINCKX, 2001). On the other hand, the Lie algebra associated with the displacement group is the set of the tangent operators, so if a subchain is a Lie group generator, the dimension of the displacement is the dimension of the tangent operator space (HERVE, 1978).

4.5 Tangent Space Formulation

Recall that the tangent operator of displacement of a rigid body is defined as :

$$\mathbf{T(t)} = \dot{\mathbf{H}}(t)\mathbf{H}(t)^{-1} \tag{4.3}$$

which computes the direction tangent of a motion (MCCARTHY, 1990). Let

$$\mathbf{H} = \begin{bmatrix} \mathbf{Q} & \mathbf{p} \\ \mathbf{0}^T & 1 \end{bmatrix} \tag{4.4}$$

then

$$\mathbf{T} = \dot{\mathbf{H}}\mathbf{H}^{-1} = \begin{bmatrix} \dot{\mathbf{Q}} & \dot{\mathbf{p}} \\ \mathbf{0}^T & 0 \end{bmatrix} \begin{bmatrix} \mathbf{Q} & \mathbf{p} \\ \mathbf{0}^T & 1 \end{bmatrix}^{-1} = \begin{bmatrix} \dot{\mathbf{Q}}\mathbf{Q}^T & \dot{\mathbf{p}} - \dot{\mathbf{Q}}\mathbf{Q}^T\mathbf{p} \\ \mathbf{0}^T & 0 \end{bmatrix} = \begin{bmatrix} \boldsymbol{\Omega} & \boldsymbol{v} \\ \mathbf{0}^T & 0 \end{bmatrix} \tag{4.5}$$

where $\boldsymbol{\Omega}$ and $\boldsymbol{v}$ are clearly defined as $\boldsymbol{\Omega} \equiv \dot{\mathbf{Q}}\mathbf{Q}^T$ and $\boldsymbol{v} \equiv \dot{\mathbf{p}} - \dot{\mathbf{Q}}\mathbf{Q}^T\mathbf{p}$. The 3×1 vector $\boldsymbol{v}$ is the velocity of a point on the link which instantaneously coincides with the origin of the reference frame, while the 3×3 skew symmetric matrix $\boldsymbol{\Omega}$ is the

angular velocity matrix related to the angular velocity vectors $\boldsymbol{\omega}$ as follows, i.e.,

$$\boldsymbol{\omega} \equiv \boldsymbol{vect}(\boldsymbol{\Omega}), \quad \boldsymbol{\Omega} \equiv \begin{bmatrix} 0 & -\omega_z & \omega_y \\ \omega_z & 0 & -\omega_x \\ -\omega_y & \omega_x & 0 \end{bmatrix}, \quad \boldsymbol{\omega} \equiv \begin{bmatrix} \omega_x \\ \omega_y \\ \omega_z \end{bmatrix}. \tag{4.6}$$

If the velocity, called *twist*, of a rigid-body is defined as the $\boldsymbol{t}$ array, i.e., $\boldsymbol{t} \equiv [\boldsymbol{\omega}^T \boldsymbol{v}^T]^T$, the bijective mapping between the tangent operator space $\{\mathbf{T}\}$ and the twist space $\{\boldsymbol{t}\}$ becomes self-evident.

A more important property of tangent operator space is its Lie algebraic structure. Since $[\mathbf{T}_a\mathbf{T}_b - \mathbf{T}_b\mathbf{T}_a]$ satisfies all the axioms for a Lie bracket, the tangent space $\{\mathbf{T}\}$ together with the product

$$[\mathbf{T}_a,\ \mathbf{T}_b] \equiv [\mathbf{T}_a\mathbf{T}_b - \mathbf{T}_b\mathbf{T}_a] \tag{4.7}$$

form a Lie algebra associated with the displacement group (STERNBERG, 1994). Many important kinematic properties of rigid body motion can thus be revealed by tangent space analysis (STRAMIGIOLI ET AL., 2002).

Under the constraints of a subchain, the only variables in the tangent operator of the EE are q_1 to q_m, by employing the derivative chain rule, we have

$$\mathbf{T}_e = \dot{\mathbf{H}}_e\mathbf{H}_e^{-1} = \sum_{i=1}^{m} \left(\frac{\partial \mathbf{H}_e}{\partial q_i} \dot{q}_i \right) \mathbf{H}_e^{-1}. \tag{4.8}$$

The pose of the EE, $\mathbf{H}_e$, can be writen in terms of the i^{th} joint as

$$\mathbf{H}_e = \mathbf{H}_{i-1}\mathbf{C}_i{}^i\mathbf{H}_e \quad \text{and} \quad {}^i\mathbf{H}_e\mathbf{H}_e^{-1} = \mathbf{C}_i^{-1}\mathbf{H}_{i-1}^{-1} \tag{4.9}$$

Using eq.(4.9), the i^{th} term of the sum of eq.(4.8) is thus written as

$$\begin{aligned}\left(\frac{\partial \mathbf{H}_e}{\partial q_i}\dot{q}_i\right)\mathbf{H}_e^{-1} &= \mathbf{H}_{i-1}\left(\frac{\partial \mathbf{C}_i}{\partial q_i}\dot{q}_i\right){}^{i}\mathbf{H}_e\mathbf{H}_e^{-1} = \mathbf{H}_{i-1}\dot{\mathbf{C}}_i{}^{i}\mathbf{H}_e\mathbf{H}_e^{-1} \\ &= \mathbf{H}_{i-1}\dot{\mathbf{C}}_i\mathbf{C}_i^{-1}\mathbf{H}_{i-1}^{-1} = \mathbf{H}_{i-1}{}^{i-1,\,i-1}\mathbf{T}_i\mathbf{H}_{i-1}^{-1} \qquad (4.10)\end{aligned}$$

where $\dot{\mathbf{C}}_i\mathbf{C}_i^{-1}$ is the tangent operator ${}^{i-1,\,i-1}\mathbf{T}_i$ expressing the motion of $\mathcal{F}_i$ relative to $\mathcal{F}_{i-1}$ and expressed in $\mathcal{F}_{i-1}$. Again, applying the derivative chain rule yieds

$${}^{i-1,i-i}\mathbf{T}_i = \dot{\mathbf{C}}_i\mathbf{C}_i^{-1} = \left(\frac{\partial \mathbf{C}_i}{\partial q_i}\mathbf{C}_i^{-1}\right)\dot{q}_i = {}^{i-1,i-1}\,\hat{\mathbf{T}}_i\dot{q}_i, \qquad (4.11)$$

where the unit tangent operator, namely ${}^{i-1,i-1}\hat{\mathbf{T}}_i$, is defined as

$${}^{i-1,i-1}\hat{\mathbf{T}}_i \equiv \frac{\partial \mathbf{C}_i}{\partial q_i}\mathbf{C}_i^{-1} \qquad (4.12)$$

Since, a change of coordinate frames from $\mathcal{F}_c$ to $\mathcal{F}_d$ of a tangent operator is computed as

$${}^{d}\mathbf{T} = {}^{d}\mathbf{H}_c{}^{c}\mathbf{T}^{c}\mathbf{H}_d, \qquad (4.13)$$

one can easily concluded that eq.(4.10) becomes

$$\left(\frac{\partial \mathbf{H}_e}{\partial q_i}\dot{q}_i\right)\mathbf{H}_e^{-1} = \mathbf{H}_{i-1}{}^{i-1,i-1}\hat{\mathbf{T}}_i\mathbf{H}_{i-1}^{-1}\dot{q}_i = {}^{i-1}\hat{\mathbf{T}}_i\dot{q}_i \qquad (4.14)$$

Now, substituation of eq.(4.14) into (4.8) yields

$$\mathbf{T}_e = \sum_{i=1}^{m}{}^{i-1}\mathbf{T}_i = \sum_{i=1}^{m}{}^{i-1}\hat{\mathbf{T}}_i\dot{q}_i \qquad (4.15)$$

which can be readily written in its twist form as

$$\boldsymbol{t}_e = \sum_{i=1}^{m}{}^{i-1}\boldsymbol{t}_i = \sum_{i=1}^{m}{}^{i-1}\hat{\boldsymbol{t}}_i\dot{q}_i. \qquad (4.16)$$

Finally, the structure equation of a PM of general topology and geometry having n subchains is given in tangent space as

$$\boldsymbol{t}_e = \sum_{i=1}^{m_j} \left({}^{i-1}\hat{\boldsymbol{t}}_{j,i} \dot{q}_{j,i} \right) = \sum_{i=1}^{m_k} \left({}^{i-1}\hat{\boldsymbol{t}}_{k,i} \dot{q}_{k,i} \right),\ \forall j,k \in \{1,\ 2,\ \cdots,\ n\},\ j \neq k \tag{4.17}$$

4.6 Tangent Space Analysis of 3-legged PMs

Following the Denavit-Hartenberg notation, the pose of $\mathcal{F}_i$ in $\mathcal{F}_{i-1}$ is as follows :

$$\mathbf{C}_i = \mathbf{B_z}\left(d_i\right)\mathbf{R_{hz}}\left(q_i\right)\mathbf{R_{hx}}\left(\alpha_i\right)\mathbf{B_x}\left(a_i\right) \text{for revolute joints} \tag{4.18}$$

$$\mathbf{C}_i = \mathbf{B_z}\left(q_i\right)\mathbf{R_{hz}}\left(\theta_i\right)\mathbf{R_{hx}}\left(\alpha_i\right)\mathbf{B_x}\left(a_i\right) \text{for prismatic joints} \tag{4.19}$$

where a_i being the link length, α_i the twist angle, d_i the offset and θ_i the rotation angle. The unit tangent operator ${}^{i-1,i-1}\hat{\mathbf{T}}_i$ can thus be writen as

$${}^{i-1,i-1}\hat{\mathbf{T}}_i = \begin{bmatrix} 0 & -1 & 0 & 0 \\ 1 & 0 & 0 & 0 \\ 0 & 0 & 0 & 0 \\ 0 & 0 & 0 & 0 \end{bmatrix} \text{(R joint)}, \quad {}^{i-1,i-1}\hat{\mathbf{T}}_i = \begin{bmatrix} 0 & 0 & 0 & 0 \\ 0 & 0 & 0 & 0 \\ 0 & 0 & 0 & 1 \\ 0 & 0 & 0 & 0 \end{bmatrix} \text{(P joint)} \tag{4.20}$$

whose corresponding twist forms are given as

$${}^{i-1,i-1}\hat{\boldsymbol{t}}_i = [0\ 0\ 1\ 0\ 0\ 0]^T \text{(R joint)}, \quad {}^{i-1,i-1}\hat{\boldsymbol{t}}_i = [0\ 0\ 0\ 0\ 0\ 1]^T \text{(P joint)} \tag{4.21}$$

Upon changing the reference frame from $\mathcal{F}_{i-1}$ to $\mathcal{F}_b$, we get

$${}^{i-1}\hat{\boldsymbol{t}}_i = \begin{bmatrix} \hat{\boldsymbol{\omega}}_i \\ \boldsymbol{p}_i \times \hat{\boldsymbol{\omega}}_i \end{bmatrix} \text{(R joint)}, \quad {}^{i-1}\hat{\boldsymbol{t}}_i = \begin{bmatrix} \mathbf{0} \\ \hat{\boldsymbol{v}}_i \end{bmatrix} \text{(P joint)} \tag{4.22}$$

where $\mathbf{0}$ is 3×1 zero vector, $\hat{\boldsymbol{\omega}}_i$, $\boldsymbol{p}_i$, and $\hat{\boldsymbol{v}}_i$ are vectors determined respectively by the joint orientation and position of a R joint, and the joint orientation of a P joint. We can see that the unit tangent vectors of R joints and P joints have very distinctive structures. In fact, if a P joint is considered as a R joint at infinity, the unit tangent vector is the normalized *Plücker* coordinates of the joint axis. This inspires us to represent topology and geometry with the normalized *Plücker* coordinates of the joint axes at a given configuration—the structure represents topology while the numerical values represent the geometry.

Let us introduces the following valiables, i.e.,

- x_i : actuated joint rate,
- $[\hat{\boldsymbol{n}}_j^T \ \hat{\boldsymbol{m}}_j^T]^T$: unit tangent vector of actuated joint,
- $\boldsymbol{y}_j$: vector composed of the passive revolute joint rates,
- $\mathbf{Y}_j$: matrix composed of the unit tangent vectors corresponding to $\boldsymbol{y}_j$,
- $\boldsymbol{z}_j$: vector composed of the passive prismatic joint rates,
- $\mathbf{Z}_j$: matrix composed of the unit tangent vectors corresponding to $\boldsymbol{z}_j$,

$$\boldsymbol{x}_j \equiv \begin{bmatrix} \hat{\boldsymbol{n}}_j \\ \hat{\boldsymbol{m}}_j \end{bmatrix}, \mathbf{Y}_j \equiv \begin{bmatrix} \mathbf{N}_j \\ \mathbf{M}_j \end{bmatrix}, \mathbf{Z}_j \equiv \begin{bmatrix} \mathbf{O}_j \\ \mathbf{K}_j \end{bmatrix}, \mathbf{W}_j \equiv \begin{bmatrix} \mathbf{N}_j & \mathbf{O}_j \\ \mathbf{M}_j & \mathbf{K}_j \end{bmatrix} \quad (4.23)$$

$$\boldsymbol{u} \equiv [\boldsymbol{y}_1^T \ \boldsymbol{z}_1^T \ \boldsymbol{y}_2^T \ \boldsymbol{z}_2^T \ \boldsymbol{y}_3^T \ \boldsymbol{z}_3^T]^T, \quad \boldsymbol{a} \equiv [x_1 \ x_2 \ x_3]^T \quad (4.24)$$

Thus, the general eq.(4.17) can written in the contexte of 3-DOF PMs as

$$\boldsymbol{t}_e = \boldsymbol{x}_1 x_1 + \mathbf{W}_1 \begin{bmatrix} \boldsymbol{y}_1 \\ \boldsymbol{z}_1 \end{bmatrix} \quad (4.25)$$

$$\boldsymbol{x}_1 x_1 + \mathbf{W}_1 \begin{bmatrix} \boldsymbol{y}_1 \\ \boldsymbol{z}_1 \end{bmatrix} = \boldsymbol{x}_2 x_2 + \mathbf{W}_2 \begin{bmatrix} \boldsymbol{y}_2 \\ \boldsymbol{z}_2 \end{bmatrix} \quad (4.26)$$

$$\boldsymbol{x}_2 x_2 + \mathbf{W}_2 \begin{bmatrix} \boldsymbol{y}_2 \\ \boldsymbol{z}_2 \end{bmatrix} = \boldsymbol{x}_3 x_3 + \mathbf{W}_3 \begin{bmatrix} \boldsymbol{y}_3 \\ \boldsymbol{z}_3 \end{bmatrix} \tag{4.27}$$

which is a set of linear equations with the tangent vector of the EE and the passive joint rates as unknowns. It is obvious that the configuration of the PM is completely determined by eqs.(4.26) and (4.27) which can be rearranged in a matrix form

$$\mathbf{W}_B \boldsymbol{u} = \mathbf{X}_B \boldsymbol{a}, \tag{4.28}$$

where $\mathbf{W}_B$ and $\mathbf{X}_B$ are defined as

$$\mathbf{W}_B \equiv \begin{bmatrix} \mathbf{W}_1 & -\mathbf{W}_2 & \mathbf{O}_3 \\ \mathbf{O}_1 & \mathbf{W}_2 & -\mathbf{W}_3 \end{bmatrix}, \quad \mathbf{X}_B \equiv \begin{bmatrix} -\boldsymbol{x}_1 & \boldsymbol{x}_2 & \mathbf{0} \\ \mathbf{0} & -\boldsymbol{x}_2 & \boldsymbol{x}_3 \end{bmatrix} \tag{4.29}$$

where $\mathbf{O}$ is zero matrix whose dimensions are determined by the adjacent block matrices. Mathematically, eqs.(4.28) and (4.29) can be underdetermined, overdetermined, or exactly determined. Each situation corresponds to a particular topological and geometrical design of 3 legged PM.

4.6.1 Isoconstrained PMs of 3-DOF

If a 3-DOF PM is isoconstrained, eq.(4.28) should be exactly constrained, implying that matrix that the 12×12 passive joint matrix, $\mathbf{W}_B$, must be invertable, i.e., a non-singular. This provides a theoretical basis for mobility analysis and for the topological and geometrical synthesis of PMs.

First of all, from the dimension of $\mathbf{W}_B$, the total number of passive joints should be 12 in order for a PM to be of 3 DOF. Then by observing the block columns of $\mathbf{W}_B$, one can concluded that none of the three subchains should have more than

6 passive joints, otherwise $\mathbf{W}_B$ will not have full column rank, that is to say, $\mathbf{W}_B$ becomes singular.

When $\mathbf{W}_B$ is square and none-singular, then by premultiplying eq.(4.28) by $\mathbf{W}_B^{-1}$, we obtain

$$\boldsymbol{u} = \mathbf{W}_B^{-1}\mathbf{X}_B\boldsymbol{a} \tag{4.30}$$

It is obvious that the DOF of the PM is equal to 3, because the 3 actuated joint variables are independent and all other joint variables are their linear combination. Therefore, by definition, the DOF of the PM is equal to 3. However, that a PM is of 3 DOFs does not necessarily mean that it is of 3 DOMs, an important issue involved in the topological and geometrical synthesis. Suppose the first two subchains have 6 passive joints apiece, leaving no passive joint for the third subchain, then according to equation (4.17), the EE can only have 1 DOM. In this case, changing the first two of the three actuated joint variables affects only the configuration of the PM, not the pose of its EE, the later being determined solely by the third actuated joint. Therefore, for a PM to have 3 DOMs, none of its subchains should have less than 2 passive joints.

Now, suppose the first subchain has 2 passive joints while the third subchain has 6 passive joints leaving 4 passive joints for the second subchain, then the first six equations of (4.28) are as the following :

$$[\mathbf{W}_1 \ -\mathbf{W}_2]\ [\boldsymbol{y}_1^T\ \boldsymbol{z}_1^T\ \boldsymbol{y}_2^T\ \boldsymbol{z}_2^T]^T = [-\boldsymbol{x}_1\ \boldsymbol{x}_2]\ [x_1\ x_2]^T \tag{4.31}$$

where $[\mathbf{W}_1 \ -\mathbf{W}_2]$ is 6×6 and non-singular, because $\mathbf{W}_B$ is non-singular. Premultiplying eq.(4.31) by $[\mathbf{W}_1 \ -\mathbf{W}_2]^{-1}$ leads to

$$[\boldsymbol{y}_1^T\ \boldsymbol{z}_1^T\ \boldsymbol{y}_2^T\ \boldsymbol{z}_2^T]^T = [\mathbf{W}_1 \ -\mathbf{W}_2]^{-1}[-\boldsymbol{x}_1\ \boldsymbol{x}_2][x_1\ x_2]^T \tag{4.32}$$

Observing eqs.(4.25) and (4.32), one knows that the tangent vector of the EE depends only on x_1 and x_2, *i.e.*, the actuated joint rates of the first two subchains, the DOM of the PM is therefore equal to 2. In order for a PM to have 3 DOMs, the possible combinations of the passive joint numbers are thus (2, 5, 5), (3, 4, 5), and (4, 4, 4).

Now, we go back to eqs.(4.25) and (4.29) to see how the DOM is affected by the disposition of the actuated joints. From eq.(4.29), the passive joint rates of the first subchain are given as :

$$\begin{bmatrix} \boldsymbol{y}_1 \\ \boldsymbol{z}_1 \end{bmatrix} = \begin{bmatrix} \underbrace{1}_{(m_1-1)\times(m_1-1)} & \mathbf{O} \end{bmatrix} \mathbf{W}_B^{-1}\mathbf{X}_B \begin{bmatrix} x_1 & x_2 & x_3 \end{bmatrix}^T \tag{4.33}$$

Let us introduces matrix $\mathbf{E}$ as follows

$$\mathbf{E} \equiv \begin{bmatrix} \underbrace{1}_{(m_1-1)\times(m_1-1)} & \mathbf{O} \end{bmatrix} \mathbf{W}_B{}^{-1}\mathbf{X}_B \tag{4.34}$$

By substituting equations (4.33) and (4.34) into equation (4.25), we get

$$\begin{aligned} \boldsymbol{t}_e &= \boldsymbol{x}_1 x_1 + \mathbf{W}_1\mathbf{E} \begin{bmatrix} x_1 & x_2 & x_3 \end{bmatrix}^T \\ &= \left[\boldsymbol{x}_1 \boldsymbol{e}_1^T + \mathbf{W}_1\mathbf{E}\right] \begin{bmatrix} x_1 & x_2 & x_3 \end{bmatrix}^T \\ &= \begin{bmatrix} \boldsymbol{x}_1 & \mathbf{W}_1 \end{bmatrix} \begin{bmatrix} \boldsymbol{e}_1 & \mathbf{E}^T \end{bmatrix}^T \begin{bmatrix} x_1 & x_2 & x_3 \end{bmatrix}^T \end{aligned} \tag{4.35}$$

It is clear that the DOM is equal to the rank of matrix $\begin{bmatrix} \boldsymbol{x}_1 & \mathbf{W}_1 \end{bmatrix} \begin{bmatrix} \boldsymbol{e}_1 & \mathbf{E}^T \end{bmatrix}^T$. A good reasoning is that if $\boldsymbol{x}_1 \in \mathit{range}\,(\mathbf{W}_1)$, the PM will lose one DOM.

Suppose

$$\boldsymbol{x}_1 = \mathbf{W}_1\boldsymbol{\xi}_1,\ \boldsymbol{\xi}_1 \in \mathbb{R}^{m_1-1},\ \|\boldsymbol{\xi}_1\|_2 \neq 0 \tag{4.36}$$

Since

$$\begin{bmatrix} \mathbf{W}_1 & -\mathbf{W}_2 & \mathbf{O}_3 \\ \mathbf{O}_1 & \mathbf{W}_2 & -\mathbf{W}_3 \end{bmatrix}^{-1} \begin{bmatrix} \mathbf{W}_1 & -\mathbf{W}_2 & \mathbf{O}_3 \\ \mathbf{O}_1 & \mathbf{W}_2 & -\mathbf{W}_3 \end{bmatrix} = \mathbf{1} \tag{4.37}$$

we have

$$\mathbf{W}_B^{-1} \begin{bmatrix} \mathbf{W}_1 \\ \mathbf{O}_1 \end{bmatrix} = \begin{bmatrix} \mathbf{1}_1 \\ \mathbf{O}_1 \end{bmatrix} \tag{4.38}$$

Rewrite eq.(4.29) as

$$\boldsymbol{u} = \mathbf{W}_B^{-1} \begin{bmatrix} -\boldsymbol{x}_1 \\ \mathbf{0} \end{bmatrix} x_1 + \mathbf{W}_B^{-1} \begin{bmatrix} \boldsymbol{x}_1 \\ -\boldsymbol{x}_2 \end{bmatrix} x_2 + \mathbf{W}_B^{-1} \begin{bmatrix} \mathbf{0} \\ \boldsymbol{x}_2 \end{bmatrix} x_3 \tag{4.39}$$

Using eqs.(4.36) and (4.38), we have

$$\mathbf{W}_B^{-1} \begin{bmatrix} -\boldsymbol{x}_1 \\ \mathbf{0} \end{bmatrix} = \mathbf{W}_B^{-1} \begin{bmatrix} -\mathbf{W}_1 \boldsymbol{\xi}_1 \\ \mathbf{O}_1 \end{bmatrix} = \begin{bmatrix} -\boldsymbol{\xi}_1 \\ \mathbf{0}_1 \end{bmatrix} \tag{4.40}$$

Substituting eq.(4.40) into eq.(4.39), we get

$$\boldsymbol{u} = \begin{bmatrix} -\boldsymbol{\xi}_1 x_1 \\ \mathbf{0}_1 \end{bmatrix} + \mathbf{W}_B^{-1} \begin{bmatrix} \boldsymbol{x}_1 \\ -\boldsymbol{x}_2 \end{bmatrix} x_2 + \mathbf{W}_B^{-1} \begin{bmatrix} \mathbf{0} \\ \boldsymbol{x}_2 \end{bmatrix} x_3 \tag{4.41}$$

So, x_1 does not appear in the solutions for $\boldsymbol{y}_2$, $\boldsymbol{z}_2$, $\boldsymbol{y}_3$, and $\boldsymbol{z}_3$. From

$$\boldsymbol{t}_e = \boldsymbol{x}_2 x_2 + \mathbf{W}_2 \begin{bmatrix} \boldsymbol{y}_2 \\ \boldsymbol{z}_2 \end{bmatrix} \tag{4.42}$$

we know that the PM loses 1 DOM. It is therefore necessary that the unit tangent vectors of the same subchain are linearly independent for the PM to have 3 DOMs.

This means that

$$\mathbf{A} \equiv \begin{bmatrix} \boldsymbol{x}_1 & \mathbf{0} & \mathbf{0} & \mathbf{W}_1 & \mathbf{O} & \mathbf{O} \\ \mathbf{0} & \boldsymbol{x}_2 & \mathbf{0} & \mathbf{O} & \mathbf{W}_2 & \mathbf{O} \\ \mathbf{0} & \mathbf{0} & \boldsymbol{x}_3 & \mathbf{O} & \mathbf{O} & \mathbf{W}_3 \end{bmatrix} \tag{4.43}$$

which we call the *joint matrix* has full column rank. From eqs.(4.25) to (4.27), (4.29), and (4.43), we have

$$\boldsymbol{t}_{3e} = \mathbf{A} \begin{bmatrix} \boldsymbol{a} \\ \boldsymbol{u} \end{bmatrix} = \mathbf{A} \begin{bmatrix} \boldsymbol{a} \\ \mathbf{W}_B^{-1}\mathbf{X}_B\boldsymbol{a} \end{bmatrix} = \mathbf{A} \begin{bmatrix} \mathbf{1} \\ \mathbf{W}_B^{-1}\mathbf{X}_B \end{bmatrix} \boldsymbol{a} = \mathbf{AB}\boldsymbol{a} \tag{4.44}$$

where matrix $\mathbf{B}$ and $\boldsymbol{t}_{3e}$ are defined as

$$\mathbf{B} \equiv \begin{bmatrix} \mathbf{1} \\ \mathbf{W}_B^{-1}\mathbf{X}_B \end{bmatrix}, \quad \boldsymbol{t}_{3e} \equiv \begin{bmatrix} \boldsymbol{t}_e \\ \boldsymbol{t}_e \\ \boldsymbol{t}_e \end{bmatrix}. \tag{4.45}$$

Equation (4.44) shows that the DOM of the PM is equal to the rank of the matrix product $\mathbf{AB}$. Now, by performing singular value decomposition of matrices $\mathbf{A}$ and $\mathbf{B}$, i.e.,

$$\mathbf{A} = \mathbf{U}_A \begin{bmatrix} \mathbf{\Lambda}_A \\ \mathbf{O}_A \end{bmatrix} \mathbf{V}_A^T, \quad \mathbf{B} = \mathbf{U}_B \begin{bmatrix} \mathbf{\Lambda}_B \\ \mathbf{O}_B \end{bmatrix} \mathbf{V}_B^T \tag{4.46}$$

we get

$$\mathbf{AB} = \mathbf{U}_A \begin{bmatrix} \mathbf{\Lambda}_A \\ \mathbf{O}_A \end{bmatrix} \mathbf{V}_A^T\mathbf{U}_B \begin{bmatrix} \mathbf{\Lambda}_B \\ \mathbf{O}_B \end{bmatrix} \mathbf{V}_B^T = \mathbf{U}_A \begin{bmatrix} \mathbf{\Lambda}_A\mathbf{V}_A^T\mathbf{U}_B \\ \mathbf{O}_A \end{bmatrix} \begin{bmatrix} \mathbf{\Lambda}_B\mathbf{V}_B^T \\ \mathbf{O}_B \end{bmatrix}$$

$$= \mathbf{U}_A \begin{bmatrix} \mathbf{\Lambda}_A \mathbf{V}_A^T \mathbf{U}_B \begin{bmatrix} \mathbf{\Lambda}_B \mathbf{V}_B^T \\ \mathbf{O}_B \end{bmatrix} \\ \mathbf{O} \end{bmatrix} \tag{4.47}$$

Since both $\mathbf{A}$ and $\mathbf{B}$ have full column rank, the diagonal matrices $\mathbf{\Lambda}_A$ and $\mathbf{\Lambda}_B$ are invertable. From a corollary of the linear algebraic theorem on the rank of a product of two matrices, i.e., if matrix one is invertable, then the rank of the product of matrix one and matrix two is equal to the rank of matrix two. We know that $\mathbf{AB}$ is of rank 3, that is to say, $\boldsymbol{t}_{3e}$ is of 3 dimensions, the PM is of 3 DOMs. Observing equation (4.45), it should be pointed out that the relative positions of the three actuated joints do not affect the DOM of the PM. Even their axes coincide, reducing the rank of matrix $\mathbf{X}_B$ to 2, matrix $\mathbf{B}$ is still of rank 3, leaving the DOM of the PM unchanged.

In summary, for an isoconstrained PM to have 3 DOFs and 3 DOMs, the necessary and sufficient conditions are as follows :

1. the passive joint number combinations of the subchains are (2, 5, 5), (3, 4, 5), or (4, 4, 4);
2. the passive joint matrix is square and non-singular;
3. the joint matrix has full column rank.

Behind the above mathematical statements is the topological and geometric information. Rewrite equation (4.28) as

$$\mathbf{V}_B \boldsymbol{u} = \mathbf{X}_B \boldsymbol{a}, \quad \mathbf{V}_B \equiv \begin{bmatrix} \mathbf{N}_1 & \mathbf{O} & -\mathbf{N}_2 & \mathbf{O} & \mathbf{O} & \mathbf{O} \\ \mathbf{M}_1 & \mathbf{K}_1 & -\mathbf{M}_2 & -\mathbf{K}_2 & \mathbf{O} & \mathbf{O} \\ \mathbf{O} & \mathbf{O} & \mathbf{N}_2 & \mathbf{O} & -\mathbf{N}_3 & \mathbf{O} \\ \mathbf{O} & \mathbf{O} & \mathbf{M}_2 & \mathbf{K}_2 & -\mathbf{M}_3 & -\mathbf{K}_3 \end{bmatrix}. \tag{4.48}$$

to reveal the special structure of the unit tangent vectors, i.e. the upper half of the

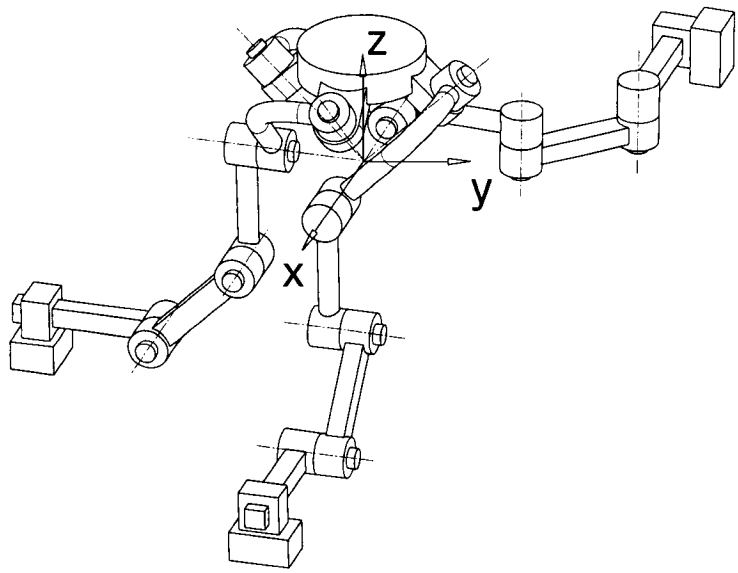

FIG. 4.4 A new isoconstrained spherical PM

tangent vector of a prismatic joint is a zero vector while the lower half is a zero vector for the tangent operator of a R joint whose axis passes through the reference origin. This can be easily verified with the new isoconstrained spherical PM shown in Fig. 4.4. Observing the block rows of the passive joint matrix, necessary conditions for it to be non-singular is that each two subchains must have at least three passive revolute joints in distinct directions; each subchain must have less than four prismatic joints, providing essential information about the overall joint composition of the PM.

If two subchains do not have passive R joints, then the first three rows vanish, seeming to allow the PM to have three joints less but still have the same number of variables as the number of equations. However, according to eq.(4.2), the three scalar equations corresponding to the orientation of the EE have only two unknowns, overdetermined in other words, implying that the PM is overconstrained.

4.6.2 Overconstrained PMs of 3 DOFs

Mechanisms that still have full cycle mobility, but do not satisfy the Chebyshev-Grubler-Kutzbach criterion, are called overconstrained mechanisms (HUNT, 1978). The overconstrained mechanisms have been intensively studied in the field of mechanisms and machine theory for over a century. Analysis of such mechanisms are mostly based on screw theory. Studies presented in (AGRAWAL ET ROTH, 1992; HUANG, 2004; KONG ET GOSSELIN, 2004; DAI ET AL., 2006) are examples of the applications of this theory to the analysis of lower-mobility PMs. The common point of these works is that the joints of the mechanism are represented by screws, hence the motion (twist) and the constraint (wrench) of the mechanism are represented by two reciprocal screw systems, the mobility issue is then transformed into a statics problem.

Our approach is rather based on geometric analysis and consists in deriving the overconstrained PMs from isoconstrained PMs by looking for geometries having zero joint rates at a non singular configuration. Replacing these joints with rigid attachments, the mechanism becomes overconstrained but keeps the original mobility. We can therefore get a better understanding of the DOM of overconstrained PMs.

In general, if the number of joint variables is less than the number of the scalar structure equations, a mechanism can only be assembled under strict geometric conditions. Moreover, extra conditions may have to be satisfied in order to have a DOF greater than zero. The planar and spherical four-bar linkages and the Bennett mechanism (HO, 1978) are good examples of this kind. These conditions correspond to the geometries of isoconstrained mechanisms under which relative motion no longer occurs at some joints.

Rewrite eq.(4.48) as

$$\underbrace{\begin{bmatrix} \mathbf{X}_B & \mathbf{V}_B \end{bmatrix}}_{12\times 15} \begin{bmatrix} \boldsymbol{a} \\ \boldsymbol{u} \end{bmatrix} = \mathbf{0}$$

If any subset of eq.(4.49) has such a form as

$$\boldsymbol{\Psi} \begin{bmatrix} \dot{q}_{k,l} \\ \dot{\boldsymbol{q}}_a \end{bmatrix} = \mathbf{0} \tag{4.49}$$

where $\boldsymbol{\Psi}$ is square and non singular, $\dot{q}_{k,l}$ is the joint rate of the l^{th} joint of the k^{th} subchain, $\dot{\boldsymbol{q}}_a$ is a vector whose components are linear combinations of the joint rates of other joints corresponding to the subset of equations, then no relative motion happens at joint (k,l). Replacing this joint with a rigid attachment, an overconstrained PM is obtained. The following two examples illustrate the above statements.

Example 1 : Translational PM

Observing the TPM shown in Fig. 4.5, we see that the last three R joints of each subchain are parallel. Since the actuated joints are prismatic, we get a subset of eq.(4.48) as the follows :

$$\begin{bmatrix} \mathbf{N}_1 & -\mathbf{N}_2 & \mathbf{O} \\ \mathbf{O} & \mathbf{N}_2 & -\mathbf{N}_3 \end{bmatrix} \begin{bmatrix} \boldsymbol{y}_1 \\ \boldsymbol{y}_2 \\ \boldsymbol{y}_3 \end{bmatrix} = \mathbf{0} \tag{4.50}$$

Let $\boldsymbol{n}_{j2}, (j = 1,2,3)$ be the first joint orientation vector of the j^{th} subchain while $\boldsymbol{n}_{j3}, (j = 1,2,3)$ be the orientation vector of joint 3, 4, and 5 of the j^{th} subchain,

then we have

$$\begin{aligned} \mathbf{N}_1 &= \begin{bmatrix} \boldsymbol{n}_{12} & \boldsymbol{n}_{13} & \boldsymbol{n}_{13} & \boldsymbol{n}_{13} \end{bmatrix} \\ \mathbf{N}_2 &= \begin{bmatrix} \boldsymbol{n}_{22} & \boldsymbol{n}_{23} & \boldsymbol{n}_{23} & \boldsymbol{n}_{23} \end{bmatrix} \\ \mathbf{N}_3 &= \begin{bmatrix} \boldsymbol{n}_{32} & \boldsymbol{n}_{33} & \boldsymbol{n}_{33} & \boldsymbol{n}_{33} \end{bmatrix} \end{aligned} \tag{4.51}$$

Substituting eq.(4.51) into (4.50), then upon rearrangement, we get

$$\begin{bmatrix} \boldsymbol{n}_{12} & \boldsymbol{n}_{13} & -\boldsymbol{n}_{22} & -\boldsymbol{n}_{23} & \mathbf{0} & \mathbf{0} \\ \mathbf{0} & \mathbf{0} & \boldsymbol{n}_{22} & \boldsymbol{n}_{23} & -\boldsymbol{n}_{32} & -\boldsymbol{n}_{33} \end{bmatrix} \begin{bmatrix} \dot{q}_{12} \\ \dot{q}_{13} + \dot{q}_{14} + \dot{q}_{15} \\ \dot{q}_{22} \\ \dot{q}_{23} + \dot{q}_{24} + \dot{q}_{25} \\ \dot{q}_{32} \\ \dot{q}_{33} + \dot{q}_{34} + \dot{q}_{35} \end{bmatrix} = \mathbf{0} \tag{4.52}$$

Obviously, $\boldsymbol{n}_{j2}, (j = 1, 2, 3)$ and $\boldsymbol{n}_{j3}, (j = 1, 2, 3)$ can be arranged such that the left hand matrix of eq.(4.52) is not singular, i.e.,

$$\begin{aligned} \dot{q}_{12} &= \dot{q}_{13} + \dot{q}_{14} + \dot{q}_{15} = 0 \\ \dot{q}_{22} &= \dot{q}_{23} + \dot{q}_{24} + \dot{q}_{25} = 0 \\ \dot{q}_{32} &= \dot{q}_{33} + \dot{q}_{34} + \dot{q}_{35} = 0 \end{aligned} \tag{4.53}$$

So, there is no relative motion at the second joint of each subchain, the joints can be replaced by rigid attachments without affecting the motion of the PM leading to an overconstrained TPM shown in Fig. 4.6.

Examples 2 : Spherical PM

A spherical PM of topology 3 – $PP\underline{R}RR$ (see Fig. 4.7) can be designed such that

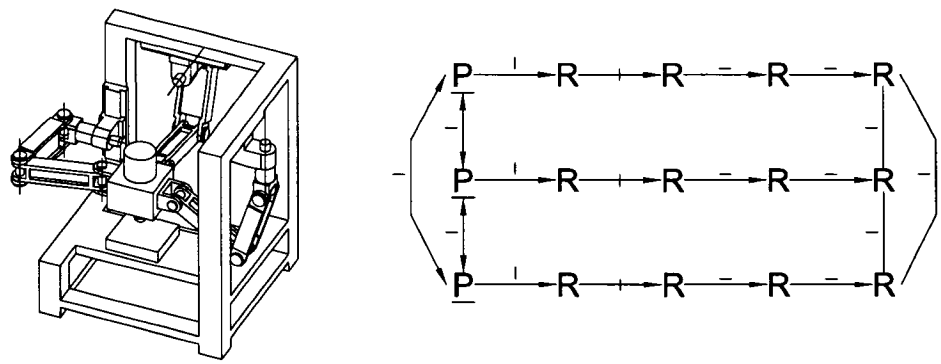

FIG. 4.5 An isoconstrained TPM of topology 3-$\underline{P}R^1R^2R^2R^2$

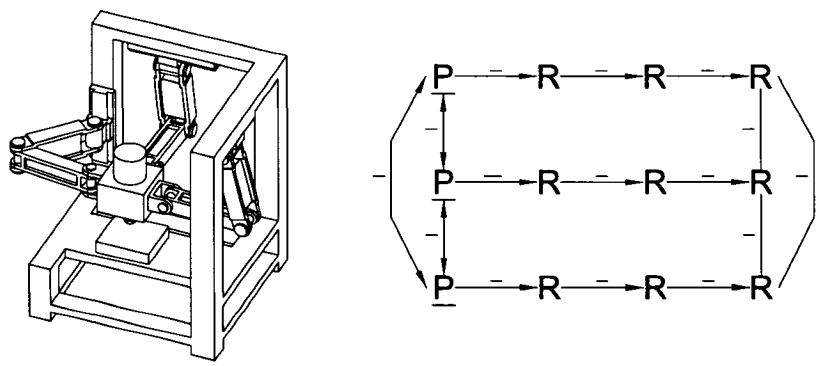

FIG. 4.6 The overconstrained TPM of topology 3-$\underline{P}R^2R^2R^2$(KIM ET TSAI, 2002)

at an initial configuration, all R joint axes are concurrent, making the lower half of their unit tangent vector vanish, then we get a subset of eqs.(4.48) as the follows

$$\begin{bmatrix} \mathbf{K}_1 & -\mathbf{K}_2 & \mathbf{O} \\ \mathbf{O} & \mathbf{K}_2 & -\mathbf{K}_3 \end{bmatrix} \begin{bmatrix} z_1 \\ z_2 \\ z_3 \end{bmatrix} = \mathbf{0} \tag{4.54}$$

The P joints can be arranged such that the left hand matrix of eq.(4.54) is not

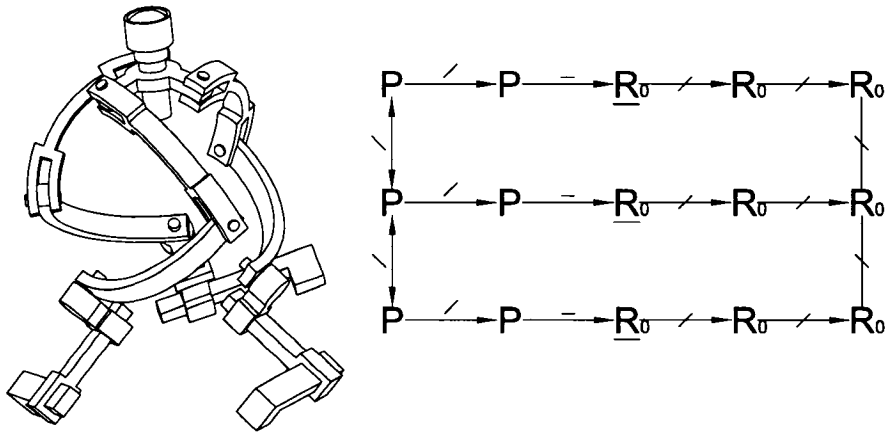

FIG. 4.7 An isoconstrained spherical PM of topology 3-$PP\underline{R}RR$

singular, leading to

$$z_1 = z_2 = z_3 = 0 \tag{4.55}$$

meaning that no relative motion occurs at any P joint. Replacing all P joints with rigid attachments leads to the overconstrained spherical PM of Fig. 4.8.

The inverse of the above process can be used to analyze overconstrained PMs by properly adding some joints which will not contribute to the motion of the mechanisms but make them isoconstrained, then all techniques available to isoconstrained mechanisms can be employed.

4.6.3 Underconstrained PMs of 3 DOFs

If the number of passive joint variables is greater than the number of scalar structure equations, then the PMs are considered as underconstrained. In general, the configuration of an underconstrained PM can not be completely controlled by the

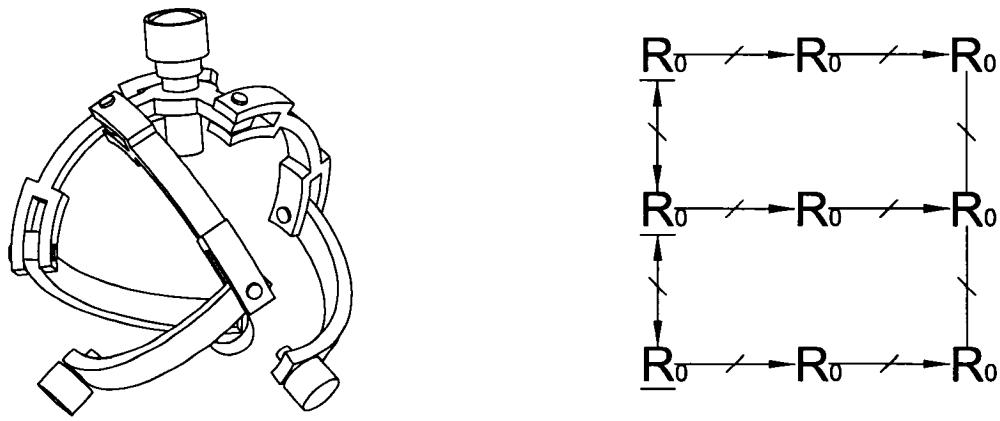

FIG. 4.8 An overconstrained spherical PM of topology 3-$\underline{R}RR$ (GOSSELIN ET HAMEL, 1994)

actuated joints because the set of structure equations can have infinitly many solutions. However, under certain conditions, the pose of the EE can be completely under the control of the actuated joints. In this case, the DOF of a PM is greater than its DOM and DOA, allowing its EE to reach a given pose with an infinite numbers of configurations. This may be useful for link obstruction avoidance. Extra actuators can be added in order to completely control the PM configuration. This is different from the redundant actuated PMs and redundant SMs because the added actuators are decoupled from the pose of the EE. Mathematically, this means that the set of eqs.(4.25) to (4.27) has infinite sets of solutions, but $\boldsymbol{t}_e$ can be solved uniquely as function of actuated joint variables. From the same reasoning, we will look into the underconstrained PMs by making an isoconstrained PM underconstrained. This can not be done by simply adding extra joints to the subchains because the DOM of the PMs has to be preserved.

Let $\mathbf{L}_j$ $(j = 1, 2, 3)$ be the matrix whose columns are the unit tangent vectors of the added joints and $\boldsymbol{v}$ be the vector whose components are the added joint rates.

Then from eq.(4.28), we get

$$\begin{bmatrix} \mathbf{W}_B & \mathbf{L}_B \end{bmatrix} \begin{bmatrix} \boldsymbol{u} \\ \boldsymbol{v} \end{bmatrix} = \mathbf{X}_B \boldsymbol{a} \tag{4.56}$$

where the overall added joint matrix $\mathbf{L}_B$ is defined as

$$\mathbf{L}_B \equiv \begin{bmatrix} \mathbf{L}_1 & -\mathbf{L}_2 & \mathbf{O} \\ \mathbf{O} & \mathbf{L}_2 & -\mathbf{L}_3 \end{bmatrix} \tag{4.57}$$

then $\boldsymbol{u}$ can be solved from eq.(4.56) as

$$\boldsymbol{u} = \mathbf{W}_B^{-1}\mathbf{X}_B\boldsymbol{a} - \mathbf{W}_B^{-1}\mathbf{L}_B\boldsymbol{v} \tag{4.58}$$

From eqs.(4.25) to (4.27), we have

$$\boldsymbol{t}_{3e} = \mathbf{X}_B\boldsymbol{a} + \mathbf{W}_D\boldsymbol{u} + \mathbf{L}_D\boldsymbol{v} \tag{4.59}$$

where $\mathbf{W}_D$ and $\mathbf{L}_D$ are defined as

$$\mathbf{W}_D \equiv \begin{bmatrix} \mathbf{W}_1 & \mathbf{O} & \mathbf{O} \\ \mathbf{O} & \mathbf{W}_2 & \mathbf{O} \\ \mathbf{O} & \mathbf{O} & \mathbf{W}_3 \end{bmatrix}, \; \mathbf{L}_D \equiv \begin{bmatrix} \mathbf{L}_1 & \mathbf{O} & \mathbf{O} \\ \mathbf{O} & \mathbf{L}_2 & \mathbf{O} \\ \mathbf{O} & \mathbf{O} & \mathbf{L}_3 \end{bmatrix}. \tag{4.60}$$

Substituting eqs.(4.58) and (4.60) into (4.59), upon rearrangement, we get

$$\boldsymbol{t}_{3e} = \left(\mathbf{X}_B + \mathbf{W}_D\mathbf{W}_B^{-1}\mathbf{X}_B\right)\boldsymbol{a} + \left(\mathbf{L}_D - \mathbf{W}_D\mathbf{W}_B^{-1}\mathbf{L}_B\right)\boldsymbol{v} \tag{4.61}$$

It is clear that in order for the added joints not to affect the DOM of the PMs, the

necessary and sufficient condition is

$$\mathbf{L}_D - \mathbf{W}_D \mathbf{W}_B^{-1} \mathbf{L}_B = \mathbf{O} \tag{4.62}$$

To investigate the subchains separately, rewrite eq.(4.62) as

$$\begin{bmatrix} \mathbf{L}_1^T & \mathbf{O}^T & \mathbf{O}^T \end{bmatrix}^T - \mathbf{W}_D \mathbf{W}_B^{-1} \begin{bmatrix} \mathbf{L}_1^T & \mathbf{O}^T \end{bmatrix}^T = \mathbf{O} \tag{4.63}$$

$$\begin{bmatrix} \mathbf{O}^T & \mathbf{L}_2^T & \mathbf{O}^T \end{bmatrix}^T - \mathbf{W}_D \mathbf{W}_B^{-1} \begin{bmatrix} -\mathbf{L}_2^T & \mathbf{L}_2^T \end{bmatrix}^T = \mathbf{O} \tag{4.64}$$

$$\begin{bmatrix} \mathbf{O}^T & \mathbf{O}^T & \mathbf{L}_2^T \end{bmatrix}^T - \mathbf{W}_D \mathbf{W}_B^{-1} \begin{bmatrix} \mathbf{O}^T & -\mathbf{L}_3^T \end{bmatrix}^T = \mathbf{O} \tag{4.65}$$

If $\mathbf{L}_1 = \mathbf{W}_1 \mathbf{X}_1$ where $\mathbf{X}_1$ has $(m_1 - 1)$ rows and as many columns as $\mathbf{L}_1$, then from eq.(4.38), we have

$$\mathbf{W}_B^{-1} \begin{bmatrix} \mathbf{L}_1 \\ \mathbf{O} \end{bmatrix} = \mathbf{W}_B^{-1} \begin{bmatrix} \mathbf{W}_1 \\ \mathbf{O} \end{bmatrix} \mathbf{X}_1 = \begin{bmatrix} \mathbf{X}_1 \\ \mathbf{O} \end{bmatrix} \tag{4.66}$$

Comparing eqs.(4.60), (4.63) and (4.66), it becomes obvious that eq.(4.63) is satisfied. This means that the unit tangent vectors of the joints added to a subchain should be linear combinations of the unit tangent vectors of the passive joints of the subchain. Figure 4.9 shows a TPM with redundant passive joints, while Fig. (4.10) shows its equivalent without redundancy. The inverse of the above process can be used to analyze underconstrained PMs by first identifying the passive joints whose unit tangent vectors are linear combinations of the unit tangent vectors of other passive joints of the same subchain, replacing them with rigid attachments, then the mechanism can be treated as isoconstrained mechanisms.

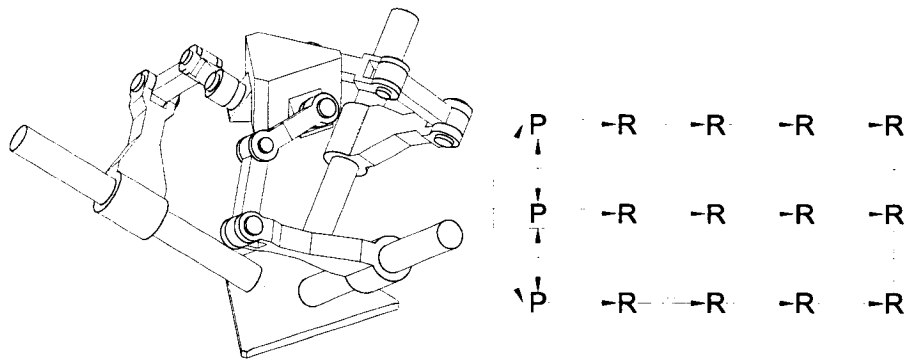

FIG. 4.9 A TPM with redundant passive joints

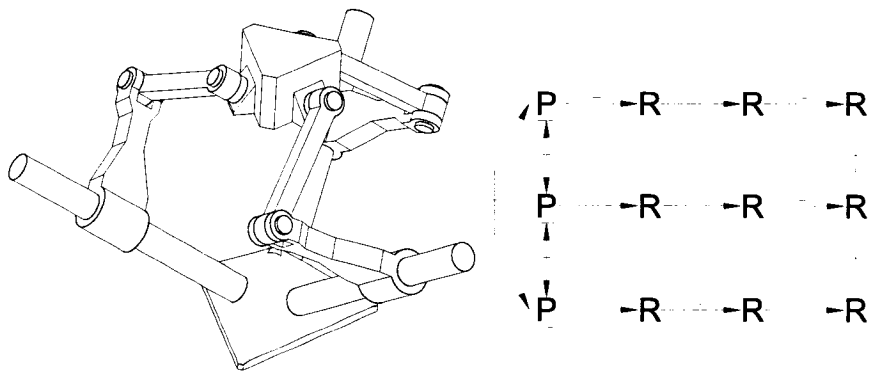

FIG. 4.10 A TPM without redundant passive joint (KONG ET GOSSELIN, 2002)

4.7 Conclusion

The kinematic modelling of the most general topology and geometry of three-degree-of-freedom PMs provides a basis for a systematic study of their kinematic properties. Deriving the tangent space structure equations from the displacement equations provides an understanding of the underlying relations between the tangent space and the displacement space. By distinguishing the degree of freedom, the degree of mobility, and the degree of actuation, a PM can be characterized more appropriately. The overall kinematic composition of an isoconstrained PM of 3 DOFs is revealed by the analysis of the structure equations and the exploration of the special structure of unit tangent vectors. The topological and geometric conditions for a PM to have 3 DOMs and be isoconstrained are derived. Any overconstrained or underconstrained PM has a corresponding isoconstrained PM whose EE has the same kinematic properties in terms of the actuated joint variables. It is therefore not necessary, in topological and geometric synthesis, to treat the overconstrained and the underconstrained cases differently because the isoconstrained designs include all overconstrained and underconstrained ones as far as the kinematic properties are concerned.

Acknowledgment

The authors acknowledge the financial support of NSERC (National Science and Engineering Research Council of Canada) under grants OGPIN-203618 and RGPIN-138478.

References

AGRAWAL, S. AND ROTH, B. (1992). Statics of in-parallel manipulator systems. *Journal of Mechanical Design - Transactions of the ASME*, **114**(4), 564 – 568.

ANGELES, J. (2002). The qualitative synthesis of parallel manipulators. In *Proceedings of the WORKSHOP on Fundamental Issues and Future Research Directions for Parallel Mechanisms and Manipulators*, Quebec City, Quebec, Canada.

ANGELES, J. (c2003). *Fundamentals of robotic mechanical systems : theory, methods, and algorithms*. Mechanical engineering series : Mechanical engineering series (Springer). Springer, New York, 2nd ed. edition.

ANGELES, J. AND GOSSELIN, C. (1988). Determination of the degree of freedom of simple and complex kinematic chains. *Transactions of the Canadian Society for Mechanical Engineers*, **12**(4), 219 – 226.

BROGARDH, C. (2002). Pkm research-important issues, as seen from a product development perspective at abb. In *Proceedings of the WORKSHOP on Fundamental Issues and Future Research Directions for Parallel Mechanisms and Manipulators*, Quebec City, Quebec, Canada, pages 68–82.

CARRICATO, M. AND PARENTI-CASTELLI, V. (2002). Singularity-free fully-isotropic translational parallel manipulators. *Proceedings of the ASME Design Engineering Technical Conference*, **5 B**, 1041 – 1050.

CLAVEL, R. (1988). Delta, a fast robot with parallel geometry. *Proceedings of the 18th International Symposium on Industrial Robots*, pages 91 – 100.

DAI, J., HUANG, Z., AND LIPKIN, H. (2006). Mobility of overconstrained parallel mechanisms. *Trans. ASME, J. Mech. Des. (USA)*, **128**(1), 220 – 9.

DENAVIT, J. AND HARTENBERG, R. S. (1954). Kinematic notation for lower-pair mechanisms based on matrices. In *American Society of Mechanical Engineers (ASME)*.

DIETMAIER, H. S. (1998). The stewart-gough platform of general geometry can have 40 real postures. In Lenarcic, J. and Husty, M., editors, *Advances in Robot Kinematics, Analysis and Control*, pages 1–10. Kluwer Academic Publishers.

GOSSELIN, C. AND ANGELES, J. (1990). Singularity analysis of closed-loop kinematic chains. *IEEE Trans. Robot. Autom. (USA)*, **6**(3), 281 – 90.

GOSSELIN, C. AND HAMEL, J.-F. (1994). The agile eye : a high-performance three-degree-of-freedom camera-orienting device. *Proceedings 1994 IEEE International Conference on Robotics and Automation (Cat. No.94CH3375-3)*, **vol.1**, 781 – 6.

GOSSELIN, C., KONG, X., FOUCAULT, S., AND BONEV, I. A. (2004). A fully decoupled 3-dof translational parallel mechanism. In *Proceedings of 2004 Parallel Kinematic Machines in Research and Practice International Conference (PKS 2004)*, Chemnitz, Germany, pages 595–610.

GOSSELIN, C., SEFRIOUI, J., AND RICHARD, M. (1994). On the direct kinematics of spherical three-degree-of-freedom parallel manipulators of general architecture. *Journal of Mechanical Design, Transactions Of the ASME*, **116**(2), 594 – 598.

GOUGH, V. (1956). Contribution to discussion of papers on research in automotive stability, control and tyre performance. *Proc. Auto Div. Inst. Mechanical Engineers.*

HERVE, J. M. (1978). Analyse structurelle des mecanismes par groupe des deplacements. left bracket structural analysis of mechanisms by set or displacements right bracket . *Mechanism & Machine Theory*, **13**(4), 437 – 450.

HERVE, J. M. (1991). Structural synthesis of parallel robots generating spatial translation. In *Proceedings of Fifth International Conference on Advanced Robotics*, pages 808–813.

HO, C. Y. (1978). Note on the existence of bennett mechanism. *Mechanism & Machine Theory*, **13**(3), 269 – 271.

HUANG, Z. (2004). Kinematics and type synthesis of lower-mobility parallel robot manipulators. *Proceeding of the 2004 the Eleventh World Congress in Mechanism and Machine Science*, pages 65 – 76.

HUNT, K. (1978). *Kinematic Geometry of Mechanisms*. Oxford University Press, London.

IFTOMM (2003). Iftomm terminology. *Mechanism and Machine Theory*, **38**, 913–912.

KIM, H. S. AND TSAI, L.-W. (2002). Evaluation of a cartesian parallel manipulator. In Lenarcic, J. and Thomas, F., editors, *Advances in Robot Kinematics, Theory and Applications*, pages 19–28. Kluwer Academic Publishers.

KONG, X. AND GOSSELIN, C. (2002). Type synthesis of linear translational parallel manipulators. In Lenarcic, J. and Thomas, F., editors, *Advances in Robot Kinematics, Theory and Applications*, pages 453–462. Kluwer Academic Publishers.

KONG, X. AND GOSSELIN, C. M. (2004). Type synthesis of 3-dof translational parallel manipulators based on screw theory. *Journal of Mechanical Design, Transactions of the ASME*, **126**(1), 83 – 92.

MCCARTHY, J. M. (1990). *An Introduction to Theoretical Kinematics*. The MIT Press, Cambridge, Massachusetts, London, England.

MERLET, J.-P. (2002). An initiative for the kinematics study of parallel manipulators. In *Proceedings of the WORKSHOP on Fundamental Issues and Future Research Directions for Parallel Mechanisms and Manipulators*, Montreal, Quebec, Canada.

MERLET, J.-P. (c1997). *Les robots paralleles*. Hermes, Paris.

RAGHAVAN, M. AND ROTH, B. (1990). Kinematic analysis of the 6r manipulator of general geometry. In *Robotics Research, Fifth International Symposium*, pages 263–269.

STERNBERG, S. (1994). *Group theory and physics*. Cambridge University Press, Cambridge.

STEWART, D. (1965). A platform with 6 degrees of freedom. In *Proc. of the Inst. of Mech. engineers, 180(Part 1, 15)*, pages 371–386.

STRAMIGIOLI, S. AND BRUYNINCKX, H. (2001). Geometry and screw theory for robotics (tutorial t9). In *IEEE International Conference on Robotics and Automation 2001*.

STRAMIGIOLI, S., MASCHKE, B., AND BIDARD, C. (2002). On the geometry of rigid-body motions : The relation between lie groups and screws. *Proceedings of the Institution of Mechanical Engineers, Part C : Journal of Mechanical Engineering Science*, **216**(1), 13 – 24.

TSAI, L.-W. (1996). Kinematics of a three-dof platform with extensible limbs. In Lenarcic, J. and Parenti-Castelli, V., editors, *Recent Advances in Robot Kinematics*, pages 401–410. Kluwer Academic Publishers.

TSAI, L.-W. (2001). *Mechanism design : enumeration of kinematic structures according to function.* Mechanical engineering series : CRC mechanical engineering series. CRC Press.

WENGER, P. AND CHABLAT, D. (2000). Kinematic analysis of a new parallel machine tool : The orthoglide. In Lenarcic, J. and Parenti-Castelli, V., editors, *Recent Advances in Robot Kinematics*, pages 305– 314. Kluwer Academic Publishers.

CHAPITRE 5

TOPOLOGICAL AND GEOMETRICAL SYNTHESIS OF THREE DEGREE-OF-FREEDOM FULLY PARALLEL MANIPULATORS BY INSTANTANEOUS KINEMATICS

Xiaoyu Wang, Luc Baron and Guy Cloutier.

Département de génie mécanique, École Polytechnique de Montréal.

P.O. 6079, station Centre-Ville, Montréal, Québec, Canada, H3C 3A7.

xiaoyu.wang@polymtl.ca

(Submitted to the *ASME Journal of Mechanical Design*)

Abstract

This paper presents a new synthesis procedure of fully parallel manipulators (PMs) of 3 degrees of freedom (DOFs) that could be implemented in a computer-aided synthesis process. Possible designs of PMs are represented by a set of unit joint-twists at an initial configuration, called here topological and geometric parameters (TGPs). This makes it possible to represent PMs of all topologies and geometries in an easy and consistent way. The kinematic bond between the end-effector (EE) and the base is then formulated as a set of equations involving TGPs, actuated-joint variables and non-actuated joint variables (passive joints). To achieve the required type of EE motion, possible topologies are first derived from tangent space analysis, and then the feasible topologies are retained by further displacement analysis. The geometries are determined such that the set of equations should be isoconstrained

when passive-joint variables are taken as unknowns. The synthesis procedure of 3-DOF PMs is illustrated with three numerical examples : one producing a new architecture of one translation and two rotations, while the other two producing existing architectures of translational PMs.

Keywords : Parallel manipulator, Synthesis, Topology, Geometry, Kinematics.

5.1 Introduction

A parallel manipulator (PM) is a closed-loop mechanism in which the end-effector (EE) is connected to the base through at least two independent kinematic chains. A fully PM is a PM with an n-DOF EE connected to the base by n independent kinematic chains, each having a single actuated joint (MERLET, 1997). Applications of PMs can be found in motion simulators, high-precision surgical tools, precision assembly tools, machine tools, and a number of industrial equipments because of their high load-carrying capacity, accurate positioning, high speed, and high capacity of acceleration (BARON, 1997). Despite of the high potential of performance offered by PMs, many applications are not yet as successful as expected (MERLET, 2002a). The closed-loop nature of PMs limits the motion of the EE and involves very complex kinematic singularities within the workspace (GOSSELIN ET ANGELES, 1990). Moreover, it is difficult to find 6-DOF PMs with orientation performance comparable to the one of serial manipulators (BROGARDH, 2002). To overcome these drawbacks, authors of (YANG ET AL., 2001) and (YANG ET AL., 1999) employed the modular design concept. An ingenious design was proposed in (HAYES ET LANGLOIS, 2005) which makes a 6-DOF PM's orienting decoupled from positioning and yields unlimited rotation. Another strategy is to connect in series two PMs of 3-DOF (the two together producing the 6-DOF mobility of the EE) in the aim to improve the overall performance and make the design easier (BROGARDH, 2002).

The advantages of this kind of hybrid manipulator are illustrated by the hybrid kinematic machine (TSAI ET JOSHI, 2002). Therefore, the synthesis of PMs of 3 DOFs has become an important design issue.

In the last two decades, numerous topologies of 3-DOF PMs have been published or disclosed in patent files. These topologies can be divided into two large categories : spherical PMs (SPMs) and translational PMs (TPMs) (GOSSELIN ET HAMEL, 1994; BARON, 2001). The SPM was proposed and systematically studied by many authors, e.g. (GOSSELIN ET AL., 1994). For TPMs, they can be further divided into two families. The first family is characterized by 3 parallelogram submechanisms which constrain the EE to a constant orientation. Many of the first family have been extensively studied and prototypes built, for example : Delta (CLAVEL, 1985), Y-Star (HERVE ET SPARACINO, 1992), Orthoglide (WENGER ET CHABLAT, 2000), and a TPM proposed by the authors of (TSAI ET STAMPER, 1997). The representative design of the second family is the 3-UPU proposed by the author of (TSAI, 1996), whose singularity problem has been the focus of a great deal of effort for several years. With the same design principle as the 3-UPU, several TPM topologies were derived (TSAI, 1999). In the meanwhile, a significant effort has also been made in 3-DOF PMs which produce displacement in both translation and rotation. PMs proposed in (CARRETERO ET AL., 2000) and (XIN-JUN ET AL., 2001) are two examples of that. The topological and geometrical synthesis of the above PMs have been accomplished mostly on a case-by-case basis (GOSSELIN ET AL., 2004).

On the design methodology side, group theory has already been applied to the topological synthesis of TPMs (HERVE, 1991). Successful examples of this application are the synthesis of Y-Star, the establishment of the displacement subgroup inventory (HERVE, 1999) and the synthesis of TPMs with doubly planar limbs (LEE ET HERVE, 2006). Group theory was also applied to synthesize SPMs (KAROUIA ET HERVE, 2002). It is noteworthy that mechanisms may produce displacements that

do not form a group (ANGELES, 2004). This limits the application of this synthesis approach. Applying screw theory to the synthesis of PMs was investigated and a detailed procedure was proposed in (LEGUAY-DURAND ET REBOULET, 1997). With this approach and similar methods, a large number of topologies of TPMs were generated (CARRICATO ET PARENTI-CASTELLI, 2002; BARON ET ANGELES, 1995; FRISOLI ET AL., 2000; KONG ET GOSSELIN, 2004). Among these topologies, there is a fully decoupled one that received special attention (KIM ET TSAI, 2002; KONG ET GOSSELIN, 2002). Generalized constraint equations having the form of ruled quadric surfaces in the image space were successfully used for planar PM synthesis which allows 3-DOF planar PMs of all topologies and geometries to have unified kinematic equations (HAYES ET AL., 2004). The above synthesis approaches deal mainly with the synthesis of parallel kinematic chains. As a result, when some joints are actuated, the kinematic properties of the mechanism as a whole were not examined systematically (GOSSELIN ET AL., 2004). To a great extent, synthesis still depends on reasoning, intuition, and experience; there is a lack of automated tool for topological synthesis (MERLET, 2002b).

In this paper, we propose a synthesis procedure in an effort to develop and eventually implement a computer-aided synthesis process. We first investigate and model the general architecture of fully PMs. Then, with the established model, instantaneous kinematic analysis is employed to derive the general conditions for the mechanism as a whole to have 3 DOF and for the EE to have 3 degrees of mobility. The mobility of the EE is characterized in its displacement tangent space and is represented by three linear independent 6-dimension arrays. The later is related to topological and geometrical parameters, actuated-joint variables, and passive-joint variables in order to match the topological and geometrical parameters to a given motion type.

5.2 Kinematic modelling

Without loss of generality, joints of more than one DOF are decomposed into a combinations of 1-DOF joints either prismatic or revolute. The EE is connected to the base by n independent serial kinematic chains. The Denavit-Hartenberg notation (DENAVIT ET HARTENBERG, 1954) for serial mechanism can therefore be used here for each so-called ***subchain*** of the PM.

The link i of serial chain j are identified by $(j,0)$ to (j,m_j), the base being $(j,0)$, and the EE being (j,m_j). The EE and the base are identified by different numbers when treated in different serial chains in order to have a unified mathematical expressions. A reference frame is attached to each link and is identified in the same way as the link. The pose of the EE, *i.e.*, its position and orientation, is defined by Cartesian variables. The relative position and orientation between links is defined by joint variables. The joint variable between link $(j,i-1)$ and (j,i) is denoted with $q_{j,i}$. The pose of the EE and the relative pose between links are defined by

- ${}^a\mathbf{H}_b$: homogeneous transformation of frame b relative to frame a ;
- $\mathbf{H}_j$: homogeneous transformation of frame j relative to the base frame ;
- $\mathbf{H}_e$: homogeneous transformation of the EE relative to the base frame.

The sequence of links in a serial chain has a corresponding sequence of homogeneous transformations that defines the pose of each link relative to its neighbor in the chain. The pose of the EE is therefore defined by the product of these transformations through every serial chain j, *i.e.*,

$$\mathbf{H}_e = \mathbf{H}_j(\boldsymbol{q}_j) = \prod_{i=1}^{m_j} {}^{j,i-1}\mathbf{H}_{j,i}(q_{j,i}), j = 1 \sim n, \boldsymbol{q}_j \equiv [q_{j,1}, q_{j,2}, \cdots, q_{j,m_j}]^T \qquad (5.1)$$

These serial chains are closed by rigidly attaching their end link frames together. The closure equations are thus obtained by equating the transformation products

of all these serial chains, say chains j and k, for example,

$$\prod_{i=1}^{m_j} {}^{j,i-1}\mathbf{H}_{j,i}(q_{j,i}) = \prod_{i=1}^{m_k} {}^{k,i-1}\mathbf{H}_{k,i}(q_{k,i}),\ \forall j,k = 1,\ \cdots,\ n \text{ and } j \neq k \tag{5.2}$$

The set of possible poses of the EE are governed by the system of eq. (5.2). The kinematic property is deeply hidden into the nonlinearity of the system. Take the generalized 3-DOF spherical PM as an example. The system reduces to a univariate 8^{th} degree polynomial (GOSSELIN ET AL., 1994). Another example of closed chains is the generalized single loop closed chain having 6 revolute joints, the famous inverse kinematic problem of serial manipulators; the system yields a univariate 16^{th} degree polynomial (RAGHAVAN ET ROTH, 1990). Obviously, the roots of these polynomials can only be computed numerically. It is extremely difficult to match the topological and geometrical parameters to the degree of freedom of the mechanism and the degree of mobility of its EE by solving directly these non-linear equations. It is reasonable that we turn our attention toward the displacement tangent space.

The concepts and theories applied in the following modelling are mainly from (ANGELES, 2003; MCCARTHY, 1990; STRAMIGIOLI ET BRUYNINCKX, 2001; STRAMIGIOLI ET AL., 2002). Let us introduce the following notions :

- ${}^{a}\mathbf{T}_{b}$: tangent operator of frame b in frame a expressed in frame a;
- $\mathbf{T}_{b}$: tangent operator of frame b in base frame expressed in base frame;
- ${}^{m,a}\mathbf{T}_{b}$: tangent operator of frame b in frame a expressed in frame m;
- ${}^{a}\mathbf{Q}_{b}$: 3×3 rotation matrix of frame b relative to frame a;
- $\mathbf{Q}_{j}$: 3×3 rotation matrix of frame j relative to the base frame;
- $\mathbf{Q}_{e}$: 3×3 rotation matrix of the EE frame relative to the base frame;
- ${}^{a}\boldsymbol{r}_{b}$: position vector of the origin of frame b in frame a;
- $\boldsymbol{r}_{j}$: position vector of the origin of frame j in the base frame;
- $\mathbf{1}$: identity matrix;

- $\mathbf{O}$: zero matrix;
- $\mathbf{0}$: 3×1 zero vector.

In general, let the homogeneous transformation of frame b with respect to frame a be given as

$$ {}^{a}\mathbf{H}_{b} = \begin{bmatrix} {}^{a}\mathbf{Q}_{b} & {}^{a}\boldsymbol{r}_{b} \\ \mathbf{0}^{T} & 1 \end{bmatrix} \tag{5.3} $$

The corresponding tangent operator is

$$ \begin{aligned} {}^{a}\mathbf{T}_{b} = {}^{a}\dot{\mathbf{H}}_{b}\,{}^{a}\mathbf{H}_{b}^{-1} &= \begin{bmatrix} {}^{a}\dot{\mathbf{Q}}_{b} & {}^{a}\dot{\boldsymbol{r}}_{b} \\ \mathbf{0}^{T} & 0 \end{bmatrix} \begin{bmatrix} {}^{a}\mathbf{Q}_{b} & {}^{a}\boldsymbol{r}_{b} \\ \mathbf{0}^{T} & 1 \end{bmatrix}^{-1} \\ &= \begin{bmatrix} {}^{a}\dot{\mathbf{Q}}_{b} & {}^{a}\dot{\boldsymbol{r}}_{b} \\ \mathbf{0}^{T} & 0 \end{bmatrix} \begin{bmatrix} {}^{a}\mathbf{Q}_{b}^{T} & -{}^{a}\mathbf{Q}_{b}^{T}{}^{a}\boldsymbol{r}_{b} \\ \mathbf{0}^{T} & 1 \end{bmatrix} \\ &= \begin{bmatrix} {}^{a}\dot{\mathbf{Q}}_{b}\,{}^{a}\mathbf{Q}_{b}^{T} & {}^{a}\dot{\boldsymbol{r}}_{b} - {}^{a}\dot{\mathbf{Q}}_{b}\,{}^{a}\mathbf{Q}_{b}^{T}{}^{a}\boldsymbol{r}_{b} \\ \mathbf{0}^{T} & 0 \end{bmatrix} = \begin{bmatrix} {}^{a}\boldsymbol{\Omega}_{b} & {}^{a}\boldsymbol{v}_{b}^{a} \\ \mathbf{0}^{T} & 0 \end{bmatrix} \end{aligned} \tag{5.4} $$

where the dot denotes differentiation with respect to time, the angular-velocity matrix ${}^{a}\boldsymbol{\Omega}_{b}$ being defined as

$$ {}^{a}\boldsymbol{\Omega}_{b} \equiv {}^{a}\dot{\mathbf{Q}}_{b}\,{}^{a}\mathbf{Q}_{b}^{T} \tag{5.5} $$

and

$$ {}^{a}\boldsymbol{v}_{b}^{a} \equiv {}^{a}\dot{\boldsymbol{r}}_{b} - {}^{a}\dot{\mathbf{Q}}_{b}\,{}^{a}\mathbf{Q}_{b}^{T}{}^{a}\boldsymbol{r}_{b} \tag{5.6} $$

is the velocity of a point on the link b that shortly establishes as the point that is instantaneously coincident with the origin of frame a. Obviously, the 3×3 skew-

symmetric matrix ${}^a\mathbf{\Omega}_b$ has only 3 independent components, *i.e.*,

$$\mathbf{\Omega} = \begin{bmatrix} 0 & -\omega_z & \omega_y \\ \omega_z & 0 & -\omega_x \\ -\omega_y & \omega_x & 0 \end{bmatrix} \tag{5.7}$$

Let us recall that the axial vector of a matrix $\mathbf{A}$ can be computed as

$$\boldsymbol{vect}(\mathbf{A}) \equiv \frac{1}{2}\begin{bmatrix} a_{32} - a_{23} \\ a_{13} - a_{31} \\ a_{21} - a_{12} \end{bmatrix}, \ \mathbf{A} \equiv \begin{bmatrix} a_{11} & a_{12} & a_{13} \\ a_{21} & a_{22} & a_{23} \\ a_{31} & a_{32} & a_{33} \end{bmatrix} \tag{5.8}$$

We thus have

$$\boldsymbol{\omega} = \boldsymbol{vect}(\mathbf{\Omega}) = [\omega_x \ \omega_y \ \omega_z]^T \tag{5.9}$$

where $\boldsymbol{\omega}$ is the corresponding angular velocity vector.

The components of the tangent operator $\mathbf{T} = \begin{bmatrix} \mathbf{\Omega} & \boldsymbol{v} \\ \mathbf{0}^T & 0 \end{bmatrix}$ can therefore be reassembled into a 6-dimension array, namely the twist $\boldsymbol{t} \equiv \begin{bmatrix} \boldsymbol{\omega} \\ \boldsymbol{v} \end{bmatrix}$. From the twist between two rigid bodies under a 1-DOF joint constraint, the type, orientation, and position of this joint can be derived. For $\boldsymbol{\omega} \neq \mathbf{0}$, we have the Chasles decomposition (McCarthy, 1990)

$$\begin{aligned} \boldsymbol{t} &= \begin{bmatrix} \boldsymbol{\omega} \\ \boldsymbol{r} \times \boldsymbol{\omega} + h\boldsymbol{\omega} \end{bmatrix} = \omega \begin{bmatrix} \hat{\boldsymbol{\omega}} \\ \boldsymbol{r} \times \hat{\boldsymbol{\omega}} + h\hat{\boldsymbol{\omega}} \end{bmatrix}, \\ \omega &= \|\boldsymbol{\omega}\|, \hat{\boldsymbol{\omega}} = \frac{\boldsymbol{\omega}}{\|\boldsymbol{\omega}\|}, \boldsymbol{r} = \frac{\boldsymbol{\omega} \times \boldsymbol{v}}{\omega^2}, h = \frac{\boldsymbol{\omega}^T \boldsymbol{v}}{\omega^2} \end{aligned} \tag{5.10}$$

where $\hat{\boldsymbol{\omega}}$ is a unit vector, while $\begin{bmatrix} \hat{\boldsymbol{\omega}} \\ \boldsymbol{r} \times \hat{\boldsymbol{\omega}} \end{bmatrix}$ is the normalized Plucker coordinates of the joint axis (ANGELES, 2003). If $h = 0$ it is a revolute joint; if $h \neq 0$ it is a screw joint; if $\boldsymbol{\omega} = \mathbf{0}$, we simply have

$$\boldsymbol{t} = \begin{bmatrix} \mathbf{0} \\ \boldsymbol{v} \end{bmatrix} = v \begin{bmatrix} \mathbf{0} \\ \hat{\boldsymbol{v}} \end{bmatrix}, v = \|\boldsymbol{v}\|, \hat{\boldsymbol{v}} = \frac{\boldsymbol{v}}{v} \tag{5.11}$$

which implies a prismatic joint in the direction defined by $\boldsymbol{v}$. The normalized twists of screw joint, revolute joint and prismatic joint are respectively

$$\hat{\boldsymbol{t}}_S = \begin{bmatrix} \hat{\boldsymbol{\omega}} \\ \boldsymbol{r} \times \hat{\boldsymbol{\omega}} + h\hat{\boldsymbol{\omega}} \end{bmatrix}_S, \hat{\boldsymbol{t}}_R = \begin{bmatrix} \hat{\boldsymbol{\omega}} \\ \boldsymbol{r} \times \hat{\boldsymbol{\omega}} \end{bmatrix}_R, \hat{\boldsymbol{t}}_P = \begin{bmatrix} \mathbf{0} \\ \hat{\boldsymbol{v}} \end{bmatrix}_P \tag{5.12}$$

Since the unit joint-twists contain both joint geometry and joint type information, we designate the set of the unit joint-twists of a mechanism at an initial configuration as its topological and geometrical parameters (TGPs). The next step is to formulate the pose and the twist of the EE of a serial chain as a function of the TGPs.

In general, for 1-DOF joint with $q(t)$ as joint variable,

$$\mathbf{T}(t) = \frac{d\mathbf{H}(q(t))}{dt}\mathbf{H}(q(t))^{-1} \tag{5.13}$$

$$\mathbf{T}(t) = \hat{\mathbf{T}}\frac{d(q(t))}{dt} \tag{5.14}$$

By combining eqs. (5.13) and (5.14), and dropping argument t for brevity since it is obvious that the items under study are functions of time,

$$\frac{d\mathbf{H}(q)}{dq} = \hat{\mathbf{T}}\mathbf{H}(q) \tag{5.15}$$

With $\hat{\mathbf{T}}$ being constant, $\mathbf{H}(q)$ can be solved from eq. (5.15) as

$$\mathbf{H}(q) = (e^{\hat{\mathbf{T}}q})\mathbf{H}(0) \tag{5.16}$$

For the i^{th} joint of a serial chain

$$^{i-1}\mathbf{H}_i(q_i) = (e^{^{i-1}\hat{\mathbf{T}}_i q_i})^{i-1}\mathbf{H}_i(0) \tag{5.17}$$

By combining eqs. (5.1) and (5.17)

$$\mathbf{H}_e = \prod_{i=1}^{n} [(e^{^{i-1}\hat{\mathbf{T}}_i q_i})^{i-1}\mathbf{H}_i(0)] \tag{5.18}$$

By changing the reference frame of $^{j-1}\hat{\mathbf{T}}_j$ from $j-1$ to 0 and with the properties of matrix exponential $(e^{\mathbf{X}})^{-1} = e^{-\mathbf{X}}$; $e^{\mathbf{H}^{-1}\mathbf{X}\mathbf{H}} = \mathbf{H}^{-1}e^{\mathbf{X}}\mathbf{H}$, the forward kinematics is derived from eq. (5.18) as

$$\begin{aligned}
\mathbf{H}_e &= \prod_{i=1}^{n} \left[\left(e^{^{i-1}\mathbf{H}_0(0)(^{0,\,i-1}\hat{\mathbf{T}}_i)\,^0\mathbf{H}_{i-1}(0)q_i} \right)^{i-1} \mathbf{H}_i(0) \right] \\
&= \prod_{i=1}^{n} \left[^{i-1}\mathbf{H}_0(0) \left(e^{(^{0,\,i-1}\hat{\mathbf{T}}_i)q_i} \right) \,^0\mathbf{H}_{i-1}(0)^{i-1}\mathbf{H}_i(0) \right] \\
&= \prod_{i=1}^{n} \left[^{i-1}\mathbf{H}_0(0) \left(e^{(^{0,\,i-1}\hat{\mathbf{T}}_i)q_i} \right) \,^0\mathbf{H}_i(0) \right]
\end{aligned} \tag{5.19}$$

that is

$$\mathbf{H}_e = \left(e^{^0\hat{\mathbf{T}}_1 q_1} e^{^{0,\,1}\hat{\mathbf{T}}_2 q_2} \cdots e^{^{0,\,n-1}\hat{\mathbf{T}}_n q_n} \right) {}^0\mathbf{H}_n(0) \tag{5.20}$$

In tangent space, from eq. (5.20), the tangent operator of the EE of a serial chain can be derived as

$$\mathbf{T}_e = \sum_{i=1}^{n} (^{0,i-1}\hat{\mathbf{T}}_i \dot{q}_i) \tag{5.21}$$

with its column form as

$$\boldsymbol{t}_e = \sum_{i=1}^{n} ({}^{0,i-1}\hat{\boldsymbol{t}}_i \dot{q}_i) \tag{5.22}$$

Since the EE is simultaneously constrained by the three serial chains ($j = 1, 2, 3$), we have

$$\boldsymbol{t}_e = \sum_{i=1}^{m_1} ({}^{0,i-1}\hat{\boldsymbol{t}}_{1,i} \dot{q}_{1,i}) = \sum_{i=1}^{m_2} ({}^{0,i-1}\hat{\boldsymbol{t}}_{2,i} \dot{q}_{2,i}) = \sum_{i=1}^{m_3} ({}^{0,i-1}\hat{\boldsymbol{t}}_{3,i} \dot{q}_{3,i}) \tag{5.23}$$

Let

$$\begin{aligned} \boldsymbol{a}_{j,i} &\equiv {}^{i-1}\hat{\boldsymbol{t}}_{j,i}, \\ \underset{\{6\times m_j\}}{\mathbf{A}_j} &\equiv \begin{bmatrix} \boldsymbol{a}_{j,1} & \cdots & \boldsymbol{a}_{j,k_j-1} & \boldsymbol{a}_{j,k_j} & \boldsymbol{a}_{j,k_j+1} & \cdots & \boldsymbol{a}_{j,m_j} \end{bmatrix}, \\ \dot{\boldsymbol{q}}_j &\equiv \begin{bmatrix} \dot{q}_{j,1} & \cdots & \dot{q}_{j,k_j-1} & \dot{q}_{j,k_j} & \dot{q}_{j,k_j+1} & \cdots & \dot{q}_{j,m_j} \end{bmatrix}^T \end{aligned} \tag{5.24}$$

we can then write eq. (5.23) in matrix form as

$$\boldsymbol{t}_e = \underset{\{6\times m_1\}}{\mathbf{A}_1}\, \dot{\boldsymbol{q}}_1 = \underset{\{6\times m_2\}}{\mathbf{A}_2}\, \dot{\boldsymbol{q}}_2 = \underset{\{6\times m_3\}}{\mathbf{A}_3}\, \dot{\boldsymbol{q}}_3 \tag{5.25}$$

The structure of $\mathbf{A}_1$, $\mathbf{A}_2$, and $\mathbf{A}_3$ corresponds to joint types and their general arrangement, *i.e.* , topology, while their numeric values correspond to kinematic dimensions, *i.e.* , the geometries. The topology and the geometries of parallel mechanisms are therefore represented by $\mathbf{A}_1$, $\mathbf{A}_2$, and $\mathbf{A}_3$ with k_1, k_2, and k_3 identify the actuated joints of the mechanism.

5.3 Tangent Space Analysis

Now, we rewrite eq. (5.24) in such a way that the actuated-joint variables are isolated from their passive-joint counterparts. Let

$$\begin{aligned}
\underset{\{6\times(m_j-1)\}}{\mathbf{B}_j} &\equiv \begin{bmatrix} \boldsymbol{a}_{j,1} & \cdots & \boldsymbol{a}_{j,k_j-1} & \boldsymbol{a}_{j,k_j+1} & \cdots & \boldsymbol{a}_{j,m_j} \end{bmatrix}, \\
x_{j,i} &\equiv \dot{q}_{j,i}, \\
\boldsymbol{x}_j &\equiv \begin{bmatrix} x_{j,1} & \cdots & x_{j,k_j-1} & x_{j,k_j} & x_{j,k_j+1} & \cdots & x_{j,m_j} \end{bmatrix}^T \\
\boldsymbol{y}_j &\equiv \begin{bmatrix} x_{j,1} & \cdots & x_{j,k_j-1} & x_{j,k_j+1} & \cdots & x_{j,m_j} \end{bmatrix}^T
\end{aligned} \tag{5.26}$$

where $\boldsymbol{y}_j$ is the passive-joint rate vector, x_{1,k_1}, x_{2,k_2}, and x_{3,k_3} are actuated-joint rate variables. Then eq. (5.25) can be written as

$$\begin{aligned}
\underset{\{6\times(m_1-1)\}}{\mathbf{B}_1}\ \boldsymbol{y}_1 + \boldsymbol{a}_{1,k_1}x_{1,k_1} &= \underset{\{6\times(m_2-1)\}}{\mathbf{B}_2}\ \boldsymbol{y}_2 + \boldsymbol{a}_{2,k_2}x_{2,k2} \\
\underset{\{6\times(m_2-1)\}}{\mathbf{B}_2}\ \boldsymbol{y}_2 + \boldsymbol{a}_{2,k_2}x_{2,k_2} &= \underset{\{6\times(m_3-1)\}}{\mathbf{B}_3}\ \boldsymbol{y}_3 + \boldsymbol{a}_{3,k_3}x_{3,k_3}
\end{aligned} \tag{5.27}$$

By rewriting eq. (5.27) in matrix form, a set of linear equations arises

$$\underbrace{\begin{bmatrix} \mathbf{B}_1 & -\mathbf{B}_2 & \mathbf{O} \\ \mathbf{O} & \mathbf{B}_2 & -\mathbf{B}_3 \end{bmatrix}}_{12\times(m_1+m_2+m_3-3)} \underbrace{\begin{bmatrix} \boldsymbol{y}_1 \\ \boldsymbol{y}_2 \\ \boldsymbol{y}_3 \end{bmatrix}}_{(m_1+m_2+m_3-3)\times 1} = \underbrace{\begin{bmatrix} -\boldsymbol{a}_{1,k_1} & \boldsymbol{a}_{2,k_2} & \mathbf{0} \\ \mathbf{0} & -\boldsymbol{a}_{2,k_2} & \boldsymbol{a}_{3,k_3} \end{bmatrix}}_{12\times 3} \underbrace{\begin{bmatrix} x_{1,k_1} \\ x_{2,k_2} \\ x_{3,k_3} \end{bmatrix}}_{3\times 1} \tag{5.28}$$

The synthesized mechanism should be iso-statically constrained when all its actuators are locked. This means that when the actuated-joint rates x_{1,k_1}, x_{2,k_2}, and x_{3,k_3} are set to zero, eq. (5.28) should have trivial solution for the passive-joint rates $\boldsymbol{y}_{1,k_1}$, ,$\boldsymbol{y}_{2,k_2}$ and $\boldsymbol{y}_{3,k_3}$ as unknowns. On the other hand, the mapping from the actuated-joints rate to the passive-joint rate should be unique. The necessary

condition for this is that the matrix on the left hand side is square and non-singular. Let

$$\underset{12\times12}{\mathbf{C}} \equiv \underbrace{\begin{bmatrix} \mathbf{B}_1 & -\mathbf{B}_2 & \mathbf{O} \\ \mathbf{O} & \mathbf{B}_2 & -\mathbf{B}_3 \end{bmatrix}}_{12\times12} \tag{5.29}$$

then we have $m_1 + m_2 + m_3 - 3 = 12$. It is obvious that the columns of each of $\mathbf{B}_1$, $\mathbf{B}_2$, and $\mathbf{B}_3$ should be linearly independent. It can therefore be concluded that the possible combinations of the numbers of joints of the three subchains are $3-6-6$, $4-5-6$, $5-5-5$, and $3-5-7$. This necessary condition does not necessarily mean that the EE will have 3 DOF. From eq. (5.28), we have

$$\begin{bmatrix} \boldsymbol{y}_1 \\ \boldsymbol{y}_2 \\ \boldsymbol{y}_3 \end{bmatrix} = \mathbf{C}^{-1} \left(\begin{bmatrix} -\boldsymbol{a}_{1,k_1} \\ 0 \end{bmatrix} x_{1,k_1} + \begin{bmatrix} \boldsymbol{a}_{2,k_2} \\ -\boldsymbol{a}_{2,k_2} \end{bmatrix} x_{2,k_2} + \begin{bmatrix} 0 \\ \boldsymbol{a}_{3,k_3} \end{bmatrix} x_{3,k_3} \right) \tag{5.30}$$

where it is clear that if $\boldsymbol{a}_{j,k_j} \in range(\underset{\{6\times(m_j-1)\}}{\mathbf{B}_j})$ then the EE will lose a DOF.

Since

$$\mathbf{C}^{-1}\mathbf{C} = \underbrace{\begin{bmatrix} \underset{(m_1-1)\times(m_1-1)}{\mathbf{1}} & \underset{(m_1-1)\times(m_2-1)}{\mathbf{O}} & \underset{(m_1-1)\times(m_3-1)}{\mathbf{O}} \\ \underset{(m_2-1)\times(m_1-1)}{\mathbf{O}} & \underset{(m_2-1)\times(m_2-1)}{\mathbf{1}} & \underset{(m_2-1)\times(m_3-1)}{\mathbf{O}} \\ \underset{(m_3-1)\times(m_1-1)}{\mathbf{O}} & \underset{(m_3-1)\times(m_2-1)}{\mathbf{O}} & \underset{(m_3-1)\times(m_3-1)}{\mathbf{1}} \end{bmatrix}}_{12\times12} \tag{5.31}$$

we have

$$\mathbf{C}^{-1}\underbrace{\begin{bmatrix}\mathbf{B}_1\\ {\scriptstyle\{6\times(m_1-1)\}}\\ \mathbf{O}\\ {\scriptstyle\{6\times(m_1-1)\}}\end{bmatrix}}_{12\times(m_1-1)} = \underbrace{\begin{bmatrix}\mathbf{1}\\ {\scriptstyle(m_1-1)\times(m_1-1)}\\ \mathbf{O}\\ {\scriptstyle(m_2-1)\times(m_1-1)}\\ \mathbf{O}\\ {\scriptstyle(m_3-1)\times(m_1-1)}\end{bmatrix}}_{12\times(m_1-1)} \tag{5.32}$$

$$\mathbf{C}^{-1}\underbrace{\begin{bmatrix}\mathbf{B}_2\\ {\scriptstyle\{6\times(m_2-1)\}}\\ -\ \mathbf{B}_2\\ {\scriptstyle\{6\times(m_2-1)\}}\end{bmatrix}}_{12\times(m_2-1)} = \underbrace{\begin{bmatrix}\mathbf{O}\\ {\scriptstyle(m_1-1)\times(m_2-1)}\\ \mathbf{1}\\ {\scriptstyle(m_2-1)\times(m_2-1)}\\ \mathbf{O}\\ {\scriptstyle(m_3-1)\times(m_2-1)}\end{bmatrix}}_{12\times(m_2-1)} \tag{5.33}$$

$$\mathbf{C}^{-1}\underbrace{\begin{bmatrix}\mathbf{O}\\ {\scriptstyle\{6\times(m_3-1)\}}\\ \mathbf{B}_3\\ {\scriptstyle\{6\times(m_3-1)\}}\end{bmatrix}}_{12\times(m_3-1)} = \underbrace{\begin{bmatrix}\mathbf{O}\\ {\scriptstyle(m_1-1)\times(m_3-1)}\\ \mathbf{O}\\ {\scriptstyle(m_2-1)\times(m_3-1)}\\ \mathbf{1}\\ {\scriptstyle(m_3-1)\times(m_3-1)}\end{bmatrix}}_{12\times(m_1-1)} \tag{5.34}$$

Let us take the 1^{st} serial chain as an example, *i.e.*, if $\boldsymbol{a}_{1,k_j} \in range(\mathbf{B_1}) \Rightarrow \exists \boldsymbol{\xi}_1 \in \mathbb{R}^{m_1-1}$ such that $\boldsymbol{a}_{1,k_1} = \mathbf{B}_1\boldsymbol{\xi}_1$, then

$$\begin{aligned}\mathbf{C}^{-1}\begin{bmatrix}-\boldsymbol{a}_{1,k_1}\\ \mathbf{0}\end{bmatrix} &= \mathbf{C}^{-1}\begin{bmatrix}-\mathbf{B}_1\\ \mathbf{0}\end{bmatrix}\boldsymbol{\xi}_1\\ &= -\underbrace{\begin{bmatrix}\mathbf{1}\\ {\scriptstyle(m_1-1)\times(m_2-1)}\\ \mathbf{O}\\ {\scriptstyle(m_2-1)\times(m_2-1)}\\ \mathbf{O}\\ {\scriptstyle(m_3-1)\times(m_2-1)}\end{bmatrix}}_{12\times(m_2-1)}\boldsymbol{\xi}_1 = -\begin{bmatrix}\boldsymbol{\xi}_1\\ \mathbf{0}\\ {\scriptstyle(m_2+m_2-2)\times 1}\end{bmatrix}\end{aligned} \tag{5.35}$$

and eq. (5.30) becomes

$$\begin{bmatrix} \boldsymbol{y}_1 \\ \boldsymbol{y}_2 \\ \boldsymbol{y}_3 \end{bmatrix} = - \begin{bmatrix} \boldsymbol{\xi}_1 x_{1,k_1} \\ \mathbf{0} \\ {\scriptstyle (m_2+m_2-2)\times 1} \end{bmatrix} + \mathbf{C}^{-1} \begin{bmatrix} \boldsymbol{a}_{2,k_2} \\ -\boldsymbol{a}_{2,k_2} \end{bmatrix} x_{2,k_2} + \mathbf{C}^{-1} \begin{bmatrix} \mathbf{0} \\ \boldsymbol{a}_{3,k_3} \end{bmatrix} x_{3,k_3} \quad (5.36)$$

It is apparent that x_{1,k_1} no longer appears in solutions for $\boldsymbol{y}_2$ and $\boldsymbol{y}_3$. However, the twist of the EE, $\boldsymbol{t}_e = \mathbf{B}_2\boldsymbol{y}_2 + \boldsymbol{a}_{2,k_2}x_{2,k_2} = \mathbf{B}_3\boldsymbol{y}_3 + \boldsymbol{a}_{3,k_3}x_{3,k_3}$ and therefore is independent of x_{1,k_1}, the EE loses 1 DOF. One can conclude that for both the mechanism and its EE to have 3 DOF, $\mathbf{A}_1$, $\mathbf{A}_2$, and $\mathbf{A}_3$ must have less than 7 columns, *i.e.*, $m_1, m_2, m_3 \leq 6$. The only possible combinations of numbers of joints along three subchains are deduced as $3-6-6$, $4-5-6$, and $5-5-5$.

5.4 The Synthesis Procedure

The type of the motion of the EE is characterized in its displacement tangent space. The EE twists are represented as 6-dimension columns. When the EE has 3 DOF, all possible EE twists must form a 3-dimension subspace. This subspace can be easily formulated as the range of a matrix of rank 3, *i.e.*, $\underset{\{6\times 3\}}{\mathbf{G}}$. From the point of view of screw theory, $range(\mathbf{G})$ is a 3-system of screw. Without loss of generality, the reference frame of the EE can be defined such that its origin coincides with the origin of the base frame. Then the motion type of the EE can be well characterized by the upper three rows and the lower three rows of the screw system. The 3-system of screw defined by the upper three rows is a $\mathbb{R}^3$ vector space formed by all possible angular velocity vectors of the EE. The 3-system of screw defined by the lower three rows is a $\mathbb{R}^3$ vector space formed by all possible velocity vectors of the origin of the EE's reference frame. The physical meaning of the two partitions can be illustrated by two examples, *i.e.*, TPMs and SPMs. For TPMs, the upper part

of the system should be a 3×3 zero matrix and the lower part should be a rank-3 3×3 matrix, because no rotation is permitted. For SPMs, the upper part of the system should be a rank-3 3×3 matrix and the lower part should be a 3×3 zero matrix, because no translation is permitted to the frame origin of the EE. As far as the motion type is concerned, the 3-system of screw can be partitioned into two 3×3 matrices to facilitate the synthesis according to a given motion type, *i.e.*

$$\mathbf{G} \equiv \begin{bmatrix} \mathbf{G}_U \\ \mathbf{G}_L \end{bmatrix}, \quad \mathbf{G}_U \equiv \begin{bmatrix} \boldsymbol{o}_1 & \boldsymbol{o}_2 & \boldsymbol{o}_3 \end{bmatrix}, \quad \mathbf{G}_L \equiv \begin{bmatrix} \boldsymbol{c}_1 & \boldsymbol{c}_2 & \boldsymbol{c}_3 \end{bmatrix} \tag{5.37}$$

where $\boldsymbol{o}_1$, $\boldsymbol{o}_2$, $\boldsymbol{o}_3$, $\boldsymbol{c}_1$, $\boldsymbol{c}_2$, and $\boldsymbol{c}_3$ are $\mathbb{R}^3$ vectors. Since the EE is constrained simultaneously by three serial chains, it follows that

$$range(\mathbf{A}_1) \cap range(\mathbf{A}_2) \cap range(\mathbf{A}_3) = range(\mathbf{G}) \tag{5.38}$$

The subspace constituted by the set of possible twists of the EE is the intersection of three subspaces generated respectively by each of the serial chains.

The first synthesis step is to construct matrices $\mathbf{A}_1$, $\mathbf{A}_2$, and $\mathbf{A}_3$ such that eq. (16) is satisfied. Instead of working in 6-dimension space, we partition matrices $\mathbf{A}_1$, $\mathbf{A}_2$, and $\mathbf{A}_3$ into upper three rows and lower three rows, designated respectively by $\underset{\{3\times m_1\}}{\mathbf{A}_{1U}}$, $\underset{\{3\times m_2\}}{\mathbf{A}_{2U}}$, $\underset{\{3\times m_3\}}{\mathbf{A}_{3U}}$, $\underset{\{3\times m_1\}}{\mathbf{A}_{1L}}$, $\underset{\{3\times m_2\}}{\mathbf{A}_{2L}}$, and $\underset{\{3\times m_3\}}{\mathbf{A}_{3L}}$. Then from eq. (5.38), one must have

$$range(\underset{\{3\times m_1\}}{\mathbf{A}_{1U}}) \cap range(\underset{\{3\times m_2\}}{\mathbf{A}_{2U}}) \cap range(\underset{\{3\times m_3\}}{\mathbf{A}_{3U}}) = range(\mathbf{G}_U) \tag{5.39}$$

$$range(\underset{\{3\times m_1\}}{\mathbf{A}_{1L}}) \cap range(\underset{\{3\times m_2\}}{\mathbf{A}_{2L}}) \cap range(\underset{\{3\times m_3\}}{\mathbf{A}_{3L}}) = range(\mathbf{G}_L) \tag{5.40}$$

It should be pointed out that eq. (5.39) and eq. (5.40) does not necessarily lead to eq. (5.38). But, as far as the motion type is concerned, eq. (5.39) and eq. (5.40)

are equivalent to eq. (5.38). Therefore, the minimum number and orientations of revolute joints for each serial chain can be determined by inspecting eq. (5.39) while the joint positions and the prismatic joint arrangement can be inferred from eq. (5.40). The general synthesis procedure can be summarized as follows :

1. Determine how many joints for each of the three serial chains. The combinations can only be $(m_1 = 3, m_2 = 6, m_3 = 6)$, $(m_1 = 4, m_2 = 5, m_3 = 6)$, or $(m_1 = 5, m_2 = 5, m_3 = 5)$.

2. Determine the subspace types of $range(\mathbf{A}_{1U})$, $range(\mathbf{A}_{2U})$, and $range(\mathbf{A}_{3U})$ such that the type of their intersection matches that of $range(\mathbf{G}_U)$. For example,
   - $range(\mathbf{G}_U)$ is null then $range(\mathbf{A}_{1U})$, $range(\mathbf{A}_{2U})$, and $range(\mathbf{A}_{3U})$ can be of (2-dimension, 2-dimension, 2-dimension),(1-dimension, 2-dimension, 3-dimension) or (null, 3-dimension, 3-dimension).
   - $range(\mathbf{G}_U)$ is 1-dimension then $range(\mathbf{A}_{1U})$, $range(\mathbf{A}_{2U})$, and $range(\mathbf{A}_{3U})$ can be of (1-dimension, 3-dimension, 3-dimension) or (2-dimension, 2-dimension, 3-dimension).

3. Determine the subspace types of $range(\mathbf{A}_{1L})$, $range(\mathbf{A}_{2L})$, and $range(\mathbf{A}_{3L})$ such that the type of their intersection matches that of $range(\mathbf{G}_L)$.

   These two steps are straight forward because we are working in the most familiar $\mathbb{R}^3$. At this stage, the motion types of all serial chains have been determined, we can either look into the rich inventory of known serial topologies for appropriate serial topologies (BARON ET ANGELES, 1995; HERVE, 1994) or proceed to the numerical steps that follow.

4. Generate $\mathbf{A}_{1U}$, $\mathbf{A}_{2U}$, and $\mathbf{A}_{3U}$ such that their ranges match those determined at step 2.

5. Construct $\mathbf{A}_{1L}$, $\mathbf{A}_{2L}$, and $\mathbf{A}_{3L}$ such that their ranges match those determined at step 3 and normalized the columns of the matrices $\mathbf{A}_1$, $\mathbf{A}_2$, and $\mathbf{A}_3$.

6. Determine which joints are to be actuated.
7. Verify if $\begin{bmatrix} \mathbf{B}_1 & -\mathbf{B}_2 & \mathbf{O} \\ \mathbf{O} & \mathbf{B}_2 & -\mathbf{B}_3 \end{bmatrix}$ is not singular and the columns of each of $\mathbf{A}_1$, $\mathbf{A}_2$, and $\mathbf{A}_3$ are linearly independent. Repeat steps 3-7 if necessary.
8. Extract the topological and the geometrical information from $\mathbf{A}_1$, $\mathbf{A}_2$, and $\mathbf{A}_3$ and verify if the subspace types of $range(\mathbf{A}_{1U})$, $range(\mathbf{A}_{2U})$, $range(\mathbf{A}_{3U})$, $range(\mathbf{A}_{1L})$, $range(\mathbf{A}_{2L})$, and $range(\mathbf{A}_{3L})$ are still those determined at step 2 and 3 upon some small displacements of the EE. If not, repeat steps 3-8.

5.5 Synthesis Examples

We illustrate the use of our synthesis procedure to the design of three PMs of different topologies and EE mobility.

Example 1

The desired motion type is 1-DOF in translation and 2-DOF in orientation.

1. This motion type can be characterized by

$$\mathbf{G}_U = \begin{bmatrix} 1 & 0 & 0 \\ 0 & 1 & 0 \\ 0 & 0 & 0 \end{bmatrix}, \quad \mathbf{G}_L = \begin{bmatrix} 0 & 0 & 0 \\ 0 & 0 & 0 \\ 0 & 0 & 1 \end{bmatrix}.$$

2. The combination of joint numbers ($m_1 = 4$, $m_2 = 5, m_3 = 6$) is selected from the set of possible number of joints for the serial chains.
3. The subspace of $range(\mathbf{G}_U)$ is of dimension 2. This can be achieved by making $range(\mathbf{A}_{1U})$ of dimension 2, $range(\mathbf{A}_{2U})$ of dimension 3, and $range(\mathbf{A}_{3U})$ of dimension 3.

4. The subspace of $range(\mathbf{G}_L)$ is of dimension 1. This can be obtained by making $range(\mathbf{A}_{1L})$ of dimension 2, $range(\mathbf{A}_{2L})$ of dimension 2, and $range(\mathbf{A}_{3L})$ of dimension 3.

5. Construct the upper parts of the TGP matrices as

$$\mathbf{A}_{1U} = \begin{bmatrix} 1 & 1 & 1 & 0 \\ 0 & 0 & 0 & 1 \\ 0 & 0 & 0 & 0 \end{bmatrix}, \mathbf{A}_{2U} = \begin{bmatrix} 0 & 0 & 0 & 0.6934 & 1 \\ 1 & 1 & 1 & 0.6934 & 0 \\ 0 & 0 & 0 & 0.6934 & 0 \end{bmatrix},$$

$$\mathbf{A}_{3U} = \begin{bmatrix} 0 & 0 & 0 & -0.7071 & 0.7071 & 0.9806 \\ 0 & 0 & 0 & -0.7071 & -0.7071 & 0 \\ 0 & 1 & 1 & 0 & 0 & 0.6934 \end{bmatrix}.$$

6. After certain several hundreds of iterations, the lower parts of the TGP matrices are chosen as

$$\mathbf{A}_{1L} = \begin{bmatrix} 0 & 0 & 0 & 0 \\ 1 & 1 & 0 & 0 \\ 1 & 0 & 1 & 0 \end{bmatrix}, \mathbf{A}_{2L} = \begin{bmatrix} 1 & 1 & 0 & 0 & 0 \\ 0 & 0 & 0 & 0 & 0 \\ 1 & 0 & 1 & 0 & 0 \end{bmatrix},$$

$$\mathbf{A}_{3L} = \begin{bmatrix} 0 & 0.7071 & 0.7071 & 0 & 0 & 0 \\ 0 & -0.7071 & 0.7071 & 0 & 0 & 0 \\ 1 & 0 & 0 & 0 & 0 & 0 \end{bmatrix}.$$

7. The first joint of each serial chain is actuated.

8. $$\det \underbrace{\begin{bmatrix} \mathbf{B}_1 & -\mathbf{B}_2 & \mathbf{O} \\ \mathbf{O} & \mathbf{B}_2 & -\mathbf{B}_3 \end{bmatrix}}_{12\times 12} = -0.481,$$

$rank(\mathbf{A_1}) = 4, rank(\mathbf{A_2}) = 5, rank(\mathbf{A_3}) = 6.$

The resulting PM is illustrated in Fig. 5.1, which is a new architecture with subchains of different topologies, *i.e.*, $\underline{\text{R}}$3R-$\underline{\text{R}}$4R-$\underline{\text{P}}$5R, where underline means an actuated joint.

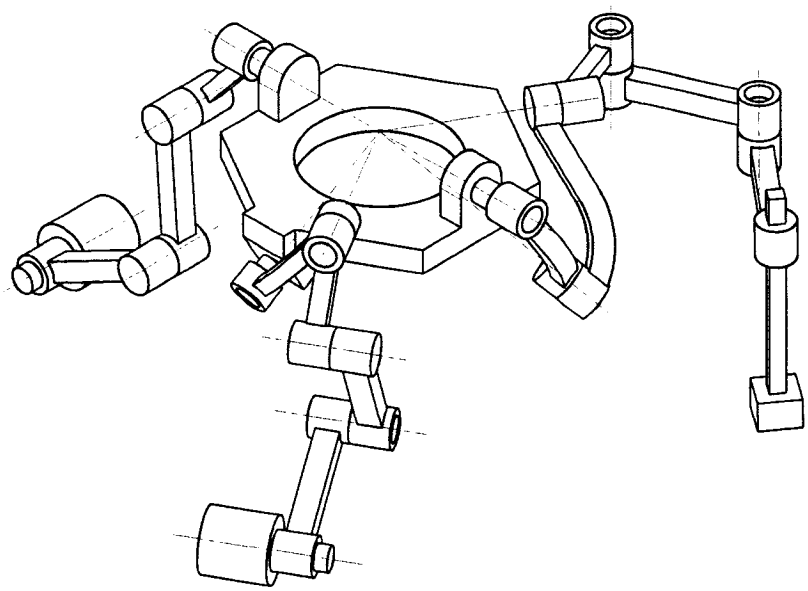

FIG. 5.1 Example 1 : A new architecture of PMs generating 1-DOF of translation and 2-DOF of rotation of topology R3R-R4R-P5R

Example 2

The desired motion type is the 3D translation at constant orientation.

1. This motion type is 3-DOF translation, *i.e.*,

$$\mathbf{G}_U = \begin{bmatrix} 0 & 0 & 0 \\ 0 & 0 & 0 \\ 0 & 0 & 0 \end{bmatrix}, \quad \mathbf{G}_L = \begin{bmatrix} 1 & 0 & 0 \\ 0 & 1 & 0 \\ 0 & 0 & 1 \end{bmatrix}.$$

2. The combination of joint numbers is chosen as $(m_1 = 5,\ m_2 = 5, m_3 = 5)$.

3. The subspace of $range(\mathbf{G}_U)$ is null. Subspaces of $range(\mathbf{A}_{1U})$, $range(\mathbf{A}_{2U})$, and $range(\mathbf{A}_{3U})$ are all of dimension 2 with their intersection being null.

4. The subspace of $range(\mathbf{G}_L)$ is of dimension 3. Subspaces of $range(\mathbf{A}_{1L})$,

$range(\mathbf{A}_{2L})$, and $range(\mathbf{A}_{3L})$ are all of dimension 3.

5. The upper parts of the TGP matrices are chosen as

$$\mathbf{A}_{1U} = \begin{bmatrix} 0 & 0 & -0.7071 & -0.7071 & 0 \\ 0 & 0 & 0.7071 & 0.7071 & 0 \\ 1 & 1 & 0 & 0 & 1 \end{bmatrix},$$

$$\mathbf{A}_{2U} = \begin{bmatrix} 0 & 0 & -0.7071 & -0.7071 & 0 \\ 0 & 0 & -0.7071 & -0.7071 & 0 \\ 1 & 1 & 0 & 0 & 1 \end{bmatrix},$$

$$\mathbf{A}_{3U} = \begin{bmatrix} -1 & -1 & 0 & 0 & -1 \\ 0 & 0 & 1 & 1 & 0 \\ 0 & 0 & 0 & 0 & 0 \end{bmatrix}.$$

6. The lower parts of the TGP matrices are chosen as

$$\mathbf{A}_{1L} = \begin{bmatrix} 1.7071 & 0.7071 & 0 & 0 & 0 \\ -0.7071 & -0.7071 & 0 & 0 & 0 \\ 0 & 0 & 1 & 0 & 0 \end{bmatrix},$$

$$\mathbf{A}_{2L} = \begin{bmatrix} 1.7071 & 0.7071 & 0 & 0 & 0 \\ 0.7071 & 0.7071 & 0 & 0 & 0 \\ 0 & 0 & 1 & 0 & 0 \end{bmatrix},$$

$$\mathbf{A}_{3L} = \begin{bmatrix} 0 & 0 & -1 & 0 & 0 \\ 0 & -0.7071 & 0 & 0 & 0 \\ 0.7071 & 0 & 0 & 0 & 0 \end{bmatrix}.$$

7. $\det \underbrace{\begin{bmatrix} \mathbf{B}_1 & -\mathbf{B}_2 & \mathbf{O} \\ \mathbf{O} & \mathbf{B}_2 & -\mathbf{B}_3 \end{bmatrix}}_{12\times 12} = 0.7071,$

$rank(\mathbf{A_1}) = 5, rank(\mathbf{A_2}) = 5, rank(\mathbf{A_3}) = 5.$

The resulting PM is illustrated in Fig. 5.2, which is an architecture that we recently proposed (WANG ET AL., 2003b) in order to have isotropic properties all the way along a circular trajectory.

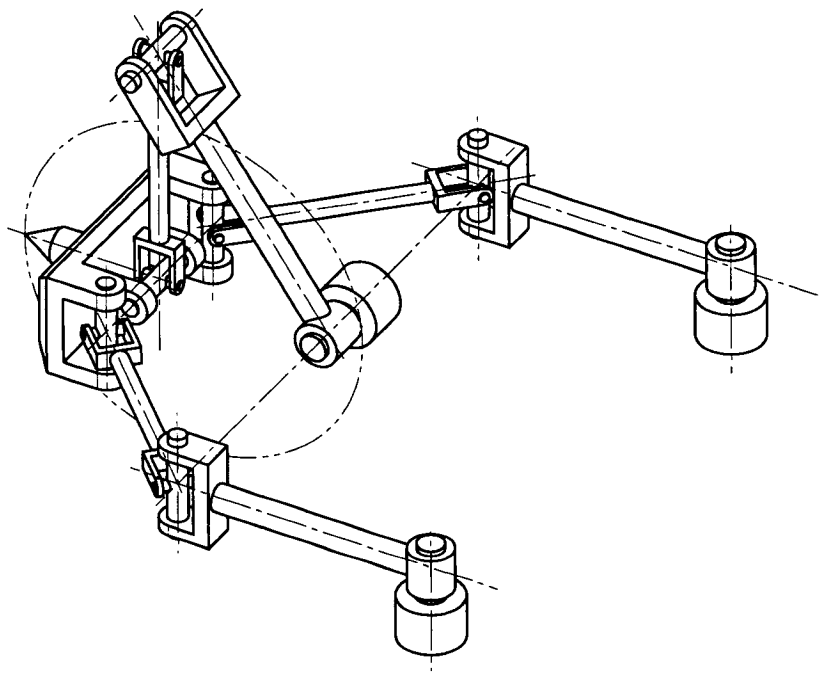

FIG. 5.2 Example 2 : An isotropic architecture of translational PM of topology 3-$\underline{R}$UU

Example 3

The desired motion type is again here the 3D translation at constant orientation.

1. This motion type is 3-DOF translation, *i.e.*,

$$\mathbf{G}_U = \begin{bmatrix} 0 & 0 & 0 \\ 0 & 0 & 0 \\ 0 & 0 & 0 \end{bmatrix}, \quad \mathbf{G}_L = \begin{bmatrix} 1 & 0 & 0 \\ 0 & 1 & 0 \\ 0 & 0 & 1 \end{bmatrix}.$$

2. The combination of joint numbers is chosen as $(m_1 = 5,\ m_2 = 5, m_3 = 5)$.
3. The subspace of $range(\mathbf{G}_U)$ is null. Subspaces of $range(\mathbf{A}_{1U})$, $range(\mathbf{A}_{2U})$, and $range(\mathbf{A}_{3U})$ are all of dimension 2 with their intersection being null.
4. The subspace of $range(\mathbf{G}_L)$ is of dimension 3. Subspaces of $range(\mathbf{A}_{1L})$, $range(\mathbf{A}_{2L})$, and $range(\mathbf{A}_{3L})$ are all of dimension 3.

This example is similar to example 2, but the geometry described through steps 5 to 7 do not allow isotropy to be reached for this PM illustrated in Fig. 5.3.

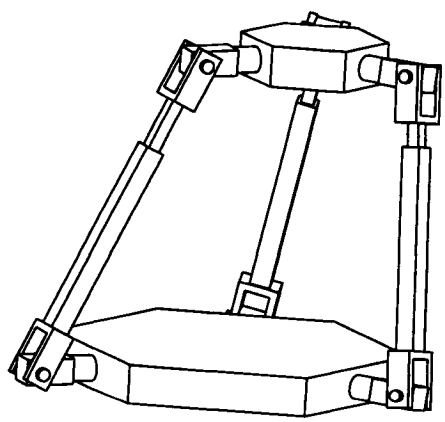

FIG. 5.3 Example 3 : An existing architecture of translational PM of topology 3-UPU

5.6 Conclusion

The concept of initial configuration is introduced. At this initial configuration, unit joint-twists of each serial chain of a PM are assembled into synthesis matrices. The structure of these matrices corresponds to joint types and their general arrangement, *i.e.*, the topology, while their numeric values correspond to kinematic dimensions, *i.e.*, the geometry. The topology and the geometry of a PM are therefore parameterized using such matrices. The kinematic model of general fully PMs of 3-DOF is established. With this model, we have the possibility of systematically synthesizing fully PMs of 3-DOF. A detailed synthesis procedure is proposed and illustrated with three examples.

Acknowledgment

The authors acknowledge the financial support of NSERC (National Science and Engineering Research Council of Canada) under grants OGPIN-203618 and RGPIN-138478.

references

ANGELES, J. (2004). The qualitative synthesis of parallel manipulators. *Journal of Mechanical Design, Transactions of the ASME*, **126**(4), 617–624.

ANGELES, J. (c2003). *Fundamentals of robotic mechanical systems : theory, methods, and algorithms.* Mechanical engineering series : Mechanical engineering series (Springer). Springer, New York, 2nd ed. edition.

BARON, L. (2001). Workspace-based design of parallel manipulators of star topology with a genetic algorithm. In *Proceedings of ASME 27th Design Automation Conference*, Pittsburg, U.S.A.

BARON, L. (c1997). *Contributions to the estimation of rigid-body motion under sensor redundancy*. PhD thesis, McGill University.

BARON, L. AND ANGELES, J. (1995). The isotropic decoupling of the direct kinematics of parallel manipulators under sensor redundancy. *Proceedings of 1995 IEEE International Conference on Robotics and Automation (Cat. No.95CH3461-1)*, **vol.2**, 1541 - 6.

BROGARDH, C. (2002). Pkm research-important issues, as seen from a product development perspective at abb. In *Proceedings of the WORKSHOP on Fundamental Issues and Future Research Directions for Parallel Mechanisms and Manipulators*, Quebec City, Quebec, Canada, pages 68–82.

CARRETERO, J. A., NAHON, M. A., AND PODHORODESKI, R. P. (2000). Workspace analysis and optimization of a novel 3-dof parallel manipulator. *International Journal of Robotics & Automation*, **15**(4), 178–88.

CARRICATO, M. AND PARENTI-CASTELLI, V. (2002). Singularity-free fully-isotropic translational parallel manipulators. *Proceedings of the ASME Design Engineering Technical Conference*, **5 B**, 1041 - 1050.

CLAVEL, R. (1985). Device for displacing and positioning an element in space. International patent, No. WO 87/03528 (1985).

DENAVIT, J. AND HARTENBERG, R. S. (1954). Kinematic notation for lower-pair mechanisms based on matrices. In *American Society of Mechanical Engineers (ASME)*.

FRISOLI, A., CHECCACCI, D., SALSEDO, F., AND BERGAMASCO, M. (2000). Synthesis by screw algebra of translating in-parallel actuated mechanisms. In Lenarcic, J. and Parenti-Castelli, V., editors, *Recent Advances in Robot Kinematics*. Kluwer Academic Publishers.

GOSSELIN, C. AND ANGELES, J. (1990). Singularity analysis of closed-loop kinematic chains. *IEEE Trans. Robot. Autom. (USA)*, **6**(3), 281 – 90.

GOSSELIN, C. AND HAMEL, J.-F. (1994). The agile eye : a high-performance three-degree-of-freedom camera-orienting device. *Proceedings 1994 IEEE International Conference on Robotics and Automation (Cat. No.94CH3375-3)*, **vol.1**, 781 – 6.

GOSSELIN, C., KONG, X., FOUCAULT, S., AND BONEV, I. A. (2004). A fully decoupled 3-dof translational parallel mechanism. In *Proceedings of 2004 Parallel Kinematic Machines in Research and Practice International Conference (PKS 2004)*, Chemnitz, Germany, pages 595–610.

GOSSELIN, C., SEFRIOUI, J., AND RICHARD, M. (1994). On the direct kinematics of spherical three-degree-of-freedom parallel manipulators of general architecture. *Journal of Mechanical Design, Transactions Of the ASME*, **116**(2), 594 – 598.

HAYES, M. AND LANGLOIS, R. (2005). Atlas : A novel kinematic architecture for six dof motion platforms. *Transactions of the Canadian Society for Mechanical Engineering*, **29**(4), 701 – 709.

HAYES, M., ZSOMBOR-MURRAY, P., AND CHEN, C. (Sept. 2004). Unified kinematic analysis of general planar parallel manipulators. *Trans. ASME, J. Mech. Des. (USA)*, **126**(5), 866 – 74.

HERVE, J. (1999). Lie group of rigid body displacements, a fundamental tool for mechanism design. *Mechanism and Machine Theory*, **34**(5), 719 – 730.

HERVE, J. M. (1991). Structural synthesis of parallel robots generating spatial translation. In *Proceedings of Fifth International Conference on Advanced Robotics*, pages 808–813.

HERVE, J. M. (1994). Mathematical group structure of the set of displacements. *Mechanism & Machine Theory*, **29**(1), 73–81.

HERVE, J. M. AND SPARACINO, F. (1992). Star, a new concept in robotics. In *Third International Workshop on Advances in Robot Kinematics*, pages 180–183.

KAROUIA, M. AND HERVE, J. M. (2002). A family of novel orientational 3-dof parallel robots. In *Proceedings of CISM-IFToMM RoManSy Symposia*, Udine, Italy, pages 359–368.

KIM, H. S. AND TSAI, L.-W. (2002). Evaluation of a cartesian parallel manipulator. In Lenarcic, J. and Thomas, F., editors, *Advances in Robot Kinematics, Theory and Applications*, pages 19–28. Kluwer Academic Publishers.

KONG, X. AND GOSSELIN, C. (2002). Type synthesis of linear translational parallel manipulators. In Lenarcic, J. and Thomas, F., editors, *Advances in Robot Kinematics, Theory and Applications*, pages 453–462. Kluwer Academic Publishers.

KONG, X. AND GOSSELIN, C. M. (2004). Type synthesis of 3-dof translational parallel manipulators based on screw theory. *Journal of Mechanical Design, Transactions of the ASME*, **126**(1), 83 – 92.

LEE, C.-C. AND HERVE, J. M. (2006). Translational parallel manipulators with doubly planar limbs. *Journal of Mechanical Design, Transactions of the ASME*, **41**(4), 433.

LEGUAY-DURAND, S. AND REBOULET, C. (1997). Design of a 3-dof parallel translating manipulator with u-p-u joints kinematic chains. In *Proceedings of the 1997 IEEE/RSJ International Conference on Intelligent Robot and Systems. Innovative Robotics for Real-World Applications. IROS '97*, pages 1637– 1642.

MCCARTHY, J. M. (1990). *An Introduction to Theoretical Kinematics*. The MIT Press, Cambridge, Massachusetts, London, England.

MERLET, J.-P. (2002a). An initiative for the kinematics study of parallel manipulators. In *Proceedings of the WORKSHOP on Fundamental Issues and Future Research Directions for Parallel Mechanisms and Manipulators*, Montreal, Quebec, Canada.

MERLET, J.-P. (2002b). Still a long way to go on the road for parallel mechanisms. In *ASME 27th Biennial Mechanisms and Robotics Conference*, Montreal, Quebec, Canada.

MERLET, J.-P. (c1997). *Les robots paralleles*. Hermes, Paris.

RAGHAVAN, M. AND ROTH, B. (1990). Kinematic analysis of the 6r manipulator of general geometry. In *Robotics Research, Fifth International Symposium*, pages 263–269.

STRAMIGIOLI, S. AND BRUYNINCKX, H. (2001). Geometry and screw theory for robotics (tutorial t9). In *IEEE International Conference on Robotics and Automation 2001*.

STRAMIGIOLI, S., MASCHKE, B., AND BIDARD, C. (2002). On the geometry of rigid-body motions : The relation between lie groups and screws. *Proceedings of the Institution of Mechanical Engineers, Part C : Journal of Mechanical Engineering Science*, **216**(1), 13 – 24.

TSAI, L.-W. (1996). Kinematics of a three-dof platform with extensible limbs. In Lenarcic, J. and Parenti-Castelli, V., editors, *Recent Advances in Robot Kinematics*, pages 401–410. Kluwer Academic Publishers.

TSAI, L.-W. (1999). The enumeration of a class of three-dof parallel manipulators. In *Proceedings of TENTH WORLD CONGRESS ON THE THEORY OF MACHINE AND MECHANISMS*, Oulu, Finland, pages 1121–1126.

TSAI, L.-W. AND JOSHI, S. (2002). Kinematic analysis of 3-dof position mechanisms for use in hybrid kinematic machines. *Journal of Mechanical Design, Transactions of the ASME*, **124**(2), 245 – 253.

TSAI, L.-W. AND STAMPER, R. (1997). A parallel manipulator with only translational degrees of freedom. Technical research report, The Institute for Systems Research, University of Maryland, U.S.A.

WANG, X., BARON, L., AND CLOUTIER, G. (2003). Kinematic modelling and isotropic conditions of a family of translational parallel manipulators. *International Conference on Control and Automation*, Montreal, Quebec, Canada, pages 173 – 177.

WENGER, P. AND CHABLAT, D. (2000). Kinematic analysis of a new parallel machine tool : The orthoglide. In Lenarcic, J. and Parenti-Castelli, V., editors, *Recent Advances in Robot Kinematics*, pages 305– 314. Kluwer Academic Publishers.

XIN-JUN, L., JINSONG, W., FENG, G., AND LI-PING, W. (2001). On the analysis of a new spatial three-degrees-of-freedom parallel manipulator. *IEEE Transactions on Robotics and Automation*, **17**(6), 959–68.

YANG, G., CHEN, I.-M., LIM, W. K., AND YEO, S. H. (1999). Design and kinematic analysis of modular reconfigurable parallel robots. *Proceedings - IEEE*

International Conference on Robotics and Automation, **4**, 2501 – 2506.

YANG, G., CHEN, I.-M., LIN, W., AND ANGELES, J. (2001). Singularity analysis of three-legged parallel robots based on passive-joint velocities. *Proceedings - IEEE International Conference on Robotics and Automation*, **3**, 2407 – 2412.

CHAPITRE 6

SYNTHESIS OF TRANSLATIONAL PARALLEL MANIPULATORS BASED ON FINITE DISPLACEMENT

Xiaoyu Wang, Luc Baron and Guy Cloutier.
Département de génie mécanique, École Polytechnique de Montréal.
P.O. 6079, station Centre-Ville, Montréal, Québec, Canada, H3C 3A7.
xiaoyu.wang@polymtl.ca

(To be submitted)

Abstract

For translational parallel manipulators (TPMs), topology synthesis methods that can be found in the literature are mainly based on screw theory, instantaneous kinematics, or group theory. Those based on screw theory or instantaneous kinematics deal only with the motion type for infinitesimal displacements at a given configuration; the motion type for finite displacements can not be properly addressed. Following the method based on group theory, topologies can be derived such that the intended motion type can be achieved for finite displacements. However, this method is limited to synthesize only the kinematic chains whose displacements are a Lie group. In this work, finite displacement equations are employed for the first time for the topology synthesis of TPMs. First of all, serial chains with less than 6 degrees of freedom (DOFs) are investigated and topology conditions for them to generate 3-DOF translation while its end-effector is under a constant orientation constraint are derived. Then the parallel manipulators (PMs) composed of

these serial chains are analyzed to find out whether and under what conditions the end-effector (EE) will keep a constant orientation through a finite workspace. This leads to a new topology synthesis approach of TPMs. In contrast with the methods based on Screw theory or instantaneous kinematics, mechanisms synthesized with this approach will have the intended motion type within a finite workspace and therefore no additional verification work is needed. Unlike the method based on Group theory, this approach is not limited by whether a serial chain can generate a Lie group displacements.

Keywords : Parallel manipulator, Translational, Kinematics, Topology, Synthesis.

6.1 Introduction

From the kinematic point of view, a mechanism is a kinematic chain with one of its links specified as the base and another one as the end-effector (EE) ; a manipulator is a mechanism with all or some of its joints actuated ; driven by the actuated joints, the EE and all other links undergo constrained motions with respect to the base (TSAI, 2001). A parallel manipulator (PM) is a closed-loop mechanism ofin which the EE is connected to the base through at least two independent kinematic chains. A fully parallel manipulator is a PM with an n-degree-of-freedom (DOF) EE connected to the base by n independent kinematic chains, each having a single actuated joint (MERLET, 1997).

Due to the closed-loop nature, the PMs possess kinematic properties which are complementary to those of traditional serial manipulators (SM). Applications of PMs can be found in motion simulators, high-precision surgical tools, precision assembly tools, machine tools, and a number of industrial equipments because of their high load-carrying capacity, accurate positioning, high speed, and high

capacity of acceleration (BARON, 1997).

Although PMs have been very successful in some applications, offering high performance, they are not yet completely accepted in some industrial areas, *e.g.* the machine-tool industry (MERLET, 2002a). Complex kinematic model and limited workspace inherent to closed-form mechanisms may explain this scenario at theoretical level (GOSSELIN ET AL., 2004). To overcome some of the drawbacks, one of the strategies is to connect in series two PMs of 3 DOF (the two together producing the 6-DOF mobility of the EE) in the aim to improve overall performance and make the design easier (BROGARDH, 2002). The advantages of this kind of hybrid manipulators are illustrated by a hybrid kinematic machine (TSAI ET JOSHI, 2002). Therefore, the synthesis of PMs of 3 DOF has become an important design issue.

During the last two decades, a great number of novel designs of PMs have been reported in the literature and enormous effort has been devoted to their kinematic studies. Amongst the representative architectures of early translational PMs (TPM), we can cite Delta PM (CLAVEL, 1988), Y-Star PM (HERVE ET SPARACINO, 1992), Orthoglide PM (WENGER ET CHABLAT, 2000), and 3-UPU PM (TSAI, 1996). Research works on these TPMs were carried out mainly on a case-by-case basis and they have little in common on synthesis and analysis methodology. As systematic synthesis approaches were gradually introduced into the topological and geometric synthesis, the number of new designs had been increasing quadratically. Based on group theory, the synthesis of a family of TPMs was realized by (HERVE, 1991). The application of group theory also leads to the synthesis of a set of spherical PMs (KAROUIA ET HERVE, 2002). Graph theory, which has been successfully used to planar mechanism synthesis, was used to enumerate some PMs (TSAI, 1999). Applying screw theory to the synthesis of PMs was investigated and a detailed procedure was proposed in (LEGUAY-DURAND ET REBOULET, 1997).

With this approach and similar methods, a large number of topologies for TPMs were generated (BARON ET ANGELES, 1995), (FRISOLI ET AL., 2000), (KONG ET GOSSELIN, 2001), (CARRICATO ET PARENTI-CASTELLI, 2002). Synthesis based on instantaneous kinematics was proposed in (WANG ET AL., 2003a). The chief drawback of the methods based on Screw theory or instantaneous kinematics is that motion type issue in finite workspace can not be properly addressed.

The objective of this work is to derived topology conditions for fully PMs to have only translational degrees of freedom within a finite workspace. This is done by using directly the finite displacement equations. The rest of this paper is organized as follows. In section 2, some basic concepts and definitions are presented. In section 3, serial kinematic chains with less than 6 DOFs are analyzed in order to derive possible subchain topologies which allow each subchain to generate 3-DOF translation while its end-effector is under a constant orientation constraint. Fully PMs composed of subchains of these topologies are analyzed in section 4. The synthesis procedure is summarized in section 5. The conclusion is drawn in section 6.

6.2 Kinematic modelling and definitions

A kinematic chain is composed of a set of rigid bodies, also called links in kinematics studies, connected by kinematic pairs. A kinematic pair is, then, the coupling of two rigid bodies so as to constrain their relative motion. The kinematic pairs are divided into two categories, namely the upper and lower kinematic pairs. An upper kinematic pair constrains two rigid bodies such that they keep a line or point contact; a lower kinematic pair constrains two rigid bodies such that a surface contact is maintained (ANGELES, 2003). A joint is a particular mechanical realization of a kinematic pair (IFToMM, 2003). There are six types of joints

corresponding to the lower kinematic pairs - spherical, cylindrical, planar, helical, revolute and prismatic. All these joints can be obtained by combining the revolute and prismatic ones. The kinematic composition of a manipulator is the essential information about the number of its links, which link is connected to which other links by what types of joints and which joints are actuated. The essential constraints are the minimum conditions for a manipulator of given kinematic composition to have the required kinematic properties. The topology of a manipulator is its kinematic composition plus the essential constraints. The geometry of a manipulator is a set of constraints on the relative locations of its joints carried by the same link. The geometry is unique to each of the manipulators of the same topology. Joint variables of a joint describe the relative position and orientation of two links coupled by the joint. The number of joint variables is the DOF of the joint.

To simplify the kinematic parametrization and without loss of generality, joints of more than one DOF are decomposed into the combinations of 1-DOF joints. Since the EE of a PM is connected to the base by independent serial kinematic chains, the Denavit-Hartenberg notation (DENAVIT ET HARTENBERG, 1954) for serial mechanism can therefore be used here for each so-called subchain of PM. The link i of serial chain j are identified by $(j,0)$ to (j,m_j) and (j,e), the base being $(j,0)$, the second last link being (j,m_j), and the EE being (j,e). The EE and the base are identified by different numbers when treated in different subchains in order to have unified mathematical expressions. A reference frame $\mathcal{F}$ is attached to each link and is identified in the same way as the link. Symbols used to formulate the kinematic model are as follows :

- b : subscript to identify the base ;
- e : subscript to identify the EE ;
- $\mathcal{F}_i$: reference frame attached to *link* i ;
- $\mathbf{Q}_c$: 3×3 orientation matrix of $\mathcal{F}_c$ with respect to $\mathcal{F}_b$;

- $\mathbf{R_z}(\theta)$: 3×3 rotation matrix about $\boldsymbol{z}$ axis with θ being the rotation angle :

$$\mathbf{R_z}(\theta) = \begin{bmatrix} \cos(\theta) & -\sin(\theta) & 0 \\ \sin(\theta) & \cos(\theta) & 0 \\ 0 & 0 & 1 \end{bmatrix};$$

- $\mathbf{R_x}(\alpha)$: 3×3 rotation matrix about $\boldsymbol{x}$ axis with α being the rotation angle :

$$\mathbf{R_x}(\alpha) = \begin{bmatrix} 1 & 0 & 0 \\ 0 & \cos(\alpha) & -\sin(\alpha) \\ 0 & \sin(\alpha) & \cos(\alpha) \end{bmatrix};$$

- $\mathbf{R_{hz}}(\theta)$: 4×4 homogeneous rotation matrix about $\boldsymbol{z}$ axis with θ being the rotation angle;
- $\mathbf{R_{hx}}(\alpha)$: 4×4 homogeneous rotation matrix about $\boldsymbol{x}$ axis with α being the rotation angle;
- $\mathbf{B_z}(d)$: 4×4 homogeneous translation matrix along $\boldsymbol{z}$ axis with d being the translation distance;
- $\mathbf{B_x}(a)$: 4×4 homogeneous translation matrix along $\boldsymbol{x}$ axis with a being the translation distance;
- $\mathbf{C}_i$: 4×4 homogeneous transformation matrix of $\mathcal{F}_i$ in $\mathcal{F}_{i-1}$;
- $\mathbf{H}_i$: 4×4 homogeneous transformation matrix of $\mathcal{F}_i$ in $\mathcal{F}_b$;
- $\boldsymbol{e}_i$: the k^{th} canonical vector which is defined as

$$\boldsymbol{e}_k \equiv \left[\underbrace{0 \ \cdots \ 0}_{k-1} \ 1 \ \underbrace{0 \ \cdots \ 0}_{n-k} \right]^T$$

whose dimension is implicit and depends on the context.

The sequence of links in a serial chain has a corresponding sequence of homogeneous transformations that defines the position and orientation of each link relative to its neighbor in the chain. The position and orientation of the EE of a PM is therefore

defined by the product of these transformations through any serial chain i, *i.e.*,

$$\begin{aligned}
\mathbf{H}_e &= \left(\prod_{j=0}^{m_i} \mathbf{C}_{i,j}\right) \mathbf{C}_{i,e},\ i = 1,\ 2,\ 3,\ \cdots \\
\mathbf{C}_{i,j} &= \mathbf{B_z}(d_{i,j})\mathbf{R_{hz}}(\theta_{i,j})\mathbf{R_{hx}}(\alpha_{i,j})\mathbf{B_x}(a_{i,j}) \\
\mathbf{C}_{i,e} &= \mathbf{B_z}(d_{i,e})\mathbf{R_{hz}}(\theta_{i,e})\mathbf{R_{hx}}(\alpha_{i,e})\mathbf{B_x}(a_{i,e})\mathbf{B_z}(d_{i,E})\mathbf{R_{hz}}(\theta_{i,E})
\end{aligned} \tag{6.1}$$

For revolute joint, $\theta_{i,j}$ is joint variable while $d_{i,j}$ is joint variable for prismatic joint. Other parameters define the geometry of the PM. Equation (6.1) is called structure equation of the mechanism (McCarthy, 1990). Under the constraints of the structure equations each link will have a particular set of positions and orientations. To characterize these sets, we adopt the following definitions :

Pose : the pose of a link is its position and orientation;

Configuration : the configuration of a mechanism is a specific arrangement of all its links under its structure constraints with each link having a specific pose;

Degree of freedom : the degree of freedom (DOF) of a mechanism is the number of independent variables in its structure equations;

Degree of mobility : the degree of mobility (DOM) of a manipulator is the number of independent variables to describe the possible poses of its EE under the structure constraints.

Configuration space : the configuration space of a manipulator is a metric space formed by the set of its possible configurations with the 2-norm of the difference between two configurations as the metric;

Orientation space : the orientation space of a manipulator is a metric space formed by the set of the possible orientations of its EE with the 2-norm of the difference between two orientations as the metric;

Position space : the position space of a manipulator is a metric space formed by the set of the possible positions of its EE with the 2-norm of the difference

between two positions as the metric;

Nature of mobility : the nature of mobility of a manipulator is the dimension of its orientation space and position space as well as the mapping between the two spaces.

To characterized the mobility of a manipulator, some concepts, derived from the topological space studies, are introduced as follows :

Path : let $0 \leq I \leq 1$, X be a metric space, and $\boldsymbol{x}, \boldsymbol{y} \in X$. A path from $\boldsymbol{x}$ to $\boldsymbol{y}$ is a continuous mapping $f : I \rightarrow X$ such that $f(0) = \boldsymbol{x}$ and $f(1) = \boldsymbol{y}$;

Connected subspace : a subspace is said to be connected if there exists at least one path between its any two elements;

Solitary subspace : a connected subspace X is said to be solitary if $\forall \boldsymbol{x}, \boldsymbol{y}$ with $\boldsymbol{x} \in X$ and $\boldsymbol{y} \notin X$ no path exists between $\boldsymbol{x}$ and $\boldsymbol{y}$;

Neighborhood : let X be a metric space and $\boldsymbol{x} \in X$. A neighborhood of $\boldsymbol{x}$ is a connected subspace, an open ball around $\boldsymbol{x}$ of radius ε, denoted by

$$B_\varepsilon(\boldsymbol{x}) \equiv \{\boldsymbol{y} \in X \mid metric(\boldsymbol{x}, \boldsymbol{y}) = \sigma, \forall \sigma < \varepsilon, \text{ with } \sigma, \varepsilon \in \mathbb{R} \text{ and } \sigma, \varepsilon > 0\}$$

Single element subspace : a solitary subspace which has only one element.

The configuration space of a PM can usually be partitioned into several solitary subspaces; a PM can not pass from one solitary subspace to another without having to be reassembled. So each solitary subspace corresponds to a so-called assembly mode. The nature of mobility of a PM may depend on assembly mode. Even within the same assembly mode, the configuration space may still be partitioned into subspaces with each of them corresponding to a different nature of mobility. The capacity of a PM to produce only translational displacements can therefore have different scopes : all assembly modes, some assembly modes or just within a configuration neighborhood. Given a PM of 3 DOF, if there exists a configuration

neighborhood within which it has 3 DOM and it is impossible for it to change the EE orientation, then it can be qualified as translational PM (TPM). The first step to the topological synthesis of TPMs is to identify the subchain topologies which allow the EE to have 3 translational DOMs while it is constrained to a constant orientation.

6.3 Possible subchain topologies for TPMs

By taking the orientation part of equation (6.1), we get

$$\mathbf{R_z}(\theta_0)\mathbf{R_x}(\alpha_0)\left[\prod_{i=1}^{m}[\mathbf{R_z}(\theta_i)\mathbf{R_x}(\alpha_i)]\right]\mathbf{R_z}(\theta_e)\mathbf{R_x}(\alpha_e)\mathbf{R_z}(\theta_E) = \mathbf{Q}_e \tag{6.2}$$

From equation (6.2), we know that imposing a constant orientation constraint only affects the revolute joints. Depending on the number of revolute joints and their relative locations, we distinguish

Single revolute joint : the only revolute joint of a subchain;

Solitary revolute joint : the revolute joint of a subchain which is parallel to non of other revolute joints of the same subchain;

Revolute link : a link carrying two revolute joints;

Skew revolute link : a link carrying two non parallel revolute joints;

H revolute link : a link carrying two parallel revolute joints;

n-H revolute link : a serial chain of $n-1$ successive H revolute links;

Conjugate skew revolute links : two revolute links with their twist angles being either equal or supplementary one another;

Hyper revolute link : the above revolute links with the presence of some prismatic joints between the revolute joints.

In the analysis of the orientation constraints presented in the following sections, subscripts identify the positions of revolute joints relative to other revolute joints in the same subchain.

6.3.1 Subchains with only one (n)-H (hpyer) revolute link

Let Θ be the sum of all revolute joint variables, then from equation (6.2), we get

$$\mathbf{R_z}(\Theta) = \mathbf{R_x}(-\alpha_0)\mathbf{R_z}(-\theta_0)\mathbf{Q}_e\mathbf{R_z}(-\theta_E)\mathbf{R_x}(-\alpha_e) \tag{6.3}$$

All entries other than Θ and $\mathbf{Q}_e$ in equation (6.3) are geometry-determined constant. It is obvious that under a constant orientation constraint, we have

$$\Theta = constant$$

which reduces the DOF of the subchain by 1. So only subchains of more than 3 DOF can have an (n)-H (hpyer) revolute link in order to produce 3 DOF translation with constant EE orientation.

6.3.2 Subchains with only one (hyper) skew revolute link

Let θ_k and θ_{k+1} be the joint variables of the joints carried by the revolute link, then from equation (6.2), we have

$$\begin{aligned} & \mathbf{R_z}\left(\sum_{i=1}^{k}\theta_i\right)\mathbf{R_x}(\alpha_k)\,\mathbf{R_z}\left(\sum_{i=k+1}^{p}\theta_{k+1}\right) \\ = \quad & \mathbf{R_x}(-\alpha_0)\,\mathbf{R_z}(-\theta_0)\,\mathbf{Q}_e\mathbf{R_z}(-\theta_E)\,\mathbf{R_x}(-\alpha_e) \end{aligned} \tag{6.4}$$

where p is the total number of revolute joints.

The only unknowns in equation (6.4) are $\sum_{i=1}^{k} \theta_i$ and $\sum_{i=k+1}^{p} \theta_{k+1}$.

Let

$$\mathbf{R_x}(-\alpha_0)\mathbf{R_z}(-\theta_0)\mathbf{Q}_e\mathbf{R_z}(-\theta_E)\mathbf{R_x}(-\alpha_e) \equiv \begin{bmatrix} l_{11} & l_{12} & l_{13} \\ l_{21} & l_{22} & l_{23} \\ l_{31} & l_{32} & l_{33} \end{bmatrix} \tag{6.5}$$

then by substituting equation (6.5) into equation (6.4), we get

$$\mathbf{R_z}\left(\sum_{i=1}^{k}\theta_i\right)\mathbf{R_x}\left(\alpha_k\right)\mathbf{R_z}\left(\sum_{i=k+1}^{p}\theta_{k+1}\right) = \begin{bmatrix} l_{11} & l_{12} & l_{13} \\ l_{21} & l_{22} & l_{23} \\ l_{31} & l_{32} & l_{33} \end{bmatrix} \tag{6.6}$$

Upon rearrangement, equation (6.6) becomes

$$\begin{aligned} \begin{bmatrix} \sin\left(\sum_{i=1}^{k}\theta_i\right) \\ -\cos\left(\sum_{i=1}^{k}\theta_i\right) \\ ctg(\alpha_k) \end{bmatrix} &= \frac{1}{\sin(\alpha_k)} \begin{bmatrix} l_{13} \\ l_{23} \\ l_{33} \end{bmatrix} \\ \begin{bmatrix} \sin\left(\sum_{i=k+1}^{p}\theta_i\right) \\ \cos\left(\sum_{i=k+1}^{p}\theta_i\right) \\ ctg(\alpha_k) \end{bmatrix} &= \frac{1}{\sin(\alpha_k)} \begin{bmatrix} l_{31} \\ l_{32} \\ l_{33} \end{bmatrix} \end{aligned} \tag{6.7}$$

From equation (6.7), we know that $\sum_{i=1}^{k} \theta_i$ and $\sum_{i=k+1}^{p} \theta_i$ are constrained to fixed values, the DOF of the subchain is reduced by 2; a subchain with only one (hyper) skew link has to have at least 5 joints in order for it to generate 3-DOF translation under constant EE orientation constraint.

6.3.3 Subchains with at least two (hyper) skew revolute links

Let f^{th} and g^{th} links be the neighboring (hyper) skew revolute links, *i.e.* $f < g$, $\alpha_f \neq 0$, $\alpha_g \neq 0$ and $\alpha_j = 0$ for $f < j < g$. Let $h \equiv g + 1$, then equation (6.2) can be written as

$$\begin{aligned}
&\prod_{i=1}^{f-1} [\mathbf{R_z}(\theta_i)\mathbf{R_x}(\alpha_i)]\, \mathbf{R_z}(\theta_f)\mathbf{R_x}(\alpha_f) \\
&\prod_{i=f+1}^{g-1} [\mathbf{R_z}(\theta_i)\mathbf{R_x}(0)]\, \mathbf{R_z}(\theta_g)\mathbf{R_x}(\alpha_g)\mathbf{R_z}(\theta_h)\mathbf{R_x}(\alpha_h) \\
&\prod_{i=h+1}^{p} [\mathbf{R_z}(\theta_i)\mathbf{R_x}(\alpha_i)] = \mathbf{R_x}(-\alpha_0)\mathbf{R_z}(-\theta_0)\mathbf{Q}_e\mathbf{R_z}(-\theta_E)\mathbf{R_x}(-\alpha_e)
\end{aligned} \tag{6.8}$$

that is

$$\begin{aligned}
&\prod_{i=1}^{f-1} [\mathbf{R_z}(\theta_i)\mathbf{R_x}(\alpha_i)]\, \mathbf{R_z}(\theta_f)\mathbf{R_x}(\alpha_f)\mathbf{R_z}\left(\sum_{i=f+1}^{g} \theta_i\right) \mathbf{R_x}(\alpha_g)\mathbf{R_z}(\theta_h)\mathbf{R_x}(\alpha_h) \\
&\prod_{i=h+1}^{p} [\mathbf{R_z}(\theta_i)\mathbf{R_x}(\alpha_i)] = \mathbf{R_x}(-\alpha_0)\mathbf{R_z}(-\theta_0)\mathbf{Q}_e\mathbf{R_z}(-\theta_E)\mathbf{R_x}(-\alpha_e)
\end{aligned} \tag{6.9}$$

Let

$$\mathbf{Q}_1 \equiv \prod_{i=1}^{f-1} [\mathbf{R_z}(\theta_i)\mathbf{R_x}(\alpha_i)]\,,\ \theta_\Sigma \equiv \sum_{i=f+1}^{g} \theta_i,\ \mathbf{Q}_2 \equiv \prod_{i=g+1}^{p} [\mathbf{R_z}(\theta_i)\mathbf{R_x}(\alpha_i)] \tag{6.10}$$

Substitution of equation (6.10) into equation (6.9) yields

$$\begin{aligned}
&\mathbf{Q}_1\mathbf{R_z}(\theta_f)\mathbf{R_x}(\alpha_f)\mathbf{R_z}(\theta_\Sigma)\mathbf{R_x}(\alpha_g)\mathbf{R_z}(\theta_h)\mathbf{R_x}(\alpha_h)\mathbf{Q}_2 \\
= \quad &\mathbf{R_x}(-\alpha_0)\mathbf{R_z}(-\theta_0)\mathbf{Q}_e\mathbf{R_z}(-\theta_E)\mathbf{R_x}(-\alpha_e)
\end{aligned} \tag{6.11}$$

Rearranging constant entries of equation (6.11) gives

$$\begin{aligned} & \mathbf{R_z}(\theta_f)\mathbf{R_x}(\alpha_f)\mathbf{R_z}(\theta_\Sigma)\mathbf{R_x}(\alpha_g)\mathbf{R_z}(\theta_h) \\ = \; & \mathbf{Q}_1^T\mathbf{R_x}(-\alpha_0)\mathbf{R_z}(-\theta_0)\mathbf{Q}_e\mathbf{R_z}(-\theta_E)\mathbf{R_x}(-\alpha_e)\mathbf{Q}_2^T\mathbf{R}_\mathbf{x}^T(\alpha_h) \end{aligned} \tag{6.12}$$

Let

$$\mathbf{Q}_1^T\mathbf{R_x}(-\alpha_0)\mathbf{R_z}(-\theta_0)\mathbf{Q}_e\mathbf{R_z}(-\theta_E)\mathbf{R_x}(-\alpha_e)\mathbf{Q}_2^T\mathbf{R}_\mathbf{x}^T(\alpha_h) \equiv \begin{bmatrix} e_{11} & e_{12} & e_{13} \\ e_{21} & e_{22} & e_{23} \\ e_{31} & e_{32} & e_{33} \end{bmatrix} \tag{6.13}$$

then substitution of equation (6.13) into equation (6.12) leads to

$$\mathbf{R_z}(\theta_f)\mathbf{R_x}(\alpha_f)\mathbf{R_z}(\theta_\Sigma)\mathbf{R_x}(\alpha_g)\mathbf{R_z}(\theta_h) = \begin{bmatrix} e_{11} & e_{12} & e_{13} \\ e_{21} & e_{22} & e_{23} \\ e_{31} & e_{32} & e_{33} \end{bmatrix} \tag{6.14}$$

Eliminate θ_h from equation (6.14) by multiplying its both sides with $\boldsymbol{e}_3$, we get

$$\mathbf{R_z}(\theta_f)\mathbf{R_x}(\alpha_f)\mathbf{R_z}(\theta_\Sigma)\mathbf{R_x}(\alpha_g)\boldsymbol{e}_3 = \begin{bmatrix} e_{13} & e_{23} & e_{23} \end{bmatrix}^T \tag{6.15}$$

Premultiplying both sides of equation (6.15) with

$$\boldsymbol{e}_3^T\mathbf{R_z}(-\theta_\Sigma)\mathbf{R_x}(-\alpha_f)\mathbf{R_z}(-\theta_f)$$

leads to

$$\sin(\alpha_f)\left[e_{13}\sin(\theta_f) - e_{23}\cos(\theta_f)\right] + e_{33}\cos(\alpha_f) = \cos(\alpha_g) \tag{6.16}$$

Under the condition that $e_{13}^2 + e_{23}^2 \neq 0$, θ_f can thus be solved from equation (6.16) as

$$\theta_f = \pm \arccos \left[\frac{\cos(\alpha_g) - e_{33}\cos(\alpha_f)}{\sin(\alpha_f)\sqrt{e_{13}^2 + e_{23}^2}} \right] - \arcsin \left(\frac{e_{13}}{\sqrt{e_{13}^2 + e_{23}^2}} \right) \tag{6.17}$$

Multiplying both sides of equation (6.15) by $\mathbf{R_x}(-\alpha_f)\mathbf{R_z}(-\theta_f)$ gives

$$\mathbf{R_z}(\theta_\Sigma)\mathbf{R_x}(\alpha_g)\boldsymbol{e}_3 = \mathbf{R_x}(-\alpha_f)\mathbf{R_z}(-\theta_f) \begin{bmatrix} e_{13} & e_{23} & e_{23} \end{bmatrix}^T \tag{6.18}$$

θ_Σ can solved from equation (6.18) as

$$\theta_\Sigma = \arcsin \frac{\boldsymbol{e}_3^T \mathbf{R_x}(-\alpha_f)\mathbf{R_z}(-\theta_f) \begin{bmatrix} e_{13} & e_{23} & e_{23} \end{bmatrix}^T}{\sin(\alpha_g)} \tag{6.19}$$

Multiplying both sides of equation (6.14) with $\mathbf{R_x}(-\alpha_g)\mathbf{R_z}(-\theta_\Sigma)\mathbf{R_x}(-\alpha_f)\mathbf{R_z}(-\theta_f)$, we have

$$\mathbf{R_z}(\theta_h) = \mathbf{R_x}(-\alpha_g)\mathbf{R_z}(-\theta_\Sigma)\mathbf{R_x}(-\alpha_f)\mathbf{R_z}(-\theta_f) \begin{bmatrix} e_{11} & e_{12} & e_{13} \\ e_{21} & e_{22} & e_{23} \\ e_{31} & e_{32} & e_{33} \end{bmatrix} \tag{6.20}$$

θ_k can be solved from equation (6.20) as

$$\theta_h = \arccos \left(\boldsymbol{e}_3^T \mathbf{R_x}(-\alpha_g)\mathbf{R_z}(-\theta_\Sigma)\mathbf{R_x}(-\alpha_f)\mathbf{R_z}(-\theta_f) \begin{bmatrix} e_{11} & e_{21} & e_{31} \end{bmatrix}^T \right) \tag{6.21}$$

From equation (6.17), (6.19), and (6.21), we know that the DOF of the subchain is reduced by 3.

If $e_{13}^2 + e_{23}^2 = 0$, since rotation matrix is orthonormal, it follows that $e_{33} = \pm 1$ and

equation (6.16) becomes

$$\cos(\alpha_f) = \pm\cos(\alpha_g) \tag{6.22}$$

That is

$$\alpha_f = \alpha_g \,, \alpha_f = -\alpha_g \,, \text{or } \alpha_f = \pi - \alpha_g \tag{6.23}$$

This means that f^{th} link and g^{th} link are conjugate. In this case equation (6.15) becomes

$$\begin{aligned}
\mathbf{R_z}(\theta_f)\mathbf{R_x}(\alpha_f)\mathbf{R_z}(\theta_\Sigma)\mathbf{R_x}(\alpha_f)\boldsymbol{e}_3 &= \boldsymbol{e}_3 \text{ for } \alpha_f = \alpha_g \\
\mathbf{R_z}(\theta_f)\mathbf{R_x}(\alpha_f)\mathbf{R_z}(\theta_\Sigma)\mathbf{R_x}(-\alpha_f)\boldsymbol{e}_3 &= \boldsymbol{e}_3 \text{ for } \alpha_f = -\alpha_g \\
\mathbf{R_z}(\theta_f)\mathbf{R_x}(\alpha_f)\mathbf{R_z}(\theta_\Sigma)\mathbf{R_x}(\pi - \alpha_f)\boldsymbol{e}_3 &= \boldsymbol{e}_3 \text{ for } \alpha_f = \pi - \alpha_g
\end{aligned}$$

which leads to

$$\left\{ \begin{array}{c} \alpha_f = \alpha_g \\ \theta_\Sigma = \pi \end{array} \right. , \left\{ \begin{array}{c} \alpha_f = -\alpha_g \\ \theta_\Sigma = 0 \end{array} \right. , \left\{ \begin{array}{c} \alpha_f = \pi - \alpha_g \\ \theta_\Sigma = 0 \end{array} \right. \tag{6.24}$$

Conjugate links in this relative configuration is said to be aligned. Substituting equation (6.24) back into equation (6.14) leads to

$$\begin{aligned}
\theta_f + \theta_h &= \arccos(e_{11}) - \pi \text{ for } \alpha_f = \alpha_g \\
\theta_f - \theta_h &= \arccos(e_{11}) \text{ for } \alpha_f = \pi - \alpha_g \text{ or } \alpha_f = -\alpha_g
\end{aligned} \tag{6.25}$$

Equations (6.24) and (6.25) reduce the DOF of the subchain by 2.

The above two situations are summarized as

– a subchain with two non conjugate (hyper) skew revolute links loose 3 DOF

when its EE is constrained in a constant orientation ;

- a subchain with two conjugate (hyper) skew revolute links loses only 2 DOF when its EE is constrained in a orientation which is reachable by aligning the two conjugate links .

To characterize a subchain by its revolute joint situations, we introduce the following definitions :

T-subchain : a subchain with only prismatic joints ;

I-subchain : a subchain whose revolute joints are all parallel ;

A-subchain : a subchain composed of one (hyper) skew revolute link and other links ;

Z-subchain : a subchain composed of two conjugate (hyper) skew revolute links and other links ;

Y-subchain : a subchain composed of at least two non conjugate (hyper) revolute links and other links.

Then, from the above analysis, the possible subchain topologies for TPMs are derived as listed in table 6.1.

TAB. 6.1 Possible subchain topologies for TPMs

	3-joint	4-joint	5-joint	6-joint
T-subchain	Yes	No	No	No
I-subchain	No	Yes	No	No
A-subchain	No	No	Yes	No
Z-subchain	No	No	Yes	Yes
Y-subchain	No	No	No	Yes

The orientation space of the EE of a 3-DOF PM under the constraints of the 3 subchains is analyzed in the next section.

6.4 Analysis of the EE orientation space of PMs of 3 DOF

The orientation space of a PM is formed by the orientation part of the set of solutions of equation (6.1). In order to synthesize topologies of TPMs, the reasoning is as follows : if

1. the orientation part of the set of solutions of equation (6.1) has only finite number of elements, (*i.e.* all solitary subspaces of the orientation space is a single element subspace, no orientation path exists between any two of them, meaning that the EE of the PM can not pass from one orientation to another without the PM having to be reassembled), and
2. each subchain allows the EE to have 3 DOMs in translation without the EE having to change orientation,

the PM is naturally a TPM.

When performing orientation analysis, we assign reference frame to (hyper) revolute link only; the prismatic joint parameters are merged into the hyper revolute link parameters in order to make the mathematical expressions concise. By rearranging equation (6.2), it follows,

$$\begin{aligned} \mathbf{Q}_{i,e}(\boldsymbol{\theta}_i) &\equiv \mathbf{R}_{\mathbf{z}}(\theta_{i,0})\mathbf{R}_{\mathbf{x}}(\alpha_{i,0}) \left[\prod_{j=1}^{p_i} [\mathbf{R}_{\mathbf{z}}(\theta_{i,j})\mathbf{R}_{\mathbf{x}}(\alpha_{i,j})] \right] \mathbf{R}_{\mathbf{x}}(\alpha_{i,e})\mathbf{R}_{\mathbf{z}}(\theta_{i,E}) \\ \boldsymbol{\theta}_i &\equiv \begin{bmatrix} \theta_{i,1} & \theta_{i,1} & \cdots & \theta_{i,p_i} \end{bmatrix}^T \end{aligned} \tag{6.26}$$

where p_i is the total number of revolute joints in i^{th} subchain. Equation (6.26) defines the orientation of the EE under the constraints of i^{th} subchain. The PM is

obtained by making the end link frames of the three subchains coincide and rigidly attached. The orientation part of the structure equations is thus given as

$$\begin{aligned} \mathbf{Q}_e = \mathbf{Q}_{1,e}(\boldsymbol{\theta}_1) &= \mathbf{Q}_{2,e}(\boldsymbol{\theta}_2) \\ \mathbf{Q}_{2,e}(\boldsymbol{\theta}_2) &= \mathbf{Q}_{3,e}(\boldsymbol{\theta}_3) \end{aligned} \tag{6.27}$$

6.4.1 PMs with a T-subchain

Under the constraint of the T-subchain, the orientation space of the EE is a single element space solely determined by the geometry of this subchain, *i.e.*

$$\mathbf{Q}_{1,e} = \mathbf{R}_{\mathbf{z}}(\theta_{1,0})\mathbf{R}_{\mathbf{x}}(\alpha_{1,0})\mathbf{R}_{\mathbf{x}}(\alpha_{1,e})\mathbf{R}_{\mathbf{z}}(\theta_{1,E}) \tag{6.28}$$

The EE will not have any displacement in orientation. From the point of view of eliminating displacements in orientation, the second and third subchains can be of any possible subchain topologies derived in the previous section (table 6.1). However, if the dimension of the orientation space of any of the other subchains is lower then 3, the PM becomes overconstrained, exact geometries of the base and the EE are necessary for equation (6.27) to have any real solution, *i.e.* for the PM to be assembled.

6.4.2 PMs with an I-subchain

Let the first subchain be an I-subchain, then from equation (6.26), we get

$$\mathbf{Q}_{1,e} = \mathbf{R}_{\mathbf{z}}(\theta_{1,0})\mathbf{R}_{\mathbf{x}}(\alpha_{1,0})\mathbf{R}_{\mathbf{z}}\left(\sum_{j=1}^{p_1}\theta_{1,j}\right)\mathbf{R}_{\mathbf{x}}(\alpha_{1,e})\mathbf{R}_{\mathbf{z}}(\theta_{1,E}) \tag{6.29}$$

If the second subchain is also I-subchain, then

$$\mathbf{Q}_{2,e} = \mathbf{R_z}(\theta_{2,0})\mathbf{R_x}(\alpha_{2,0})\mathbf{R_z}\left(\sum_{j=1}^{p_2}\theta_{2,j}\right)\mathbf{R_x}(\alpha_{2,e})\mathbf{R_z}(\theta_{2,E}) \tag{6.30}$$

Substituting equations (6.29) and (6.30) into equation (6.27) yields

$$\begin{aligned} & \mathbf{R_z}\left(\sum_{j=1}^{p_1}\theta_{1,j}\right)\mathbf{R_x}(\alpha_{1,e})\mathbf{R_z}(\theta_{1,E})\mathbf{R_z}(-\theta_{2,E})\mathbf{R_x}(-\alpha_{2,e}) \\ = \quad & \mathbf{R_x}(-\alpha_{1,0})\mathbf{R_z}(-\theta_{1,0})\mathbf{R_z}(\theta_{2,0})\mathbf{R_x}(\alpha_{2,0})\mathbf{R_z}\left(\sum_{j=1}^{p_2}\theta_{2,j}\right) \end{aligned} \tag{6.31}$$

Let

$$\begin{aligned} \begin{bmatrix} g_{11} & g_{12} & g_{13} \end{bmatrix}^T &\equiv \mathbf{R_x}(\alpha_{1,e})\mathbf{R_z}(\theta_{1,E})\mathbf{R_z}(-\theta_{2,E})\mathbf{R_x}(-\alpha_{2,e})\boldsymbol{e}_3 \\ \begin{bmatrix} g_{21} & g_{22} & g_{23} \end{bmatrix}^T &\equiv \mathbf{R_x}(-\alpha_{1,0})\mathbf{R_z}(-\theta_{1,0})\mathbf{R_z}(\theta_{2,0})\mathbf{R_x}(\alpha_{2,0})\boldsymbol{e}_3 \end{aligned} \tag{6.32}$$

which depend only on the geometry of the subchains. By comparing equations (6.31) and (6.32), we get

$$\mathbf{R_z}\left(\sum_{j=1}^{p_1}\theta_{1,j}\right)\begin{bmatrix} g_{11} & g_{12} & g_{13} \end{bmatrix}^T = \begin{bmatrix} g_{21} & g_{22} & g_{23} \end{bmatrix}^T \tag{6.33}$$

If $g_{13} \neq g_{23}$, then equation (6.33) has no real solution, the PM can not be assembled. If $g_{13} = g_{23}$, then from equations (6.33) we get

$$\sum_{j=1}^{p_1}\theta_{1,j} = \arccos\left(\frac{g_{11}g_{21} + g_{12}g_{22}}{g_{11}^2 + g_{12}^2}\right)$$

leading to a single element orientation space; the third subchain can be of any topology listed in table 6.1.

If the second subchain is an A-subchain, then from equation equation (6.26), we have

$$\begin{aligned} & \mathbf{R_z}\left(\sum_{j=1}^{f_2}\theta_{2,j}\right)\mathbf{R_x}(\alpha_{2,f})\mathbf{R_z}\left(\sum_{j=f_2+1}^{p_2}\theta_{2,j}\right) \\ = \quad & \mathbf{R_x}(-\alpha_{2,0})\mathbf{R_z}(-\theta_{2,0})\mathbf{Q}_e\mathbf{R_z}(-\theta_{2,E})\mathbf{R_x}(-\alpha_{2,e}) \end{aligned} \tag{6.34}$$

By rearranging equations (6.29) and (6.34), we get

$$\mathbf{Q}_e\mathbf{R_z}(-\theta_{1,E})\mathbf{R_x}(-\alpha_{1,e}) = \mathbf{R_z}(\theta_{1,0})\mathbf{R_x}(\alpha_{1,0})\mathbf{R_z}\left(\sum_{j=1}^{p_1}\theta_{1,j}\right) \tag{6.35}$$

$$\begin{aligned} & \mathbf{Q}_e\mathbf{R_z}(-\theta_{2,E})\mathbf{R_x}(-\alpha_{2,e}) \\ = \quad & \mathbf{R_z}(\theta_{2,0})\mathbf{R_x}(\alpha_{2,0})\mathbf{R_z}\left(\sum_{j=1}^{f_2}\theta_{2,j}\right)\mathbf{R_x}(\alpha_{2,f_2})\mathbf{R_z}\left(\sum_{j=f_2+1}^{p_2}\theta_{2,j}\right) \end{aligned} \tag{6.36}$$

From equations (6.35) and (6.36), we can solve

$$\cos\left(\sum_{j=1}^{p_1}\theta_{1,j}\right) = \frac{-A_3C_3 \pm \sqrt{A_3^2B_3^2 + B_3^4 - B_3^2C_3^2}}{A_3^2 + B_3^2}$$

$$\cos\left(\sum_{j=1}^{f_2}\theta_{2,j}\right) = \frac{-A_1C_1 \pm \sqrt{A_1^2B_1^2 + B_1^4 - B_1^2C_1^2}}{A_1^2 + B_1^2}$$

$$\cos\left(\sum_{j=f_2+1}^{p_2}\theta_{2,j}\right) = \frac{-A_2C_2 \pm \sqrt{A_2^2B_2^2 + B_2^4 - B_2^2C_2^2}}{A_2^2 + B_2^2}$$

where the right hand entries are all geometry-determined parameters.

It is clear that under the constraints of an I-subchain and an A-subchain, the EE has only two possible orientations, each corresponding to an assembly mode; given an assembly mode, it is impossible for the EE to change orientation. The third subchain can be of any topologies listed in table 6.1.

6.4.3 PMs with three A-subchains

Let f_i^{th} $(i = 1, 2, 3)$ (hyper) revolute link be the (hyper) skew revolute link of i^{th} A-subchain, then from equation (6.26), we have

$$\begin{aligned}\mathbf{Q}_{i,e} &= \mathbf{R_z}(\theta_{i,0})\mathbf{R_x}(\alpha_{i,0})\mathbf{R_z}\left(\sum_{j=1}^{f_i}\theta_{i,j}\right)\mathbf{R_x}(\alpha_{i,f_i}) \\ &\quad \mathbf{R_z}\left(\sum_{j=f_i+1}^{p_i}\theta_{i,j}\right)\mathbf{R_x}(\alpha_{i,e})\mathbf{R_z}(\theta_{i,E}),\ i = 1,\ 2,\ 3 \end{aligned} \tag{6.37}$$

Let

$$\mathbf{g}_i \equiv \begin{bmatrix} a_i & b_i & c_i \end{bmatrix}^T \equiv \mathbf{R_z}(\theta_{i,0})\mathbf{R_x}(\alpha_{i,0})\boldsymbol{e}_3,\ i = 1,\ 2,\ 3 \tag{6.38}$$

which is function of the base geometry, and

$$\begin{aligned}\mathbf{h}_i &\equiv \begin{bmatrix} x_i & y_i & z_i \end{bmatrix}^T \\ &\equiv \mathbf{R_z}(\theta_{i,0})\mathbf{R_x}(\alpha_{i,0})\mathbf{R_z}\left(\sum_{j=1}^{f_i}\theta_{i,j}\right)\mathbf{R_x}(\alpha_{i,f_i})\mathbf{R_z}\left(\sum_{j=f_i+1}^{p_i}\theta_{i,j}\right)\boldsymbol{e}_3 \\ &\quad i = 1,\ 2,\ 3 \end{aligned} \tag{6.39}$$

By substituting equation (6.39) into equation (6.37), we have

$$\mathbf{h}_i = \mathbf{Q}_{i,e}\mathbf{R_z}(-\theta_{i,E})\mathbf{R_x}(-\alpha_{i,e})\boldsymbol{e}_3,\ i = 1,\ 2,\ 3 \tag{6.40}$$

Since $\mathbf{Q}_{1,e} = \mathbf{Q}_{2,e} = \mathbf{Q}_{3,e} = \mathbf{Q}_e$, $\mathbf{Q}_{i,e}$ $(i = 1, 2, 3)$ can be eliminated by taking the scalar product of equation (6.40), *i.e*

$$\begin{aligned}\lambda_1 &\equiv \mathbf{h}_1^T\mathbf{h}_2 = \boldsymbol{e}_3^T\mathbf{R_x}(\alpha_{1,e})\mathbf{R_z}(\theta_{1,E} - \theta_{2,E})\mathbf{R_x}(-\alpha_{2,e})\boldsymbol{e}_3 \\ \lambda_2 &\equiv \mathbf{h}_2^T\mathbf{h}_3 = \boldsymbol{e}_3^T\mathbf{R_x}(\alpha_{2,e})\mathbf{R_z}(\theta_{2,E} - \theta_{3,E})\mathbf{R_x}(-\alpha_{3,e})\boldsymbol{e}_3\end{aligned}$$

$$\lambda_3 \equiv \mathbf{h}_3^T \mathbf{h}_1 = \boldsymbol{e}_3^T \mathbf{R}_{\mathbf{x}}(\alpha_{3,e}) \mathbf{R}_{\mathbf{z}}(\theta_{3,E} - \theta_{1,E}) \mathbf{R}_{\mathbf{x}}(-\alpha_{1,e}) \boldsymbol{e}_3 \tag{6.41}$$

With equations (6.38) and (6.39), taking the scalar products between $\mathbf{g}_i$ and $\mathbf{h}_i$ $(i = 1, 2, 3)$ leads to

$$d_i \equiv \mathbf{g}_i^T \mathbf{h}_i = \boldsymbol{e}_3^T \mathbf{R}_{\mathbf{x}}(\alpha_{i,f_i}) \boldsymbol{e}_3, \; i = 1, \; 2, \; 3 \tag{6.42}$$

which is function of the geometries of the base, the EE, and the (hyper) skew revolute links.

Writing equations (6.41) in scalar form gives

$$x_1 x_2 + y_1 y_2 + z_1 z_2 - \lambda_1 = 0 \tag{6.43}$$

$$u x_2 + v y_2 + w z_2 - \lambda_2 = 0 \tag{6.44}$$

$$u x_1 + v y_1 + w z_1 - \lambda_3 = 0 \tag{6.45}$$

where $u \equiv x_3$, $v \equiv y_3$, and $w \equiv z_3$. $\mathbf{h}_i$ $(i = 1, 2, 3)$ being unit vector leads to

$$x_1^2 + y_1^2 + z_1^2 - 1 = 0 \tag{6.46}$$

$$x_2^2 + y_2^2 + z_2^2 - 1 = 0 \tag{6.47}$$

$$u^2 + v^2 + w^2 - 1 = 0 \tag{6.48}$$

Writing equation (6.42) in scalar form gives

$$a_1 x_1 + b_1 y_1 + c_1 z_1 - d_1 = 0 \tag{6.49}$$

$$a_2 x_2 + b_2 y_2 + c_2 z_2 - d_2 = 0 \tag{6.50}$$

$$a_3 u + b_3 v + c_3 w - d_3 = 0 \tag{6.51}$$

Equations from (6.43) to (6.51) are a set of 9 equations with 9 unknown, *i.e.*

$$x_1,\ y_1,\ z_1,\ x_2,\ y_2,\ z_2,\ u,\ v,\ w$$

Eliminate x_1 from equations (6.45) and (6.46) with equation (6.49), we get

$$ud_1 + (va_1 - ub_1)y_1 + (wa_1 - uc_1)z_1 - a_1\lambda_3 = 0 \quad (6.52)$$

$$-a_1^2 + d_1^2 - 2b_1d_1y_1 + (a_1^2 + b_1^2)y_1^2 + (-2c_1d_1 + 2b_1c_1y_1)z_1 + (a_1^2 + c_1^2)z_1^2 = 0 \quad (6.53)$$

Using equation (6.52) to eliminate y_1 from equation (6.53) yields

$$\begin{aligned}
& a_1^2\left[\left(u^2+v^2\right)d_1^2 - 2vb_1d_1\lambda_3 + 2ua_1\left(vb_1 - d_1\lambda_3\right) + b_1^2\left(-u^2+\lambda_3^2\right)\right] \\
+\ & a_1^4\left(-v^2+\lambda_3^2\right) - 2a_1^2\left(-w\left(ua_1+vb_1\right) + \left(u^2+v^2\right)c_1\right)z_1d_1 \\
+\ & 2a_1^2\left(w\left(a_1^2+b_1^2\right) - \left(ua_1+vb_1\right)\right)z_1\lambda_3 + \left(v^2+w^2\right)z_1^2a_1^4 \\
+\ & a_1^2\left(u^2+w^2\right)z_1^2b_1^2 - 2a_1^2vwb_1c_1z_1^2 + a_1^2\left(u^2+v^2\right)z_1^2c_1^2 \\
-\ & 2ua_1^3\left(vb_1 - w_1c_1\right)z_1^2 = 0
\end{aligned} \quad (6.54)$$

Eliminate x_2 from equations (6.44) and (6.47) with equation (6.50), we get

$$ud_2 + (va_2 - ub_2)y_2 + (wa_2 - uc_2)z_2 - a_2\lambda_2 = 0 \quad (6.55)$$

$$-a_2^2 + d_2^2 - 2b_2d_2y_2 + (a_2^2 + b_2^2)y_2^2 + (-2c_2d_2 + 2b_2c_2y_2)z_2 + (a_2^2 + c_2^2)z_2^2 = 0 \quad (6.56)$$

y_2 in equation (6.56) can be eliminated by using equation (6.55), we get

$$\begin{aligned}
& a_2^2\left[\left(u^2+v^2\right)d_2^2 - 2vb_2d_2\lambda_2 + 2ua_2\left(vb_2 - d_2\lambda_2\right) + b_2^2\left(-u^2+\lambda_2^2\right)\right] \\
+\ & a_2^4\left(-v^2+\lambda_2^2\right) - 2a_2^2\left(-w\left(ua_2+vb_2\right) + \left(u^2+v^2\right)c_2\right)z_2d_2 \\
+\ & 2a_2^2\left(w\left(a_2^2+b_2^2\right) - \left(ua_2+vb_2\right)\right)z_2\lambda_2 + \left(v^2+w^2\right)z_2^2a_2^4 \\
+\ & a_2^2\left(u^2+w^2\right)z_2^2b_2^2 - 2a_2^2vwb_2c_2z_2^2 + \left(u^2+v^2\right)z_2^2a_2^2c_2^2
\end{aligned}$$

$$- \quad 2ua_2^3 (vb_2 - w_2c_2) z_2^2 = 0 \tag{6.57}$$

Eliminate x_1 from equation (6.43) with equation (6.49), we get

$$a_1y_1y_2 - x_2(-d_1 + b_1y_1 + c_1z_1) + a_1z_1z_2 - a_1\lambda_1 = 0 \tag{6.58}$$

y_1 can be eliminated from equation (6.58) with (6.52)

$$\begin{aligned} &(va_1 - ub_1)(d_1x_2 - c_1x_2z_1 + a_1z_1z_2 - a_1\lambda_1) + \\ &b_1x_2(ud_1 + wa_1z_1 - uc_1z_1 - a_1\lambda_3) - a_1y_2(ud_1 + wa_1z_1 - uc_1z_1 - a_1\lambda_3) = 0 \end{aligned} \tag{6.59}$$

Eliminate x_2 from equation (6.59) with equation (6.50), we get

$$\begin{aligned} &-va_1^2a_2\lambda_1 + ua_1a_2b_1\lambda_1 + d_2(va_1d_1 + wa_1b_1z_1 - va_1c_1z_1 - a_1b_1\lambda_3) \\ &+y_2(-ua_1a_2d_1 - wa_1^2a_2z_1 + ua_1a_2c_1z_1 + a_1^2a_2\lambda_3) \\ &-b_2y_2(va_1d_1 + wa_1b_1z_1 - va_1c_1z_1 - a_1b_1\lambda_3) + \\ &z_2(va_1^2a_2z_1 - ua_1a_2b_1z_1 - c_2(va_1d_1 + wa_1b_1z_1 - va_1c_1z_1 - a_1b_1\lambda_3) = 0 \end{aligned} \tag{6.60}$$

Eliminate y_2 from equation (6.60) with equation (6.55), we get

$${}^2A(u,v,w)\, z_1z_2 + {}^2B(u,v,w)\, z_1 + {}^2C(u,v,w)\, z_2 + {}^2D(u,v,w) = 0 \tag{6.61}$$

where ${}^2A(u,v,w)$, ${}^2B(u,v,w)$, ${}^2C(u,v,w)$, and ${}^2D(u,v,w)$ are quadratic function of u, v, and w.

Eliminate z_2 from equation (6.61) with equation (6.57), we get

$$(va_2 - ub_2)^2 \left({}^4A_0(u,v,w)\, z_1^2 + {}^4A_1(u,v,w)\, z_1 + {}^4A_2(u,v,w)\right) = 0 \tag{6.62}$$

where ${}^4A(u,v,w)_i$ $(i = 0,1,2)$ is quartic function of u, v, and w. Rewrite equa-

tion (6.54) as

$$ {}^{2}B_0(u,v,w)\, z_1^2 + {}^{2}B_1(u,v,w)\, z_1 + {}^{2}B_2(u,v,w) = 0 \tag{6.63} $$

where ${}^{2}B_i$ $(i = 0, 1, 2)$ is quadratic function of u, v, and w.

For equations (6.62) and (6.63) with z_1 as unknown to have real solutions, the Sylvester resultant must be zero, *i.e.*

$$ (va_2 - ub_2)^4 \begin{vmatrix} {}^{4}A_0(u,v,w) & {}^{4}A_1(u,v,w) & {}^{4}A_2(u,v,w) & 0 \\ 0 & {}^{4}A_0(u,v,w) & {}^{4}A_1(u,v,w) & {}^{4}A_2(u,v,w) \\ {}^{2}B_0(u,v,w) & {}^{2}B_1(u,v,w) & {}^{2}B_2(u,v,w) & 0 \\ 0 & {}^{2}B_0(u,v,w) & {}^{2}B_1(u,v,w) & {}^{2}B_2(u,v,w) \end{vmatrix} = 0 \tag{6.64} $$

Expanding equation (6.64) leads to

$$ {}^{8}C(u,v,w)\,(va_2 - ub_2)^4\,(va_1 - ub_1)^4 = 0 \tag{6.65} $$

where ${}^{8}C(u,v,w)$ is 8^{th} order polynomial of u, v, and w.

Eliminating w from equation (6.48) with equation (6.51) gives

$$ v^2(b_3^2 + c_3^2) + 2v(ua_3b_3 - b_3d_3) + u^2\left(a_3^2 + c_3^2\right) - 2ua_3d_3 - c_3^2 + d_3^2 = 0 \tag{6.66} $$

Similarly, eliminating w from equation (6.65) with equation (6.51) gives

$$ {}^{8}D(u,v)\,(va_2 - ub_2)^4\,(va_1 - ub_1)^4 = 0 \tag{6.67} $$

where ${}^{8}D(u,v,w)$ is 8^{th} order polynomial of u, v, and w.

If $(va_2 - ub_2)(va_1 - ub_1) \neq 0$, then

$$^8D(u, v) = 0 \tag{6.68}$$

Eliminating v from equation (6.68) with equation(6.66) leads to

$$\sum_{i=0}^{16} k_i u^i = 0 \tag{6.69}$$

where k_i $(i = 0 \sim 16)$ is geometry dependent coefficient.

If $(va_2 - ub_2) = 0$, then from equation (6.66), we have

$$\begin{aligned} & u^2\left(a_1^2a_3^2 + 2a_1a_3b_1b_3 + b_1^2b_3^2 + a_1^2c_3^2 + b_1^2a_3^2\right) \\ - \; & 2ua_1\left(a_1a_3d_3 + b_1b_3d_3\right) - a_1^2\left(c_3^2 - d_3^2\right) = 0 \end{aligned} \tag{6.70}$$

If $(va_1 - ub_1) = 0$, similarly, we get

$$\begin{aligned} & u^2\left(a_2^2a_3^2 + 2a_2a_3b_2b_3 + b_2^2b_3^2 + a_2^2c_3^2 + b_2^2a_3^2\right) \\ - \; & 2ua_2\left(a_2a_3d_3 + b_2b_3d_3\right) - a_2^2\left(c_3^2 - d_3^2\right) = 0 \end{aligned} \tag{6.71}$$

From equations (6.69)$\sim$(6.71), we know that the set of equations (6.43)$\sim$(6.51) has only finite number of solutions, *i.e.* the EE can have only finite number of orientations with each orientation corresponding to an assembly mode. Given an assembly mode, it is impossible for the EE to change orientation.

6.4.4 PMs with three Z-subchains

Let f_i^{th} and g_i^{th} $(i = 1, 2, 3)$ (hyper) revolute links be the conjugate links, then from equation (6.26), we get

$$\begin{aligned}\mathbf{Q}_e &= \mathbf{R_z}(\theta_{i,\,0})\mathbf{R_x}(\alpha_{i,\,0})\mathbf{R_z}\left(\sum_{j=1}^{f_i}\theta_{i,\,j}\right)\mathbf{R_x}(\alpha_{i,\,f_i}) \\ &\quad \mathbf{R_z}\left(\sum_{j=f_i+1}^{g_i}\theta_{i,\,j}\right)\mathbf{R_x}(\alpha_{i,\,f_i})\mathbf{R_z}\left(\sum_{j=g_i+1}^{p_i}\theta_{i,\,j}\right)\mathbf{R_x}(\alpha_{i,\,e})\mathbf{R_z}(\theta_{i,\,E}) \quad (6.72)\end{aligned}$$

Let

$$\varphi_i \equiv \sum_{j=1}^{f_i}\theta_{i,\,j},\ \phi_i \equiv \sum_{j=f_i+1}^{g_i}\theta_{i,\,j},\ \psi_i \equiv \sum_{j=g_i+1}^{p_i}\theta_{i,\,j}$$

From equation (6.72), we get

$$\begin{aligned}&\mathbf{R_z}(\theta_{i,\,0})\mathbf{R_x}(\alpha_{i.\,0})\mathbf{R_z}(\varphi_i)\mathbf{R_x}(\alpha_{i,\,f_i})\mathbf{R_z}(\phi_i) \\ &\mathbf{R_x}(\alpha_{i,\,f_i})\mathbf{R_z}(\psi_i)\mathbf{R_x}(\alpha_{i,\,e})\mathbf{R_z}(\theta_{i,\,E}-\theta_{k,\,E})\mathbf{R_x}(-\alpha_{k,\,e}) \\ =\ &\mathbf{R_z}(\theta_{k,\,0})\mathbf{R_x}(\alpha_{k,\,0})\mathbf{R_z}(\varphi_k)\mathbf{R_x}(\alpha_{k,\,f_k}) \\ &\mathbf{R_z}(\phi_k)\mathbf{R_x}(\alpha_{k,\,f_k})\mathbf{R_z}(\psi_k),\ i,\ k\ =\ 1,\ 2,\ 3;\ i \neq k \qquad (6.73)\end{aligned}$$

Equation (6.73) is equivalent to 6 scalar equations with 9 unknowns, having infinite number of solutions. So what is to be investigated is whether there exists a configuration neighborhood within which the PM has only translational displacement.

From the analysis of the last section, we know that if the two conjugate (hyper) skew revolute links are aligned, the subchain can allow the EE to have 3-DOM displacement with a constant orientation.

Let $\Phi \equiv \left\| \begin{array}{c} \pi - \phi_1 \\ \pi - \phi_2 \\ \pi - \phi_3 \end{array} \right\|_2$. If $\Phi = 0$, the two (hyper) conjugate revolute links of each subchain are aligned and equation (6.72) can be written as

$$\mathbf{Q}_e = \mathbf{R_z}(\theta_{i,\,0})\mathbf{R_x}(\alpha_{i,\,0})\mathbf{R_z}(\varphi_i + \psi_i + \pi)\mathbf{R_x}(\alpha_{i,\,e})\mathbf{R_z}(\theta_{i,\,E}) \text{ for } i = 1,\ 2,\ 3 \quad (6.74)$$

while equation (6.73) as

$$\begin{aligned} & \mathbf{R_z}(\varphi_i + \psi_i + \pi)\mathbf{R_x}(\alpha_{i,\,e})\mathbf{R_z}(\theta_{i,\,E} - \theta_{k,\,E})\mathbf{R_x}(-\alpha_{k,\,e}) \\ = \ & \mathbf{R_x}(-\alpha_{i,\,0})\mathbf{R_z}(\theta_{k,\,0} - \theta_{i,\,0})\mathbf{R_x}(\alpha_{k,\,0})\mathbf{R_z}(\varphi_k + \psi_k + \pi) \\ & \text{for } i,\ k = 1,\ 2,\ 3;\ i \neq k \end{aligned} \quad (6.75)$$

Let

$$\begin{aligned} \boldsymbol{\lambda}_{i,\,k} &\equiv \mathbf{R_x}(\alpha_{i,\,e})\mathbf{R_z}(\theta_{i,\,E} - \theta_{k,\,E})\mathbf{R_x}(-\alpha_{k,\,e})\boldsymbol{e}_3 \\ \boldsymbol{\mu}_{i,\,k} &\equiv \mathbf{R_x}(-\alpha_{i,\,0})\mathbf{R_z}(\theta_{k,\,0} - \theta_{i,\,0})\mathbf{R_x}(\alpha_{k,\,0})\boldsymbol{e}_3,\ i,\ k = 1,\ 2,\ 3;\ i \neq k \end{aligned} \quad (6.76)$$

which depend only on the geometry, then

$$\mathbf{R_z}(\varphi_i + \psi_i + \pi)\boldsymbol{\lambda}_{i,\,k} = \boldsymbol{\mu}_{i,\,k} \quad (6.77)$$

If the PM has such a geometry that

$$\boldsymbol{e}_3^T\boldsymbol{\lambda}_{i,\,k} = \boldsymbol{e}_3^T\boldsymbol{\mu}_{i,\,k},\ i,\ k = 1,\ 2,\ 3;\ i \neq k \quad (6.78)$$

then from equations (6.74) and (6.77) we know that the EE has an unique orientation when the two (hyper) conjugate revolute links of each subchain are aligned, and φ_i $(i = 1, 2, 3)$ can take any value so long as $\varphi_i + \psi_i$ $(i = 1, 2, 3)$ satisfies

equation (6.77). Equation (6.77) also shows that when the two conjugate links are aligned, a Z-subchain has the same effect as an I-subchain. The next step is to see if the EE can be constrained to this orientation through out a configuration neighborhood.

Let

$$\begin{aligned} \mathbf{g}_i &\equiv \mathbf{R_z}(\theta_{i,0})\mathbf{R_x}(\alpha_{i,0})\boldsymbol{e}_3 \\ \mathbf{h}_i &\equiv \mathbf{R_z}(\theta_{i,0})\mathbf{R_x}(\alpha_{i,0})\mathbf{R_z}(\varphi_i)\mathbf{R_x}(\alpha_{i,f_i})\mathbf{R_z}(\phi_i)\mathbf{R_x}(\alpha_{i,f_i})\boldsymbol{e}_3 \\ &\quad \text{for } i = 1,\ 2,\ 3 \end{aligned} \tag{6.79}$$

where $\mathbf{g}_i$ and $\mathbf{h}_i$ $(i = 1, 2, 3)$ are respectively the first and last revolute joint orientation. If $\Phi = 0$, from equations (6.79) we get

$$\mathbf{h}_i|_{\Phi=0} = \mathbf{R_z}(\theta_{i,0})\mathbf{R_x}(\alpha_{i,0})\boldsymbol{e}_3 = \mathbf{g}_i \text{ for } i = 1,\ 2,\ 3 \tag{6.80}$$

Since $\mathbf{h}_1$, $\mathbf{h}_2$, and $\mathbf{h}_3$ are respectively the last revolute joint orientation of each subchain, they should undergo the same rotation with respect to $\mathbf{h}_1|_{\Phi=0}$, $\mathbf{h}_2|_{\Phi=0}$, and $\mathbf{h}_3|_{\Phi=0}$. Therefore $\exists\mathbf{Q}$, a rotation matrix, such that

$$\mathbf{h}_i = \mathbf{Q}\,\mathbf{h}_i|_{\Phi=0} = \mathbf{Q}\mathbf{g}_i,\ i = 1,\ 2,\ 3 \tag{6.81}$$

Let the unit vector $\mathbf{s}$ be the rotation axis of $\mathbf{Q}$, *i.e.*

$$\mathbf{s} = \mathbf{Q}\mathbf{s} \tag{6.82}$$

Taking the scalar product between equations (6.81) and (6.82) yields

$$\mathbf{h}_i^T\mathbf{s} = \mathbf{g}_i^T\mathbf{s} \Leftrightarrow \left(\mathbf{h}_i^T - \mathbf{g}_i^T\right)\mathbf{s} = 0,\ i = 1,\ 2,\ 3 \tag{6.83}$$

From equation (6.79), we have

$$\begin{aligned} \mathbf{h}_i - \mathbf{g}_i &= \mathbf{R_z}(\theta_{i,\,0})\mathbf{R_x}(\alpha_{i,\,0})\mathbf{R_z}(\varphi_i)\mathbf{R_x}(\alpha_{i,\,f_i}) \\ &\quad [\mathbf{R_z}(\phi_i)\mathbf{R_x}(\alpha_{i,\,f_i}) - \mathbf{R_z}(\pi)\mathbf{R_x}(\alpha_{i,\,f_i})]\,\boldsymbol{e}_3,\ i = 1,\ 2,\ 3 \end{aligned} \tag{6.84}$$

Upon simplification of equation (6.84), we get

$$\begin{aligned} \mathbf{h}_i - \mathbf{g}_i &= 2\sin(\alpha_{i,\,f_i})\sin(\pi/2 - \phi_i/2)\,\mathbf{R_z}(\theta_{i,\,0})\mathbf{R_x}(\alpha_{i,\,0})\mathbf{R_z}(\varphi_i) \\ &\quad \mathbf{R_x}(\alpha_{i,\,f_i})\begin{bmatrix} \cos(\pi/2 - \phi_i/2) & \sin(\pi/2 - \phi_i/2) & 0 \end{bmatrix}^T \end{aligned} \tag{6.85}$$

Comparing equations (6.83) and (6.85), we have

$$\begin{bmatrix} \cos(\pi/2 - \phi_i/2) & \sin(\pi/2 - \phi_i/2) & 0 \end{bmatrix} \mathbf{M}_i(\varphi_i)\,\mathbf{s} = 0 \tag{6.86}$$

where

$$\mathbf{M}_i(\varphi_i) \equiv [\mathbf{R_z}(\theta_{i,\,0})\mathbf{R_x}(\alpha_{i,\,0})\mathbf{R_z}(\varphi_i)\mathbf{R_x}(\alpha_{i,\,f_i})]^T \tag{6.87}$$

From equation (6.86), we know that with Φ approaching $\mathbf{0}$, we have

$$\begin{bmatrix} 1 & 0 & 0 \end{bmatrix} \left[\lim_{\Phi \to 0} \mathbf{M}_i(\varphi_i)\right] \mathbf{s} = 0 \tag{6.88}$$

and

$$\begin{bmatrix} \begin{bmatrix} 1 & 0 & 0 \end{bmatrix} \left[\lim_{\Phi \to 0} \mathbf{M}_1(\varphi_1)\right] \\ \begin{bmatrix} 1 & 0 & 0 \end{bmatrix} \left[\lim_{\Phi \to 0} \mathbf{M}_2(\varphi_2)\right] \\ \begin{bmatrix} 1 & 0 & 0 \end{bmatrix} \left[\lim_{\Phi \to 0} \mathbf{M}_3(\varphi_3)\right] \end{bmatrix} \mathbf{s} = 0 \tag{6.89}$$

Let

$$N(\vartheta) \equiv \det \begin{bmatrix} [1 & 0 & 0\,]\mathbf{M}_1(\varphi_1) \\ [1 & 0 & 0\,]\mathbf{M}_2(\varphi_2) \\ [1 & 0 & 0\,]\mathbf{M}_3(\varphi_3) \end{bmatrix}, \ \vartheta \equiv \ [\varphi_1 \quad \varphi_2 \quad \varphi_3\,]^T \tag{6.90}$$

then from equation (6.89) we know that

$$\lim_{\Phi \to 0} N(\vartheta) = 0 \tag{6.91}$$

From equation (6.91), we may conclude that if the PM is put into a configuration where $\Phi = 0$ but $|N(\vartheta)| \gg 0$, then within a neighborhood of this configuration, Φ will remains 0, *i.e.* the EE will keep a constant orientation. In fact, this is true, since

1. $N(\vartheta)$ is continuous,
2. $\lim_{\Phi \to 0} N(\vartheta) = 0$,
3. if $\Phi = 0$, ϑ can take any element in $\mathbb{R}^3$,

$\exists \vartheta_0 \in \mathbb{R}^3$ and $\delta_0 > 0$, such that $\Phi = 0$ and $|N(\vartheta_0)| > \delta_0$, leading to that in configuration space, along any path from a configuration where $\Phi = 0$ and $\vartheta = \vartheta_0$ to a configuration where $|N(\vartheta)| > \varepsilon_0 \ll \delta_0, \varepsilon_0 > 0$ we have $\Phi = 0$ because from the limit definition, we have $\forall \varepsilon_0 > 0$, $\delta_0 > 0$, $\varepsilon_0 \ll \delta_0$, $\exists \sigma > 0$, such that if $0 < \Phi < \sigma$ then $|N(\vartheta)| < \varepsilon_0$, implying that for Φ to pass from 0 to σ, it is necessary that $|N(\vartheta)| < \varepsilon_0$.

If every subchain of the PM allows the EE to have 3 DOM in translation while keeping a constant orientation, then the PM is TPM within a neighborhood of the configuration where $\Phi = 0$ and $\vartheta = \vartheta_0$.

When the PM reaches a configuration where $\Phi = 0$ and $|N(\vartheta)| = 0$, the Z-subchain

can leave the aligned configuration passing to a general configuration and can no longer constrain the EE's orientation.

6.5 Topological synthesis of TPMs

With the analyses carried out in the previous sections, the topological synthesis of TPMs becomes straightforward and can be summarized as follows :

The first step is to determine the type of each subchain. The type of the first subchain can be of any of those listed in table 6.1. Depending on the choice of the first subchain, the second and third can be determined such that a constant orientation configuration neighborhood exists.

1. If the first subchain is a T-subchain, then the second and the third can be any of those listed in table 6.1 ;
2. If the first subchain is an I-subchain or a Z-subchain, then at least one of the second and the third should not be an Y-subchain ;
3. If the first subchain is an A-subchain, then the second and the third must be an A-subchain.

This can also serve as a verification for the synthesis based on instantaneous kinematics.

Then, the next step is to determine the topology of a subchain of a given type so as to generate 3 DOMs in translation. This can be done by using the synthesis methods for serial kinematic chains.

6.6 Conclusion

The proposed kinematic model applies to the most general topologies and geometries of 3-DOF PMs and therefore allows a thorough analysis of how the translational displacement and the configuration of a PM are affected by a constant orientation constraint on the EE. The topological constraints are derived for a serial kinematic chain of less than 6 joints to produce 3-DOF translation with a constant orientation of the EE. This, together with the proposed concepts, such as revolute link, A-subchain, serial kinematic chains can be effectively characterized. The analysis of the orientation solutions of the forward kinematics of all subchain combinations confirms which kinds of combination can produce a constant EE orientation in a finite configuration space. The finite configuration space may be the entire configuration space, a particular assembly mode, or a neighborhood in the configuration space. It is mathematically proven that a 3-DOF PM can produce only translation within a neighborhood of its configuration space but loose this capacity outside the neighborhood.

Acknowledgment

The authors acknowledge the financial support of NSERC (National Science and Engineering Research Council of Canada) under grants OGPIN-203618 and RGPIN-138478.

References

ANGELES, J. (c2003). *Fundamentals of robotic mechanical systems : theory, methods, and algorithms.* Mechanical engineering series : Mechanical engineering

series (Springer). Springer, New York, 2nd ed. edition.

BARON, L. (c1997). *Contributions to the estimation of rigid-body motion under sensor redundancy*. PhD thesis, McGill University.

BARON, L. AND ANGELES, J. (1995). The isotropic decoupling of the direct kinematics of parallel manipulators under sensor redundancy. *Proceedings of 1995 IEEE International Conference on Robotics and Automation (Cat. No.95CH3461-1)*, **vol.2**, 1541 - 6.

BROGARDH, C. (2002). Pkm research-important issues, as seen from a product development perspective at abb. In *Proceedings of the WORKSHOP on Fundamental Issues and Future Research Directions for Parallel Mechanisms and Manipulators*, Quebec City, Quebec, Canada, pages 68–82.

CARRICATO, M. AND PARENTI-CASTELLI, V. (2002). Singularity-free fully-isotropic translational parallel manipulators. *Proceedings of the ASME Design Engineering Technical Conference*, **5 B**, 1041 - 1050.

CLAVEL, R. (1988). Delta, a fast robot with parallel geometry. *Proceedings of the 18th International Symposium on Industrial Robots*, pages 91 - 100.

DENAVIT, J. AND HARTENBERG, R. S. (1954). Kinematic notation for lower-pair mechanisms based on matrices. In *American Society of Mechanical Engineers (ASME)*.

FRISOLI, A., CHECCACCI, D., SALSEDO, F., AND BERGAMASCO, M. (2000). Synthesis by screw algebra of translating in-parallel actuated mechanisms. In Lenarcic, J. and Parenti-Castelli, V., editors, *Recent Advances in Robot Kinematics*. Kluwer Academic Publishers.

GOSSELIN, C., KONG, X., FOUCAULT, S., AND BONEV, I. A. (2004). A fully decoupled 3-dof translational parallel mechanism. In *Proceedings of 2004 Parallel Kinematic Machines in Research and Practice International Conference (PKS 2004)*, Chemnitz, Germany, pages 595–610.

HERVE, J. M. (1991). Structural synthesis of parallel robots generating spatial translation. In *Proceedings of Fifth International Conference on Advanced Robotics*, pages 808–813.

HERVE, J. M. AND SPARACINO, F. (1992). Star, a new concept in robotics. In *Third International Workshop on Advances in Robot Kinematics*, pages 180–183.

IFTOMM (2003). Iftomm terminology. *Mechanism and Machine Theory*, **38**, 913–912.

KAROUIA, M. AND HERVE, J. M. (2002). A family of novel orientational 3-dof parallel robots. In *Proceedings of CISM-IFToMM RoManSy Symposia*, Udine, Italy, pages 359–368.

KONG, X. AND GOSSELIN, C. (2001). Generation of parallel manipulators with three translational degrees of freedom based on screw theory. In Agency, T. C. S., editor, *Symposium 2001 sur les mécanismes,les machines et la mécatronique de CCToMM*, Saint-Hubert, Montréal, Québec, Canada.

LEGUAY-DURAND, S. AND REBOULET, C. (1997). Design of a 3-dof parallel translating manipulator with u-p-u joints kinematic chains. In *Proceedings of the 1997 IEEE/RSJ International Conference on Intelligent Robot and Systems. Innovative Robotics for Real-World Applications. IROS '97*, pages 1637– 1642.

MCCARTHY, J. M. (1990). *An Introduction to Theoretical Kinematics*. The MIT Press, Cambridge, Massachusetts, London, England.

MERLET, J.-P. (2002). An initiative for the kinematics study of parallel manipulators. In *Proceedings of the WORKSHOP on Fundamental Issues and Future Research Directions for Parallel Mechanisms and Manipulators*, Montreal, Quebec, Canada.

MERLET, J.-P. (c1997). *Les robots paralleles*. Hermes, Paris.

TSAI, L.-W. (1996). Kinematics of a three-dof platform with extensible limbs. In Lenarcic, J. and Parenti-Castelli, V., editors, *Recent Advances in Robot Kinematics*, pages 401–410. Kluwer Academic Publishers.

TSAI, L.-W. (1999). The enumeration of a class of three-dof parallel manipulators. In *Proceedings of TENTH WORLD CONGRESS ON THE THEORY OF MACHINE AND MECHANISMS*, Oulu, Finland, pages 1121–1126.

TSAI, L.-W. (2001). *Mechanism design : enumeration of kinematic structures according to function*. Mechanical engineering series : CRC mechanical engineering series. CRC Press.

TSAI, L.-W. AND JOSHI, S. (2002). Kinematic analysis of 3-dof position mechanisms for use in hybrid kinematic machines. *Journal of Mechanical Design, Transactions of the ASME*, **124**(2), 245 – 253.

WANG, X., BARON, L., AND CLOUTIER, G. (2003). Design manifold of translational parallel manipulators. In l'Agence spatiale canadienne, editor, *Proceedings of 2003 CCToMM Symposium on Mechanisms, Machines, and Mechatronics*, Montreal, Quebec, Canada, pages 231–239.

WENGER, P. AND CHABLAT, D. (2000). Kinematic analysis of a new parallel machine tool : The orthoglide. In Lenarcic, J. and Parenti-Castelli, V., editors, *Recent Advances in Robot Kinematics*, pages 305– 314. Kluwer Academic Publishers.

CHAPITRE 7

TOPOLOGICAL AND GEOMETRIC MODELLING OF TRANSLATIONAL PARALLEL MANIPULATOR

Xiaoyu Wang, Luc Baron and Guy Cloutier.
Département de génie mécanique, École Polytechnique de Montréal.
P.O. 6079, station Centre-Ville, Montréal, Québec, Canada, H3C 3A7.
xiaoyu.wang@polymtl.ca

(To be submitted)

Abstract

This paper presents a kinematic modelling of translational parallel manipulators (TPMs) of different topologies. The concept of initial configuration is at first introduced. Based on the initial configuration a continuous topological and geometric parametrization is carried out. A special frame assignment is then performed. In order to treat the revolute joints and the prismatic ones in a unified way, joint variables are normalized, making the geometric model and the Jacobian matrix dimension-homogeneous. With the proposed kinematic model, design parameter space is continuous, a great advantage for implementing global optimization algorithms, simulated annealing, evolutionary algorithms for instance. The inverse kinematic problem is investigated using extensively matrix manipulation and it is found that there exists a closed-form solution if no serial kinematic chain linking the base to the end-effector has more than 5 joints. A numerical approach

for the forward kinematic problem is proposed. The whole work forms a basis for simultaneous synthesis of topology and geometry of TPMs.

Keywords : Parallel manipulator, Translational, Kinematics, Topology, Geometry, Synthesis.

7.1 Introduction

A parallel manipulator (PM) is a closed-loop mechanism in which the end-effector is connected to the base through at least two independent kinematic chains (MERLET, 1997). Due to the closed-loop nature, PMs provide, in general, high load-carrying capacity, accurate positioning, high speed, and high capacity of acceleration (ANGELES, 2003). The closed-loop nature also implies very complex kinematic model, singularities, and limited workspace (GOSSELIN ET ANGELES, 1990). Another drawback which attract researchers' attention is the performance in orientation space of 6-DOF PMs. It is difficult to find 6-DOF PMs with orientation performance comparable to serial manipulators (BROGARDH, 2002). To overcome these drawbacks, authors of (ZANGANEH ET ANGELES, 1998) proposed a modular solution, employing a hybrid structure. Another solution is to connect two 3-DOF PMs to produce 6-DOF motion in order to improve the overall performance and make the design easier. This can be illustrated by the hybrid kinematic machine (TSAI ET JOSHI, 2002). Therefore, the kinematic studies of 3-DOF PMs have become an important design issue.

Early designs of 3-DOF PMs have been realized mostly by resorting to researchers' experience, intuition, and ingenuity. Agile eye PM is the earliest design of spherical PM (GOSSELIN ET HAMEL, 1994). Delta PM is among the most successful translational PMs (TPM) (CLAVEL, 1985). Other TPM designs which have been under

extensive studies include 3-UPU PM (TSAI, 1996), Orthoglide PM (WENGER ET CHABLAT, 2000). Kinematic studies of these 3-DOF PMs have been mostly accomplished on a case-by-case basis (GOSSELIN ET AL., 2004). Parallel to these well known designs, a great deal of effort has been made on the topological synthesis methodology. Y-Star PM (HERVE ET SPARACINO, 1992) is the first TPM synthesized based on the group theory. Another synthesis approach is based on screw theory. This approach was explained in detail and demonstrated by examples in (LEGUAY-DURAND ET REBOULET, 1997). With these systematic approaches, several large families of PM topologies have been proposed. On TPM side, we can cite (KONG ET GOSSELIN, 2004), while (KAROUIA ET HERVE, 2002) can be cited for spherical PMs. The most distinctive topology of TPMs was proposed independently by (KONG ET GOSSELIN, 2001) and (KIM ET TSAI, 2002), it is a fully decoupled TPM.

Although the considerable advantages and the enormous effort by researchers, applications of PMs are far from what we have expected, there is still a long way to go on the road to put into full play of PMs (MERLET, 2002b). Topological and geometric synthesis is still an open problem for PMs of less than 6 DOF (MERLET, 2002a). The work presented in this paper is motivated by the need for systematic topological and geometric synthesis of TPMs.

In section 3, we investigate how to represent joint type with continuous variables and how to parameterize the topology. In section 4, we study the integrated topology and geometry representation. In section 5, an original frame assignment is proposed by which parameter singularity can be avoided, a generalized kinematic modelling is proposed. Particular aspects of kinematic model for TPMs are detailed in section 6. In section 7, inverse kinematic problem is fully investigated. Section 8 deals with forward kinematic problem and a numerical solution is proposed. The Jacobian matrix is formulated in section 9 and the topological and geometric syn-

thesis procedure is presented in section 10. The conclusion is presented in the last section.

7.2 Nomenclature

- b : subscript to identify the base;
- e : subscript to identify the end-effector;
- $\mathcal{F}_i$: reference frame attached to *link* i;
- $\mathbf{G}_i$: 3×3 orientation matrix of $\mathcal{F}_i$ with respect to $\mathcal{F}_{i-1}$ at the initial configuration;
- $\mathbf{G_h}_i$: 4×4 homogeneous orientation matrix of $\mathcal{F}_i$ with respect to $\mathcal{F}_{i-1}$ at the initial configuration;
- ${}^d\boldsymbol{\rho}_c$: 3×1 position vector of the origin of $\mathcal{F}_c$ in $\mathcal{F}_d$;
- $\boldsymbol{\rho}_i$: 3×1 position vector of the origin of $\mathcal{F}_i$ in $\mathcal{F}_{i-1}$;
- $\boldsymbol{p}_i$: 3×1 position vector of the origin of $\mathcal{F}_i$ in $\mathcal{F}_b$
- $\mathbf{A}_i$: 3×3 orientation matrix of $\mathcal{F}_i$ with respect to $\mathcal{F}_{i-1}$;
- ${}^d\mathbf{Q}_c$: 3×3 orientation matrix of $\mathcal{F}_c$ with respect to $\mathcal{F}_d$;
- $\mathbf{Q}_c$: 3×3 orientation matrix of $\mathcal{F}_c$ with respect to $\mathcal{F}_b$;
- $\mathbf{R_z}(\theta)$: 3×3 rotation matrix about $\boldsymbol{z}$ axis with θ being the rotation angle :

$$\mathbf{R_z}(\theta) = \begin{bmatrix} \cos(\theta) & -\sin(\theta) & 0 \\ \sin(\theta) & \cos(\theta) & 0 \\ 0 & 0 & 1 \end{bmatrix};$$

- $\mathbf{R_{hz}}(\theta)$: 4×4 homogeneous rotation matrix about $\boldsymbol{z}$ axis with θ being the rotation angle;
- $\mathbf{B_x}(r)$: 4×4 homogeneous translation matrix along $\boldsymbol{x}$ axis with r being the translation distance;
- $\mathbf{C}_i$: 4×4 homogeneous transformation matrix of $\mathcal{F}_i$ in $\mathcal{F}_{i-1}$;
- $\mathbf{H}_i$: 4×4 homogeneous transformation matrix of $\mathcal{F}_i$ in $\mathcal{F}_b$;
- ${}^d\mathbf{H}_c$: 4×4 homogeneous transformation matrix of $\mathcal{F}_c$ in $\mathcal{F}_d$;

– $\boldsymbol{e}_i$: the k^{th} canonical vector which is defined as

$$\boldsymbol{e}_k \equiv \left[\underbrace{0 \cdots 0}_{k-1} \; 1 \; \underbrace{0 \cdots 0}_{n-k} \right]^T$$

whose dimension is implicit and depends on the context;

– ${}^{d}\mathbf{T}_c$: tangent operator of $\mathcal{F}_c$ in $\mathcal{F}_d$ expressed in $\mathcal{F}_b$;

– ${}^{f,\,d}\mathbf{T}_c$: tangent operator of $\mathcal{F}_c$ in $\mathcal{F}_d$ expressed in $\mathcal{F}_f$;

– ${}^{d}\boldsymbol{t}_c$: tangent vector of $\mathcal{F}_c$ in $\mathcal{F}_d$ expressed in $\mathcal{F}_b$;

– ${}^{f,\,d}\boldsymbol{t}_c$: tangent vector of $\mathcal{F}_c$ in $\mathcal{F}_d$ expressed in $\mathcal{F}_f$;

– $\boldsymbol{t}_c$: tangent vector of $\mathcal{F}_c$ in $\mathcal{F}_b$ expressed in $\mathcal{F}_b$.

7.3 Topological Representation

Suppose two links coupled by a revolute joint and a reference frame is attached to each of them; at an initial configuration, the origins of the two reference frames $\mathcal{F}_{i-1}$ and $\mathcal{F}_i$ coincide; the joint axis is parallel to the z-axis of $\mathcal{F}_{i-1}$ and intersects the negative side of the x-axis of $\mathcal{F}_{i-1}$ at right angle (Fig. 7.1).

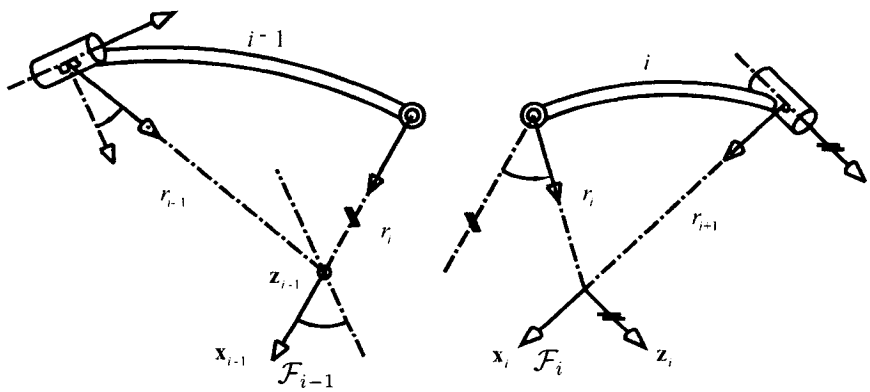

FIG. 7.1 Two links coupled by a revolute joint

The relative orientation and position are given as

$$\mathbf{A}_i = \mathbf{R}_{\mathbf{z}}(\theta_i)\mathbf{G}_i \tag{7.1}$$

$$\boldsymbol{\rho}_i = -r_i\boldsymbol{e}_1 + r_i\mathbf{R}_{\mathbf{z}}(\theta_i)\boldsymbol{e}_1 \tag{7.2}$$

$$\boldsymbol{\rho}_i = \begin{bmatrix} r_i\cos(\theta_i) - r_i \\ r_i\sin(\theta_i) \\ 0 \end{bmatrix} = \begin{bmatrix} -2r_i\sin^2(\theta_i/2) \\ r_i\sin(\theta_i) \\ 0 \end{bmatrix} \tag{7.3}$$

Instead of taking θ_i as joint joint variable, we define

$$q_i = r_i\theta_i \tag{7.4}$$

to measure the relative pose of the two links and q_i is referred to as normalized joint variable. In addition, we define

$$w_i = \frac{1}{r_i} \tag{7.5}$$

Then from equations (7.3), (7.4), and (7.5), we have

$$\boldsymbol{\rho}_i = \begin{bmatrix} -2\sin^2(w_iq_i/2)/w_i \\ \sin(w_iq_i)/w_i \\ 0 \end{bmatrix} \tag{7.6}$$

It is evident that

$$\lim_{w_i\to 0}\boldsymbol{\rho}_i = \begin{bmatrix} 0 \\ q_i \\ 0 \end{bmatrix}$$
$$\lim_{w_i\to 0}\mathbf{A}_i = \lim_{w_i\to 0}\left[\mathbf{R}_{\mathbf{z}}\left(w_iq_i\right)\mathbf{G}_i\right] = \mathbf{G}_i \tag{7.7}$$

Equation (7.7) is just the relative pose of the two links when they are coupled by a prismatic joint. With the above formulation, revolute joints and prismatic ones

can be treated in a unified way and the normalization of the joint variable is the key to achieve this.

Although it is a well-known fact that a prismatic joint is actually a revolute joint at infinity, the two types of joints are always treated differently and the type of a joint is always represented by a boolean variable : a joint can only be either revolute or prismatic, nothing in-between.

Inspired by this observation and the basic concept of fuzzy logic, we introduce the concept : **joint nature** which is a non negative real number to characterize the level of the "revoluteness" of a joint. In the above example, it is just w_i defined by equation (7.5). This allows us to deal the prismatic joints and the revolute ones in the same way.

Definition : *the type of a joint in a kinematic chain is represented by a pair* (κ, w) *where* κ *is a natural number identifying its orientation from other joints, while* w *is a non negative number characterizing its membership to revolute joint.*

The topology of a fully parallel mechanism of n-DOF is represented by n matrices with each matrix representing a subchain from the base to the end-effector :

$$\begin{bmatrix} \kappa_{j,1} & \kappa_{j,2} & \cdots & \kappa_{j,m_j-1} & \kappa_{j,m_j} \\ w_{j,1} & w_{j,2} & \cdots & w_{j,m_j-1} & w_{j,m_j} \end{bmatrix}, j = 1, 2, \cdots, n \tag{7.8}$$

where m_j is the total number of joints of j^{th} subchain.

This numerical representation is aimed at simultaneous synthesis of both topology and geometry.

7.4 Geometric Representation

Instead of describing separately the geometry of each link, we describe an initial configuration. This is done by giving the coordinates of all joint axes with respect to the global reference frame.

Definition : *the location of a joint axis at an initial configuration is represented by a triple* $(\hat{\boldsymbol{n}}, \hat{\boldsymbol{m}}, w)$ *where* $\hat{\boldsymbol{n}}$ *is a unit vector defining the orientation of the joint axis,* $\hat{\boldsymbol{m}}$ *is a unit vector indicating the direction of the moment of* $\hat{\boldsymbol{n}}$ *with respect to the origin of the global reference frame,* w *is the nature of the joint.*

It is here that the topology information is integrated into the geometric definition.

The *Plücker* coordinates of the joint axis is simply

$$\boldsymbol{l} = \begin{bmatrix} w\hat{\boldsymbol{n}} \\ \hat{\boldsymbol{m}} \end{bmatrix} \tag{7.9}$$

With this representation, it should be avoided to position the joint such that its axis is too close to the origin of the global reference frame, because this will lead to parameter singularity, that is w will approach infinity. This does not limit the representation method, because it the relative location of the joints that defines the geometry, changing the reference frame does not change the geometry.

The topology and geometry of a fully parallel mechanism of n-DOF is represented by n matrices with each matrix representing a subchain from the base to the end-effector :

$$\begin{bmatrix} \hat{\boldsymbol{n}}_{j,1} & \hat{\boldsymbol{n}}_{j,2} & \cdots & \hat{\boldsymbol{n}}_{j,m_j-1} & \hat{\boldsymbol{n}}_{j,m_j} \\ \hat{\boldsymbol{m}}_{j,1} & \hat{\boldsymbol{m}}_{j,2} & \cdots & \hat{\boldsymbol{m}}_{j,m_j-1} & \hat{\boldsymbol{m}}_{j,m_j} \\ w_{j,1} & w_{j,2} & \cdots & w_{j,m_j-1} & w_{j,m_j} \end{bmatrix}, j = 1, 2, \cdots, n \tag{7.10}$$

where m_j is the total number of joints of j^{th} subchain.

Those are the design parameters, they are continuous and suffer from no parameter singularity problem.

7.5 kinematic modelling of general PMs

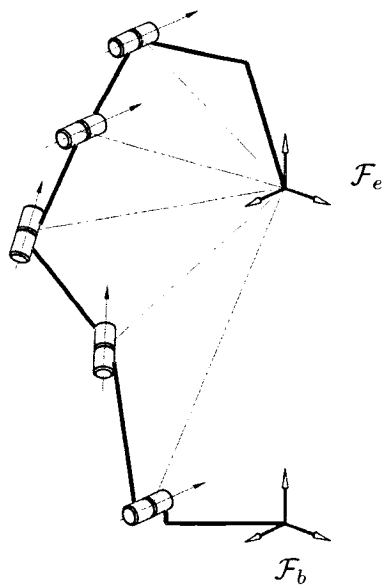

FIG. 7.2 End-effector reference frame

The reference frames for all links are defined at the initial configuration and this is done by following the rules given below :

1. Locate the reference frame for the end-effector such that no joint axis passes through its origin (Fig. 7.2) ;
2. Change the reference frame of the topological and geometric parameters to the end-effector frame : recall that ${}^b\boldsymbol{\rho}_e$ and ${}^b\mathbf{Q}_e$ denote respectively the position and the orientation of the end-effector frame in the base frame. For

every joint (the subscript is dropped off for simplicity), if ${}^{b}w = 0$ then

$$\begin{aligned} {}^{e}\hat{\boldsymbol{n}} &= {}^{e}\mathbf{Q}_{b}\,{}^{b}\hat{\boldsymbol{n}} \\ {}^{e}\hat{\boldsymbol{m}} &= {}^{e}\mathbf{Q}_{b}\,{}^{b}\hat{\boldsymbol{m}} \\ {}^{e}w &= 0 \end{aligned} \tag{7.11}$$

otherwise, let P be a point on the axis, ${}^{b}\boldsymbol{r}$ and ${}^{e}\boldsymbol{r}$ denote its positions in the base frame and in the end-effector frame respectively, we then have

$$\begin{aligned} {}^{e}\hat{\boldsymbol{n}} &= {}^{e}\mathbf{Q}_{b}\,{}^{b}\hat{\boldsymbol{n}} \\ {}^{e}\boldsymbol{r} &= {}^{e}\mathbf{Q}_{b}({}^{b}\boldsymbol{r} - {}^{b}\boldsymbol{\rho}_{e}) \\ {}^{e}\boldsymbol{m} &= {}^{e}\boldsymbol{r} \times {}^{e}\hat{\boldsymbol{n}} = {}^{e}\mathbf{Q}_{b}({}^{b}\boldsymbol{r} \times {}^{b}\hat{\boldsymbol{n}} - {}^{b}\boldsymbol{\rho}_{e} \times {}^{b}\hat{\boldsymbol{n}}) \end{aligned} \tag{7.12}$$

Let $\left[{}^{b}\boldsymbol{\rho}_{e}\times\right]$ denote the cross product matrix associated with ${}^{b}\boldsymbol{\rho}_{e}$, since

$${}^{b}\boldsymbol{r} \times {}^{b}\hat{\boldsymbol{n}} = {}^{b}\boldsymbol{m} = {}^{b}\hat{\boldsymbol{m}}/{}^{b}w \tag{7.13}$$

by substituting equation (7.13) into (7.12), we have

$${}^{e}\boldsymbol{m} = -{}^{e}\mathbf{Q}_{b}\left[{}^{b}\boldsymbol{\rho}_{e}\times\right]{}^{b}\hat{\boldsymbol{n}} + {}^{e}\mathbf{Q}_{b}\,{}^{b}\hat{\boldsymbol{m}}/{}^{b}w \tag{7.14}$$

then, the *Plücker* coordinates of the axis in the end-effector frame can be computed as

$$\begin{bmatrix} {}^{e}\hat{\boldsymbol{n}} \\ {}^{e}\boldsymbol{m} \end{bmatrix} = \begin{bmatrix} {}^{e}\mathbf{Q}_{b} & \mathbf{O} \\ -{}^{e}\mathbf{Q}_{b}\left[{}^{b}\boldsymbol{\rho}_{e}\times\right] & {}^{e}\mathbf{Q}_{b} \end{bmatrix} \begin{bmatrix} {}^{b}\hat{\boldsymbol{n}} \\ {}^{b}\hat{\boldsymbol{m}}/{}^{b}w \end{bmatrix} \tag{7.15}$$

Finally, ${}^{e}w = 1/\|{}^{e}\boldsymbol{m}\|_{2}$ and ${}^{e}\hat{\boldsymbol{m}} = {}^{e}\boldsymbol{m}/{}^{e}w$.

3. Links of subchain j from the base to the end-effector are identified by $link(j, 0)$

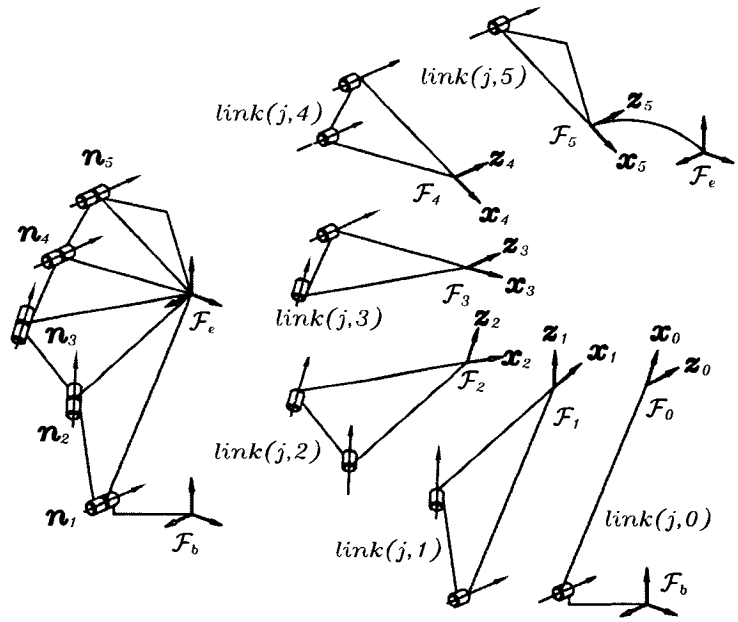

FIG. 7.3 Link reference frames

to $link(j, m_j)$, the base being $link(j, 0)$ and the end-effector being $link(j, m_j)$; joint coupling $link(j, i-1)$ and $link(j, i)$ is identified by $joint(j, i)$; frame $\mathcal{F}_{j,i}$ is attached to $link(j, i)(Fig.\ 7.3)$; the base and the end-effector have multiple rigidly attached frames with each of them corresponding to an individual subchain;

4. The reference frame for $link(j, i)$ is defined such that

$$ {}^{e}\mathbf{Q}_{j,i} = \left[{}^{e}\hat{\boldsymbol{m}}_{j,i+1} \times {}^{e}\hat{\boldsymbol{n}}_{j,i+1},\ {}^{e}\hat{\boldsymbol{m}}_{j,i+1},\ {}^{e}\hat{\boldsymbol{n}}_{j,i+1} \right] \tag{7.16} $$

$$ {}^{e}\boldsymbol{\rho}_{j,i} = \mathbf{0} \tag{7.17} $$

the $\boldsymbol{z}$-axis of $\mathcal{F}_{j,i}$ being parallel to the axis of $joint(j, i+1)$ and the $\boldsymbol{x}$-axis intersecting the the axis of $joint(j, i+1)$ and pointing from the intersecting point to the origin of the end-effector frame (Fig. 7.4). The $\boldsymbol{y}$-axis is determined as usual by the right-hand rule.

5. The normalized joint variable of $joint(j,i)$ is denoted by $q_{j,i}$, the rotation angle with respect to the initial configuration is denoted by $\theta_{j,i}$ and

$$\theta_{j,i} = w_{j,i} q_{j,i} \tag{7.18}$$

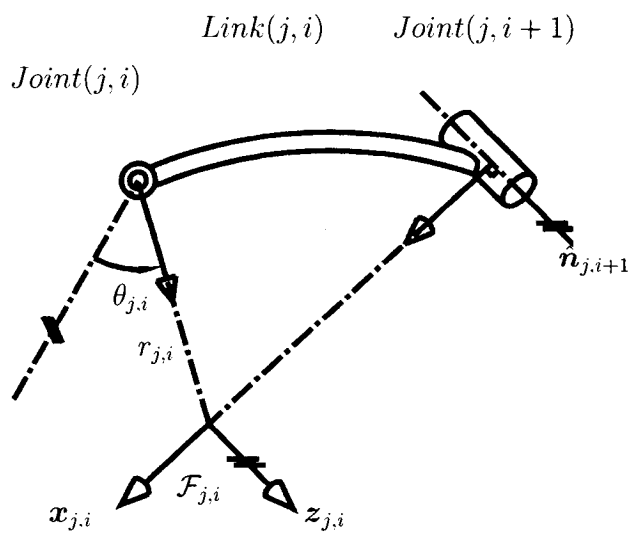

FIG. 7.4 Reference frame definition for $link(i,j)$

6. Compute the link geometry matrices from ${}^{b}\mathbf{Q}_{e}$, ${}^{e}\mathbf{Q}_{j,0}$, $\cdots$, and ${}^{e}\mathbf{Q}_{j,m_j}$: for $\mathbf{G}_{j,1}$ to $\mathbf{G}_{j,m_j-1}$

$$\mathbf{G}_{j,i} = {}^{j,i-1}\mathbf{Q}_{e}\,{}^{e}\mathbf{Q}_{j,i} \tag{7.19}$$

$\mathbf{G}_{j,0}$, $\mathbf{G}_{j,m_j}$, and $\mathbf{G}_{j,e}$ are treated differently, *i.e.*

$$\mathbf{G}_{j,0} = {}^{b}\mathbf{Q}_{e}\,{}^{e}\mathbf{Q}_{j,0} \tag{7.20}$$

$$\mathbf{G}_{j,m_j} = \mathbf{1} \tag{7.21}$$

$$\mathbf{G}_{j,e} = {}^{j,m_j}\mathbf{Q}_{e} \tag{7.22}$$

The sequence of links in each subchain has a corresponding sequence of homogeneous transformations that defines the pose of each link relative to its neighbor in

the chain. The pose of the end-effector is therefore constrained by the product of these transformations through every subchain. With the above frame assignment, the pose of $link(j,i)$ with respect to $link(j,i-1)$ is given as

$$\mathbf{C}_{j,i} = \mathbf{B}_{\mathbf{x}}(-\frac{1}{w_{j,i}})\mathbf{R}_{\mathbf{hz}}(w_{j,i}q_{j,i})\mathbf{B}_{\mathbf{x}}(\frac{1}{w_{j,i}})\mathbf{G}_{\mathbf{h}j,i} \tag{7.23}$$

The corresponding 3×3 orientation matrix is given as

$$\mathbf{A}_{j,i} = \mathbf{R}_{\mathbf{z}}(w_{j,i}q_{j,i})\mathbf{G}_{j,i} \tag{7.24}$$

The corresponding position is given as

$$\boldsymbol{\rho}_{j,i} = -\frac{\boldsymbol{e}_1}{w_{j,i}} + \mathbf{R}_{\mathbf{z}}(w_{j,i}q_{j,i})\frac{\boldsymbol{e}_1}{w_{j,i}} \tag{7.25}$$

This leads to

$$\boldsymbol{\rho}_{j,i} = \begin{bmatrix} \frac{1}{w_{j,i}}\cos(w_{j,i}q_{j,i}) - \frac{1}{w_{j,i}} \\ \frac{1}{w_{j,i}}\sin(w_{j,i}q_{j,i}) \\ 0 \end{bmatrix} = \begin{bmatrix} -\frac{2}{w_{j,i}}\sin^2\left(\frac{w_{j,i}q_{j,i}}{2}\right) \\ \frac{1}{w_{j,i}}\sin(w_{j,i}q_{j,i}) \\ 0 \end{bmatrix} \tag{7.26}$$

When $w_{j,i}$ approaches 0, we have

$$\lim_{w_{j,i}\to 0} \mathbf{A}_{j,i} = \mathbf{G}_{j,i} \tag{7.27}$$

$$\lim_{w_{j,i}\to 0} \boldsymbol{\rho}_{j,i} = \begin{bmatrix} 0 \\ q_{j,i} \\ 0 \end{bmatrix} \tag{7.28}$$

This corresponds to the situation of a prismatic joint.

The pose of the end-effector under the structure constraint of subchain j is

$$\mathbf{H}_e = \mathbf{H}_{j,0}\left(\prod_{i=1}^{m_j}\mathbf{C}_{j,i}\right)\mathbf{C}_{j,e},\ i = 1, 2, \cdots, m_j \tag{7.29}$$

In terms of orientation and position, equation (7.29) can be written as

$$\mathbf{Q}_e = \mathbf{Q}_{j,0}\left(\prod_{i=1}^{m_j}\mathbf{A}_{j,i}\right)\mathbf{A}_{j,e},\ i = 1, 2, \cdots, m_j \tag{7.30}$$

$$\mathbf{Q}_{j,i} = \mathbf{Q}_{j,0}\prod_{k=1}^{i}\mathbf{A}_{j,k},\ k = 1, 2, \cdots, i \tag{7.31}$$

$$\boldsymbol{p}_{j,i} = \boldsymbol{p}_{j,0} + \sum_{k=1}^{i}\left(\mathbf{Q}_{j,k-1}\boldsymbol{\rho}_{j,k}\right),\ k = 1, 2, \cdots, i \tag{7.32}$$

$$\boldsymbol{p}_{j,e} = \boldsymbol{p}_{j,0} + \sum_{i=1}^{m_j}\left(\mathbf{Q}_{j,i-1}\boldsymbol{\rho}_{j,i}\right) + \mathbf{Q}_{j,m_j}\boldsymbol{\rho}_{j,e},\ i = 1, 2, \cdots, m_j \tag{7.33}$$

Equations (7.31) and (7.32) are used to compute the orientation and position of links other than the base and the end-effector.

For a PM of n degree of freedom, the n subchains are closed by rigidly attaching together their fist link frames and last link frames respectively. The structure equations are obtained by equating the transformation products defined by equation (7.29) of all subchains, *i.e.*, $\forall j,\ k = 1, 2, \cdots, n$ and $j \neq k$

$$\mathbf{H}_{j,0}\left(\prod_{i=1}^{m_j}\mathbf{C}_{j,i}\right)\mathbf{C}_{j,e} = \mathbf{H}_{k,0}\left(\prod_{i=1}^{m_k}\mathbf{C}_{k,i}\right)\mathbf{C}_{k,e} \tag{7.34}$$

7.6 Kinematic model of TPMs

In our previous work, it was concluded that for the kinematic model of a PM of 3 DOF to be neither underdetermined nor overdetermined and for it to be a TPM,

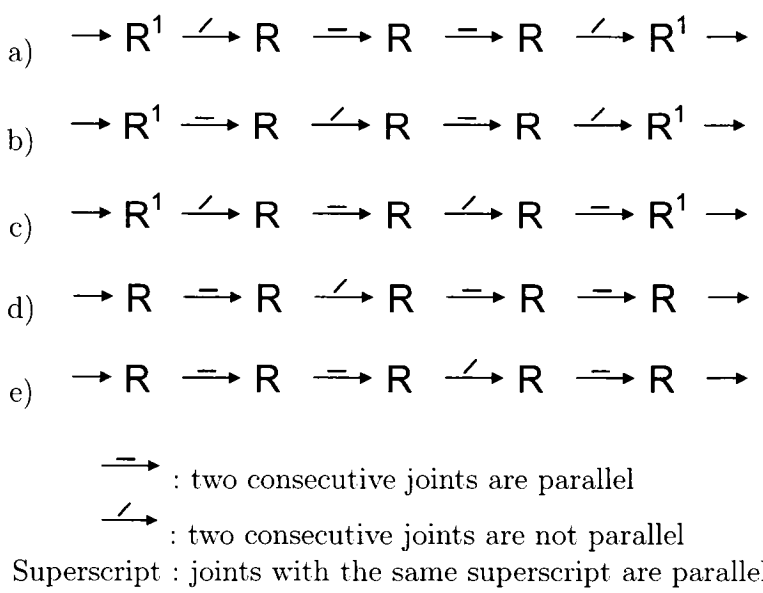

FIG. 7.5 Topologies of 5-revolute-joint subchains

the following conditions must be satisfied :

1. The joint number distributions among the three subchains are (3, 6, 6), (4, 5, 6) or (5, 5, 5);
2. Joints of 3-joint subchain are all prismatic ones;
3. Kinematic composition of a 4-joint subchain is one of the followins :
   - 3 parallel revolute joints and one prismatic joint;
   - 2 parallel revolute joints and 2 prismatic joints;
   - one revolute joint and 3 prismatic joints;
4. the topology of a 5-joint subchain is one of those shown in Fig. (7.5).

From the topological and geometrical representation (7.10), the tangent vector (or twist) corresponding to the j^th subchain is

$$\boldsymbol{t}_j = \begin{bmatrix} w_{j,1}\hat{\boldsymbol{n}}_{j,1} & w_{j,2}\hat{\boldsymbol{n}}_{j,2} & w_{j,3}\hat{\boldsymbol{n}}_{j,3} & w_{j,4}\hat{\boldsymbol{n}}_{j,4} & w_{j,5}\hat{\boldsymbol{n}}_{j,5} \\ \hat{\boldsymbol{m}}_{j,1} & \hat{\boldsymbol{m}}_{j,2} & \hat{\boldsymbol{m}}_{j,3} & \hat{\boldsymbol{m}}_{j,4} & \hat{\boldsymbol{m}}_{j,5} \end{bmatrix} \begin{bmatrix} \dot{q}_1 \\ \dot{q}_2 \\ \dot{q}_3 \\ \dot{q}_4 \\ \dot{q}_5 \end{bmatrix} \tag{7.35}$$

where the dot denotes differentiation with respect to time. The normalized Jacobian matrix is

$$\mathbf{J}_j = \begin{bmatrix} w_{j,1}\hat{\boldsymbol{n}}_{j,1} & w_{j,2}\hat{\boldsymbol{n}}_{j,2} & w_{j,3}\hat{\boldsymbol{n}}_{j,3} & w_{j,4}\hat{\boldsymbol{n}}_{j,4} & w_{j,5}\hat{\boldsymbol{n}}_{j,5} \\ \hat{\boldsymbol{m}}_{j,1} & \hat{\boldsymbol{m}}_{j,2} & \hat{\boldsymbol{m}}_{j,3} & \hat{\boldsymbol{m}}_{j,4} & \hat{\boldsymbol{m}}_{j,5} \end{bmatrix} \tag{7.36}$$

Investigating the topologies shown in (Fig. 7.5), there are two groups of joints for each topology; joints of the same group are parallel each other. Given a topology shown in (Fig. 7.5), let the joints in group one be represented by

$$\begin{pmatrix} \hat{\boldsymbol{n}}_{g1} & \hat{\boldsymbol{n}}_{g1} \\ \hat{\boldsymbol{m}}_{g1,\,1} & \hat{\boldsymbol{m}}_{g1,\,2} \\ w_{g1,\,1} & w_{g1,\,2} \end{pmatrix}$$

while group two by

$$\begin{pmatrix} \hat{\boldsymbol{n}}_{g2} & \hat{\boldsymbol{n}}_{g2} & \hat{\boldsymbol{n}}_{g2} \\ \hat{\boldsymbol{m}}_{g2,\,1} & \hat{\boldsymbol{m}}_{g2,\,2} & \hat{\boldsymbol{m}}_{g2,\,3} \\ w_{g2,\,1} & w_{g2,\,2} & w_{g2,\,3} \end{pmatrix}$$

and let

$$\mathbf{X} \equiv \begin{bmatrix} w_{g1,1}\hat{\boldsymbol{n}}_{g1} & w_{g1,2}\hat{\boldsymbol{n}}_{g1} & w_{g2,1}\hat{\boldsymbol{n}}_{g2} & w_{g2,2}\hat{\boldsymbol{n}}_{g2} & w_{g2,3}\hat{\boldsymbol{n}}_{g2} \\ \hat{\boldsymbol{m}}_{g1,1} & \hat{\boldsymbol{m}}_{g1,2} & \hat{\boldsymbol{m}}_{g2,1} & \hat{\boldsymbol{m}}_{g2,2} & \hat{\boldsymbol{m}}_{g2,3} \end{bmatrix}$$

It is obious that

$$range(\mathbf{J}) = range(\mathbf{X})$$

If $w_{g1,1} = w_{g1,2} = 0$ or $w_{g2,1} = w_{g2,2} = w_{g2,3} = 0$, the rank of $\mathbf{J}$ will be reduced by 2 because the upper three rows of $\mathbf{X}$ becomes rank one submatrix, meaning that the inverse instantaneous kinematic model becomes a set of four independent linear equations with five unknowns, an underdetermined system. Noticing also that $w \geq 0$, we can conclude that

$$w_{g1,1} + w_{g1,2} > 0$$
$$w_{g2,1} + w_{g2,2} + w_{g2,3} > 0$$

7.7 Inverse kinematics of TPMs

The inverse kinematics of 3-joint subchain and 4-joint subchain are straight forward, so their solutions will not be presented here.

For inverse kinematics of 6-joint subchains, depending on topology and geometry, some of them can have closed-form solutions but most of them can only be solved numerically. How to find all solutions to this problem and how to compute them efficiently have been a subject of intensive studies for several decades. Efforts have been concentrated on individual topologies, no non-iterative formulation can apply to a wide range of topologies. In the context of simultaneous topological and

geometrical synthesis of PM, the adaptability of the solution to different topologies is of most importance, so the numerical method becomes a natural choice, the adaptability being preferred to the efficiency in this case.

We will focus on closed-form solutions for 5-joint subchains.

From the previous section we know that for all 5-joint subchains there are always two joints in one direction while the other three in another direction. So the basic idea to solve the inverse kinematic problem is to project the EE position vector onto the vector representing the three parallel joint direction in order to eliminate the three parallel joint variables and reduce the problem to the solution of a quadratic polynomial with one of the other two parallel joint variables as unknown. We will present solutions for two kinds of subchains. Solutions for the rest of the subchains can be found in the appendices.

7.7.1 Subchains of $R^1R^1R^2R^2R^2$

7.7.1.1 Solve q_1 and q_2

a) Non of $joint(1)$ or $joint(2)$ is at infinity ($w_1w_2 \neq 0$)

Rewrite equation (7.30) and (7.33) as

$$\mathbf{Q}_e = \mathbf{A}_0\mathbf{A}_1\mathbf{A}_2\mathbf{A}_3\mathbf{A}_4\mathbf{A}_5\mathbf{A}_e \tag{7.37}$$

$$\boldsymbol{p}_e = \boldsymbol{\rho}_0 + \mathbf{Q}_0\boldsymbol{\rho}_1 + \mathbf{Q}_1\boldsymbol{\rho}_2 + \mathbf{Q}_2\boldsymbol{\rho}_3 + \mathbf{Q}_3\boldsymbol{\rho}_4 + \mathbf{Q}_4\boldsymbol{\rho}_5 + \mathbf{Q}_5\boldsymbol{\rho}_e \tag{7.38}$$

Upon rearrangement, equation (7.38) can be written as

$$\mathbf{Q}_0^T(\boldsymbol{p}_e - \boldsymbol{\rho}_0 - \mathbf{Q}_2\boldsymbol{\rho}_3 - \mathbf{Q}_3\boldsymbol{\rho}_4 - \mathbf{Q}_4\boldsymbol{\rho}_5 - \mathbf{Q}_5\boldsymbol{\rho}_e) = \boldsymbol{\rho}_1 + \mathbf{Q}_0^T\mathbf{Q}_1\boldsymbol{\rho}_2 \tag{7.39}$$

where

$$\boldsymbol{\rho}_1 = -\frac{\boldsymbol{e}_1}{w_1} + \mathbf{R}_{\mathbf{z}}(w_1 q_1)\frac{\boldsymbol{e}_1}{w_1} \tag{7.40}$$

Since $joint(1)$ and $joint(2)$ are parallel one another, $joint(3)$, $joint(4)$, and $joint(5)$ are parallel each other, $\mathbf{G}_1$, $\mathbf{G}_3$ and $\mathbf{G}_4$ are simply rotation matrices about $\boldsymbol{z}$-axis. Let

$$\mathbf{G}_1 \equiv \mathbf{R}_{\mathbf{z}}(-\beta_1),\ \mathbf{G}_3 \equiv \mathbf{R}_{\mathbf{z}}(-\beta_3),\ \mathbf{G}_4 \equiv \mathbf{R}_{\mathbf{z}}(-\beta_4) \tag{7.41}$$

Since $\mathbf{Q}_1 = \mathbf{Q}_0\mathbf{A}_1$ and $\mathbf{A}_1 = \mathbf{R}_{\mathbf{z}}(w_1 q_1)\mathbf{R}_{\mathbf{z}}(-\beta_2)$, we have

$$\begin{aligned}\mathbf{Q}_1\boldsymbol{\rho}_2 &= \mathbf{Q}_0\mathbf{R}_{\mathbf{z}}(w_1 q_1)\mathbf{R}_{\mathbf{z}}(-\beta_2)\left[-\frac{\boldsymbol{e}_1}{w_2} + \mathbf{R}_{\mathbf{z}}(w_2 q_2)\frac{\boldsymbol{e}_1}{w_2}\right] \\ &= \mathbf{Q}_0\left[-\mathbf{R}_{\mathbf{z}}(w_1 q_1)\mathbf{R}_{\mathbf{z}}(-\beta_2)\frac{\boldsymbol{e}_1}{w_2} + \mathbf{R}_{\mathbf{z}}(w_1 q_1 + w_2 q_2)\mathbf{R}_{\mathbf{z}}(-\beta_2)\frac{\boldsymbol{e}_1}{w_2}\right]\end{aligned} \tag{7.42}$$

The end-effector having a constant orientation means

$$w_1 q_1 + w_2 q_2 = 0 \tag{7.43}$$

Therefore, equation (7.42) becomes

$$\mathbf{Q}_1\boldsymbol{\rho}_2 = \mathbf{Q}_0\left[-\mathbf{R}_{\mathbf{z}}(w_1 q_1)\mathbf{R}_{\mathbf{z}}(-\beta_2)\frac{\boldsymbol{e}_1}{w_2} + \mathbf{R}_{\mathbf{z}}(-\beta_2)\frac{\boldsymbol{e}_1}{w_2}\right] \tag{7.44}$$

By substituting equations (7.25) and (7.44) into the right hand of equation (7.39), we get

$$\begin{aligned}\boldsymbol{\rho}_1 + \mathbf{Q}_0^T\mathbf{Q}_1\boldsymbol{\rho}_2 &= -\frac{\boldsymbol{e}_1}{w_1} + \mathbf{R}_{\mathbf{z}}(w_1 q_1)\frac{\boldsymbol{e}_1}{w_1} - \mathbf{R}_{\mathbf{z}}(w_1 q_1)\mathbf{R}_{\mathbf{z}}(-\beta_2)\frac{\boldsymbol{e}_1}{w_2} + \mathbf{R}_{\mathbf{z}}(-\beta_2)\frac{\boldsymbol{e}_1}{w_2} \\ &= \mathbf{R}_{\mathbf{z}}(w_1 q_1)\left[\frac{\boldsymbol{e}_1}{w_1} - \mathbf{R}_{\mathbf{z}}(-\beta_2)\frac{\boldsymbol{e}_1}{w_2}\right] - \left[\frac{\boldsymbol{e}_1}{w_1} - \mathbf{R}_{\mathbf{z}}(-\beta_2)\frac{\boldsymbol{e}_1}{w_2}\right] \\ &= \mathbf{R}_{\mathbf{z}}(w_1 q_1)\,\mathbf{u} - \mathbf{u}\end{aligned} \tag{7.45}$$

where

$$\boldsymbol{u} \equiv \begin{bmatrix} u_1 & u_2 & u_3 \end{bmatrix}^T = \frac{\boldsymbol{e}_1}{w_1} - \mathbf{R}_{\mathbf{z}}(-\beta_2)\frac{\boldsymbol{e}_1}{w_2} \tag{7.46}$$

is a geometry dependent vector. By adding equation (7.39) to equation (7.45), we get

$$\mathbf{Q}_0^T(\boldsymbol{p}_e - \boldsymbol{\rho}_0 - \mathbf{Q}_2\boldsymbol{\rho}_3 - \mathbf{Q}_3\boldsymbol{\rho}_4 - \mathbf{Q}_4\boldsymbol{\rho}_5 - \mathbf{Q}_5\boldsymbol{\rho}_e) = \mathbf{R}_{\mathbf{z}}(w_1q_1)\,\mathbf{u} - \mathbf{u} \tag{7.47}$$

Multiplying both sides of equation (7.47) by $\mathbf{Q}_0$ leads to

$$\boldsymbol{p}_e - \boldsymbol{\rho}_0 + \mathbf{Q}_0\boldsymbol{u} - \mathbf{Q}_2\boldsymbol{\rho}_3 - \mathbf{Q}_3\boldsymbol{\rho}_4 - \mathbf{Q}_4\boldsymbol{\rho}_5 - \mathbf{Q}_5\boldsymbol{\rho}_e = \mathbf{Q}_0\mathbf{R}_{\mathbf{z}}(w_1q_1)\,\boldsymbol{u} \tag{7.48}$$

By projecting both sides of equation (7.48) onto $\mathbf{Q}_4\boldsymbol{e}_3$, we get

$$\begin{aligned} \boldsymbol{e}_3^T\mathbf{Q}_4^T(\boldsymbol{p}_e - \boldsymbol{\rho}_0 + \mathbf{Q}_0\boldsymbol{u}) &- \boldsymbol{e}_3^T\mathbf{Q}_4^T\mathbf{Q}_2\boldsymbol{\rho}_3 - \boldsymbol{e}_3^T\mathbf{Q}_4^T\mathbf{Q}_3\boldsymbol{\rho}_4 \\ &- \boldsymbol{e}_3^T\mathbf{Q}_4^T\mathbf{Q}_4\boldsymbol{\rho}_5 - \boldsymbol{e}_3^T\mathbf{Q}_4^T\mathbf{Q}_5\boldsymbol{\rho}_e \\ &= \boldsymbol{e}_3^T\mathbf{Q}_4^T\mathbf{Q}_0\mathbf{R}_{\mathbf{z}}(w_1q_1)\,\boldsymbol{u} \end{aligned} \tag{7.49}$$

Since $Joint(3)$, $joint(4)$ and $joint(5)$ are parallel each other, we have

$$\boldsymbol{e}_3^T\mathbf{Q}_4^T = \boldsymbol{e}_3^T\mathbf{Q}_2^T \Rightarrow \boldsymbol{e}_3^T\mathbf{Q}_4^T\mathbf{Q}_2 = \boldsymbol{e}_3^T\mathbf{Q}_2^T\mathbf{Q}_2 = \boldsymbol{e}_3^T \tag{7.50}$$

$$\boldsymbol{e}_3^T\mathbf{Q}_4^T = \boldsymbol{e}_3^T\mathbf{Q}_3^T \Rightarrow \boldsymbol{e}_3^T\mathbf{Q}_4^T\mathbf{Q}_3 = \boldsymbol{e}_3^T\mathbf{Q}_3^T\mathbf{Q}_3 = \boldsymbol{e}_3^T \tag{7.51}$$

Substitute equations (7.50) and (7.51) into equation (7.49), then

$$\begin{aligned} \boldsymbol{e}_3^T\mathbf{Q}_4^T(\boldsymbol{p}_e - \boldsymbol{\rho}_0 + \mathbf{Q}_0\boldsymbol{u}) &- \boldsymbol{e}_3^T\boldsymbol{\rho}_3 - \boldsymbol{e}_3^T\boldsymbol{\rho}_4 \\ &- \boldsymbol{e}_3^T\boldsymbol{\rho}_5 - \boldsymbol{e}_3^T\mathbf{Q}_4^T\mathbf{Q}_5\boldsymbol{\rho}_e \\ &= \boldsymbol{e}_3^T\mathbf{Q}_4^T\mathbf{Q}_0\mathbf{R}_{\mathbf{z}}(w_1q_1)\,\boldsymbol{u} \end{aligned} \tag{7.52}$$

Observing equation (7.26), we know that

$$\boldsymbol{e}_3^T \boldsymbol{\rho} \;=\; 0 \tag{7.53}$$

in addition to

$$\begin{aligned} \mathbf{Q}_5 \;&=\; \mathbf{Q}_4\mathbf{A}_5 = \mathbf{Q}_4\mathbf{R}_{\mathbf{z}}\left(w_5 q_5\right)\mathbf{G}_5 \\ &\Rightarrow\; \mathbf{Q}_4^T\mathbf{Q}_5 = \mathbf{R}_{\mathbf{z}}\left(w_5 q_5\right)\mathbf{G}_5 \\ &\Rightarrow\; \boldsymbol{e}_3^T\mathbf{Q}_4^T\mathbf{Q}_5 = \boldsymbol{e}_3^T\mathbf{G}_5 \end{aligned} \tag{7.54}$$

$$\begin{aligned} \mathbf{Q}_e = \mathbf{Q}_4\mathbf{A}_5\mathbf{A}_e \;&=\; \mathbf{Q}_4\mathbf{R}_{\mathbf{z}}\left(w_5 q_5\right)\mathbf{G}_5\mathbf{G}_e \\ \Rightarrow \mathbf{Q}_4 \;&=\; \mathbf{Q}_e\mathbf{G}_e^T\mathbf{G}_5^T\mathbf{R}_{\mathbf{z}}\left(w_5 q_5\right)^T \\ \Rightarrow \mathbf{Q}_4\boldsymbol{e}_3 \;&=\; \mathbf{Q}_e\mathbf{G}_e^T\mathbf{G}_5^T\boldsymbol{e}_3 \\ \Rightarrow \boldsymbol{e}_3^T\mathbf{Q}_4^T \;&=\; \boldsymbol{e}_3^T\mathbf{G}_5\mathbf{G}_e\mathbf{Q}_e^T \end{aligned} \tag{7.55}$$

Substituting equations (7.53), (7.54), and (7.55) into equation (7.52) yields

$$\boldsymbol{e}_3^T\mathbf{G}_5\mathbf{G}_e\mathbf{Q}_e^T\left(\boldsymbol{p}_e - \boldsymbol{\rho}_0 + \mathbf{Q}_0\boldsymbol{u}\right) - \boldsymbol{e}_3^T\mathbf{G}_5\boldsymbol{\rho}_e = \boldsymbol{e}_3^T\mathbf{G}_5\mathbf{G}_e\mathbf{Q}_e^T\mathbf{Q}_0\mathbf{R}_{\mathbf{z}}\left(w_1 q_1\right)\boldsymbol{u} \tag{7.56}$$

Let

$$\begin{aligned} \boldsymbol{v}^T &\equiv \begin{bmatrix} v_1 & v_2 & v_3 \end{bmatrix} = \boldsymbol{e}_3^T\mathbf{G}_5\mathbf{G}_e\mathbf{Q}_e^T\mathbf{Q}_0 \\ k &= \boldsymbol{e}_3^T\mathbf{G}_5\mathbf{G}_e\mathbf{Q}_e^T\left(\boldsymbol{p}_e - \boldsymbol{\rho}_0 + \mathbf{Q}_0\boldsymbol{u}\right) - \boldsymbol{e}_3^T\mathbf{G}_5\boldsymbol{\rho}_e \end{aligned} \tag{7.57}$$

which depend only on the geometry, then

$$\boldsymbol{v}^T\mathbf{R}_{\mathbf{z}}\left(w_1 q_1\right)\boldsymbol{u} = k \tag{7.58}$$

with its scalar form being as

$$(v_1u_1 + v_2u_2)\cos(w_1q_1) + (v_2u_1 - v_1u_2)\sin(w_1q_1) = k - v_3u_3 \tag{7.59}$$

From equation (7.59), q_1 can be easily solved and q_2 is then computed from (7.43)

b) $Joint(1)$ **is at infinity** $(w_1 = 0, w_2 \neq 0)$

If $w_1 = 0$ and $w_2 \neq 0$, from equation (7.43) we have

$$q_2 = 0 \tag{7.60}$$

and equation (7.44) becomes

$$\mathbf{Q}_2\boldsymbol{\rho}_1 = 0 \tag{7.61}$$

By substituting equations (7.28) and (7.61) into the right hand of equation (7.39), we have

$$\boldsymbol{\rho}_1 + \mathbf{Q}_0^T\mathbf{Q}_1\boldsymbol{\rho}_2 = \begin{bmatrix} 0 & q_1 & 0 \end{bmatrix}^T \tag{7.62}$$

Combining equations (7.39) and (7.62) leads to

$$\boldsymbol{p}_e - \boldsymbol{\rho}_0 - \mathbf{Q}_2\boldsymbol{\rho}_3 - \mathbf{Q}_3\boldsymbol{\rho}_4 - \mathbf{Q}_4\boldsymbol{\rho}_5 - \mathbf{Q}_5\boldsymbol{\rho}_e = \mathbf{Q}_0\begin{bmatrix} 0 & q_1 & 0 \end{bmatrix}^T \tag{7.63}$$

Projecting both sides of equation (7.63) onto $\mathbf{Q}_4\boldsymbol{e}_3$ results in

$$\begin{aligned} \boldsymbol{e}_3^T\mathbf{Q}_4^T(\boldsymbol{p}_e - \boldsymbol{\rho}_0) &- \boldsymbol{e}_3^T\mathbf{Q}_4^T\mathbf{Q}_2\boldsymbol{\rho}_3 - \boldsymbol{e}_3^T\mathbf{Q}_4^T\mathbf{Q}_3\boldsymbol{\rho}_4 \\ &- \boldsymbol{e}_3^T\mathbf{Q}_4^T\mathbf{Q}_4\boldsymbol{\rho}_5 - \boldsymbol{e}_3^T\mathbf{Q}_4^T\mathbf{Q}_5\boldsymbol{\rho}_e \\ &= \boldsymbol{e}_3^T\mathbf{Q}_4^T\mathbf{Q}_0\begin{bmatrix} 0 & q_1 & 0 \end{bmatrix}^T \end{aligned} \tag{7.64}$$

By substituting equations (7.50) and (7.51) into equation (7.64), we get

$$\begin{aligned} \boldsymbol{e}_3^T \mathbf{Q}_4^T (\boldsymbol{p}_e - \boldsymbol{\rho}_0) &- \boldsymbol{e}_3^T \boldsymbol{\rho}_3 - \boldsymbol{e}_3^T \boldsymbol{\rho}_4 \\ &- \boldsymbol{e}_3^T \boldsymbol{\rho}_5 - \boldsymbol{e}_3^T \mathbf{Q}_4^T \mathbf{Q}_5 \boldsymbol{\rho}_e \\ &= \boldsymbol{e}_3^T \mathbf{Q}_4^T \mathbf{Q}_0 \begin{bmatrix} 0 & q_1 & 0 \end{bmatrix}^T \end{aligned} \tag{7.65}$$

Substitution of equations (7.53), (7.54), and (7.55) into equation (7.65) gives

$$\boldsymbol{e}_3^T \mathbf{G}_5 \mathbf{G}_e \mathbf{Q}_e^T (\boldsymbol{p}_e - \boldsymbol{\rho}_0) - \boldsymbol{e}_3^T \mathbf{G}_5 \boldsymbol{\rho}_e = \boldsymbol{e}_3^T \mathbf{G}_5 \mathbf{G}_e \mathbf{Q}_e^T \mathbf{Q}_0 \begin{bmatrix} 0 & q_1 & 0 \end{bmatrix}^T \tag{7.66}$$

Now we introduce intermediate variables

$$\begin{aligned} k &= \boldsymbol{e}_3^T \mathbf{G}_5 \mathbf{G}_e \mathbf{Q}_e^T (\boldsymbol{p}_e - \boldsymbol{\rho}_0) - \boldsymbol{e}_3^T \mathbf{G}_5 \boldsymbol{\rho}_e \\ \boldsymbol{u}^T &= \begin{bmatrix} u_1 & u_2 & u_3 \end{bmatrix}^T = \boldsymbol{e}_3^T \mathbf{G}_5 \mathbf{G}_e \mathbf{Q}_e^T \mathbf{Q}_0 \end{aligned}$$

which are geometry-dependent only, then we have

$$\boldsymbol{u} \begin{bmatrix} 0 & q_1 & 0 \end{bmatrix}^T = k \tag{7.67}$$

i.e.

$$u_2 q_1 = k \tag{7.68}$$

q_1 is therefore solved.

c) $Joint(2)$ **is at infinity** $(w_2 = 0, w_1 \neq 0)$

If $w_2 = 0$ and $w_1 \neq 0$, from equations (7.43) and (7.28), we have

$$q_1 = 0,\ \boldsymbol{\rho}_1 = \mathbf{0},\ \boldsymbol{\rho}_2 = \begin{bmatrix} 0 & q_2 & 0 \end{bmatrix}^T \tag{7.69}$$

Then, since $\mathbf{Q}_1 = \mathbf{Q}_0\mathbf{A}_1$ and $\mathbf{A}_1 = \mathbf{R_z}(w_1q_1)\,\mathbf{R_z}(-\beta_2)$, we have

$$\begin{aligned}\mathbf{Q}_1\boldsymbol{\rho}_2 &= \mathbf{Q}_0\mathbf{R_z}(w_1q_1)\,\mathbf{R_z}(-\beta_2)\begin{bmatrix}0 & q_2 & 0\end{bmatrix}^T \\ &= \mathbf{Q}_0\mathbf{R_z}(-\beta_2)\begin{bmatrix}0 & q_2 & 0\end{bmatrix}^T \end{aligned} \tag{7.70}$$

Comparing equations (7.39), (7.69) and (7.70) yields

$$\boldsymbol{p}_e - \boldsymbol{\rho}_0 - \mathbf{Q}_2\boldsymbol{\rho}_3 - \mathbf{Q}_3\boldsymbol{\rho}_4 - \mathbf{Q}_4\boldsymbol{\rho}_5 - \mathbf{Q}_5\boldsymbol{\rho}_e = \mathbf{Q}_0\mathbf{R_z}(-\beta_2)\begin{bmatrix}0 & q_1 & 0\end{bmatrix}^T \tag{7.71}$$

Equation (7.71) is different from equation (7.63) only by element $\mathbf{R_z}(-\beta_2)$. Similarly to the deduction process for the case of $w_1 = 0, w_2 \neq 0$, we get

$$\boldsymbol{e}_3^T\mathbf{G}_5\mathbf{G}_e\mathbf{Q}_e^T(\boldsymbol{p}_e - \boldsymbol{\rho}_0) - \boldsymbol{e}_3^T\mathbf{G}_5\boldsymbol{\rho}_e = \boldsymbol{e}_3^T\mathbf{G}_5\mathbf{G}_e\mathbf{Q}_e^T\mathbf{Q}_0\mathbf{R_z}(-\beta_2)\begin{bmatrix}0 & q_2 & 0\end{bmatrix}^T \tag{7.72}$$

Introduce intermediate variables

$$\begin{aligned} k &= \boldsymbol{e}_3^T\mathbf{G}_5\mathbf{G}_e\mathbf{Q}_e^T(\boldsymbol{p}_e - \boldsymbol{\rho}_0) - \boldsymbol{e}_3^T\mathbf{G}_5\boldsymbol{\rho}_e \\ \boldsymbol{u}^T = \begin{bmatrix}u_1 & u_2 & u_3\end{bmatrix}^T &= \boldsymbol{e}_3^T\mathbf{G}_5\mathbf{G}_e\mathbf{Q}_e^T\mathbf{Q}_0\mathbf{R_z}(-\beta_2)\end{aligned}$$

we then get

$$\boldsymbol{u}\begin{bmatrix}0 & q_2 & 0\end{bmatrix}^T = k \tag{7.73}$$

i.e.

$$u_2q_2 = k \tag{7.74}$$

q_2 is solved.

7.7.1.2 Solve q_3, q_4, and q_5

With q_1 and q_2 having been solved, $\mathbf{Q}_1$, $\mathbf{Q}_2$, $\boldsymbol{p}_1$, and $\boldsymbol{p}_2$ are known. In addition, $\mathbf{Q}_5$ is also known because

$$\mathbf{Q}_e = \mathbf{Q}_5\mathbf{A}_e = \mathbf{Q}_5\mathbf{G}_e \Rightarrow \mathbf{Q}_5 = \mathbf{Q}_e\mathbf{G}_e^T$$

Consequently, equation (7.38) can be written as

$$\boldsymbol{p}_e = \boldsymbol{p}_2 + \mathbf{Q}_2\boldsymbol{\rho}_3 + \mathbf{Q}_3\boldsymbol{\rho}_4 + \mathbf{Q}_4\boldsymbol{\rho}_5 + \mathbf{Q}_5\boldsymbol{\rho}_e \tag{7.75}$$

Substitute equation (7.25) into (7.75), we then get

$$\begin{aligned}\boldsymbol{p}_e = \boldsymbol{p}_2 \;+\; & \mathbf{Q}_2\left[-\frac{\boldsymbol{e}_1}{w_3} + \mathbf{R}_{\mathbf{z}}\left(w_3q_3\right)\frac{\boldsymbol{e}_1}{w_3}\right] + \mathbf{Q}_3\left[-\frac{\boldsymbol{e}_1}{w_4} + \mathbf{R}_{\mathbf{z}}\left(w_4q_4\right)\frac{\boldsymbol{e}_1}{w_4}\right] \\ + \; & \mathbf{Q}_4\left[-\frac{\boldsymbol{e}_1}{w_5} + \mathbf{R}_{\mathbf{z}}\left(w_5q_5\right)\frac{\boldsymbol{e}_1}{w_5}\right] + \mathbf{Q}_5\boldsymbol{\rho}_e\end{aligned}$$

that is, upon rearrangement

$$\begin{aligned}\boldsymbol{p}_e = \boldsymbol{p}_2 \;-\; & \mathbf{Q}_2\frac{\boldsymbol{e}_1}{w_3} + \mathbf{Q}_2\mathbf{R}_{\mathbf{z}}\left(w_3q_3\right)\frac{\boldsymbol{e}_1}{w_3} - \mathbf{Q}_3\frac{\boldsymbol{e}_1}{w_4} + \mathbf{Q}_3\mathbf{R}_{\mathbf{z}}\left(w_4q_4\right)\frac{\boldsymbol{e}_1}{w_4} \\ - \; & \mathbf{Q}_4\frac{\boldsymbol{e}_1}{w_5} + \mathbf{Q}_4\mathbf{R}_{\mathbf{z}}\left(w_5q_5\right)\frac{\boldsymbol{e}_1}{w_5} + \mathbf{Q}_5\boldsymbol{\rho}_e\end{aligned} \tag{7.76}$$

Write $\mathbf{Q}_3$ and $\mathbf{Q}_4$ in terms of geometry and joint variables, *i.e.*

$$\begin{aligned}\mathbf{Q}_3 &= \mathbf{Q}_2\mathbf{R}_{\mathbf{z}}\left(w_3q_3\right)\mathbf{G}_3 = \mathbf{Q}_2\mathbf{R}_{\mathbf{z}}\left(w_3q_3\right)\mathbf{R}_{\mathbf{z}}\left(-\beta_3\right) \\ \mathbf{Q}_4 &= \mathbf{Q}_3\mathbf{R}_{\mathbf{z}}\left(w_4q_4\right)\mathbf{G}_4 = \mathbf{Q}_3\mathbf{R}_{\mathbf{z}}\left(w_4q_4\right)\mathbf{R}_{\mathbf{z}}\left(-\beta_4\right) \\ \mathbf{Q}_e = \mathbf{Q}_4\mathbf{A}_5\mathbf{A}_e = \mathbf{Q}_4\mathbf{R}_{\mathbf{z}}\left(w_5q_5\right)\mathbf{G}_5\mathbf{G}_e &\Rightarrow \mathbf{Q}_4\mathbf{R}_{\mathbf{z}}\left(w_5q_5\right) = \mathbf{Q}_e\mathbf{G}_e^T\mathbf{G}_5^T\end{aligned} \tag{7.77}$$

Substitute equations (7.77) into equation (7.76), then we get

$$\begin{aligned} \boldsymbol{p}_e = \boldsymbol{p}_2 \;&-\; \mathbf{Q}_2\frac{\boldsymbol{e}_1}{w_3} + \mathbf{Q}_2\mathbf{R}_{\mathbf{z}}\left(w_3q_3\right)\frac{\boldsymbol{e}_1}{w_3} - \mathbf{Q}_2\mathbf{R}_{\mathbf{z}}\left(w_3q_3\right)\mathbf{R}_{\mathbf{z}}\left(-\beta_3\right)\frac{\boldsymbol{e}_1}{w_4} \\ &+\; \mathbf{Q}_3\mathbf{R}_{\mathbf{z}}\left(w_4q_4\right)\frac{\boldsymbol{e}_1}{w_4} - \mathbf{Q}_3\mathbf{R}_{\mathbf{z}}\left(w_4q_4\right)\mathbf{R}_{\mathbf{z}}\left(-\beta_4\right)\frac{\boldsymbol{e}_1}{w_5} \\ &+\; \mathbf{Q}_e\mathbf{G}_e^T\mathbf{G}_5^T\frac{\boldsymbol{e}_1}{w_5} + \mathbf{Q}_5\boldsymbol{\rho}_e \end{aligned} \tag{7.78}$$

This can be simplified as

$$\begin{aligned} \boldsymbol{p}_e = \boldsymbol{p}_2 \;&-\; \mathbf{Q}_2\frac{\boldsymbol{e}_1}{w_3} + \mathbf{Q}_2\mathbf{R}_{\mathbf{z}}\left(w_3q_3\right)\left[\frac{\boldsymbol{e}_1}{w_3} - \mathbf{R}_{\mathbf{z}}\left(-\beta_3\right)\frac{\boldsymbol{e}_1}{w_4}\right] \\ &+\; \mathbf{Q}_3\mathbf{R}_{\mathbf{z}}\left(w_4q_4\right)\left[\frac{\boldsymbol{e}_1}{w_4} - \mathbf{R}_{\mathbf{z}}\left(-\beta_4\right)\frac{\boldsymbol{e}_1}{w_5}\right] \\ &+\; \mathbf{Q}_e\mathbf{G}_e^T\mathbf{G}_5^T\frac{\boldsymbol{e}_1}{w_5} + \mathbf{Q}_5\boldsymbol{\rho}_e \end{aligned} \tag{7.79}$$

Arranging all terms involving q_4 to the left hand of equation (7.79) leads to

$$\begin{aligned} &\mathbf{Q}_2^T\mathbf{Q}_3\mathbf{R}_{\mathbf{z}}\left(w_4q_4\right)\left[\frac{\boldsymbol{e}_1}{w_4} - \mathbf{R}_{\mathbf{z}}\left(-\beta_4\right)\frac{\boldsymbol{e}_1}{w_5}\right] \\ = \;&\mathbf{Q}_2^T\left(\boldsymbol{p}_e - \boldsymbol{p}_2 - \mathbf{Q}_5\boldsymbol{\rho}_e + \mathbf{Q}_2\frac{\boldsymbol{e}_1}{w_3} - \mathbf{Q}_e\mathbf{G}_e^T\mathbf{G}_5^T\frac{\boldsymbol{e}_1}{w_5}\right) \\ &-\mathbf{R}_{\mathbf{z}}\left(w_3q_3\right)\left[\frac{\boldsymbol{e}_1}{w_3} - \mathbf{R}_{\mathbf{z}}\left(-\beta_3\right)\frac{\boldsymbol{e}_1}{w_4}\right] \end{aligned} \tag{7.80}$$

Although scalar equations obtained from expanding equation (7.80) will allow us to deal with all situations of *joint*(3) and/or *joint*(4) and/or *joint*(5) being at infinity, we prefer to do some symbolic computations for each of these situations, because those cases involve more simplified equation and can provide a better computational efficiency.

a) $w_3w_4w_5 \neq 0$

By introducing the following intermediate variables

$$\boldsymbol{p} = \mathbf{Q}_2^T \left(\boldsymbol{p}_e - \boldsymbol{p}_2 - \mathbf{Q}_5 \boldsymbol{\rho}_e + \mathbf{Q}_2 \frac{\boldsymbol{e}_1}{w_3} - \mathbf{Q}_e \mathbf{G}_e^T \mathbf{G}_5^T \frac{\boldsymbol{e}_1}{w_5} \right)$$
$$\boldsymbol{u} = \left[\frac{\boldsymbol{e}_1}{w_3} - \mathbf{R}_{\mathbf{z}} \left(-\beta_3 \right) \frac{\boldsymbol{e}_1}{w_4} \right], \ \boldsymbol{v} = \left[\frac{\boldsymbol{e}_1}{w_4} - \mathbf{R}_{\mathbf{z}} \left(-\beta_4 \right) \frac{\boldsymbol{e}_1}{w_5} \right]$$

equation (7.80) can be written as

$$\boldsymbol{p} - \mathbf{R}_{\mathbf{z}} \left(w_3 q_3 \right) \boldsymbol{u} = \mathbf{Q}_2^T \mathbf{Q}_3 \mathbf{R}_{\mathbf{z}} \left(w_4 q_4 \right) \boldsymbol{v} \tag{7.81}$$

Take 2-norm of equation (7.81) to eliminate q_4 :

$$\begin{aligned} \boldsymbol{p}^T \boldsymbol{p} + \boldsymbol{u}^T \boldsymbol{u} - 2 \boldsymbol{p}^T \mathbf{R}_{\mathbf{z}} \left(w_3 q_3 \right) \boldsymbol{u} &= \boldsymbol{v}^T \boldsymbol{v} \Rightarrow \\ \boldsymbol{p}^T \mathbf{R}_{\mathbf{z}} \left(w_3 q_3 \right) \boldsymbol{u} &= \frac{\boldsymbol{p}^T \boldsymbol{p} + \boldsymbol{u}^T \boldsymbol{u} - \boldsymbol{v}^T \boldsymbol{v}}{2} \end{aligned} \tag{7.82}$$

Write equation (7.82) in scalar form :

$$\left(p_1 u_1 + p_2 u_2 \right) \cos \left(w_3 q_3 \right) + \left(p_2 u_1 - p_1 u_2 \right) \sin \left(w_3 q_3 \right) = \frac{\boldsymbol{p}^T \boldsymbol{p} + \boldsymbol{u}^T \boldsymbol{u} - \boldsymbol{v}^T \boldsymbol{v}}{2} - p_3 u_3 \tag{7.83}$$

q_3 can be solved from equation (7.83).

Rewrite equation (7.81) as

$$\mathbf{R}_{\mathbf{z}} \left(w_4 q_4 \right) \boldsymbol{v} = \mathbf{Q}_3^T \mathbf{Q}_2 \left[\boldsymbol{p} - \mathbf{R}_{\mathbf{z}} \left(w_3 q_3 \right) \boldsymbol{u} \right] \tag{7.84}$$

Then, q_4 can be computed from equation (7.84) and q_5 can be computed from the fact that $w_3 q_3 + w_4 q_4 + w_5 q_5 = 0$.

b) $w_3 w_4 w_5 = 0$

To better reveal implications of one or two of the w_3, w_4, and w_5 approaching zero,

rewrite equation (7.75) as

$$\mathbf{Q}_2^T\left(\boldsymbol{p}_e - \boldsymbol{p}_2 - \mathbf{Q}_5\boldsymbol{\rho}_e\right) = \boldsymbol{\rho}_3 + \mathbf{A}_3\boldsymbol{\rho}_4 + \mathbf{A}_3\mathbf{A}_4\boldsymbol{\rho}_5 \tag{7.85}$$

Recall that

$$\begin{aligned}
\mathbf{A}_3 &= \mathbf{R}_\mathbf{z}\left(w_3q_3\right)\mathbf{G}_3 = \mathbf{R}_\mathbf{z}\left(w_3q_3\right)\mathbf{R}_\mathbf{z}\left(-\beta_3\right) = \mathbf{R}_\mathbf{z}\left(w_3q_3 - \beta_3\right)\\
\mathbf{A}_3\mathbf{A}_4 &= \mathbf{A}_3\mathbf{R}_\mathbf{z}\left(w_4q_4\right)\mathbf{G}_4 = \mathbf{A}_3\mathbf{R}_\mathbf{z}\left(w_4q_4\right)\mathbf{R}_\mathbf{z}\left(-\beta_4\right)\\
&= \mathbf{R}_\mathbf{z}\left(w_3q_3 + w_4q_4 - \beta_3\right)\mathbf{R}_\mathbf{z}\left(-\beta_4\right) = \mathbf{R}_\mathbf{z}\left(w_3q_3 + w_4q_4 - \beta_3 - \beta_4\right)\\
\mathbf{Q}_e &= \mathbf{Q}_2\mathbf{A}_3\mathbf{A}_4\mathbf{A}_5\mathbf{A}_e = \mathbf{Q}_2\mathbf{A}_3\mathbf{A}_4\mathbf{R}_\mathbf{z}\left(w_5q_5\right)\mathbf{G}_5\mathbf{G}_e\\
&= \mathbf{Q}_2\mathbf{R}_\mathbf{z}\left(w_3q_3 + w_4q_4 + w_5q_5 - \beta_3 - \beta_4\right)\mathbf{G}_5\mathbf{G}_e\\
&\Rightarrow \mathbf{R}_\mathbf{z}\left(w_3q_3 + w_4q_4 + w_5q_5 - \beta_3 - \beta_4\right) = \mathbf{Q}_2^T\mathbf{Q}_e\mathbf{G}_e^T\mathbf{G}_5^T
\end{aligned} \tag{7.86}$$

and let

$$\boldsymbol{p}_a \equiv \mathbf{Q}_2^T\left(\boldsymbol{p}_e - \boldsymbol{p}_2 - \mathbf{Q}_5\boldsymbol{\rho}_e\right) \tag{7.87}$$

which is known, then from equations (7.25), (7.85), (7.86) and (7.87), we have

$$\begin{aligned}
\boldsymbol{p} &= \boldsymbol{\rho}_3 + \mathbf{A}_3\boldsymbol{\rho}_4 + \mathbf{A}_3\mathbf{A}_4\boldsymbol{\rho}_5\\
&= \left[-\frac{\boldsymbol{e}_1}{w_3} + \mathbf{R}_\mathbf{z}\left(w_3q_3\right)\frac{\boldsymbol{e}_1}{w_3}\right] + \mathbf{R}_\mathbf{z}\left(w_3q_3 - \beta_3\right)\left[-\frac{\boldsymbol{e}_1}{w_4} + \mathbf{R}_\mathbf{z}\left(w_4q_4\right)\frac{\boldsymbol{e}_1}{w_4}\right]\\
&+ \mathbf{R}_\mathbf{z}\left(w_3q_3 + w_4q_4 - \beta_3\right)\mathbf{R}_\mathbf{z}\left(-\beta_4\right)\left[-\frac{\boldsymbol{e}_1}{w_5} + \mathbf{R}_\mathbf{z}\left(w_5q_5\right)\frac{\boldsymbol{e}_1}{w_5}\right]
\end{aligned} \tag{7.88}$$

If two of w_3, w_4, and w_5 are equal to zero, then the third joint variable is zero because $w_3q_3 + w_4q_4 + w_5q_5 = 0$. In these cases, according equation (7.28), the kinematic equations reduce to a set of linear equations :

1. if $w_3 = w_4 = 0$, then equation (7.88) becomes

$$\boldsymbol{p} = \boldsymbol{e}_2 q_3 + \mathbf{R}_{\mathbf{z}}(-\beta_3)\,\boldsymbol{e}_2 q_4 \tag{7.89}$$

2. if $w_4 = w_5 = 0$, then equation (7.88) becomes

$$\boldsymbol{p} = \mathbf{R}_{\mathbf{z}}(-\beta_3)\,\boldsymbol{e}_2 q_4 + \mathbf{R}_{\mathbf{z}}(-\beta_3 - \beta_4)\,\boldsymbol{e}_2 q_5 \tag{7.90}$$

3. if $w_5 = w_3 = 0$, then equation (7.88) becomes

$$\boldsymbol{p} = \boldsymbol{e}_2 q_3 + \mathbf{R}_{\mathbf{z}}(-\beta_3 - \beta_4)\,\boldsymbol{e}_2 q_5 \tag{7.91}$$

These are simple sets of linear equations with joint variables as unknown and can be easily solved.

Cases of only one joint being at infinity are discussed below :

1. if w_3=0, then equation (7.88) can be written as

$$\begin{aligned} \boldsymbol{p} = \boldsymbol{e}_2 q_3 \;&+\; \mathbf{R}_{\mathbf{z}}(-\beta_3)\left[-\frac{\boldsymbol{e}_1}{w_4} + \mathbf{R}_{\mathbf{z}}(w_4 q_4)\frac{\boldsymbol{e}_1}{w_4}\right] \\ &+\; \mathbf{R}_{\mathbf{z}}(w_4 q_4 - \beta_3 - \beta_4)\left[-\frac{\boldsymbol{e}_1}{w_5} + \mathbf{R}_{\mathbf{z}}(w_5 q_5)\frac{\boldsymbol{e}_1}{w_5}\right] \end{aligned} \tag{7.92}$$

Upon rearrangement of equation (7.92), we get

$$\begin{aligned} &\boldsymbol{p} + \mathbf{R}_{\mathbf{z}}(-\beta_3)\frac{\boldsymbol{e}_1}{w_4} - \mathbf{Q}_2^T \mathbf{Q}_e \mathbf{G}_e^T \mathbf{G}_5^T \frac{\boldsymbol{e}_1}{w_5} - \boldsymbol{e}_2 q_3 \\ =\;& \mathbf{R}_{\mathbf{z}}(-\beta_3)\,\mathbf{R}_{\mathbf{z}}(w_4 q_4)\left[\frac{\boldsymbol{e}_1}{w_4} - \mathbf{R}_{\mathbf{z}}(-\beta_4)\frac{\boldsymbol{e}_1}{w_5}\right] \end{aligned} \tag{7.93}$$

Taking 2-norm of equation (7.93) can eliminate q_4 and a quadratic equation with q_3 as unknown is obtained and can be easily solved;

2. if w_4=0, then equation (7.88) can be written as

$$\begin{aligned} \boldsymbol{p} &= \left[-\frac{\boldsymbol{e}_1}{w_3} + \mathbf{R_z}\left(w_3 q_3\right)\frac{\boldsymbol{e}_1}{w_3}\right] + \mathbf{R_z}\left(w_3 q_3 - \beta_3\right)\boldsymbol{e}_2 q_4 \\ &+ \mathbf{R_z}\left(w_3 q_3 - \beta_3 - \beta_4\right)\left[-\frac{\boldsymbol{e}_1}{w_5} + \mathbf{R_z}\left(w_5 q_5\right)\frac{\boldsymbol{e}_1}{w_5}\right] \end{aligned} \tag{7.94}$$

Upon rearrangement of equation (7.94), we get

$$\begin{aligned} &\boldsymbol{p} + \frac{\boldsymbol{e}_1}{w_3} - \mathbf{Q}_2^T\mathbf{Q}_e\mathbf{G}_e^T\mathbf{G}_5^T\frac{\boldsymbol{e}_1}{w_5} \\ &= \mathbf{R_z}\left(w_3 q_3\right)\left[\frac{\boldsymbol{e}_1}{w_3} + \mathbf{R_z}\left(-\beta_3\right)\boldsymbol{e}_2 q_4 - \mathbf{R_z}\left(-\beta_3 - \beta_4\right)\frac{\boldsymbol{e}_1}{w_5}\right] \end{aligned} \tag{7.95}$$

Taking 2-norm of equation (7.95) can eliminate q_3 and a quadratic equation with q_4 as unknown is obtained and can be easily solved;

3. if w_5=0, then equation (7.88) can be written as

$$\begin{aligned} \boldsymbol{p} = &\left[-\frac{\boldsymbol{e}_1}{w_3} + \mathbf{R_z}\left(w_3 q_3\right)\frac{\boldsymbol{e}_1}{w_3}\right] + \mathbf{R_z}\left(w_3 q_3 - \beta_3\right)\left[-\frac{\boldsymbol{e}_1}{w_4} + \mathbf{R_z}\left(w_4 q_4\right)\frac{\boldsymbol{e}_1}{w_4}\right] \\ &+\mathbf{R_z}\left(w_3 q_3 + w_4 q_4 - \beta_3\right)\mathbf{R_z}\left(-\beta_4\right)\boldsymbol{e}_2 q_5 \end{aligned} \tag{7.96}$$

Upon rearrangement of equation (7.96), we get

$$\begin{aligned} &\boldsymbol{p} + \frac{\boldsymbol{e}_1}{w_3} - \mathbf{R_z}\left(-\beta_3\right)\frac{\boldsymbol{e}_1}{w_4} - \mathbf{R_z}\left(-\beta_3 - \beta_4\right)\boldsymbol{e}_2 q_5 \\ &= \mathbf{R_z}\left(w_3 q_3\right)\left[\frac{\boldsymbol{e}_1}{w_3} - \mathbf{R_z}\left(-\beta_3\right)\frac{\boldsymbol{e}_1}{w_4}\right] \end{aligned} \tag{7.97}$$

Taking 2-norm of equation (7.97) can eliminate q_3 and a quadratic equation with q_5 as unknown is obtained and can be easily solved.

7.7.2 Subchains of $R^1R^1R^2R^2R^1$

7.7.2.1 Solve q_3 and q_4

Rewrite equation (7.38) as

$$\mathbf{p}_e - \rho_0 - \mathbf{Q}_0\rho_1 - \mathbf{Q}_1\rho_2 - \mathbf{Q}_4\rho_5 - \mathbf{Q}_5\rho_e = \mathbf{Q}_2\rho_3 + \mathbf{Q}_3\rho_4 \tag{7.98}$$

Since $joint(1)$, $joint(2)$, and $joint(5)$ are parallel, we have

$$\begin{aligned}
\mathbf{e}_3^T\mathbf{Q}_0^T\mathbf{Q}_1 &= \mathbf{e}_3^T,\ \mathbf{e}_3^T\mathbf{Q}_0^T\mathbf{Q}_4 = \mathbf{e}_3^T \\
\mathbf{e}_3^T\mathbf{Q}_0^T\mathbf{Q}_2 &= \mathbf{e}_3^T\mathbf{Q}_0^T\mathbf{Q}_1\mathbf{A}_2 = \mathbf{e}_3^T\mathbf{R}_\mathbf{z}(w_2q_2)\,\mathbf{G}_2 = \mathbf{e}_3^T\mathbf{G}_2 \\
\mathbf{e}_3^T\mathbf{Q}_0^T\mathbf{Q}_3 &= \mathbf{e}_3^T\mathbf{Q}_0^T\mathbf{Q}_2\mathbf{A}_3 = \mathbf{e}_3^T\mathbf{G}_2\mathbf{R}_\mathbf{z}(w_3q_3)\,\mathbf{R}_\mathbf{z}(-\beta_3)
\end{aligned} \tag{7.99}$$

Multiplying equation (7.98) with $\mathbf{e}_3^T\mathbf{Q}_0$ gives

$$\mathbf{e}_3^T\mathbf{Q}_0^T(\mathbf{p}_e - \rho_0 - \mathbf{Q}_5\rho_e) = \mathbf{e}_3^T\mathbf{G}_2\rho_3 + \mathbf{e}_3^T\mathbf{G}_2\mathbf{R}_\mathbf{z}(w_3q_3)\,\mathbf{R}_\mathbf{z}(-\beta_3)\,\rho_4 \tag{7.100}$$

If $w_3w_4 \neq 0$, substitute $\boldsymbol{\rho}$ given by equation (7.25) into equation (7.100), then

$$\begin{aligned}
\mathbf{e}_3^T\mathbf{Q}_0^T(\mathbf{p}_e - \rho_0 - \mathbf{Q}_5\rho_e) &= \mathbf{e}_3^T\mathbf{G}_2\left[-\frac{\mathbf{e}_1}{w_3} + \mathbf{R}_\mathbf{z}(w_3q_3)\frac{\mathbf{e}_1}{w_3}\right] \\
&+\mathbf{e}_3^T\mathbf{G}_2\mathbf{R}_\mathbf{z}(w_3q_3)\,\mathbf{R}_\mathbf{z}(-\beta_3)\left[-\frac{\mathbf{e}_1}{w_4} + \mathbf{R}_\mathbf{z}(w_4q_4)\frac{\mathbf{e}_1}{w_4}\right]
\end{aligned} \tag{7.101}$$

q_4 can be eliminated by the fact that $w_3q_3 + w_4q_4 = 0$. After being simplified, equation (7.101) becomes

$$\begin{aligned}
&\mathbf{e}_3^T\mathbf{Q}_0^T(\mathbf{p}_e - \rho_0 - \mathbf{Q}_5\rho_e) + \mathbf{e}_3^T\mathbf{G}_2\frac{\mathbf{e}_1}{w_3} - \mathbf{e}_3^T\mathbf{G}_2\mathbf{R}_\mathbf{z}(-\beta_3)\frac{\mathbf{e}_1}{w_4} \\
&\qquad = \mathbf{e}_3^T\mathbf{G}_2\mathbf{R}_\mathbf{z}(w_3q_3)\left[\frac{\mathbf{e}_1}{w_3} - \mathbf{R}_\mathbf{z}(-\beta_3)\frac{\mathbf{e}_1}{w_4}\right]
\end{aligned} \tag{7.102}$$

So, q_3 is ready to be solved. For $w_3 w_4 = 0$, the solution is similar to $R^1R^1R^2R^2R^2$.

7.7.2.2 Solve q_1, q_2, and q_5

Rewrite equation (7.38) as

$$\mathbf{p}_e - \rho_0 - \mathbf{Q}_5\rho_e = \mathbf{Q}_0\rho_1 + \mathbf{Q}_1\rho_2 + \mathbf{Q}_2\left(\rho_3 + \mathbf{A}_3\rho_4\right) + \mathbf{Q}_4\rho_5 \tag{7.103}$$

where $\rho_3 + \mathbf{A}_3\rho_4$ is known. Substitute $\boldsymbol{\rho}$ given by equation (7.25) into equation (7.103), then

$$\begin{aligned}\mathbf{p}_e - \rho_0 - \mathbf{Q}_5\rho_e = \quad & \mathbf{Q}_0\left[-\frac{\mathbf{e}_1}{w_1} + \mathbf{R}_{\mathbf{z}}\left(w_1q_1\right)\frac{\mathbf{e}_1}{w_1}\right] + \mathbf{Q}_1\left[-\frac{\mathbf{e}_1}{w_2} + \mathbf{R}_{\mathbf{z}}\left(w_2q_2\right)\frac{\mathbf{e}_1}{w_2}\right] \\ & + \mathbf{Q}_2\left(\rho_3 + \mathbf{A}_3\rho_4\right) + \mathbf{Q}_4\left[-\frac{\mathbf{e}_1}{w_5} + \mathbf{R}_{\mathbf{z}}\left(w_5q_5\right)\frac{\mathbf{e}_1}{w_5}\right]\end{aligned} \tag{7.104}$$

a) $w_1w_2w_5 \neq 0$

Recall that

$$\mathbf{Q}_e = \mathbf{Q}_4\mathbf{A}_5\mathbf{A}_e = \mathbf{Q}_4\mathbf{R}_{\mathbf{z}}\left(w_5q_5\right)\mathbf{G}_5\mathbf{G}_e \Rightarrow \mathbf{Q}_4\mathbf{R}_{\mathbf{z}}\left(w_5q_5\right) = \mathbf{Q}_e\mathbf{G}_e^T\mathbf{G}_5^T \tag{7.105}$$

After simplification, equation (7.104) becomes

$$\begin{aligned}&\mathbf{p}_e - \rho_0 + \mathbf{Q}_0\frac{\mathbf{e}_1}{w_1} - \mathbf{Q}_5\rho_e \\ &-\mathbf{Q}_e\mathbf{G}_e^T\mathbf{G}_5^T\frac{\mathbf{e}_1}{w_5} - \mathbf{Q}_0\mathbf{R}_{\mathbf{z}}\left(w_1q_1\right)\left[\frac{\mathbf{e}_1}{w_1} - \mathbf{R}_{\mathbf{z}}\left(-\beta_1\right)\frac{\mathbf{e}_1}{w_2}\right] = \\ &\mathbf{Q}_1\mathbf{R}_{\mathbf{z}}\left(w_2q_2\right)\left[\frac{\mathbf{e}_1}{w_2} + \mathbf{G}_2\left(\rho_3 + \mathbf{A}_3\rho_4\right) - \mathbf{G}_2\mathbf{R}_{\mathbf{z}}\left(w_3q_3\right)\mathbf{G}_3\mathbf{R}_{\mathbf{z}}\left(w_4q_4\right)\mathbf{G}_4\frac{\mathbf{e}_1}{w_5}\right]\end{aligned} \tag{7.106}$$

Let

$$\begin{aligned}
\boldsymbol{p} &= \mathbf{p}_e - \rho_0 + \mathbf{Q}_0\frac{\mathbf{e}_1}{w_1} - \mathbf{Q}_5\rho_e - \mathbf{Q}_e\mathbf{G}_e^T\mathbf{G}_5^T\frac{\mathbf{e}_1}{w_5} \\
\boldsymbol{u} &= \left[\frac{\mathbf{e}_1}{w_1} - \mathbf{R_z}\left(-\beta_1\right)\frac{\mathbf{e}_1}{w_2}\right] \\
\boldsymbol{v} &= \left[\frac{\mathbf{e}_1}{w_2} + \mathbf{G}_2\left(\rho_3 + \mathbf{A}_3\rho_4\right) - \mathbf{G}_2\mathbf{R_z}\left(w_3q_3\right)\mathbf{G}_3\mathbf{R_z}\left(w_4q_4\right)\mathbf{G}_4\frac{\mathbf{e}_1}{w_5}\right]
\end{aligned}$$

Then

$$\boldsymbol{p} - \mathbf{Q}_0\mathbf{R_z}\left(w_1q_1\right)\boldsymbol{u} = \mathbf{Q}_1\mathbf{R_z}\left(w_2q_2\right)\boldsymbol{v} \tag{7.107}$$

Take the 2-norm of equation (7.107) to eliminate q_2, that is

$$2\boldsymbol{p}^T\mathbf{Q}_0\mathbf{R_z}\left(w_1q_1\right)\boldsymbol{u} = \boldsymbol{p}^T\boldsymbol{p} + \boldsymbol{u}^T\boldsymbol{u} - \boldsymbol{v}^T\boldsymbol{v} \tag{7.108}$$

q_1 can therefore be easily solved. q_2 can be solved by substituting q_1 back into equation (7.106) and q_5 is solve by $w_1q_1 + w_2q_2 + w_5q_5 = 0$.

b) $w_1w_2w_5 = 0$

If two of w_1, w_2, and w_5 are equal to 0, equation (7.104) simply become a set of linear equations :

1. if $w_1 = w_2 = 0$, then equation (7.104) can be written as

$$\begin{aligned}
\mathbf{Q}_0\mathbf{e}_2q_1 + \mathbf{Q}_0\mathbf{R_z}\left(-\beta_1\right)\mathbf{e}_2q_2 = \mathbf{p}_e - \rho_0 - \mathbf{Q}_5\rho_e \\
-\mathbf{Q}_0\mathbf{R_z}\left(-\beta_1\right)\mathbf{G}_2\left(\rho_3 + \mathbf{A}_3\rho_4\right)
\end{aligned} \tag{7.109}$$

2. if $w_2 = w_5 = 0$, then equation (7.104) can be written as

$$\mathbf{Q}_0\mathbf{R_z}\left(-\beta_1\right)\mathbf{e}_2q_2 + \mathbf{Q}_0\mathbf{R_z}\left(-\beta_1\right)\mathbf{G}_2\mathbf{R_z}\left(w_3q_3\right)\mathbf{G}_3\mathbf{R_z}\left(w_4q_4\right)\mathbf{G}_4\mathbf{e}_2q_5$$

$$= \mathbf{p}_e - \rho_0 - \mathbf{Q}_5\rho_e - \mathbf{Q}_0\mathbf{R}_\mathbf{z}\left(-\beta_1\right)\mathbf{G}_2\left(\rho_3 + \mathbf{A}_3\rho_4\right) \quad (7.110)$$

3. if $w_5 = w_1 = 0$, then equation (7.104) can be written as

$$\begin{aligned}\mathbf{Q}_0\mathbf{e}_2q_1 + \mathbf{Q}_0\mathbf{R}_\mathbf{z}\left(-\beta_1\right)\mathbf{G}_2\mathbf{R}_\mathbf{z}\left(w_3q_3\right)\mathbf{G}_3\mathbf{R}_\mathbf{z}\left(w_4q_4\right)\mathbf{G}_4\mathbf{e}_2q_5 \\ = \mathbf{p}_e - \rho_0 - \mathbf{Q}_5\rho_e - \mathbf{Q}_0\mathbf{R}_\mathbf{z}\left(-\beta_1\right)\mathbf{G}_2\left(\rho_3 + \mathbf{A}_3\rho_4\right) \quad (7.111)\end{aligned}$$

Equations from (7.109) to (7.111) are sets of linear equations with joint variables as unknowns and can be easily solved.

The followings are the situations of only one of w_1, w_2, and w_5 being equal to 0 :

1. if $w_1 = 0$, then equation (7.104) can be written as

$$\mathbf{p} - \mathbf{Q}_0\mathbf{e}_2q_1 = \mathbf{Q}_0\mathbf{R}_\mathbf{z}\left(-\beta_1\right)\mathbf{R}_\mathbf{z}\left(w_2q_2\right)\mathbf{u} \quad (7.112)$$

   where

$$\begin{aligned}\mathbf{p} &= \mathbf{p}_e - \rho_0 - \mathbf{Q}_5\rho_e - \mathbf{Q}_e\mathbf{G}_e^T\mathbf{G}_5^T\frac{\mathbf{e}_1}{w_5} + \mathbf{Q}_0\mathbf{R}_\mathbf{z}\left(-\beta_1\right)\frac{\mathbf{e}_1}{w_2} \\ \mathbf{u} &= \frac{\mathbf{e}_1}{w_2} + \mathbf{G}_2\left(\rho_3 + \mathbf{A}_3\rho_4\right) - \mathbf{G}_2\mathbf{R}_\mathbf{z}\left(-\beta_3\right)\mathbf{G}_4\frac{\mathbf{e}_1}{w_5}\end{aligned}$$

   By taking the 2-norm of equation (7.112), q_2 can be eliminated and q_1 can be solved from a quadratic polynomial;

2. if $w_2 = 0$, then equation (7.104) can be written as

$$\mathbf{p} = \mathbf{Q}_0\mathbf{R}_\mathbf{z}\left(w_1q_1\right)\left[\mathbf{R}_\mathbf{z}\left(-\beta_1\right)\mathbf{e}_2q_2 + \mathbf{u}\right] \quad (7.113)$$

   where

$$\mathbf{p} = \mathbf{p}_e - \rho_0 - \mathbf{Q}_5\rho_e + \mathbf{Q}_0\frac{\mathbf{e}_1}{w_1} - \mathbf{Q}_e\mathbf{G}_e^T\mathbf{G}_5^T\frac{\mathbf{e}_1}{w_5}$$

$$\mathbf{u} = \frac{\mathbf{e}_1}{w_1} + \mathbf{R_z}(-\beta_1)\,\mathbf{G}_2(\rho_3 + \mathbf{A}_3\rho_4) - \mathbf{R_z}(-\beta_1)\,\mathbf{G}_2\mathbf{R_z}(-\beta_3)\,\mathbf{G}_4\frac{\mathbf{e}_1}{w_5}$$

By taking the 2-norm of equation (7.113), q_1 can be eliminated and q_2 can be solved from a quadratic polynomial;

3. if $w_5 = 0$, then equation (7.104) can be written as

$$\mathbf{p} - \mathbf{v}q_5 = \mathbf{Q}_0\mathbf{R_z}(w_1 q_1)\,\mathbf{v} \tag{7.114}$$

where

$$\begin{aligned}
\mathbf{p} &= \mathbf{p}_e - \rho_0 - \mathbf{Q}_5\rho_e + \mathbf{Q}_0\frac{\mathbf{e}_1}{w_1} - \mathbf{Q}_0\mathbf{R_z}(-\beta_1)\frac{\mathbf{e}_1}{w_2} \\
&\quad -\mathbf{Q}_0\mathbf{R_z}(-\beta_1)\,\mathbf{G}_2(\rho_3 + \mathbf{A}_3\rho_4) \\
\mathbf{u} &= \mathbf{Q}_0\mathbf{R_z}(-\beta_1)\,\mathbf{G}_2\mathbf{R_z}(-\beta_3)\,\mathbf{G}_4\mathbf{e}_2 \\
\mathbf{v} &= \left[\frac{\mathbf{e}_1}{w_1} - \mathbf{R_z}(-\beta_1)\frac{\mathbf{e}_1}{w_2}\right]
\end{aligned}$$

By taking the 2-norm of equation (7.114), q_1 can be eliminated and q_5 can be solved from a quadratic polynomial.

7.8 Forward kinematics of TPMs

The forward kinematic problem is to determine the pose of the end-effector when the joint variables of the actuated joints are known. A TPM has 15 joints, only 3 of them being actuated and the rest 12 are passive joints. Observing the structure equation of a TPM (7.34), it is equivalent to a set of 12 non linear equations with the passive joint variables as unknown. Finding all solutions of this problem is beyond the scope of this work. We are interested in finding solutions when the end-effector keeps its orientation it has at the initial configuration. Under this premise, the number of unknowns in the structure equations can be reduced by 6.

Since closed-form solutions depend greatly on judicious kinematic modelling for a specific topology and demand a great deal of symbolic mathematical manipulation, it is therefore not adaptable for simultaneous topological and geometric synthesis for which a wide range of topologies need to be dealt with. So a reasonable choice is to employ numerical solutions based on a general kinematic model.

To improve the efficiency of the numerical solutions, we will do some preprocess to the kinematic model to eliminate as many unknowns as possible and instead of solving the passive joint variables, we transform the problem into solving the end-effector's position. By doing so, we can always limit our initial guess within a reasonable range, not too far from the end-effector's position at the initial configuration.

In what follows, we present the process to eliminate all passive joint variables and to transform the problem to a set of equations with the end-effector position as unknown.

7.8.1 Position manifold

The structural constraints imposed by each subchain together with the constant orientation constraint on the end-effector form a position manifold. This manifold can be derived by eliminating the passive joint variables.

We take the $R^1R^1R^2R^2R^1$ subchain to illustrate the deduction of the position manifold. The first joint is supposed to be the actuated joint.

Rewrite equation (7.38) as

$$\mathbf{p}_e - \rho_0 - \mathbf{Q}_0\rho_1 - \mathbf{Q}_5\rho_e = \mathbf{Q}_1\rho_2 + \mathbf{Q}_2\rho_3 + \mathbf{Q}_3\rho_4 + \mathbf{Q}_4\rho_5 \tag{7.115}$$

Substitute $\boldsymbol{\rho}$ given by equation (7.25) into equation (7.115), then

$$\begin{aligned}
&\mathbf{Q}_1^T \mathbf{p}_e - \mathbf{Q}_1^T \left(\rho_0 + \mathbf{Q}_0 \rho_1 + \mathbf{G}_e^T \mathbf{G}_5^T \rho_e + \mathbf{Q}_e \mathbf{G}_e^T \mathbf{G}_5^T \frac{\mathbf{e}_1}{w_5} \right) + \frac{\mathbf{e}_1}{w_2} \\
= \; & \mathbf{R}_{\mathbf{z}} (w_2 q_2) \, \mathbf{G}_2 \left[\mathbf{G}_2^T \frac{\mathbf{e}_1}{w_2} - \frac{\mathbf{e}_1}{w_3} + \mathbf{R}_{\mathbf{z}} (-\beta_3) \frac{\mathbf{e}_1}{w_4} - \mathbf{R}_{\mathbf{z}} (-\beta_3) \, \mathbf{G}_4 \frac{\mathbf{e}_1}{w_5} \right] \\
& + \mathbf{R}_{\mathbf{z}} (w_2 q_2) \, \mathbf{G}_2 \mathbf{R}_{\mathbf{z}} (w_3 q_3) \left[\frac{\mathbf{e}_1}{w_3} - \mathbf{R}_{\mathbf{z}} (-\beta_3) \frac{\mathbf{e}_1}{w_4} \right]
\end{aligned} \tag{7.116}$$

Let

$$\begin{aligned}
\mathbf{a}_1 &= -\mathbf{Q}_1^T \left(\rho_0 + \mathbf{Q}_0 \rho_1 + \mathbf{G}_e^T \mathbf{G}_5^T \rho_e + \mathbf{Q}_e \mathbf{G}_e^T \mathbf{G}_5^T \frac{\mathbf{e}_1}{w_5} \right) + \frac{\mathbf{e}_1}{w_2} \\
\mathbf{a}_2 &= \mathbf{G}_2^T \frac{\mathbf{e}_1}{w_2} - \frac{\mathbf{e}_1}{w_3} + \mathbf{R}_{\mathbf{z}} (-\beta_3) \frac{\mathbf{e}_1}{w_4} - \mathbf{R}_{\mathbf{z}} (-\beta_3) \, \mathbf{G}_4 \frac{\mathbf{e}_1}{w_5} \\
\mathbf{a}_3 &= \frac{\mathbf{e}_1}{w_3} - \mathbf{R}_{\mathbf{z}} (-\beta_3) \frac{\mathbf{e}_1}{w_4}
\end{aligned} \tag{7.117}$$

then

$$\mathbf{Q}_1^T \mathbf{p}_e + \mathbf{a}_1 = \mathbf{R}_{\mathbf{z}} (w_2 q_2) \, \mathbf{G}_2 \left[\mathbf{a}_2 + \mathbf{R}_{\mathbf{z}} (w_3 q_3) \, \mathbf{a}_3 \right] \tag{7.118}$$

Multiply both sides of equation (7.118) with $\mathbf{e}_3^T \mathbf{Q}_1^T$ to eliminate q_2

$$\mathbf{e}_3^T \mathbf{Q}_1^T \mathbf{p}_e + \mathbf{e}_3^T \mathbf{a}_1 = \mathbf{e}_3^T \mathbf{G}_2 \mathbf{a}_2 + \mathbf{e}_3^T \mathbf{G}_2 \mathbf{R}_{\mathbf{z}} (w_3 q_3) \, \mathbf{a}_3 \tag{7.119}$$

Let

$$\mathbf{a}_4^T = \mathbf{e}_3^T \mathbf{G}_2 \tag{7.120}$$

then expanding equation (7.119) leads to

$$\begin{aligned}
&(a_{31} a_{41} + a_{32} a_{42}) \cos (w_3 q_3) + (-a_{32} a_{41} + a_{31} a_{42}) \sin (w_3 q_3) \\
&\qquad = \mathbf{e}_3^T \mathbf{Q}_1^T \mathbf{p}_e + \mathbf{e}_3^T \mathbf{a}_1 - \mathbf{e}_3^T \mathbf{G}_2 \mathbf{a}_2 - a_{33} a_{43}
\end{aligned} \tag{7.121}$$

Let

$$\begin{aligned} \mathbf{a}_5 &= \mathbf{e}_3^T \mathbf{Q}_1^T \\ f_{11} &= a_{31}a_{41} + a_{32}a_{42} \\ f_{12} &= -a_{32}a_{41} + a_{31}a_{42} \\ f_{13} &= \mathbf{e}_3^T \mathbf{a}_1 - \mathbf{e}_3^T \mathbf{G}_2 \mathbf{a}_2 - a_{33}a_{43} \end{aligned}$$

then equation (7.121) can be written as

$$f_{11}\cos(w_3 q_3) + f_{12}\sin(w_3 q_3) = \mathbf{p}_e^T \mathbf{a}_5 + f_{13} \tag{7.122}$$

Take the 2-norm of equation (7.118) to eliminate q_2 :

$$\mathbf{p}_e^T \mathbf{p}_e + 2\mathbf{p}_e^T \mathbf{Q}_1 \mathbf{a}_1 + \mathbf{a}_1^T \mathbf{a}_1 = \mathbf{a}_2^T \mathbf{a}_2 + 2\mathbf{a}_2^T \mathbf{R}_{\mathbf{z}}(w_3 q_3)\,\mathbf{a}_3 + \mathbf{a}_3^T \mathbf{a}_3 \tag{7.123}$$

Expanding the second term on the right hand of equation (7.123) gives

$$\begin{aligned} &2(a_{31}a_{21} + a_{32}a_{22})\cos(w_3 q_3) + 2(-a_{32}a_{21} + a_{31}a_{22})\sin(w_3 q_3) \\ &\quad = \mathbf{p}_e^T \mathbf{p}_e + 2\mathbf{p}_e^T \mathbf{Q}_1 \mathbf{a}_1 + \mathbf{a}_1^T \mathbf{a}_1 - \mathbf{a}_2^T \mathbf{a}_2 - \mathbf{a}_3^T \mathbf{a}_3 - a_{33}a_{23} \end{aligned} \tag{7.124}$$

Let

$$\begin{aligned} \mathbf{a}_6 &= 2\mathbf{Q}_1 \mathbf{a}_1 \\ f_{21} &= 2(a_{31}a_{21} + a_{32}a_{22}) \\ f_{22} &= 2(-a_{32}a_{21} + a_{31}a_{22}) \\ f_{13} &= \mathbf{a}_1^T \mathbf{a}_1 - \mathbf{a}_2^T \mathbf{a}_2 - \mathbf{a}_3^T \mathbf{a}_3 - a_{33}a_{23} \end{aligned} \tag{7.125}$$

then, equation (7.124) can be written as

$$f_{21}\cos(w_3q_3) + f_{22}\sin(w_3q_3) = \mathbf{p}_e^T\mathbf{p}_e + \mathbf{p}_e^T\mathbf{a}_6 + f_{23} \tag{7.126}$$

From equations (7.122) and (7.126) we get

$$\begin{aligned}(f_{11}f_{22} - f_{12}f_{21})\cos(w_3q_3) &= -f_{12}\mathbf{p}_e^T\mathbf{p}_e + \mathbf{p}_e^T(-f_{12}\mathbf{a}_6 + f_{22}\mathbf{a}_5) \\ &\quad -f_{12}f_{23} + f_{13}f_{22} \qquad (7.127)\\ (f_{11}f_{22} - f_{12}f_{21})\sin(w_3q_3) &= f_{11}\mathbf{p}_e^T\mathbf{p}_e + \mathbf{p}_e^T(f_{11}\mathbf{a}_6 - f_{21}\mathbf{a}_5) \\ &\quad +f_{11}f_{23} - f_{13}f_{21} \qquad (7.128)\end{aligned}$$

Let

$$\begin{aligned} b_1 &= -f_{12} \\ \mathbf{u} &= -f_{12}\mathbf{a}_6 + f_{22}\mathbf{a}_5 \\ b_2 &= -f_{12}f_{23} + f_{13}f_{22} \\ b_3 &= f_{11} \\ \mathbf{v} &= f_{11}\mathbf{a}_6 - f_{21}\mathbf{a}_5 \\ b_4 &= f_{11}f_{23} - f_{13}f_{21} \\ b_5 &= (f_{11}f_{22} - f_{12}f_{21})^2 + (f_{11}f_{22} - f_{12}f_{21})^2 \end{aligned}$$

By taking the square sum of equations (7.127) and (7.128), the position manifold is obtained as the following :

$$\left(b_1\mathbf{p}_e^T\mathbf{p}_e + \mathbf{p}_e^T\mathbf{u} + b_2\right)^2 + \left(b_3\mathbf{p}_e^T\mathbf{p}_e + \mathbf{p}_e^T\mathbf{v} + b_4\right)^2 - b_5 = 0 \tag{7.129}$$

For manifold (7.129), if one joint is at infinity, the manifolds become a quadratic

equation :

$$\mathbf{p}_e^T\mathbf{p}_e + \mathbf{p}_e^T\mathbf{D}_1\mathbf{p}_e + \mathbf{p}_e^T\mathbf{u} + b = 0 \tag{7.130}$$

If two joints are at infinity, the manifold become a linear equation :

$$\mathbf{p}_e^T\mathbf{u} + b = 0 \tag{7.131}$$

For subchains of $R^1R^1R^2R^2R^2$ and $R^1R^2R^2R^2R^1$, since there are three parallel joints, under a constant orientation constraint, the end-effector will only undergo planar motion. The position manifold can be easily derived from the general kinematic model and has the form of equation (7.131).

7.8.2 Numerical solution

Let

$$\boldsymbol{p}_e \equiv \begin{bmatrix} x & y & z \end{bmatrix}^T \tag{7.132}$$

where x, y, and z are the Cartesian coordinates of the origin of the end-effector frame. It is obvious that the position manifolds are polynomials in x, y, and z. Let $F_j(x, y, z)$ denote the position manifold of j^{th} subchain, then the forward kinematic problem can be stated as the solution of the following set of polynomial equations :

$$F_1(x, y, z) = F_2(x, y, z) = F_3(x, y, z) = 0 \tag{7.133}$$

The number of monomials of a fourth-order polynomial in three variables makes it cumbersome to program the algorithms. So instead of expanding the manifolds to explicit polynomials in x, y, and z, we keep the compact vector form and present the following rules to compute the partial derivatives :

$\mathbf{D}$ and $\boldsymbol{u}$ are constant matrix and vector respectively,

$$\begin{aligned}
\frac{\partial\left(\mathbf{p}_e^T\mathbf{p}_e\right)}{\partial x} &= 2\mathbf{p}_e^T\mathbf{e}_1,\ \frac{\partial\left(\mathbf{p}_e^T\mathbf{p}_e\right)}{\partial y} = 2\mathbf{p}_e^T\mathbf{e}_2,\ \frac{\partial\left(\mathbf{p}_e^T\mathbf{p}_e\right)}{\partial z} = 2\mathbf{p}_e^T\mathbf{e}_3 \\
\frac{\partial\left(\mathbf{p}_e^T\mathbf{u}\right)}{\partial x} &= \mathbf{e}_1^T\mathbf{u},\ \frac{\partial\left(\mathbf{p}_e^T\mathbf{u}\right)}{\partial y} = \mathbf{e}_2^T\mathbf{u},\ \frac{\partial\left(\mathbf{p}_e^T\mathbf{u}\right)}{\partial z} = \mathbf{e}_3^T\mathbf{u} \\
\frac{\partial\left(\mathbf{p}_e^T\mathbf{D}\mathbf{p}_e\right)}{\partial x} &= \mathbf{e}_1^T\mathbf{D}\mathbf{p}_e + \mathbf{p}_e^T\mathbf{D}\mathbf{e}_1 \\
\frac{\partial\left(\mathbf{p}_e^T\mathbf{D}\mathbf{p}_e\right)}{\partial y} &= \mathbf{e}_2^T\mathbf{D}\mathbf{p}_e + \mathbf{p}_e^T\mathbf{D}\mathbf{e}_2 \\
\frac{\partial\left(\mathbf{p}_e^T\mathbf{D}\mathbf{p}_e\right)}{\partial z} &= \mathbf{e}_3^T\mathbf{D}\mathbf{p}_e + \mathbf{p}_e^T\mathbf{D}\mathbf{e}_3
\end{aligned}$$

Following the above rules, the partial derivative of equation (7.129) with respect to x is computed as

$$\begin{aligned}
\frac{\partial F\left(x,\ y,\ z\right)}{\partial x} &= 2\left(b_1\mathbf{p}_e^T\mathbf{p}_e + \mathbf{p}_e^T\mathbf{u} + b_2\right)\left(2b_1\mathbf{p}_e^T\mathbf{e}_1 + \mathbf{e}_1^T\mathbf{u}\right) \\
&\quad +2\left(b_3\mathbf{p}_e^T\mathbf{p}_e + \mathbf{p}_e^T\mathbf{v} + b_4\right)\left(2b_3\mathbf{p}_e^T\mathbf{e}_1 + \mathbf{e}_1^T\mathbf{v}\right)
\end{aligned}$$

At this point, the Newton-Raphson method is ready to be implemented to find the solution of equation (7.133) :

1. Start at an initial guess $\boldsymbol{p}$;
2. Compute the values of $F_1(x,y,z)$, $F_1(x,y,z)$, and $F_1(x,y,z)$
3. Compute the Jacobian matrix :

$$\mathbf{P} = \begin{bmatrix}
\frac{\partial F_1(x,\ y,\ z)}{\partial x} & \frac{\partial F_1(x,\ y,\ z)}{\partial y} & \frac{\partial F_1(x,\ y,\ z)}{\partial z} \\
\frac{\partial F_2(x,\ y,\ z)}{\partial x} & \frac{\partial F_2(x,\ y,\ z)}{\partial y} & \frac{\partial F_2(x,\ y,\ z)}{\partial z} \\
\frac{\partial F_3(x,\ y,\ z)}{\partial x} & \frac{\partial F_3(x,\ y,\ z)}{\partial y} & \frac{\partial F_3(x,\ y,\ z)}{\partial z}
\end{bmatrix}$$

4. Compute the step of the next iteration :

$$\Delta \mathbf{p} = \mathbf{P}^{-1} \left[\begin{array}{ccc} F_1(x,\ y,\ z) & F_2(x,\ y,\ z) & F_3(x,\ y,\ z) \end{array} \right]^T$$

5. If the predefined precision or maximum number of iterations is reached, end the process ;
6. $\mathbf{p} = \mathbf{p} - \Delta \mathbf{p}$ and perform the next iteration, change the initial guess if necessary.

7.9 Jacobian matrix

The Jacobian matrix plays an important role in evaluating the performance of a PM. The set of Jacobian matrices form a metric space. Traditionally, for a Jacobian matrix, the columns corresponding to prismatic joints have zero elements in the angular velocity rows, while those corresponding to revolute joints have unit vectors in the angular velocity part. The drawbacks are :

- Two Jacobian matrices of different topologies are always in two isolated subspaces, no path exists between them, making a great number of potential designs missing ;
- A revolute joint far enough from the global reference will surely cause singularity of the Jacobian matrix and make it impossible to evaluate the design. In practice, there exist many ways to actuate a revolute joint, slider-crank mechanism for instance ; a revolute joint may even be realized by a slightly curved guide and driven by slightly curved rack gear allowing the joint axis to be placed very far away from the manipulator reference frame. If a revolute joint is not an angle-driven one, then the traditional formulation of the Jacobian matrix will not work.

In this work, to make Jacobian metric space a continuous one, the joint variables are

normalized and the angular velocity part of a Jacobian matrix can have any element in $\mathbb{R}^3$; a revolute joint approaching infinity will not necessarily leads to a singular Jacobian matrix. This allows the whole spectrum of topologies and geometries to be taken into consideration and be evaluated.

7.9.1 Jacobian matrix of subchains

Considering an n-joint subchain, following the tangent operator definition and equation (7.23), we have

$$ {}^{i-1,\,i-1}\mathbf{T}_i = \dot{\mathbf{C}}_i\mathbf{C}_i^{-1} = \mathbf{B}_x\left(-\frac{1}{w_i}\right)\frac{d\mathbf{R_{hz}}\left(w_iq_i\right)}{dt}\mathbf{R_{hz}}\left(w_iq_i\right)^{-1}\mathbf{B}_x\left(\frac{1}{w_i}\right) \tag{7.134} $$

Since

$$ \frac{d\mathbf{R_{hz}}\left(w_iq_i\right)}{dt}\mathbf{R_{hz}}\left(w_iq_i\right)^{-1} = \begin{bmatrix} 0 & -w_i & 0 & 0 \\ w_i & 0 & 0 & 0 \\ 0 & 0 & 0 & 0 \\ 0 & 0 & 0 & 0 \end{bmatrix}\dot{q}_i \tag{7.135} $$

therefore

$$ {}^{i-1,\,i-1}\mathbf{T}_i = \begin{bmatrix} 0 & -w_i & 0 & 0 \\ w_i & 0 & 0 & 1 \\ 0 & 0 & 0 & 0 \\ 0 & 0 & 0 & 0 \end{bmatrix}\dot{q}_i \tag{7.136} $$

The corresponding tangent vector is

$$ {}^{i-1,\,i-1}\boldsymbol{t}_i = \begin{bmatrix} w_i\boldsymbol{e}_3 \\ \boldsymbol{e}_2 \end{bmatrix}\dot{q}_i \tag{7.137} $$

Let

$$\mathbf{S}_i \equiv \begin{bmatrix} \mathbf{Q}_i & \mathbf{Q}_i \\ [\boldsymbol{p}_i\times]\,\mathbf{Q}_i & \mathbf{Q}_i \end{bmatrix} \tag{7.138}$$

which is the tangent vector coordinate transformation matrix, then

$${}^{i-1}\boldsymbol{t}_i = \mathbf{S}_{i-1}\,{}^{i-1,\,i-1}\boldsymbol{t}_i = \mathbf{S}_{i-1}\begin{bmatrix} w_i\boldsymbol{e}_3 \\ \boldsymbol{e}_2 \end{bmatrix}\dot{q}_i \tag{7.139}$$

Let

$$\begin{bmatrix} \boldsymbol{\varpi}_i \\ \boldsymbol{\chi}_i \end{bmatrix} \equiv \mathbf{S}_{i-1}\begin{bmatrix} w_i\boldsymbol{e}_3 \\ \boldsymbol{e}_2 \end{bmatrix} \tag{7.140}$$

then the Jacobian matrix of the subchain is given as :

$$\mathbf{J} = \begin{bmatrix} \boldsymbol{\varpi}_1 & \boldsymbol{\varpi}_2 & \cdots & \boldsymbol{\varpi}_n \\ \boldsymbol{\chi}_1 & \boldsymbol{\chi}_2 & \cdots & \boldsymbol{\chi}_n \end{bmatrix} \tag{7.141}$$

7.9.2 Jacobian matrix of TPMs

Let the tangent vector of the end-effector be denoted by

$$\boldsymbol{t}_e \equiv \begin{bmatrix} \boldsymbol{\omega}_e \\ \boldsymbol{v}_e \end{bmatrix} \tag{7.142}$$

Suppose the first joint is actuated and let

$$\boldsymbol{q}_j \equiv \begin{bmatrix} q_{j2} & q_{j3} & \cdots & q_{jm_j} \end{bmatrix}^T,\ j = 1,\ 2,\ 3 \tag{7.143}$$

$$\boldsymbol{q} \equiv \begin{bmatrix} q_{11} & q_{21} & q_{31} \end{bmatrix}^T \tag{7.144}$$

then

$$\begin{bmatrix} \boldsymbol{\omega}_e \\ \boldsymbol{v}_e \end{bmatrix} = \begin{bmatrix} \boldsymbol{\varpi}_{j2} & \boldsymbol{\varpi}_{j3} & \cdots & \boldsymbol{\varpi}_{jm_j} \\ \boldsymbol{\chi}_{j2} & \boldsymbol{\chi}_{j3} & \cdots & \boldsymbol{\chi}_{jm_j} \end{bmatrix} \dot{\boldsymbol{q}}_j + \begin{bmatrix} \boldsymbol{\varpi}_{11} & \boldsymbol{\varpi}_{21} & \boldsymbol{\varpi}_{31} \\ \boldsymbol{\chi}_{11} & \boldsymbol{\chi}_{21} & \boldsymbol{\chi}_{31} \end{bmatrix} \boldsymbol{e}_j \boldsymbol{e}_j^T \dot{\boldsymbol{q}},\ j = 1,\ 2,\ 3 \tag{7.145}$$

They are 18 linear equations with 18 unknown. $\dot{\boldsymbol{q}}_j$ can be easily solved as linear combination of $\dot{q}_1$, $\dot{q}_2$, and $\dot{q}_3$:

$$\dot{\boldsymbol{q}}_j = \mathbf{F}_j \dot{\boldsymbol{q}},\ j = 1,\ 2,\ 3 \tag{7.146}$$

where $\mathbf{F}_j$ is known. Therefore

$$\begin{bmatrix} \boldsymbol{\omega}_e \\ \boldsymbol{v}_e \end{bmatrix} = \mathbf{F}_j \dot{\boldsymbol{q}} + \begin{bmatrix} \boldsymbol{\varpi}_{11} & \boldsymbol{\varpi}_{21} & \boldsymbol{\varpi}_{31} \\ \boldsymbol{\chi}_{11} & \boldsymbol{\chi}_{21} & \boldsymbol{\chi}_{31} \end{bmatrix} \boldsymbol{e}_j \boldsymbol{e}_j^T \dot{\boldsymbol{q}},\ j = 1,\ 2,\ 3 \tag{7.147}$$

the Jacobian matrix is computed as

$$\mathbf{J} = \mathbf{F}_j + \begin{bmatrix} \boldsymbol{\varpi}_{11} & \boldsymbol{\varpi}_{21} & \boldsymbol{\varpi}_{31} \\ \boldsymbol{\chi}_{11} & \boldsymbol{\chi}_{21} & \boldsymbol{\chi}_{31} \end{bmatrix} \boldsymbol{e}_j \boldsymbol{e}_j^T,\ j = 1,\ 2,\ or\ 3 \tag{7.148}$$

7.10 Synthesis procedure

By definition, the end-effector of a TPM is always connected to the base by three serial kinematic chains. Since a TPM is defined by the nature, the orientation and the position of each of its joints at an initial configuration, its topological and geometric synthesis is, in fact, the synthesis of the three subchains. To describe the j^{th} subchain, parameters introduced in section 3 are summarized as the followings :

1. $m_j \in \mathbb{N}$: the number of joints;
2. $\kappa_{j1}, \kappa_{j2}, \cdots, \kappa_{jm_j} \in \mathbb{N}$: identify which joints have the same orientation;

3. $\hat{\boldsymbol{n}}_{j1}, \hat{\boldsymbol{n}}_{j2}, \cdots, \hat{\boldsymbol{n}}_{jm_j}$: unit vectors representing the joint orientations;
4. $\hat{\boldsymbol{m}}_{j1}, \hat{\boldsymbol{m}}_{j2}, \cdots, \hat{\boldsymbol{m}}_{jm_j}$: unit vectors representing the orientations of the moments of the above unit vectors when each of them is aligned to a different joint axis;
5. $w_{j1}, w_{j2}, \cdots, w_{jm_j}$: joint natures;

The following is the topological and geometric synthesis procedure :

1. Determine m_1, m_2, and m_3 such that the triple
   $(m_1, m_2, m_3) \in \{(5,5,5), (4,5,6), (3,6,6)\}$
2. For $j = 1, 2, 3$, if
   (a) m_j =3 then
   - $w_{j1} = w_{j2} = w_{j3} = 0$ (no revolute joint);
   - $\boldsymbol{\kappa}_j$=$(\kappa_{j1}, \kappa_{j2}, \kappa_{j3}) \in \{(1,1,2), (1,2,1), (1,1,2)\}$
   - according to $\boldsymbol{\kappa}_j$, construct $\hat{\boldsymbol{n}}_{j1}$, $\hat{\boldsymbol{n}}_{j2}$, $\hat{\boldsymbol{n}}_{j3}$, and then $\hat{\boldsymbol{m}}_{j1}$, $\hat{\boldsymbol{m}}_{j2}$, $\hat{\boldsymbol{m}}_{j3}$

   (b) m_j =4 then
   - construct $(w_{j1}, w_{j2}, w_{j3}, w_{j4})$ such that $w_{j1}w_{j2}w_{j3}w_{j4} = 0$ (at least one prismatic joint).
   - Let $S \equiv \{k \mid k = 1,2,3,4; w_{jk} \neq 0\}$ (the set of revolute joint subscripts), construct $(\kappa_{j1}, \kappa_{j2}, \kappa_{j3}, \kappa_{j4})$ such that $\forall c,\ d \in S,\ \kappa_{jc} = \kappa_{jd}$ (all revolute joints are parallel);
   - according to $\boldsymbol{\kappa}_j$, construct $\hat{\boldsymbol{n}}_{j1} \sim \hat{\boldsymbol{n}}_{j4}$ and then $\hat{\boldsymbol{m}}_{j1} \sim \hat{\boldsymbol{m}}_{j4}$

   (c) m_j =5 then
   - construct $\boldsymbol{\kappa}_j$=$(\kappa_{j1}, \kappa_{j2}, \kappa_{j3}, \kappa_{j4}, \kappa_{j5})$ such that

$$\boldsymbol{\kappa}_j \in \{(1,1,2,2,2),(2,2,2,1,1),(2,1,1,2,2),(1,2,2,2,1),(2,2,1,1,2)\}$$

   - Let $S_1 \equiv \{k \mid k = 1 \sim 5; \kappa_{jk} = 1\}$, $S_2 \equiv \{k \mid k = 1 \sim 5; \kappa_{jk} = 2\}$,

construct $(w_{j1}, w_{j2}, w_{j3}, w_{j4}, w_{j5})$ such that $w_{jc} + w_{jd} > 0$ if $c, d \in S_1$ and $w_{jc} + w_{jd} + w_{jf} > 0$ if $c, d, f \in S_2$;

- according to $\boldsymbol{\kappa}_j$, construct $\hat{\boldsymbol{n}}_{j1} \sim \hat{\boldsymbol{n}}_{j5}$ and then $\hat{\boldsymbol{m}}_{j1} \sim \hat{\boldsymbol{m}}_{j5}$

(d) m_j =6 then there is no special constraint on the topological and geometric parameters.

Algorithms for the above process can be easily implemented to perform automatic topology and geometry generation. After that, kinematic model can also be establish automatically by following the procedure proposed in section 4. The performance evaluation can then be carried out according to different evaluation criteria.

7.11 Conclusion

Fundamental issues concerning simultaneous topological and geometric synthesis of TPMs were systematically studied. First of all, the concept of initial configuration was introduced, making it possible to represent revolute joints and prismatic joints in a unified way. Then a singularity-free parametrization of both topology and geometry was proposed. After that, joint variables were normalized, which enables the joint type to be seamlessly incorporated into kinematic model, it is no longer necessary to reformulate the kinematic model when a revolute joint is replaced by a prismatic one or vice versa. Inverse and forward kinematic problems were investigated, detailed solutions were proposed, and the Jacobian matrix was formulated, making the proposed kinematic model ready to be used for kinematic synthesis. Finally, a topological and geometric synthesis procedure was presented which was aimed at automatic generation of topologies and geometries of TPMs.

Acknowledgment

The authors acknowledge the financial support of NSERC (National Science and Engineering Research Council of Canada) under grants OGPIN-203618 and RGPIN-138478.

7.12 Appendix 1 : Inverse kinematics of TPMs

7.12.1 Subchains of $R^1R^1R^1R^2R^2$

Knowing $Joint(1)$, $Joint(2)$, and $Joint(3)$ being parallel, let

$$\mathbf{G}_1 = \mathbf{R}_\mathbf{z}(-\beta_1), \ \mathbf{G}_2 = \mathbf{R}_\mathbf{z}(-\beta_1) \tag{7.149}$$

Since $w_1q_1 + w_2q_2 + w_3q_3 = 0$, we have

$$\begin{aligned} \mathbf{Q}_3 &= \mathbf{Q}_0\mathbf{A}_1\mathbf{A}_2\mathbf{A}_3 \\ &= \mathbf{Q}_0\mathbf{R}_\mathbf{z}(-w_1q_1)\,\mathbf{R}_\mathbf{z}(-\beta_1)\,\mathbf{R}_\mathbf{z}(-w_2q_2)\,\mathbf{R}_\mathbf{z}(-\beta_2)\,\mathbf{R}_\mathbf{z}(-w_3q_3)\,\mathbf{G}_3 \\ &= \mathbf{Q}_0\mathbf{R}_\mathbf{z}(-\beta_1-\beta_2)\,\mathbf{G}_3 \end{aligned} \tag{7.150}$$

So $\mathbf{Q}_3$ is known.

Rewrite equation (7.38) as

$$\boldsymbol{p}_e - \boldsymbol{\rho}_0 - \mathbf{Q}_0\boldsymbol{\rho}_1 - \mathbf{Q}_1\boldsymbol{\rho}_2 - \mathbf{Q}_2\boldsymbol{\rho}_3 - \mathbf{Q}_5\boldsymbol{\rho}_e = \mathbf{Q}_3(\boldsymbol{\rho}_4 + \mathbf{A}_4\boldsymbol{\rho}_5) \tag{7.151}$$

where

$$\begin{aligned}\boldsymbol{\rho}_4 + \mathbf{A}_4\boldsymbol{\rho}_5 = & - \frac{\boldsymbol{e}_1}{w_4} + \mathbf{R}_{\mathbf{z}}(w_4 q_4)\frac{\boldsymbol{e}_1}{w_4} \\ & + \mathbf{R}_{\mathbf{z}}(w_4 q_4)\mathbf{R}_{\mathbf{z}}(-\beta_4)\left[-\frac{\boldsymbol{e}_1}{w_5} + \mathbf{R}_{\mathbf{z}}(w_5 q_5)\frac{\boldsymbol{e}_1}{w_5}\right] \end{aligned} \tag{7.152}$$

If $w_4 w_5 \neq 0$, since $w_4 q_4 + w_5 q_5 = 0$, equation (7.152) can be written as

$$\boldsymbol{\rho}_4 + \mathbf{A}_4\boldsymbol{\rho}_5 = \mathbf{R}_{\mathbf{z}}(w_4 q_4)\left[\frac{\boldsymbol{e}_1}{w_4} - \mathbf{R}_{\mathbf{z}}(-\beta_4)\frac{\boldsymbol{e}_1}{w_5}\right] - \frac{\boldsymbol{e}_1}{w_4} + \mathbf{R}_{\mathbf{z}}(-\beta_4)\frac{\boldsymbol{e}_1}{w_5} \tag{7.153}$$

Let

$$\boldsymbol{u} = \begin{bmatrix} u_1 & u_2 & u_3 \end{bmatrix} = \frac{\boldsymbol{e}_1}{w_4} - \mathbf{R}_{\mathbf{z}}(-\beta_4)\frac{\boldsymbol{e}_1}{w_5}$$

then equation (7.153) can be written as

$$\boldsymbol{\rho}_4 + \mathbf{A}_4\boldsymbol{\rho}_5 = \mathbf{R}_{\mathbf{z}}(w_4 q_4)\,\boldsymbol{u} - \boldsymbol{u} \tag{7.154}$$

Given the first three joint axes being parallel, we have

$$\begin{aligned} \boldsymbol{e}_3^T\mathbf{Q}_0^T = \boldsymbol{e}_3^T\mathbf{Q}_1^T \Rightarrow \boldsymbol{e}_3^T\mathbf{Q}_0^T\mathbf{Q}_1 = \boldsymbol{e}_3^T \\ \boldsymbol{e}_3^T\mathbf{Q}_0^T = \boldsymbol{e}_3^T\mathbf{Q}_2^T \Rightarrow \boldsymbol{e}_3^T\mathbf{Q}_0^T\mathbf{Q}_2 = \boldsymbol{e}_3^T \end{aligned} \tag{7.155}$$

Multiplying equation (7.151) with $\boldsymbol{e}_3^T\mathbf{Q}_0^T$ gives

$$\boldsymbol{e}_3^T\mathbf{Q}_0^T(\boldsymbol{p}_e - \boldsymbol{\rho}_0 - \mathbf{Q}_5\boldsymbol{\rho}_e) = \boldsymbol{e}_3^T\mathbf{Q}_0^T\mathbf{Q}_3(\boldsymbol{\rho}_4 + \mathbf{A}_4\boldsymbol{\rho}_5) \tag{7.156}$$

Combining equations (7.154) and (7.156) gives

$$\boldsymbol{e}_3^T\mathbf{Q}_0^T(\boldsymbol{p}_e - \boldsymbol{\rho}_0 - \mathbf{Q}_5\boldsymbol{\rho}_e) + \boldsymbol{e}_3^T\mathbf{Q}_0^T\mathbf{Q}_3\boldsymbol{u} = \boldsymbol{e}_3^T\mathbf{Q}_0^T\mathbf{Q}_3\mathbf{R}_{\mathbf{z}}(w_4 q_4)\,\boldsymbol{u} \tag{7.157}$$

Equation (7.157) has the same form as equation (7.56) and is ready to be solved for q_4. For $joint(4)$ or $joint(5)$ being at infinity, the treatment is similar to $R^1R^1R^2R^2R^2$.

Having solved q_4 and q_5, since

$$\boldsymbol{p}_e = \boldsymbol{p}_3 + \mathbf{Q}_3\boldsymbol{\rho}_4 + \mathbf{Q}_4\boldsymbol{\rho}_5 + \mathbf{Q}_5\boldsymbol{\rho}_e \Rightarrow \boldsymbol{p}_3 = \boldsymbol{p}_e - \mathbf{Q}_3\boldsymbol{\rho}_4 - \mathbf{Q}_4\boldsymbol{\rho}_5 - \mathbf{Q}_5\boldsymbol{\rho}_e \tag{7.158}$$

and from (7.150), we have

$$\begin{aligned} \mathbf{Q}_4 &= \mathbf{Q}_3\mathbf{A}_4 = \mathbf{Q}_0\mathbf{R}_{\mathbf{z}}\left(-\beta_1 - \beta_2\right)\mathbf{G}_3\mathbf{R}_{\mathbf{z}}\left(w_4q_4 - \beta_4\right) \\ \mathbf{Q}_5 &= \mathbf{Q}_4\mathbf{A}_5 = \mathbf{Q}_0\mathbf{R}_{\mathbf{z}}\left(-\beta_1 - \beta_2\right)\mathbf{G}_3\mathbf{R}_{\mathbf{z}}\left(w_4q_4 + w_5q_5 - \beta_4\right)\mathbf{G}_5 \end{aligned} \tag{7.159}$$

So $\boldsymbol{p}_3$ is known. Write $\boldsymbol{p}_3$ in function of q_1, q_2, and q_3 :

$$\boldsymbol{p}_3 = \boldsymbol{\rho}_0 + \mathbf{Q}_0\boldsymbol{\rho}_1 + \mathbf{Q}_1\boldsymbol{\rho}_2 + \mathbf{Q}_2\boldsymbol{\rho}_3 \tag{7.160}$$

Equation (7.160) has the same form as equation (7.75) and can solved similarly and will not be repeated here.

7.12.2 Subchains of $R^1R^2R^2R^2R^1$

Rewrite equation (7.38) as

$$-\mathbf{Q}_1\boldsymbol{\rho}_2 - \mathbf{Q}_2\boldsymbol{\rho}_3 - \mathbf{Q}_3\boldsymbol{\rho}_4 = \boldsymbol{\rho}_0 - \boldsymbol{p}_e + \mathbf{Q}_0\boldsymbol{\rho}_1 + \mathbf{Q}_4\boldsymbol{\rho}_5 + \mathbf{Q}_5\boldsymbol{\rho}_e \tag{7.161}$$

Since $joint(2)$, $joint(3)$, and $joint(4)$ are parallel, we have

$$\boldsymbol{e}_3^T\mathbf{Q}_1^T = \boldsymbol{e}_3^T\mathbf{Q}_2^T \Rightarrow \boldsymbol{e}_3^T\mathbf{Q}_1^T\mathbf{Q}_2 = \boldsymbol{e}_3^T$$

$$
\begin{aligned}
\boldsymbol{e}_3^T\mathbf{Q}_1^T &= \boldsymbol{e}_3^T\mathbf{Q}_3^T \Rightarrow \boldsymbol{e}_3^T\mathbf{Q}_1^T\mathbf{Q}_3 = \boldsymbol{e}_3^T \\
\mathbf{Q}_1 &= \mathbf{Q}_0\mathbf{A}_1 = \mathbf{Q}_0\mathbf{R}_{\mathbf{z}}\left(w_1q_1\right)\mathbf{G}_1 \\
&\Rightarrow \boldsymbol{e}_3^T\mathbf{Q}_1^T\mathbf{Q}_0 = \boldsymbol{e}_3^T\mathbf{G}_1^T\mathbf{R}_{\mathbf{z}}\left(-w_1q_1\right) \\
\mathbf{Q}_4 &= \mathbf{Q}_1\mathbf{R}_{\mathbf{z}}\left(w_2q_2 + w_3q_3 + w_4q_4 - \beta_2 - \beta_3\right)\mathbf{G}_4 \\
&\Rightarrow \boldsymbol{e}_3^T\mathbf{Q}_1^T\mathbf{Q}_4 = \boldsymbol{e}_3^T\mathbf{G}_4 \\
\boldsymbol{e}_3^T\mathbf{Q}_1^T\mathbf{Q}_5 &= \boldsymbol{e}_3^T\mathbf{Q}_1^T\mathbf{Q}_4\mathbf{R}_{\mathbf{z}}\left(w_5q_5\right)\mathbf{G}_5 = \boldsymbol{e}_3^T\mathbf{G}_4\mathbf{R}_{\mathbf{z}}\left(w_5q_5\right)\mathbf{G}_5 \qquad (7.162)
\end{aligned}
$$

Multiplying equation (7.161) with $\boldsymbol{e}_3^T\mathbf{Q}_1^T$ yields

$$
\begin{aligned}
\boldsymbol{e}_3^T\mathbf{Q}_1^T\left(\boldsymbol{\rho}_0 - \boldsymbol{p}_e\right) &+ \boldsymbol{e}_3^T\mathbf{G}_1^T\mathbf{R}_{\mathbf{z}}\left(-w_1q_1\right)\boldsymbol{\rho}_1 \\
&+ \boldsymbol{e}_3^T\mathbf{G}_4\boldsymbol{\rho}_5 + \boldsymbol{e}_3^T\mathbf{G}_4\mathbf{R}_{\mathbf{z}}\left(w_5q_5\right)\mathbf{G}_5\boldsymbol{\rho}_e = 0 \qquad (7.163)
\end{aligned}
$$

Since $w_1q_1 + w_5q_5 = 0$, if $w_1w_2 \neq 0$, equation (7.163) can be simplified as

$$
\begin{aligned}
&\boldsymbol{e}_3^T\mathbf{G}_1^T\mathbf{R}_{\mathbf{z}}\left(-w_1q_1\right)\left[\mathbf{Q}_0^T\left(\boldsymbol{\rho}_0 - \boldsymbol{p}_e\right) - \frac{\boldsymbol{e}_1}{w_1}\right] \\
&+\boldsymbol{e}_3^T\mathbf{G}_4\mathbf{R}_{\mathbf{z}}\left(-w_1q_1\right)\left(\frac{\boldsymbol{e}_1}{w_5} + \mathbf{G}_5\boldsymbol{\rho}_e\right) = -\boldsymbol{e}_3^T\left(\mathbf{G}_1^T\frac{\boldsymbol{e}_1}{w_1} - \mathbf{G}_4\frac{\boldsymbol{e}_1}{w_5}\right) \qquad (7.164)
\end{aligned}
$$

q_1 is the only unknown in equation (7.164) and can be easily solved. q_5 can be solved by $w_1q_1 + w_5q_5 = 0$. For $joint(1)$ or $joint(5)$ being at infinity, the treatment is similar to $R^1R^1R^2R^2R^2$.

Having solved q_1 and q_5, $\boldsymbol{\rho}_1$, $\mathbf{Q}_1$, $\mathbf{Q}_4$, $\mathbf{Q}_5$, and $\boldsymbol{\rho}_5$ become known. From equation (7.38), we have

$$
\mathbf{Q}_1^T\left(\mathbf{p}_e - \rho_0 - \mathbf{Q}_0\rho_1 - \mathbf{Q}_5\rho_e - \mathbf{Q}_4\rho_5\right) = \rho_2 + \mathbf{A}_2\rho_3 + \mathbf{A}_2\mathbf{A}_3\rho_4 \qquad (7.165)
$$

The left side of equation (7.165) is known and the only unknowns in the right hand are q_3, q_4, and q_5 which can be solved by using the same techniques as for

equation (7.75)

7.12.3 Subchains of $R^1R^2R^2R^1R^1$

7.12.3.1 Solve q_2 and q_3

Rewrite equation (7.38) as

$$\mathbf{p}_e - \rho_0 - \mathbf{Q}_0\rho_1 - \mathbf{Q}_3\rho_4 - \mathbf{Q}_4\rho_5 - \mathbf{Q}_5\rho_e = \mathbf{Q}_1\rho_2 + \mathbf{Q}_2\rho_3 \tag{7.166}$$

Since

$$\begin{aligned}
\mathbf{e}_3^T\mathbf{Q}_0^T\mathbf{Q}_1 &= \mathbf{e}_3^T\mathbf{Q}_0^T\mathbf{Q}_0\mathbf{R}_\mathbf{z}\left(-w_1q_1\right)\mathbf{G}_1 = \mathbf{e}_3^T\mathbf{G}_1 \\
\mathbf{e}_3^T\mathbf{Q}_0^T\mathbf{Q}_2 &= \mathbf{e}_3^T\mathbf{G}_1\mathbf{R}_\mathbf{z}\left(w_2q_2\right)\mathbf{R}_\mathbf{z}\left(-\beta_2\right) \\
\mathbf{e}_3^T\mathbf{Q}_0^T &= \mathbf{e}_3^T\mathbf{Q}_3^T \Rightarrow \mathbf{e}_3^T\mathbf{Q}_0^T\mathbf{Q}_3 = \mathbf{e}_3^T \\
\mathbf{e}_3^T\mathbf{Q}_0^T &= \mathbf{e}_3^T\mathbf{Q}_4^T \Rightarrow \mathbf{e}_3^T\mathbf{Q}_0^T\mathbf{Q}_4 = \mathbf{e}_3^T \\
\mathbf{e}_3^T\mathbf{Q}_0^T\mathbf{Q}_5 &= \mathbf{e}_3^T\mathbf{Q}_0^T\mathbf{Q}_e\mathbf{G}_e^T
\end{aligned}$$

Multiplying equation (7.166) with $\mathbf{e}_3^T\mathbf{Q}_0^T$ gives

$$\mathbf{e}_3^T\mathbf{Q}_0^T\left(\mathbf{p}_e - \rho_0\right) - \mathbf{e}_3^T\mathbf{Q}_0^T\mathbf{Q}_e\mathbf{G}_e^T\rho_e = \mathbf{e}_3^T\mathbf{G}_1\rho_2 + \mathbf{e}_3^T\mathbf{G}_1\mathbf{R}_\mathbf{z}\left(w_2q_2\right)\mathbf{R}_\mathbf{z}\left(-\beta_2\right)\rho_3 \tag{7.167}$$

If $w_2 = 0$ and $w_3 \neq 0$, since $w_2q_2 + w3q_3 = 0$ we have $w_2q2 = w_3q_3 = 0$. Combining equations (7.26), (7.28), and (7.167) gives

$$\mathbf{e}_3^T\mathbf{Q}_0^T\left(\mathbf{p}_e - \rho_0\right) - \mathbf{e}_3^T\mathbf{Q}_0^T\mathbf{Q}_e\mathbf{G}_e^T\rho_e = \mathbf{e}_3^T\mathbf{G}_1\mathbf{e}_2q_2 \tag{7.168}$$

q_2 can be easily solved.

Similarly, if $w_3 = 0$ and $w_2 \neq 0$, we have

$$\mathbf{e}_3^T \mathbf{Q}_0^T (\mathbf{p}_e - \rho_0) - \mathbf{e}_3^T \mathbf{Q}_0^T \mathbf{Q}_e \mathbf{G}_e^T \rho_e = \mathbf{e}_3^T \mathbf{G}_1 \mathbf{R}_\mathbf{z} (-\beta_2) \mathbf{e}_2 q_3 \tag{7.169}$$

q_3 can be easily solved.

If $w_2 w_3 \neq 0$, substitute $\boldsymbol{\rho}$ given by equation (7.25) into equation (7.167), then

$$\begin{aligned} \mathbf{e}_3^T \mathbf{Q}_0^T (\mathbf{p}_e - \rho_0) - \mathbf{e}_3^T \mathbf{Q}_0^T \mathbf{Q}_e \mathbf{G}_e^T \rho_e + \mathbf{e}_3^T \mathbf{G}_1 \frac{\mathbf{e}_1}{w_2} - \mathbf{e}_3^T \mathbf{G}_1 \mathbf{R}_\mathbf{z} (-\beta_2) \frac{\mathbf{e}_1}{w_3} \\ = \mathbf{e}_3^T \mathbf{G}_1 \mathbf{R}_\mathbf{z} (w_2 q_2) \left[\frac{\mathbf{e}_1}{w_2} - \mathbf{R}_\mathbf{z} (-\beta_2) \frac{\mathbf{e}_1}{w_3} \right] \end{aligned} \tag{7.170}$$

q_2 can be easily solved. q_3 can be solved by $w_2 q_2 + w_3 q_3 = 0$.

7.12.3.2 Solve q_1, q_4, and q_5

Rewrite equation (7.38) as

$$\mathbf{p}_e = \rho_0 + \mathbf{Q}_0 \rho_1 + \mathbf{Q}_1 (\rho_2 + \mathbf{A}_2 \rho_3) + \mathbf{Q}_3 \rho_4 + \mathbf{Q}_4 \rho_5 + \mathbf{Q}_5 \rho_e \tag{7.171}$$

where $\rho_2 + \mathbf{A}_2 \rho_3$ is known. Substitute $\boldsymbol{\rho}$ given by equation (7.25) into equation (7.103), then

$$\begin{aligned} &\mathbf{p}_e - \rho_0 - \mathbf{Q}_e \mathbf{G}_e^T \rho_e = \mathbf{Q}_0 \rho_1 \\ &+ \mathbf{Q}_0 \mathbf{R}_\mathbf{z} (w_1 q_1) \mathbf{G}_1 (\rho_2 + \mathbf{A}_2 \rho_3) \\ &+ \mathbf{Q}_0 \mathbf{R}_\mathbf{z} (w_1 q_1) \mathbf{G}_1 \mathbf{R}_\mathbf{z} (-\beta_2) \mathbf{G}_3 \rho_4 \\ &+ \mathbf{Q}_0 \mathbf{R}_\mathbf{z} (w_1 q_1) \mathbf{G}_1 \mathbf{R}_\mathbf{z} (-\beta_2) \mathbf{G}_3 \mathbf{R}_\mathbf{z} (w_4 q_4) \mathbf{R}_\mathbf{z} (-\beta_4) \rho_5 \end{aligned} \tag{7.172}$$

If two of $Joint(1)$, $Joint(4)$, and $Joint(5)$ are at infinity, we have

1. $w_1 = w_4 = 0$

$$\mathbf{Q}_0\mathbf{e_2}q_1 + \mathbf{Q}_0\mathbf{G}_1\mathbf{R_z}\left(-\beta_2\right)\mathbf{G}_3\mathbf{e_2}q_4 = \mathbf{p}_e - \rho_0 - \mathbf{Q}_e\mathbf{G}_e^T\rho_e - \mathbf{Q}_0\mathbf{G}_1\left(\rho_2 + \mathbf{A}_2\rho_3\right) \tag{7.173}$$

2. $w_4 = w_5 = 0$

$$\mathbf{Q}_0\mathbf{G}_1\mathbf{R_z}\left(-\beta_2\right)\mathbf{G}_3\mathbf{e_2}q_4 + \mathbf{Q}_0\mathbf{G}_1\mathbf{R_z}\left(-\beta_2\right)\mathbf{G}_3\mathbf{R_z}\left(-\beta_4\right)\mathbf{e_2}q_5 = \mathbf{p}_e - \rho_0 - \mathbf{Q}_e\mathbf{G}_e^T\rho_e - \mathbf{Q}_0\mathbf{G}_1\left(\rho_2 + \mathbf{A}_2\rho_3\right) \tag{7.174}$$

3. $w_5 = w_1 = 0$

$$\mathbf{Q}_0\mathbf{e_2}q_1 + \mathbf{Q}_0\mathbf{G}_1\mathbf{R_z}\left(-\beta_2\right)\mathbf{G}_3\mathbf{R_z}\left(-\beta_4\right)\mathbf{e_2}q_5 = \mathbf{p}_e - \rho_0 - \mathbf{Q}_e\mathbf{G}_e^T\rho_e - \mathbf{Q}_0\mathbf{G}_1\left(\rho_2 + \mathbf{A}_2\rho_3\right) \tag{7.175}$$

They are sets of linear equations and can be easily solved.

If one of $Joint(1)$, $Joint(4)$, and $Joint(5)$ are at infinity, we have

1. $w_1 = 0$

$$\mathbf{p} - \mathbf{Q}_0\mathbf{e_2}q_1 = \mathbf{Q}_0\mathbf{G}_1\mathbf{R_z}\left(-\beta_2\right)\mathbf{G}_3\mathbf{R_z}\left(w_4q_4\right)\mathbf{u} \tag{7.176}$$

$$\begin{aligned}\mathbf{p} &= \mathbf{p}_e - \rho_0 - \mathbf{Q}_e\mathbf{G}_e^T\rho_e - \mathbf{Q}_0\mathbf{G}_1\left(\rho_2 + \mathbf{A}_2\rho_3\right) \\ &\quad - \mathbf{Q}_e\mathbf{G}_e^T\mathbf{G}_5^T\frac{\mathbf{e}_1}{w_5} + \mathbf{Q}_0\mathbf{G}_1\mathbf{R_z}\left(-\beta_2\right)\mathbf{G}_3\frac{\mathbf{e}_1}{w_4} \\ \mathbf{u} &= \left[\frac{\mathbf{e}_1}{w_4} - \mathbf{R_z}\left(-\beta_4\right)\frac{\mathbf{e}_1}{w_5}\right]\end{aligned}$$

2. $w_4 = 0$

$$\mathbf{p} = \mathbf{Q}_0\rho_1\mathbf{R_z}\left(w_1q_1\right)\left[\mathbf{G}_1\mathbf{R_z}\left(-\beta_2\right)\mathbf{G}_3\mathbf{e_2}q_4 + \mathbf{u}\right] \tag{7.177}$$

$$\begin{aligned}
\mathbf{p} &= \mathbf{p}_e - \rho_0 - \mathbf{Q}_e\mathbf{G}_e^T\rho_e + \mathbf{Q}_0\rho_1\frac{\mathbf{e}_1}{w_1} - \mathbf{Q}_e\mathbf{G}_e^T\mathbf{G}_5^T\frac{\mathbf{e}_1}{w_5} \\
&\quad - \mathbf{Q}_0\mathbf{R_z}\left(w_1q_1\right)\mathbf{G}_1\left(\rho_2 + \mathbf{A}_2\rho_3\right) \\
\mathbf{u} &= \frac{\mathbf{e}_1}{w_1} - \mathbf{G}_1\mathbf{R_z}\left(-\beta_2\right)\mathbf{G}_3\mathbf{R_z}\left(-\beta_4\right)\frac{\mathbf{e}_1}{w_5}
\end{aligned}$$

3. $w_5 = 0$

$$\mathbf{p} - \mathbf{Q}_e\mathbf{G}_e^T\mathbf{G}_5^T\mathbf{e_2}q_4 = \mathbf{Q}_0\mathbf{R_z}\left(w_1q_1\right)\mathbf{u} \tag{7.178}$$

$$\begin{aligned}
\mathbf{p} &= \mathbf{p}_e - \rho_0 - \mathbf{Q}_e\mathbf{G}_e^T\rho_e + \mathbf{Q}_0\frac{\mathbf{e}_1}{w_1} - \mathbf{Q}_e\mathbf{G}_e^T\mathbf{G}_5^T\mathbf{R_z}\left(-\beta_4\right)\frac{\mathbf{e}_1}{w_4} \\
\mathbf{u} &= \frac{\mathbf{e}_1}{w_1} + \mathbf{G}_1\left(\rho_2 + \mathbf{A}_2\rho_3\right) - \mathbf{G}_1\mathbf{R_z}\left(-\beta_2\right)\mathbf{G}_3\frac{\mathbf{e}_1}{w_4}
\end{aligned}$$

$w_1w_4w_5 \neq 0$

$$\mathbf{p} - \mathbf{Q}_0\mathbf{R_z}\left(w_1q_1\right)\mathbf{u} = \mathbf{Q}_3\mathbf{R_z}\left(w_4q_4\right)\mathbf{v} \tag{7.179}$$

$$\begin{aligned}
\mathbf{p} &= \mathbf{p}_e - \rho_0 - \mathbf{Q}_e\mathbf{G}_e^T\rho_e - \mathbf{Q}_e\mathbf{G}_e^T\mathbf{G}_5^T\frac{\mathbf{e}_1}{w_5} + \mathbf{Q}_0\frac{\mathbf{e}_1}{w_1} \\
\mathbf{u} &= \frac{\mathbf{e}_1}{w_1} + \mathbf{G}_1\left(\rho_2 + \mathbf{A}_2\rho_3\right) - \mathbf{G}_1\mathbf{R_z}\left(-\beta_2\right)\mathbf{G}_3\frac{\mathbf{e}_1}{w_4} \\
\mathbf{v} &= \frac{\mathbf{e}_1}{w_4} - \mathbf{R_z}\left(-\beta_4\right)\frac{\mathbf{e}_1}{w_5}
\end{aligned}$$

The solution of the above equations is similar to the case for $R^1R^1R^2R^2R^1$.

7.13 Appendix 2 : Position manifold

b) $R^1R^1R^1R^2R^2$ and $R^1R^2R^2R^1R^1$

Rewrite equation (7.115) as

$$\begin{aligned}
&\mathbf{Q}_1^T\mathbf{p}_e + \mathbf{Q}_1^T\left(-\rho_0 - \mathbf{Q}_0\rho_1 - \mathbf{Q}_e\mathbf{G}_e^T\rho_e - \mathbf{Q}_e\mathbf{G}_e^T\mathbf{G}_5^T\frac{\mathbf{e}_1}{w_5}\right) + \frac{\mathbf{e}_1}{w_2} \\
= \;& \mathbf{R}_\mathbf{z}(w_2q_2)\frac{\mathbf{e}_1}{w_2} - \mathbf{A}_2\frac{\mathbf{e}_1}{w_3} + \mathbf{A}_2\mathbf{R}_\mathbf{z}(w_3q_3)\frac{\mathbf{e}_1}{w_3} - \mathbf{A}_2\mathbf{A}_3\frac{\mathbf{e}_1}{w_4} \\
&+\mathbf{A}_2\mathbf{A}_3\mathbf{R}_\mathbf{z}(w_4q_4)\frac{\mathbf{e}_1}{w_4} - \mathbf{A}_2\mathbf{A}_3\mathbf{A}_4\frac{\mathbf{e}_1}{w_5}
\end{aligned} \tag{7.180}$$

Since

$$\begin{aligned}
\mathbf{A}_2 &= \mathbf{R}_\mathbf{z}(w_2q_2)\,\mathbf{R}_\mathbf{z}(-\beta_2) \\
\mathbf{A}_2\mathbf{A}_3 &= \mathbf{R}_\mathbf{z}(-\beta_2)\,\mathbf{G}_3 \\
\mathbf{A}_2\mathbf{A}_3\mathbf{A}_4 &= \mathbf{R}_\mathbf{z}(-\beta_2)\,\mathbf{G}_3\mathbf{R}_\mathbf{z}(w_4q_4)\,\mathbf{R}_\mathbf{z}(-\beta_4)
\end{aligned}$$

equation (7.180) can be written as

$$\begin{aligned}
&\mathbf{Q}_1^T\mathbf{p}_e + \mathbf{Q}_1^T\left(-\rho_0 - \mathbf{Q}_0\rho_1 - \mathbf{Q}_e\mathbf{G}_e^T\rho_e - \mathbf{Q}_e\mathbf{G}_e^T\mathbf{G}_5^T\frac{\mathbf{e}_1}{w_5}\right) + \frac{\mathbf{e}_1}{w_2} \\
&-\mathbf{R}_\mathbf{z}(-\beta_2)\left[\frac{\mathbf{e}_1}{w_3} - \mathbf{G}_3\frac{\mathbf{e}_1}{w_4}\right] \\
= \;& \mathbf{R}_\mathbf{z}(w_2q_2)\left[\frac{\mathbf{e}_1}{w_2} - \mathbf{R}_\mathbf{z}(-\beta_2)\frac{\mathbf{e}_1}{w_3}\right] \\
&+\mathbf{R}_\mathbf{z}(-\beta_2)\,\mathbf{G}_3\mathbf{R}_\mathbf{z}(w_4q_4)\left[\frac{\mathbf{e}_1}{w_4} - \mathbf{R}_\mathbf{z}(-\beta_4)\frac{\mathbf{e}_1}{w_5}\right]
\end{aligned} \tag{7.181}$$

Let

$$\mathbf{a}_1 = \mathbf{Q}_1^T\left(-\rho_0 - \mathbf{Q}_0\rho_1 - \mathbf{Q}_e\mathbf{G}_e^T\rho_e - \mathbf{Q}_e\mathbf{G}_e^T\mathbf{G}_5^T\frac{\mathbf{e}_1}{w_5}\right)$$

$$
\begin{aligned}
& + \frac{\mathbf{e}_1}{w_2} - \mathbf{R_z}\left(-\beta_2\right)\left[\frac{\mathbf{e}_1}{w_3} - \mathbf{G}_3\frac{\mathbf{e}_1}{w_4}\right] \\
\mathbf{a}_2 &= -\left[\frac{\mathbf{e}_1}{w_4} - \mathbf{R_z}\left(-\beta_4\right)\frac{\mathbf{e}_1}{w_5}\right] \\
\mathbf{a}_3 &= \frac{\mathbf{e}_1}{w_2} - \mathbf{R_z}\left(-\beta_2\right)\frac{\mathbf{e}_1}{w_3}
\end{aligned}
$$

then equation (7.181) becomes

$$
\mathbf{Q}_1^T\mathbf{p}_e + \mathbf{a}_1 + \mathbf{R_z}\left(-\beta_2\right)\mathbf{G}_3\mathbf{R_z}\left(w_4q_4\right)\mathbf{a}_2 = \mathbf{R_z}\left(w_2q_2\right)\mathbf{a}_3 \tag{7.182}
$$

Multiply both sides of equation (7.182) with $\mathbf{e}_3^T$ to eliminate q_2 :

$$
\mathbf{e}_3^T\mathbf{Q}_1^T\mathbf{p}_e + \mathbf{e}_3^T\mathbf{a}_1 + \mathbf{e}_3^T\mathbf{G}_3\mathbf{R_z}\left(w_4q_4\right)\mathbf{a}_2 = \mathbf{e}_3^T\mathbf{a}_3 \tag{7.183}
$$

Let

$$
\mathbf{a}_4^T = \mathbf{e}_3^T\mathbf{G}_3
$$

then expanding the third term of equation (7.183) leads to

$$
\begin{aligned}
\left(a_{21}a_{41} + a_{22}a_{42}\right)\cos\left(w_3q_3\right) + \left(-a_{22}a_{41} + a_{21}a_{42}\right)\sin\left(w_3q_3\right) = \\
-\mathbf{e}_3^T\mathbf{Q}_1^T\mathbf{p}_e - \mathbf{e}_3^T\mathbf{a}_1 - a_{23}a_{43}
\end{aligned} \tag{7.184}
$$

Let

$$
\begin{aligned}
f_{11} &= a_{21}a_{41} + a_{22}a_{42} \\
f_{12} &= -a_{22}a_{41} + a_{21}a_{42} \\
f_{13} &= -\mathbf{e}_3^T\mathbf{a}_1 - a_{23}a_{43}
\end{aligned}
$$

then equation (7.184) can written as

$$f_{11}\cos(w_3q_3) + f_{12}\sin(w_3q_3) = -\mathbf{e}_3^T\mathbf{Q}_1^T\mathbf{p}_e + f_{13} \tag{7.185}$$

Take the 2-norm of equation (7.182), then

$$\begin{aligned}\mathbf{p}_e^T\mathbf{p}_e + 2\mathbf{p}_e^T\mathbf{Q}_1\mathbf{a}_1 + 2\left(\mathbf{p}_e^T\mathbf{Q}_1 + \mathbf{a}_1^T\right)\mathbf{R}_\mathbf{z}(-\beta_2)\mathbf{G}_3\mathbf{R}_\mathbf{z}(w_4q_4)\mathbf{a}_2 \\ = -\mathbf{a}_1^T\mathbf{a}_1 - \mathbf{a}_2^T\mathbf{a}_2 + \mathbf{a}_3^T\mathbf{a}_3\end{aligned} \tag{7.186}$$

Let

$$\begin{aligned}\mathbf{a}_5 &= 2\mathbf{Q}_1\mathbf{a}_1 \\ &\quad \left(\mathbf{p}_e^T\mathbf{a}_6 + g_1\right)\cos(w_4q_4) + \left(\mathbf{p}_e^T\mathbf{a}_7 + g_2\right)\sin(w_4q_4) \\ &= 2\left(\mathbf{p}_e^T\mathbf{Q}_1 + \mathbf{a}_1^T\right)\mathbf{R}_\mathbf{z}(-\beta_2)\mathbf{G}_3\mathbf{R}_\mathbf{z}(w_4q_4)\mathbf{a}_2\end{aligned}$$

then equation (7.182) can be written as

$$\begin{aligned}&\left(\mathbf{p}_e^T\mathbf{a}_6 + g_1\right)\cos(w_4q_4) + \left(\mathbf{p}_e^T\mathbf{a}_7 + g_2\right)\sin(w_4q_4) \\ =\ & -\mathbf{p}_e^T\mathbf{p}_e - \mathbf{p}_e^T\mathbf{a}_5 - \mathbf{a}_1^T\mathbf{a}_1 - \mathbf{a}_2^T\mathbf{a}_2 + \mathbf{a}_3^T\mathbf{a}_3\end{aligned} \tag{7.187}$$

From equations (7.185) and (7.187), we have

$$\begin{aligned}&\left[\mathbf{p}_e^T\left(f_{11}\mathbf{a}_7 - f_{12}\mathbf{a}_6\right) + f_{11}g_2 - f_{12}g_1\right]\cos(w_3q_3) \\ =\ & f_{12}\mathbf{p}_e^T\mathbf{p}_e - \mathbf{p}_e^T\mathbf{a}_7\mathbf{e}_3^T\mathbf{Q}_1^T\mathbf{p}_e + g_2\mathbf{p}_e^T\left(\mathbf{Q}_1\mathbf{e}_3 + f_{13}\mathbf{a}_7 + f_{12}\mathbf{a}_5\right) \\ & + f_{12}\left(\mathbf{a}_1^T\mathbf{a}_1 + \mathbf{a}_2^T\mathbf{a}_2 - \mathbf{a}_3^T\mathbf{a}_3\right) + f_{13}g_2\end{aligned} \tag{7.188}$$

$$\begin{aligned}&\left[\mathbf{p}_e^T\left(f_{11}\mathbf{a}_7 - f_{12}\mathbf{a}_6\right) + f_{11}g_2 - f_{12}g_1\right]\sin(w_4q_4) \\ =\ & -f_{11}\mathbf{p}_e^T\mathbf{p}_e + \mathbf{p}_e^T\mathbf{a}_6\mathbf{e}_3^T\mathbf{Q}_1^T\mathbf{p}_e + \mathbf{p}_e^T\left(-f_{11}\mathbf{a}_5 - f_{13}\mathbf{a}_6 + g_1\mathbf{Q}_1\mathbf{e}_3\right)\end{aligned}$$

$$-f_{11}\left(\mathbf{a}_1^T\mathbf{a}_1+\mathbf{a}_2^T\mathbf{a}_2-\mathbf{a}_3^T\mathbf{a}_3\right)_e-f_{13}g_1 \tag{7.189}$$

Let

$$\begin{aligned}
b_1 &= f_{12}\\
\mathbf{D}_1 &= -\mathbf{a}_7\mathbf{e}_3^T\mathbf{Q}_1^T\\
\mathbf{u} &= g_2\left(\mathbf{Q}_1\mathbf{e}_3+f_{13}\mathbf{a}_7+f_{12}\mathbf{a}_5\right)\\
b_2 &= f_{12}\left(\mathbf{a}_1^T\mathbf{a}_1+\mathbf{a}_2^T\mathbf{a}_2-\mathbf{a}_3^T\mathbf{a}_3\right)+f_{13}g_2\\
b_3 &= -f_{11}\\
\mathbf{D}_2 &= \mathbf{a}_6\mathbf{e}_3^T\mathbf{Q}_1^T\\
\mathbf{v} &= -f_{11}\mathbf{a}_5-f_{13}\mathbf{a}_6+g_1\mathbf{Q}_1\mathbf{e}_3\\
b_4 &= -f_{11}\left(\mathbf{a}_1^T\mathbf{a}_1+\mathbf{a}_2^T\mathbf{a}_2-\mathbf{a}_3^T\mathbf{a}_3\right)_e-f_{13}g_1\\
\mathbf{w} &= f_{11}\mathbf{a}_7-f_{12}\mathbf{a}_6\\
b_5 &= f_{11}g_2-f_{12}g_1
\end{aligned}$$

then equations (7.188) and (7.189) can be written as

$$b_1\mathbf{p}_e^T\mathbf{p}_e+\mathbf{p}_e^T\mathbf{D}_1\mathbf{p}_e+\mathbf{p}_e^T\mathbf{u}+b_2 = \left(\mathbf{p}_e^T\mathbf{w}+b_5\right)\cos\left(w_3q_3\right) \tag{7.190}$$

$$b_3\mathbf{p}_e^T\mathbf{p}_e+\mathbf{p}_e^T\mathbf{D}_2\mathbf{p}_e+\mathbf{p}_e^T\mathbf{v}+b_4 = \left(\mathbf{p}_e^T\mathbf{w}+b_5\right)\sin\left(w_4q_4\right) \tag{7.191}$$

The square sum of equations (7.190) and (7.191) leads to the position manifold :

$$\begin{aligned}
&\left(b_1\mathbf{p}_e^T\mathbf{p}_e+\mathbf{p}_e^T\mathbf{D}_1\mathbf{p}_e+\mathbf{p}_e^T\mathbf{u}+b_2\right)^2\\
+\;&\left(b_3\mathbf{p}_e^T\mathbf{p}_e+\mathbf{p}_e^T\mathbf{D}_2\mathbf{p}_e+\mathbf{p}_e^T\mathbf{v}+b_4\right)^2-\left(\mathbf{p}_e^T\mathbf{w}+b_5\right)^2=0
\end{aligned} \tag{7.192}$$

For manifold (7.192), if one joint is at infinity, the manifold becomes a quadratic

equation :

$$\mathbf{p}_e^T\mathbf{p}_e + \mathbf{p}_e^T\mathbf{D}_1\mathbf{p}_e + \mathbf{p}_e^T\mathbf{u} + b = 0 \tag{7.193}$$

If two joints are at infinity, the manifold becomes a linear equation :

$$\mathbf{p}_e^T\mathbf{u} + b = 0 \tag{7.194}$$

References

ANGELES, J. (c2003). *Fundamentals of robotic mechanical systems : theory, methods, and algorithms.* Mechanical engineering series : Mechanical engineering series (Springer). Springer, New York, 2nd ed. edition.

BROGARDH, C. (2002). Pkm research-important issues, as seen from a product development perspective at abb. In *Proceedings of the WORKSHOP on Fundamental Issues and Future Research Directions for Parallel Mechanisms and Manipulators*, Quebec City, Quebec, Canada, pages 68–82.

CLAVEL, R. (1985). Device for displacing and positioning an element in space. International patent, No. WO 87/03528 (1985).

GOSSELIN, C. AND ANGELES, J. (1990). Singularity analysis of closed-loop kinematic chains. *IEEE Trans. Robot. Autom. (USA)*, **6**(3), 281 – 90.

GOSSELIN, C. AND HAMEL, J.-F. (1994). The agile eye : a high-performance three-degree-of-freedom camera-orienting device. *Proceedings 1994 IEEE International Conference on Robotics and Automation (Cat. No.94CH3375-3)*, **vol.1**, 781 – 6.

GOSSELIN, C., KONG, X., FOUCAULT, S., AND BONEV, I. A. (2004). A fully decoupled 3-dof translational parallel mechanism. In *Proceedings of 2004 Paral-*

lel Kinematic Machines in Research and Practice International Conference (PKS 2004), Chemnitz, Germany, pages 595–610.

HERVE, J. M. AND SPARACINO, F. (1992). Star, a new concept in robotics. In *Third International Workshop on Advances in Robot Kinematics*, pages 180–183.

KAROUIA, M. AND HERVE, J. M. (2002). A family of novel orientational 3-dof parallel robots. In *Proceedings of CISM-IFToMM RoManSy Symposia*, Udine, Italy, pages 359–368.

KIM, H. S. AND TSAI, L.-W. (2002). Evaluation of a cartesian parallel manipulator. In Lenarcic, J. and Thomas, F., editors, *Advances in Robot Kinematics, Theory and Applications*, pages 19–28. Kluwer Academic Publishers.

KONG, X. AND GOSSELIN, C. (2001). Generation of parallel manipulators with three translational degrees of freedom based on screw theory. In Agency, T. C. S., editor, *Symposium 2001 sur les mécanismes,les machines et la mécatronique de CCToMM*, Saint-Hubert, Montréal, Québec, Canada.

KONG, X. AND GOSSELIN, C. M. (2004). Type synthesis of 3-dof translational parallel manipulators based on screw theory. *Journal of Mechanical Design, Transactions of the ASME*, **126**(1), 83 – 92.

LEGUAY-DURAND, S. AND REBOULET, C. (1997). Design of a 3-dof parallel translating manipulator with u-p-u joints kinematic chains. In *Proceedings of the 1997 IEEE/RSJ International Conference on Intelligent Robot and Systems. Innovative Robotics for Real-World Applications. IROS '97*, pages 1637– 1642.

MERLET, J.-P. (2002a). An initiative for the kinematics study of parallel manipulators. In *Proceedings of the WORKSHOP on Fundamental Issues and Future Research Directions for Parallel Mechanisms and Manipulators*, Montreal, Quebec,

Canada.

MERLET, J.-P. (2002b). Still a long way to go on the road for parallel mechanisms. In *ASME 27th Biennial Mechanisms and Robotics Conference*, Montreal, Quebec, Canada.

MERLET, J.-P. (c1997). *Les robots paralleles*. Hermes, Paris.

TSAI, L.-W. (1996). Kinematics of a three-dof platform with extensible limbs. In Lenarcic, J. and Parenti-Castelli, V., editors, *Recent Advances in Robot Kinematics*, pages 401–410. Kluwer Academic Publishers.

TSAI, L.-W. AND JOSHI, S. (2002). Kinematic analysis of 3-dof position mechanisms for use in hybrid kinematic machines. *Journal of Mechanical Design, Transactions of the ASME*, **124**(2), 245 – 253.

WENGER, P. AND CHABLAT, D. (2000). Kinematic analysis of a new parallel machine tool : The orthoglide. In Lenarcic, J. and Parenti-Castelli, V., editors, *Recent Advances in Robot Kinematics*, pages 305– 314. Kluwer Academic Publishers.

ZANGANEH, K. AND ANGELES, J. (1998). Formalism for the analysis and design of modular kinematic structures. *International Journal of Robotics Research*, **17**(7), 720 – 730.

CHAPITRE 8

DISCUSSION GÉNÉRALE

Dans tous les domaines d'activités humaines, le niveau d'exigence ne cesse d'augmenter. Les manipulateurs ne sont pas d'exceptions. D'une part, de plus en plus d'applications exigent des performances plus élevées de la part des manipulateurs. D'autre part, dictées par la considération économique, les contraintes sur le temps consacré à la conception et à l'optimisation de nos produits deviennent primordiales. L'adaptation des techniques existantes étant limitée, il nous faut dorénavant concevoir de nouveaux mécanismes plus performants et plus adaptés. Il faut aussi développer des outils de synthèse automatisés afin de réduire le temps du cycle de conception et d'obtenir les résultats optimaux. C'est à partir de ce constat que nous avons orienté nos travaux de recherche vers les MPs qui sont relativement nouveaux dans la scène de la robotique et nous avons visé à développer un environnement de synthèse topologique et géométrique des MPTs.

L'objectif général de cette thèse était de résoudre les problèmes dans la synthèse des MPs. Notre intérêt s'est porté sur les MPs à 3 degrés de liberté, et plus particulièrement, aux MPTs.

Traditionnellement, la synthèse des manipulateurs s'effectue en deux étapes. La première consiste à choisir une topologie qui convient a priori aux contraintes de satisfaction de la tâche. Ensuite, un paramétrage est effectué afin d'établir un modèle de synthèse des manipulateurs de la topologie choisie. La première problématique de cette méthode concerne le choix optimal de la topologie. Puisque le choix de la topologie est principalement basé sur nos connaissances antérieures, notre expérience,

notre intuition, et notre ingéniosité, on ne sait d'aucune manière si la topologie choisie est optimale ou non. La deuxième problématique concerne la correspondance entre le modèle de synthèse établi et les manipulateurs visés, c'est-à-dire qu'une partie des manipulateurs générés par le modèle ne satisfont même pas aux critères de base tels que le DDL et le DDM, tandis que ceux qui y satisfont ne représentent qu'une petite partie des manipulateurs visés. La troisième problématique concerne l'implantation d'une méthode de synthèse automatisée. Chaque topologie choisie nécessitant un paramétrage personnalisé, il est impossible d'automatiser le processus de synthèse. En premier lieu, notre objectif a nécessité une étude approfondie de l'aspect topologique et géométrique des manipulateurs spatiaux afin de résoudre le problème de correspondance entre le modèle de synthèse et les manipulateurs visés. L'idée était d'identifier et d'introduire dans la modélisation topologique des éléments dimensionnels et géométriques qui sont essentiels à déterminer le DDL, le DDM, et la NDM d'un manipulateur. Ces éléments dimensionnels et géométriques que nous appelons contraintes essentielles permettent d'établir un modèle de synthèse qui représente mieux les manipulateurs visés. L'introduction des contraintes essentielles a aussi nécessité une nouvelle approche de représentation topologique, car les méthodes existantes ne sont pas adaptées à la nouvelle définition de la topologie. Le diagramme topologique que nous avons proposé permet une meilleure représentation des DDL, DDM, et NDM et facilite la synthèse manuelle ou automatisée et la documentation de cette dernière.

Contrairement aux MSs, le problème des DDL, DDM, NDM des MPs est un problème très complexe qui a mérité une analyse systématique. Tels que démontrés dans le chapitre quatre, le DDL, le DDM, et le degré de motorisation d'un MP peuvent être différents les uns les autres. Du point de vue mécanique, un MP peut être isocontraint, surcontraint, ou souscontraint et les modélisations respectives sont conséquemment très différentes. Du point de vue mathématique, il s'agit

des systèmes d'équations non linéaires exactement déterminé, surdéterminé, ou indéterminé. En ce qui concerne la modélisation, chaque manipulateur surcontraint ou souscontraint nécessite une modélisation personnalisée et un traitement mathématique particulier. Étant donné le nombre infini des cas surcontraints et souscontraints, il est impossible de les traiter de façon automatique. L'analyse effectuée dans le chapitre quatre a démontré que chaque manipulateur surcontraint ou souscontraint a un équivalent parmi les manipulateurs isocontraints dont la propriété cinématique de l'effecteur lui est identique comme une fonction des variables des joints actionnés. Ce constat permet de ne pas traiter les manipulateurs surcontraints ou souscontraints de façon cas par cas et plutôt de les traiter de manière uniforme en prenant leur équivalent dans les manipulateurs isocontraints. L'aproche que nous avons proposée pour déterminer la topologie et la géométrie d'un manipulateur à partir des DDL et DDM permet de générer tous les manipulateurs visés dont ceux surcontraints et ceux souscontraints se déduisent à partir de leurs équivalents.

Les méthodes existantes de synthèse en fonction de la NDM sont basées principalement sur la théorie des groupes de Lie ou la théorie des visseurs. Celle basée sur la théorie des groupes de Lie ne permet de générer que les manipulateurs dont les souschaînes génèrent des déplacements des groupes de Lie. Cependant, la plupart des souschaînes génèrent pas de groupes de Lie, cette méthode est grandement limitée. La méthode basée sur la théorie des visseurs consiste à transformer un système de torseurs de vitesse à un système de torseurs de force en utilisant la réciprocité. Le problème de synthèse cinématique est ainsi transformé à un problème statique. Cette transformation ne réduit pas le niveau de difficulté de la synthèse. L'approche que nous avons proposée consiste à déduire la topologie et la géométrie directement du système de torseurs de vitesse qui est donc plus efficace que celle basée sur la théorie des visseurs. Comme la synthèse basée sur la théorie des visseurs qui s'effec-

tue à une configuration particulière, notre approche soufre aussi de l'inconvénient de garantir la NDM dans un espace de travail.

L'analyse de l'orientation de l'effecteur dans l'espace de travail a pour objectif de déduire les conditions pour qu'un manipulateur soit un MPT. L'analyse a démontré qu'il existe trois catégories de MPTs. L'effecteur des manipulateurs de la première catégorie ne peut pas changer d'orientation à travers leur espace de travail de tous les modes d'assemblage. Les manipulateurs de la deuxième catégorie ne sont les MPTs que pour certains modes d'assemblage tandis que les manipulateurs de la troisième catégorie ne sont les MPTs que pour un sousespace de travail d'un seul mode d'assemblage. Le problème de mobilité des MPTs dans l'espace de travail a été entièrement résolu.

Avec les méthodes de synthèse existantes, la synthèse topologique et géométrique s'effectue de façon séquentielle, c'est-à-dire que l'on choisit la topologie en premier, puis pour chaque topologie la synthèse géométrique est effectuée. De toute évidence, cette manière ne permet pas de déterminer à la fois la topologie et la géométrie afin d'obtenir les résultats optimaux. Pour résoudre ce problème, il a été nécessaire d'introduire la topologie en tant que variable de synthèse. La plus simple façon de ce faire est de représenter la topologie par une série de variables booléennes qui correspondent respectivement à la nature de chacun des couples cinématiques. Puisque les variables booléennes ne prennent que les valeurs 0 ou 1, cette méthode ne permet pas à un ensemble de designs évoluent vers un autre ensemble de designs de manière continue. Jusqu'à date, aucun travail n'a été réalisé avec succès à cet égard. La méthode que nous avons proposée de représenter la nature des couples cinématiques avec des variables continues permet de pallier cet inconvénient.

L'ensemble des travaux réalisés dans cette thèse permettront l'implantation d'un système de synthèse automatisé des MPTs. Ceci sera réalisable grâce à l'usage de

plus en plus courant de l'outil informatique et à l'extension de ses capacités de calcul.

CONCLUSION

Les travaux réalisé dans cette thèse permettent d'une part la résolution des problèmes fondamentaux de la synthèse cinématique des manipulateurs et d'autre part la mise au point d'une méthode de synthèse topologique et géométrique des MPTs.

Que ce soit un MS ou un MP, il est essentiel d'aborder l'aspect topologique et géométrique afin de mettre en place un système de synthèse cinématique. L'étude de la littérature que nous avons réalisée a démontré que jusqu'à présent le sujet de topologie et géométrie n'a pas été traité de manière rigoureuse. Une définition adéquate de topologie est essentielle afin d'effectuer efficacement la conception qualitative. Elle est aussi indispensable à la synthèse géométrique pour que l'espace de paramètres de synthèse corresponde aux manipulateurs visés. L'étude de ce sujet que nous avons réalisée ainsi que la représentation topologique que nous avons proposée dans le chapitre trois représentent un apport original à cet égard.

La première question qui s'impose à la synthèse est de déterminer la topologie et la géométrie afin d'avoir le DDM demandé. L'originalité de notre réalisation à cette question est d'avoir déduit les conditions topologiques et géométriques pour un MP d'avoir 3 DDM et d'être isocontraint. Ceci a été réalisé grâce à une analyse systématique dans l'esspace tangentiel. Les situations surcontrainte et souscontrainte ont aussi été abordée, et ce basé sur celle isocontrainte, permettant de les traiter de façon uniforme.

Par la suite, nous avons traité la NDM des MPs à 3 DDLs. En représentant la NDM par deux matrices 3×3, nous avons proposé une approche de synthèse topologique et géométrique en fonction de la NDM. Application de cette approche nous a permis de contribuer une nouvelle architecture de MP à 3 DDLs. Puisque cette approche

s'appuie sur l'analyse de l'espace tangentiel qui dépend de la configuration, la NDM d'un manipulateur ainsi obtenu peut changer avec sa configuration. Vérifier si un manipulateur satisfait à la NDM partout dans un espace de travail reste une problématique à étudier.

Pour résoudre cette problématique dans la synthèse des MPTs, nous avons effectué une analyse dans l'espace de déplacement. Cette analyse nous a permis de déduire quelles sont les topologies qui ne permettent à l'effecteur d'avoir la mobilité qu'en translation. À ce point-ci, notre approche de synthèse topologique a été complétée.

La synthèse topologique ou géométrique est un problème qui est grandement étudié depuis des années. Par contre, la synthèse conjointe topologie et géométrie des MPs reste un problème ouvert car les récents travaux sur la question consistent encore soit à trouver de nouvelles topologies soit à optimiser la performance d'un manipulateur d'une topologie donnée. Cependant, la propriété cinématique d'un manipulateur dépend autant de la topologie que de la géométrie. Ce constat nous a amené à proposer un modèle cinématique qui prenne en compte la topologie et la géométrie. Pour cela, nous avons intégré la nature des couples cinématiques en tant que variables de synthèse dans le modèle cinématique, ce qui nous permet d'envisager, lors de la synthèse d'un manipulateur, toutes les topologies en vue de satisfaire une tâche donnée. Cette démarche constitue une de nos contributions originales. Par ailleurs, nous avons résolu les problèmes des MGD et MGI à partir du modèle proposé. Ceci est une contribution importante pour la mise en place des algorithmes d'évaluation et d'optimisation dans le but d'automatiser le processus de synthèse.

L'ensemble des travaux réalisés dans cette thèse constituent une plate-forme de synthèse topologique et géométrique des MPs.

En perspective, les éléments présentés dans cette thèse peuvent être intégrés avec les méthodes d'optimisation globale et peuvent être utilisés pour produire un environnement de synthèse topologique et géométrique automatisée des MPs.

Enfin, un travail de fond sur l'évaluation de performance et la mise ensemble de tous les éléments nécessaires sont indispensables afin de réaliser la conception automatisée des MPs.

RÉFÉRENCES

AGRAWAL, S. ET ROTH, B. (1992). Statics of in-parallel manipulator systems. *Journal of Mechanical Design - Transactions of the ASME*, **114**(4), 564 – 568.

AGRAWAL, S. K. (1991). Study of an in-parallel mechanism using reciprocal screws. In *Proceedings of the Ninth World Congress on the Theory of Machines and Mechanisms*, pages 405– 408.

ANGELES, J. (1982). *Spatial Kinematic Chains. Analysis, Synthesis, Optimization.* Springer-Verlag, Berlin.

ANGELES, J. (2002). The qualitative synthesis of parallel manipulators. In *Proceedings of the WORKSHOP on Fundamental Issues and Future Research Directions for Parallel Mechanisms and Manipulators*, Quebec City, Quebec, Canada.

ANGELES, J. (2004). The qualitative synthesis of parallel manipulators. *Journal of Mechanical Design, Transactions of the ASME*, **126**(4), 617–624.

ANGELES, J. (c2003). *Fundamentals of robotic mechanical systems : theory, methods, and algorithms.* Mechanical engineering series : Mechanical engineering series (Springer). Springer, New York, 2nd ed. edition.

ANGELES, J. ET GOSSELIN, C. (1988). Determination of the degree of freedom of simple and complex kinematic chains. *Transactions of the Canadian Society for Mechanical Engineers*, **12**(4), 219 – 226.

BALKAN, T., KEMAL OZGOREN, M., SAHIR ARIKAN, M., ET MURAT BAYKURT, H. (2001). A kinematic structure-based classification and compact kinematic equations for six-dof industrial robotic manipulators. *Mechanism and Machine Theory*, **36**(7), 817 – 832.

BARON, L. (2001). Workspace-based design of parallel manipulators of star topology with a genetic algorithm. In *Proceedings of ASME 27th Design Automation Conference*, Pittsburg, U.S.A.

BARON, L. (c1997). *Contributions to the estimation of rigid-body motion under sensor redundancy*. PhD thesis, McGill University.

BARON, L. ET ANGELES, J. (1995). The isotropic decoupling of the direct kinematics of parallel manipulators under sensor redundancy. *Proceedings of 1995 IEEE International Conference on Robotics and Automation (Cat. No.95CH3461-1)*, **vol.2**, 1541 – 6.

BARON, L. ET ANGELES, J. (2000). The direct kinematics of parallel manipulators under joint-sensor redundancy. *IEEE Trans. Robot. Autom. (USA)*, **16**(1), 12 – 19.

BARON, L., WANG, X., ET CLOUTIER, G. (2002). The isotropic conditions of parallel manipulators of delta topology. In Lenarcic, J. et Thomas, F., editors, *Advances in Robot Kinematics, Theory and Applications*, pages 357–367. Kluwer Academic Publishers.

BENNETT, G. (1903). A new mechanism. *Engineering*.

BIRGLEN, L. (2002). Haptic devices based on parallel mechanisms : State of the art. ParalleMIC - the Parallel Mechanisms Information Center, http ://www.parallemic.org/Reviews/Review003.html.

BIRGLEN, L., GOSSELIN, C., POULIOT, N., MONSARRAT, B., ET LALIBERTE, T. (2002). SHaDe, a new 3-dof haptic device. *IEEE Trans. Robot. Autom. (USA)*, **18**(2), 166 – 75.

BONEV, I. (2003). The true origins of parallel robots. ParalleMIC - the Parallel Mechanisms Information Center, http ://www.parallemic.org/Review007.html.

BOUDREAU, R., DARENFED, S., ET GOSSELIN, C. (1998). On the computation of the direct kinematics of parallel manipulators using polynomial networks. *IEEE Trans. Syst. Man Cybern. A, Syst. Humans (USA)*, **28**(2), 213 - 20.

BROGARDH, C. (2002). Pkm research-important issues, as seen from a product development perspective at abb. In *Proceedings of the WORKSHOP on Fundamental Issues and Future Research Directions for Parallel Mechanisms and Manipulators*, Quebec City, Quebec, Canada, pages 68–82.

CARRETERO, J. A., NAHON, M. A., ET PODHORODESKI, R. P. (2000). Workspace analysis and optimization of a novel 3-dof parallel manipulator. *International Journal of Robotics & Automation*, **15**(4), 178–88.

CARRICATO, M. ET PARENTI-CASTELLI, V. (2002). Singularity-free fully-isotropic translational parallel manipulators. *Proceedings of the ASME Design Engineering Technical Conference*, **5 B**, 1041 - 1050.

CHAILLET, N. ET PERRARD, C. (2001). Robotique industrielle - evolutions technologique, offre, perspective et enjeux. Actualité, Université de Franche-Comté, No. 153, http ://www.univ-fcomte.fr/actualite/en-direct/num153.

CHEDMAIL, P. (1998). Optimization of multi-dof mechanisms. In Angeles, J. et Zakhariev, E., editors, *Computational Methods in Mechanisms System*, pages 97–130. Springer Verlag.

CHEN, P. ET ROTH, B. (1969). A unified theory for finitely and infinitesimally seperated position problems of kinematic synthesis. *ASME Journal of Engineering for Industry, Series B*, **91**, 203–208. Record Number : 2800.

CLAVEL, R. (1985). Device for displacing and positioning an element in space. International patent, No. WO 87/03528 (1985).

CLAVEL, R. (1988). Delta, a fast robot with parallel geometry. *Proceedings of*

the 18th International Symposium on Industrial Robots, pages 91 – 100.

COMPANY, O. (2000). *Machines-outils rapides a structure parallele Methodologie de conception, applications et nouveaux concepts.* PhD thesis, Universite Montpellier II, Sciences et Techniques du Languedoc, France.

CRAIG, J. J. (1986). *Introduction to robotics : mechanics & control.* Addison-Wesley Pub. Co., Reading, Mass.

CROSSLEY, F. (1962). Contribution to gruebler's theory in number synthesis of plane mechanisms. *American Society of Mechanical Engineers – Papers*, pages 5 –15.

CROSSLEY, F. (1965). Permutations of kinematic chains of eight members or less from graph – theoretic viewpoint. *Developments in Theoretical and Applied Mechanics*, **2**, 467 – 486.

DAI, J., HUANG, Z., ET LIPKIN, H. (2006). Mobility of overconstrained parallel mechanisms. *Trans. ASME, J. Mech. Des. (USA)*, **128**(1), 220 – 9.

DENAVIT, J. ET HARTENBERG, R. S. (1954). Kinematic notation for lower-pair mechanisms based on matrices. In *American Society of Mechanical Engineers (ASME).*

DIETMAIER, H. S. (1998). The stewart-gough platform of general geometry can have 40 real postures. In Lenarcic, J. et Husty, M., editors, *Advances in Robot Kinematics, Analysis and Control*, pages 1–10. Kluwer Academic Publishers.

DOBRJANSKYJ, L. ET FREUDENSTEIN, F. (1967). Some applications of graph theory to structural analysis of mechanisms. *American Society of Mechanical Engineers – Transactions – Journal of Engineering for Industry*, **89**(1), 153 – 158.

ENGELBERGER, J. (1964). Role of industrial robots in improving production operations. *Automation*, **11**(6), 62 – 67.

FREUDENSTEIN, F. ET MAKI, E. (1965). On a theory for the type synthesis of mechanism. In *Proceedings of the 11th International Congress of Applied Mechanics*, Springer, Berlin, pages 420–428.

FREUDENSTEIN, F. ET MAKI, E. (1979). Creation of mechanisms according to kinematic structure and function. *Journal of Environment and Planning*, **6**, 375–391.

FREUDENSTEIN, F. ET WOO, L. (1974). Kinematic structure of mechanisms. In *Basic Questions of Design Theory*. North Holland, Amsterdam, Holland,.

FRISOLI, A., CHECCACCI, D., SALSEDO, F., ET BERGAMASCO, M. (2000). Synthesis by screw algebra of translating in-parallel actuated mechanisms. In Lenarcic, J. et Parenti-Castelli, V., editors, *Recent Advances in Robot Kinematics*. Kluwer Academic Publishers.

GOSSELIN, C. ET ANGELES, J. (1990). Singularity analysis of closed-loop kinematic chains. *IEEE Trans. Robot. Autom. (USA)*, **6**(3), 281 – 90.

GOSSELIN, C. ET HAMEL, J.-F. (1994). The agile eye : a high-performance three-degree-of-freedom camera-orienting device. *Proceedings 1994 IEEE International Conference on Robotics and Automation (Cat. No.94CH3375-3)*, **vol.1**, 781 – 6.

GOSSELIN, C., KONG, X., FOUCAULT, S., ET BONEV, I. A. (2004). A fully decoupled 3-dof translational parallel mechanism. In *Proceedings of 2004 Parallel Kinematic Machines in Research and Practice International Conference (PKS 2004)*, Chemnitz, Germany, pages 595–610.

GOSSELIN, C., SEFRIOUI, J., ET RICHARD, M. (1994). On the direct kinematics of spherical three-degree-of-freedom parallel manipulators of general architecture. *Journal of Mechanical Design, Transactions Of the ASME*, **116**(2), 594 – 598.

GOSSELIN, C. M., RICARD, R., ET NAHON, M. A. (1995). Comparison of archi-

tectures of parallel mechanisms for workspace and kinematic properties. *American Society of Mechanical Engineers, Design Engineering Division (Publication) DE*, **82**(1), 951 – 958.

GOSSELIN, M. (1988). *Kinematic Analysis, Optimization and Programming of Parallel Robotic Manipulator.* PhD thesis, McGill University, Montreal, Canada.

GOUGH, V. (1956). Contribution to discussion of papers on research in automotive stability, control and tyre performance. *Proc. Auto Div. Inst. Mechanical Engineers.*

GOURDEAU, R. (1997). Object-oriented programming for robotic manipulator simulation. *IEEE Robotics & Automation Magazine*, **4**(3), 21 – 29.

GWINNETT, J. (1931). Amusement devices. US Patent No. 1,789,680.

HAYATI, S. ET MIRMIRANI, M. (Winter 1985). Improving the absolute positioning accuracy of robot manipulators. *J. Robot. Syst. (USA)*, **2**(4), 397 – 413.

HAYES, M. ET LANGLOIS, R. (2005). Atlas : A novel kinematic architecture for six dof motion platforms. *Transactions of the Canadian Society for Mechanical Engineering*, **29**(4), 701 – 709.

HAYES, M., ZSOMBOR-MURRAY, P., ET CHEN, C. (Sept. 2004). Unified kinematic analysis of general planar parallel manipulators. *Trans. ASME, J. Mech. Des. (USA)*, **126**(5), 866 – 74.

HERVE, J. (1999). Lie group of rigid body displacements, a fundamental tool for mechanism design. *Mechanism and Machine Theory*, **34**(5), 719 – 730.

HERVE, J. M. (1978). Analyse structurelle des mecanismes par groupe des deplacements. left bracket structural analysis of mechanisms by set or displacements right bracket . *Mechanism & Machine Theory*, **13**(4), 437 – 450.

HERVE, J. M. (1991). Structural synthesis of parallel robots generating spatial translation. In *Proceedings of Fifth International Conference on Advanced Robotics*, pages 808–813.

HERVE, J. M. (1994). Mathematical group structure of the set of displacements. *Mechanism & Machine Theory*, **29**(1), 73–81.

HERVE, J. M. ET SPARACINO, F. (1992). Star, a new concept in robotics. In *Third International Workshop on Advances in Robot Kinematics*, pages 180–183.

HO, C. Y. (1978). Note on the existence of bennett mechanism. *Mechanism & Machine Theory*, **13**(3), 269 – 271.

HUANG, Z. (2004). Kinematics and type synthesis of lower-mobility parallel robot manipulators. *Proceeding of the 2004 the Eleventh World Congress in Mechanism and Machine Science*, pages 65 – 76.

HUNT, K. (1978). *Kinematic Geometry of Mechanisms*. Oxford University Press, London.

HUNT, K. H. (1982a). Geometry of robotics devices. *Mechanical Engineering Transactions*, **7**(4), 213–220. Record Number : 2700 1982.

HUNT, K. H. (1982b). Structural kinematics of in parallel actuated robot arms. Record Number : 2710 Proceedings Title : Design and Production Engineering Technical Conference Place of Meeting : Washington.

IFTOMM (2003). Iftomm terminology. *Mechanism and Machine Theory*, **38**, 913–912.

ISO (1981). Kinematic diagrams - graphical symbols. ISO 3952-1, 1981.

KAROUIA, M. ET HERVE, J. M. (2002). A family of novel orientational 3-dof parallel robots. In *Proceedings of CISM-IFToMM RoManSy Symposia*, Udine, Italy, pages 359–368.

KHALIL, W. ET KLEINFINGER, J. (1986). A new geometric notation for open and closed-loop robots. *Proceedings 1986 IEEE International Conference on Robotics and Automation (Cat. No.86CH2282-2)*, pages 1174 – 9.

KIM, H. S. ET TSAI, L.-W. (2002). Evaluation of a cartesian parallel manipulator. In Lenarcic, J. et Thomas, F., editors, *Advances in Robot Kinematics, Theory and Applications*, pages 19–28. Kluwer Academic Publishers.

KONG, X. ET GOSSELIN, C. (2001). Generation of parallel manipulators with three translational degrees of freedom based on screw theory. In Agency, T. C. S., editor, *Symposium 2001 sur les mécanismes,les machines et la mécatronique de CCToMM*, Saint-Hubert, Montréal, Québec, Canada.

KONG, X. ET GOSSELIN, C. (2002). Type synthesis of linear translational parallel manipulators. In Lenarcic, J. et Thomas, F., editors, *Advances in Robot Kinematics, Theory and Applications*, pages 453–462. Kluwer Academic Publishers.

KONG, X. ET GOSSELIN, C. M. (2004). Type synthesis of 3-dof translational parallel manipulators based on screw theory. *Journal of Mechanical Design, Transactions of the ASME*, **126**(1), 83 – 92.

LEDERMANN, W. (1973). *Introduction to group theory*. Longman, London.

LEE, C.-C. ET HERVE, J. M. (2006). Translational parallel manipulators with doubly planar limbs. *Journal of Mechanical Design, Transactions of the ASME*, **41**(4), 433.

LEGUAY-DURAND, S. ET REBOULET, C. (1997). Design of a 3-dof parallel translating manipulator with u-p-u joints kinematic chains. In *Proceedings of the 1997 IEEE/RSJ International Conference on Intelligent Robot and Systems. Innovative Robotics for Real-World Applications. IROS '97*, pages 1637– 1642.

McCarthy, J. M. (1990). *An Introduction to Theoretical Kinematics.* The MIT Press, Cambridge, Massachusetts, London, England.

Merlet, J.-P. (2002a). An initiative for the kinematics study of parallel manipulators. In *Proceedings of the WORKSHOP on Fundamental Issues and Future Research Directions for Parallel Mechanisms and Manipulators*, Montreal, Quebec, Canada.

Merlet, J.-P. (2002b). Still a long way to go on the road for parallel mechanisms. In *ASME 27th Biennial Mechanisms and Robotics Conference*, Montreal, Quebec, Canada.

Merlet, J.-P. (c1997). *Les robots paralleles.* Hermes, Paris.

Ozgoren, M. (2002). Topological analysis of 6-joint serial manipulators and their inverse kinematic solutions. *Mechanism and Machine Theory*, **37**(5), 511 – 547.

ParalleMIC (2002). Terminology. ParalleMIC - the Parallel Mechanisms Information Center.

Park, F. C. et Bobrow, J. E. (1995). Geometric optimization algorithms for robot kinematic design. *Journal of Robotic Systems*, **12**(6), 453 – 463.

Pierrot, F. (1991). *Robots pleinement paralleles legers : Conception, Modelisation et Commande.* PhD thesis, Universite Montpellier II, Montpellier, France.

Pollard, W. (1940). Spray painting machine. US Patent, No. 2,213,108.

Powell, I. (1982). The kinematic analysis and simulation of the parallel topology manipulator. *Marconi Rev. (UK)*, **45**(226), 121 – 38.

Raghavan, M. et Roth, B. (1990). Kinematic analysis of the 6r manipulator of general geometry. In *Robotics Research, Fifth International Symposium*, pages 263–269.

RAMSTEIN, E. (1999). *Contribution a la formation generale d'un probleme de synthese de mécanismes et resolution.* PhD thesis, Universite de Nantes, Ecole doctorale science pour l'ingenieur de Nantes, France.

SMITH, R. (1886). Diagrams of kinematics. *Engineer.*

STERNBERG, S. (1994). *Group theory and physics.* Cambridge University Press, Cambridge.

STEWART, D. (1965). A platform with 6 degrees of freedom. In *Proc. of the Inst. of Mech. engineers, 180(Part 1, 15)*, pages 371–386.

STRAMIGIOLI, S. ET BRUYNINCKX, H. (2001). Geometry and screw theory for robotics (tutorial t9). In *IEEE International Conference on Robotics and Automation 2001.*

STRAMIGIOLI, S., MASCHKE, B., ET BIDARD, C. (2002). On the geometry of rigid-body motions : The relation between lie groups and screws. *Proceedings of the Institution of Mechanical Engineers, Part C : Journal of Mechanical Engineering Science*, **216**(1), 13 – 24.

SU, H., COLLINS, C., ET MCCARTHY, J. (2002). Classification of rrss linkages. *Mechanism and Machine Theory*, **37**(11), 1413 – 1433.

THE ASSOCIATION OF GERMAN ENGINEERS (1993). Symbols for the kinematic structure description of industrial robots. Guideline 2681.

TSAI, L.-W. (1996). Kinematics of a three-dof platform with extensible limbs. In Lenarcic, J. et Parenti-Castelli, V., editors, *Recent Advances in Robot Kinematics*, pages 401–410. Kluwer Academic Publishers.

TSAI, L.-W. (1999). The enumeration of a class of three-dof parallel manipulators. In *Proceedings of TENTH WORLD CONGRESS ON THE THEORY OF MACHINE AND MECHANISMS*, Oulu, Finland, pages 1121–1126.

TSAI, L.-W. (2001). *Mechanism design : enumeration of kinematic structures according to function.* Mechanical engineering series : CRC mechanical engineering series. CRC Press.

TSAI, L.-W. ET JOSHI, S. (2001). Comparison study of architectures of four 3 degree-of-freedom translational parallel manipulators. *Proceedings - IEEE International Conference on Robotics and Automation*, **2**, 1283 – 1288.

TSAI, L.-W. ET JOSHI, S. (2002). Kinematic analysis of 3-dof position mechanisms for use in hybrid kinematic machines. *Journal of Mechanical Design, Transactions of the ASME*, **124**(2), 245 – 253.

TSAI, L.-W. ET STAMPER, R. (1997). A parallel manipulator with only translational degrees of freedom. Technical research report, The Institute for Systems Research, University of Maryland, U.S.A.

WANG, L.-C. ET OEN, K.-T. (2002). Numerical direct kinematic analysis of fully parallel linearly actuated platform type manipulators. *J. Robot. Syst. (USA)*, **19**(8), 391 – 400.

WANG, X., BARON, L., ET CLOUTIER, G. (2003a). Design manifold of translational parallel manipulators. In l'Agence spatiale canadienne, editor, *Proceedings of 2003 CCToMM Symposium on Mechanisms, Machines, and Mechatronics*, Montreal, Quebec, Canada, pages 231–239.

WANG, X., BARON, L., ET CLOUTIER, G. (2003b). Kinematic modelling and isotropic conditions of a family of translational parallel manipulators. *IEEE International Conference on Control and Automation*,Montreal, Quebec, Canada, pages 173 – 177.

WANG, X., BARON, L., ET CLOUTIER, G. (2004). The design of parallel manipulators of delta topology under isotropic constraint. In Huang, T., editor,

Proceedings of the 11th World Congress in Mechanism and Machine Science, volume 1, Tianjin, China, pages 202–206. China Machinery Press.

WENGER, P. ET CHABLAT, D. (2000). Kinematic analysis of a new parallel machine tool : The orthoglide. In Lenarcic, J. et Parenti-Castelli, V., editors, *Recent Advances in Robot Kinematics*, pages 305– 314. Kluwer Academic Publishers.

WIKIPEDIA (2006). Robot. Wikipédia : L'encyclopédie libre http ://fr.wikipedia.org/wiki/Robot.

XIN-JUN, L., JINSONG, W., FENG, G., ET LI-PING, W. (2001). On the analysis of a new spatial three-degrees-of-freedom parallel manipulator. *IEEE Transactions on Robotics and Automation*, **17**(6), 959–68.

YANG, D. ET LEE, T. (1984). Feasibility study of a platform type of robotic manipulator from a kinematic viewpoint. *Journal of Mechanisms, Transmissions and Automation in Design*, **106**, 191–198.

YANG, G., CHEN, I.-M., LIM, W. K., ET YEO, S. H. (1999). Design and kinematic analysis of modular reconfigurable parallel robots. *Proceedings - IEEE International Conference on Robotics and Automation*, **4**, 2501 – 2506.

YANG, G., CHEN, I.-M., LIN, W., ET ANGELES, J. (2001). Singularity analysis of three-legged parallel robots based on passive-joint velocities. *Proceedings - IEEE International Conference on Robotics and Automation*, **3**, 2407 – 2412.

ZANGANEH, K. ET ANGELES, J. (1998). Formalism for the analysis and design of modular kinematic structures. *International Journal of Robotics Research*, **17**(7), 720 – 730.

ZHUANG, H., ROTH, Z., ET HAMANO, F. (1992). A complete and parametrically continuous kinematic model for robot manipulators. *IEEE Trans. Robot. Autom. (USA)*, **8**(4), 451 – 63.

ZLATANOV, D., BONEV, I., ET GOSSELIN, C. (2002). Constraint singularities as configuration space singularities. ParalleMIC - the Parallel Mechanisms Information Center, http ://www.parallemic.org/Reviews/Review008.html.